FACULTY OF ENGINEERING AND APPLIED SCIENCE

INSTITUTE OF SOUND AND VIBRATION RESEARCH

INJECTION PUMP AS A SOURCE OF ENGINE NOISE

by

Henry L. Pullen

A Thesis submitted for the Degree of
Master of Philosophy

University of Southampton

July, 1980

TO MY WIFE

UNIVERSITY OF SOUTHAMPTON

ABSTRACT

FACULTY OF ENGINEERING AND APPLIED SCIENCE

INSTITUTE OF SOUND AND VIBRATION RESEARCH

Master of Philosophy

INJECTION PUMP AS A SOURCE OF ENGINE NOISE

by Henry L. Pullen

The thesis deals with a study of the origins of in-line fuel injection pump noise and vibration for automotive diesel engines covering a large range of size and design configurations.

A detailed study is made on the basic exciting characteristics of the pump hydraulic forces and the correlation of these with the exciting propensities of the gas force. This is carried out both from theoretical and experimental bases. Also the basic differences between the engine structure and the injection pump structure are determined and techniques for assessing the contribution of injection equipment noise to the total engine noise are established, including their particular sound radiation efficiencies.

It is found that the injection pump noise is radiated mainly by the pump surfaces and that the pump induced vibration of the engine structure are not a major contributing factor to overall engine noise.

Other factors which are important in generating injection pump noise are also considered. These are mainly the effects of drive coupling details, drive gear "back lash" and basic pump mounting systems.

ACKNOWLEDGEMENTS

I would like to thank Professor Priede for the opportunity given to me to undertake this investigation and for his encouragement and expert guidance throughout.

I am extremely grateful to my supervisor Dr. Lalor and to Dr. Anderton and Mr. Grover for their advice and assistance and to the technical staff of the I.S.V.R. Automotive Group for their assistance in building and maintaining the special rigs used during this project.

Thanks are also to LUCAS CAV Ltd, London, for their assistance in initiating this project, the use of their laboratory equipment, supplying hardware and their expert advice at all times.

Finally, I record my thanks and gratitude to my wife who not only undertook the exact task of typing the thesis but also gave continuous support in every aspect during my seemingly endless pre-occupation with this work.

TABLE OF CONTENTS

LIST OF FIGURES

CHAPTER 3

CHAPTER 4

CHAPTER 5

CHAPTER 5 (Continued)

CHAPTER 6

1. INTRODUCTION

The fuel injection equipment is an integral part of a diesel engine which, due to the extreme pressure and rapidity of the fuel delivery process, develops impulsive exciting forces similar to those of the rapid pressure rise resulting from diesel combustion. Because of this similarity, noise produced by the fuel injection equipment has (particularly of in-line systems) for many years been a controversial subject.

For a long time there was a school of thought that the characteristic noise of diesel engines was mainly due to the mechanical operation of the fuel injection equipment. Subsequently, however, this has been disproved by many and varied investigations and it was found that injection equipment was seldom the predominant noise source of the engine. With the improvements to diesel combustion systems (smoother cylinder pressure development), engine mechanical noise, and engine structure design, in some instances the fuel injection equipment can become a source of noise of major significance. However, this is not the general case as in parallel with these developments considerable attention also has been paid by the pump manufacturers to produce quieter fuel injection pump designs.

Even though pump noise is normally lower than the other engine noise sources, in practice it is found that the actual difference can vary widely according to injection characteristics, mechanical design and methods of drive and mounting to the engine structure. Therefore there is a need to have a clearer understanding of the actual mechanism of generation of the pump noise itself, i.e. radiation of noise from the pump structure and the interaction between the pump structure and engine structure to which vibration forces from the pump are transmitted.

This thesis is based on a study of in-line pump noise and vibration. Investigations deal with the detailed study of the exciting characteristics of the pump hydraulic pressure and the correlation of these with the exciting propensities of the gas force from theoretical and experimental bases. The exciting forces when considered with the structural characteristics of the pump are related to the characteristics of the emitted noise. The analysis

of the interaction between the vibrating structures of the engine and pump forms a large part of the thesis which includes the study of the force paths and the relevant details of engine and pump structure responses.

Finally a practical study is made on techniques of reducing the noise from fuel pumps by the investigation related to pump drive and mounting systems.

2. LITERATURE SURVEY

2.1. Historical Review of Injection System Evolution

The satisfactory functioning of any diesel engine largely depends on the accuracy of the fuel injection system. Both speed and power are regulated by the quantity of fuel injected. The instant of fuel injected controls the efficiency and economical running of the engine.

The diesel engine has progressed in accordance with the improvements made in fuel injection. This has not only been incidental to the development of the diesel engine, but has been the primary factor, the rest of the improvements being based on the further opportunities presented by increased efficiency in injecting fuel.

A.F. Evan (2.1) stated that although solid or airless injection was contemplated by all diesel pioneers, Priestman (2.2); A. Stuart (2.3); and Capitaine (2.4), R. Diesel (2.5) himself, gave it up in preference for air injection for two very good reasons. The first was because he could not accomplish the process properly, and the second was that he had available means for producing blast injection, as he used blast air in his early coal dust experiment.

McKechnie (2.6) is rightly credited with the establishment of an air-less injection for large diesel engines and the Vickers firm turned out a considerable number of ships' diesels with this form of injection. His first arrangement was to raise an accumulator plunger by a snail cam, then deliver the oil, the snail cam subsequently allowing the spring activated plunger to come into action.

Hornsby's (2.7) did something of this kind, at least it appears so superficially, as they had a snail cam which raised a plunger, but it was really a hammer and on its release it descended and struck the plunger a hard blow; excellent for commencement of injection though its utility ceased there.

Blackstone's (2.8) were given considerable credit for their accumulator system. It gave quite good performance where low pressures and moderate speeds were employed. The accumulator consisted of a free plunger in two halves. These were thimble-shaped and enveloped a stiff compression spring, an initial load was applied by a bolt. A metering pump delivered oil during the cycle to the chamber of this pump, from which there was a branch to the jet. The oil displaced the plunger outwards by the extent of the oil delivery. A heavy lever was actuated

by the engine mechanism and during its travel it engaged the end of the plunger, forcing it in and compressing the spring still further. This motion continued until the lever made contact with the admission valve when the plunger spring expanded to its internal stop and delivered the oil.

Over the years from around 1905 many diesel engineers developed various types of fuel injection systems with the main emphasis on metering the fuel and controlling the rate of injection.

In the year 1919, Robson (2.9) designed a pump which had a conventional suction and delivery valve and a cam operated spring loaded plunger. This pump proved to be the prototype of the majority of pumps now in use.

Harland and Wolf (2.10) were, in 1926, responsible for a long stroke pump, the plunger had harmonic motion and interconnecting with this plunger was a spill valve communicating from the delivery chamber to the suction chamber, this valve being adjustable for quantity. There was also a separate eccentric operating suction valve which could be adjusted in phase to time the commencement of injection. The important feature of this particular valve was the release of pressure above the delivery valve.

For many years diesel engines had air-blast injection systems, i.e. the fuel was injected by air pressure of higher intensity than the compression in the cylinder. Although the system was capable of giving good atomization and penetration of the fuel, the power required to drive the blast-air compressors amounted to some 10% of the power of the engine. It was, however, unsuitable for small high speed diesel engines and so the solid-injection or air-less injection system came into being with a separate pump and fuel spraying nozzle provided for each cylinder.

Frazer M. Evan (2.11) stated that the classis design of the "in-line" fuel injection pump was originated by Robert Bosch Company (2.12) in Stuttgart. The success of the Bosch injection system was largely dependent on three basic design features, none of which was originated by Bosch. The first of these features was the method of pump delivery control by means of a helically-grooved slide valve formed in the head of a rotatable pump plunger to communicate with inlet and spill ports in the barrel wall. The second feature of the Bosch system

was the use of a closed injector nozzle with a differential needle valve, but this but this goes back at least as far as a patent by Ruston (2.13) in 1909. The third feature was the so-called 'Atlas' type unloading delivery valve (2.14) patented by the Atlas Diesel Company in 1924. This delivery valve drops the pipe line pressure at the end of injection to give rapid closure of the nozzle valve. The patent rights were acquired by Bosch.

Bosch's (2.12) own major contributions were in choosing the right elements to achieve a successful system, in meticulous attention to detail design and simplification; and in parallel development of production techniques to enable the equipment to be produced in quantity and economically.

In 1938 the manufacture of pumps and injectors to the Bosch design was taken over in this country by C.A.V. Ltd, Acton, London.

Up to the present day, in-line fuel injection pumps are still used extensively, namely on large diesel engines above say 1.5 litres per cylinder capacity.

Significant development in recent years has been directed towards the design of pumps of simple construction and smaller physical size which has been necessary as the small high speed diesel engines have become increasingly used. This, in the main part, has been based on rotary and distribution system.

2.2. Literature Survey of Fuel Injection Pump Noise

Considerable research has been carried out to reduce noise of diesel engines. This has been initiated because of the ever increasing demand for diesel driven transport vehicles which are major contributors to environmental noise pollution problems.

Most of the noise sources appertaining to the diesel engine have received extensive investigation with the exception of the fuel injection pump and literature on noise produced by fuel injection equipment is very limited.

From the work carried out by Austen and Priede (2.15) the following observations were made.

(1) The noise produced by the operation of the fuel injection system is comprised of (a) noise emitted by the surfaces of the injection system and (b) noise emitted by the engine surfaces to which vibration from the injection system is transmitted.

(2) The force responsible for the pump structure vibration is the hydraulic pressure in the pump chamber which acts between the camshaft and top of the pump. The excitation is produced by two distinct transients, i.e. the "pumping" transient and "spill" transient, their magnitude being dependent on factors such as cam rate, plunger diameter, injector pipe bore diameter and nozzle discharge area.

Mounting a conventional pump on a special bracket attached to an engine structure, Priede (2.16) considered that the hydraulic force acting normal to the camshaft can be resolved into two components, i.e. the horizontal force which causes bodily movement of the pump and the vertical force producing bending of the camshaft. Further investigations were carried out to reduce noise by reducing the basic camshaft vibrations by (a) fitting a heavy flywheel to minimise the effect of impulsive torque fluctuations; (b) by using larger camshaft diameter and (c) by fitting a plain bronze bearing block underneath the camshaft on the machined portion between the two centre cams. Shims were placed between the block and the pump housing in order to vary the bearing clearance. Fitting and adjusting the clearance of this centre bearing gave noise reductions of some 2 to 9 dB over the frequency range 200 Hz to 2000 Hz. In conclusion Priede states that the predominant noise of the injection pump arises from bending vibration of the pump camshaft, excited by rapid changes of fluid pressure in the pump elements. The emitted noise lies in the frequency range between 500 Hz to 800 Hz depending on the length of the camshaft.

Zimmerman (2.17) found that by running an in-line pump at various stages of assembly (inside an anechoic chamber) the noise of the unassembled pump in which only the camshaft turned was extremely low and hardly protruded above the background noise level of the test rig. Assembling the pump with tappets and tappet springs produced an increase in the noise by some 12 dB. Assembly of the plungers and pressure valves, together with the filling of the suction gallery with fuel, increased the noise by a further 2.5 dB even though the delivery valves were not operating since no fuel was being injected. When the fuel rack was fully opened there was a further increase of noise by some 5 to 15 dB(A).

Zimmerman also stated that one of the decisive factors of the cam drive was the actual cam shape which served to produce a particular

injection law at the nozzle as required by the combustion system. From investigations on various cam shapes an eccentric cam was the quietest. Somewhat more noisier was the tangential and circular arc cams. However, the general emitted noise due to the cam profile is about equal indicating that the cam shape was not an important parameter.

Methods of noise reduction by vibration damping the external walls of the pump have been considered. Zimmerman (2.17) showed a comparison between a cast iron housing without centre bearing and an aluminium housing with centre bearing. At idling and half-load conditions the cast iron housing was found to be quieter. With full injection quantity and higher speeds, the aluminium housing was found to be quieter. He also found that delivery valves are known to be an important source of vibration and noise. The greatest noise reduction was achieved by the combination of plastic valves with steel-rubber-steel seatings. However, it was found that these valve constructions could not be used in production.

From measurements on a running engine Zimmerman found that the influence of the injection pump on the total noise radiated could mainly be observed within the immediate vicinity of the pump and the noise emitted by the pump was chiefly due to bodily vibrations transmitted from the crankcase.

Russell (2.18) found that the rate at which the noise of an in-line pump increases with speed was related to the spectrum shape of the noise generating forces. Two major components were found, one being the hydraulic pressure pulse in the barrel, the other being impact as the delivery valve closes.

When a triangular repetitive force, such as the hydraulic pressure pulse, developed in the barrel, is subjected to Fourier Analysis, a series of spectrum lines results, with the fundamental at firing frequency. The lower harmonics are of similar level to the fundamental The overall envelope of the harmonics falls at approximately 40 dB/ decade increase in frequency above the frequency at which the pulse duration is half period.

From a specific investigation Russell showed four modes of pump vibration :

(1) cambox bending in the horizontal plane at 1.0 KHz.,

(2) flexing about the mounting at or near 1.25 KHz.,

(3) cambox plate resonances at and above 2.0 KHz. and

(4) panel modes of inspection cover at 3.5 KHz.

All these modes were efficient radiators of noise, so increasing their natural frequencies would not significantly affect the radiation efficiency.

Russell concluded on noise treatments that there was little scope for reducing the peak pumping pressure, or smoothing the barrel pressure waveform, as both lead to excessive smoke emissions and fuel consumption by the engine. Structural modifications to reduce high frequency vibration response involves stiffening the cambox with large ribs and re-timing troublesome modes to higher frequencies where there is less excitation.

3. BASIC ORIGINS OF INJECTION PUMP NOISE - RELATION BETWEEN EXCITING FORCES VIBRATION AND NOISE

The injection system is required to inject fuel at a precisely defined rate, time and pressure which is dictated by engine performance considerations. Thus deliberate changes to the hydraulic pressure characteristics for control of noise are basically ruled out. Since the injection characteristics require a high rate of pressure rise and correspondingly rapid pressure drop when injection is terminated it is obvious that the structure of the injection pump has to be extremely stiff. Flexibility in the drive could alter the required characteristics of injection and therefore the drive should also have considerable torsional stiffness. The injection pump itself cannot be vibration isolated from the engine structure and thus when fitted to an engine it forms an integral part of the engine structure. The same argument applies to injectors which must be rigidly mounted to the cylinder head to provide an adequate seal against cylinder pressure.

3.1. Principles of Fuel Injection Pump Design and Operation

On in-line engines, the fuel injection pump is usually mounted at the side of the engine. The pump may be base mounted to a supporting bracket attached to the engine casing or flange mounted to the engine timing gear case or end plate. Incorporated with the pump is the governor mechanism, excess fuel device for easy starting, stop control and sometimes an automatic advance device. Some types of pump are lubricated from the engine lubricating system via drillings in the pump mounting flange.

For these investigations most of the work has been carried out on a common type six element in-line high speed fuel injection pump which is relatively compact and lightweight. The main pump housing is split into two halves; the upper half machined from steel containing the fuel passages and pumping elements and the lower half cast in light alloy, housing the camshaft, tappets and control rod.

A complete pumping element - one required for each cylinder - consists of the operating cam which is engine driven, cam follower or tappet, plunger and barrel, return spring and delivery valve. The plunger is rotated within the barrel by a control fork which is clamped to the control rod which in turn is operated by the governor.

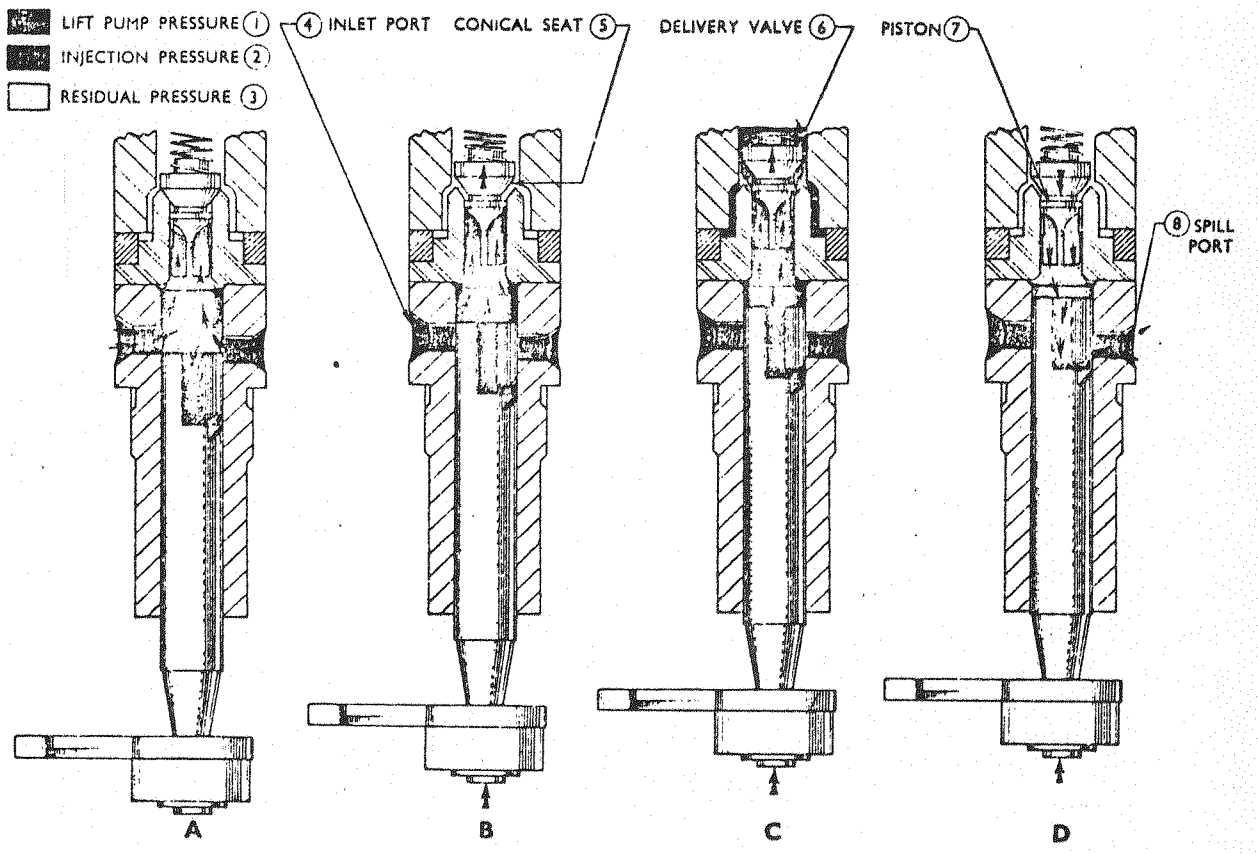

FIG 3·1

A pumping element is shown in Figure 3.1 in the various stages of its operating cycle. At (A) the plunger is at the bottom of its stroke and fuel under lift pump pressure fills the pumping element via the two ports in the barrel. At this stage the pressure in the barrel is not sufficient to lift the delivery valve off its seating against the action of the spring. As the camshaft rotates the plunger rises until position (B) is reached cutting off both the inlet and exit ports. Further upward movement of the plunger pressurises the fuel and begins to lift the delivery valve off its seat.

When fuel pressure is sufficient to lift the delivery valve completely off its seat, and the piston clear of its guide (C) fuel passes along the pipe line to the injector. The fuel pressure developed by the plunger lifts the injector needle valve off its seating against the action of the spring and allows fuel in a highly atomized state to be sprayed in the cylinder.

Fuel continues to be injected until the plunger reaches position (D) when the upper edge of the helical groove has uncovered the lower edge of the spill port and allows fuel under high pressure to leak back down the centre drilling in the plunger and out through the helical grooves into the fuel galleries of the pump body. This reduces the fuel pressure in the barrel and the delivery valve spring, assisted by the high pressure remaining in the pipe line, causes the valve to close rapidly.

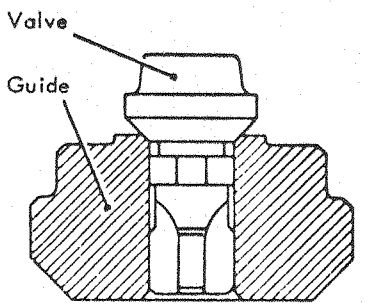

FIG 3.2 DILIVERY VALVE ASSEY

The sudden, if slight, reduction in pipe line pressure is sufficient to allow the injector needle valve to snap shut under force of its spring, hence preventing fuel from dribbling from the injector which would cause carbon build-up on the injector tip.

The delivery valve, Figure 3.2, also acts as a non-return valve and maintains residual pressure in the injector pipe line.

Figure 3.3 shows a typical indicator diagram taken from the fuel pipe under operating conditions. The full horizontal line is atmospheric pressure, and the dotted line the "trapped" pipe pressure from the previous cycle. Operations begin at point (a), where, due to the forward motion of the fuel pump plunger, the pressure rises: there is no opening of the injector nozzle.

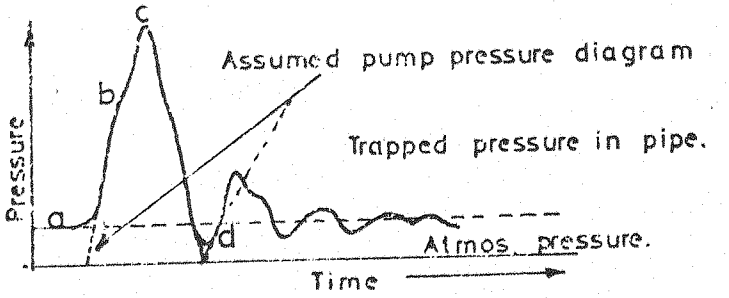

FIG. 3·3

At point (b), the injector "release pressure", the needle lifts and there is a momentary drop in pressure rate due to the sudden instantaneous increase in the volume of the system caused by motion of the needle. The

magnitude of this drop in pressure is determined almost entirely by the lift and diameter of the needle. The shape of the curve between points (b) and (c) is most important and is determined by a number of factors in combination. Bearing in mind that the needle is fully lifted against its stop and the nozzle orifice is open, whether the pressure will rise as shown or will remain constant or even fall, depends on the outflow from the nozzle at the rate of supply from the pump; the latter depends on the plunger size and cam rate.

At point (c) the spill valve or port in the pump opens and the pressure falls. Here again, the rate of fall of pressure depends on a number of factors, the most important of which are the type of delivery valve used, the rate of opening of the spill port or valve and the rapidity with which the injector needle snaps down when the pressure at that point has fallen to the calculated closing pressure. These three factors in combination also determine the residual pressure in the line, from which the cycle of operation begins.

Point (d) is invariably lower than this residual pressure due to the wave effect. From point (c) onwards the residual wave effect gradually dies out and leaves the line charged with the trapped-pipe pressure.

An important feature in the design of a fuel injection system is the type and magnitude of the residual pressure wave. It can, under certain conditions, cause a secondary opening of the injector which can cause erratic and inefficient combustion in the engine cylinder.

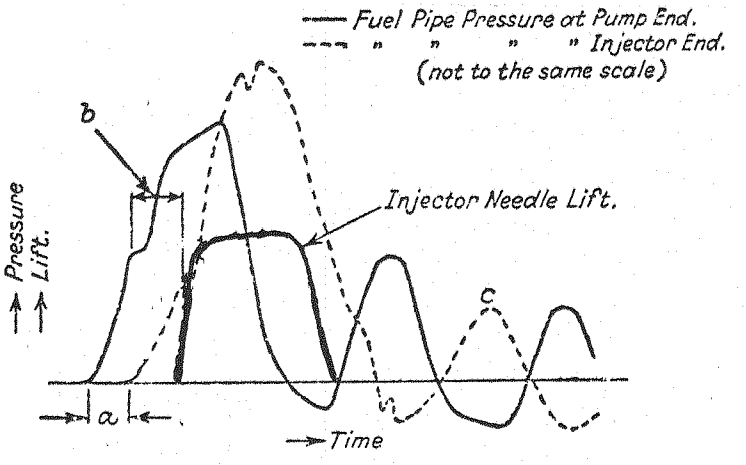

FIG. 3·4.

From Figure 3.4 distance (a) represents the time for the first pressure impulse to travel from the pump to the injector. The speed is that of sound in the fluid corrected for pipe diameter.

Distance (b) measured at the pressure at which the needle of the injector opens, is invariably found to be slightly greater than (a), due to the effect of friction in the pipe as the pressure waves build up.

The relative degree of control exercised by the pump and pipe respectively on the injection process is shown by the phasing of the full and dotted lines. It will be seen that due to the length of fuel pipe the greater part of the injection takes place whilst spill is actually in progress at the fuel pump end, the transmitted pressure wave at the injector end being in sole control. The rapid fall of pressure caused by the spill results in the residual waves shown and these waves have the peculiar property that their speed is one half of the theoretical speed of sound in the entrapped column of oil between the injector and the pump delivery valve. There appears to be no doubt that the oil column is behaving as an open ended pipe with consequent halving of its natural frequency, due probably to some instability of fuel pump delivery valve.

The fundamental differences between the conditions just after spill and those obtained at (a) are that whereas in the former at the "end" of the pipe are the injector needle and the delivery valve, in the latter the "ends" are the injector needle and top of the pump plunger. It is at point (c) that secondary opening of injector needle is liable to occur.

3.2. Considerations of the Basic Principles of Generation of Injector, Pump Noise and the Relationship with Engine Structure

When considering the mechanism of generation of noise in a diesel engine it is clear that both the exciting forces developed in the engine and the exciting forces developed in the pump each excite both the pump and engine structure at the same time, i.e. noise and vibration attributable to either cannot be simply identified. The clear understanding of the mechanism of vibration and noise generation thus is very complex with interconnected vibration paths from one vibratory system to another. This is illustrated by comparing a cross-sectioned drawing of an engine with its equivalent system. (Figure 3.5).

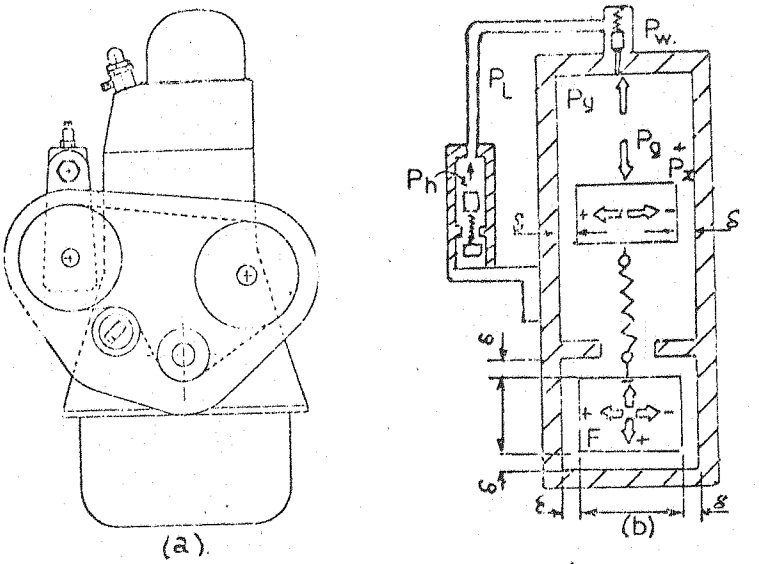

FIG. 3·5

There are two major forces which develop within the engine structure.

(1) Unidirectional exciting forces (rapid rise of gas force) resulting from combustion P_g and $(P_g + P_I)$ acting during the period around T.D.C. are responsible for combustion induced noise.

(2) Reversible forces (F) which develop in the crank mechanism and are responsible for various impacts and thus mechanically induced noise.

In the injection system there are three distinct forces as illustrated in Figure 3.5.

(1) Pump chamber hydraulic pressure force P_h acting on the lower part of the pump structure and which is also responsible for the impulsive torque of the pump.

(2) High pressure pipe line hydraulic force P_L which acts only on a small top part of the pump and throughout the pipe line up to the injector. This pressure is variable along the length of the pipe due to pressure waves.

(3) Mechanical impact forces P_W in the injector system, namely delivery valves seating and injector needle opening and closing.

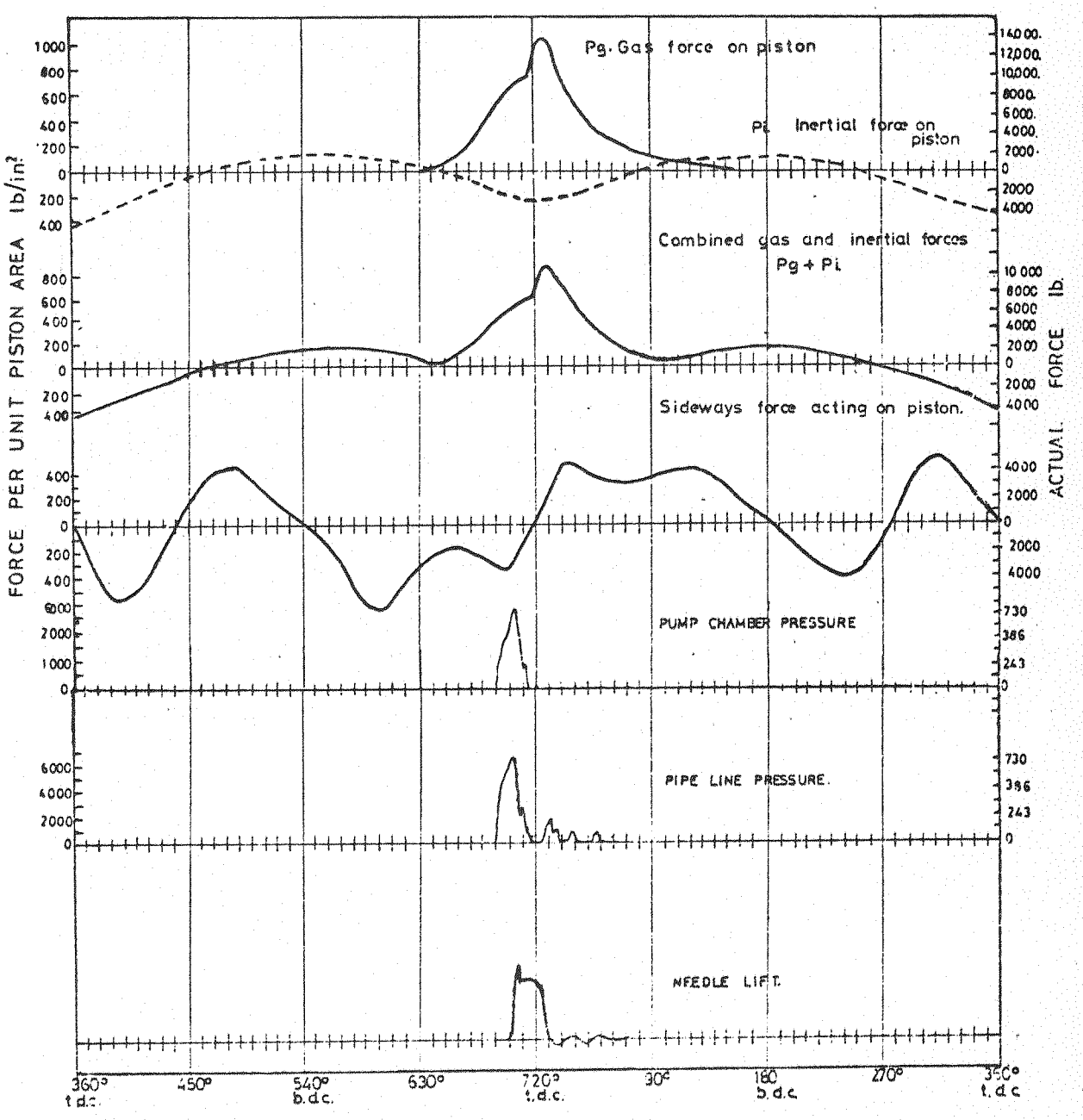

FIG 3·6 COMPARISON OF ENGINE AND INJECTION SYSTEM EXCITING FORCE DIAGRAMS.

The comparison of the main engine and injection system exciting force diagrams is illustrated in Figure 3.6. plotted on the basis of engine crank angle.

Since the engine system and the injection system are excited almost simultaneously, as illustrated in Figure 3.6., the precise identification of the generation of noise is almost impossible. A series of tests, however, can be devised to understand the problem to a reasonable extent. These are described below -

(1) The engine cannot be run with its own exciting forces only present (i.e. with the absence of injection system forces).

In the running engine, by the lead covering technique, it is possible to identify radiation of the injection pump noise. Here the pump noise emitted would be the result of all the exciting forces present in the engine. The exciting forces of the injection system, however, may be predominant.

(2) The injection system can be run on a fuel pump test rig and its vibration characteristics and noise determined. The mounting structure can be made non-responsive and it is possible to obtain accurately the radiation of pump noise.

(3) The injection system can be run on its own as fitted to the engine structure. In this instance the engine is stationary (non-running) and the pump is motored via its timing gear.

In this instance the lead covering technique enables the radiation of noise from the pump alone to be determined as well as the radiation from various engine surfaces excited by the injection system forces. It is also possible to remove the injectors and thus assess the contribution of the injector exciting forces. In this case, however, the vibration characteristics of the engine would not be wholly realistic since the damping characteristics of the engine structure existing in the running state cannot be reproduced.

(4) The engine can be motored with fully operational injection system. To avoid ignition a fuel resistant to ignition can be used. This test would give more reasonable representation of the engine structure condition as regards damping, oil temperature and its viscosity. There are, however, additional exciting forces being introduced, namely those responsible for the engine mechanically induced noise.

Based on these considerations various possible alternative test techniques are used for the investigations presented in the thesis. The fourth test technique however, has been omitted in this study.

3.3. Theoretical Assessment of Exciting Propensities of Hydraulic Pump Chamber Pressures

Approximation of the actual pump chamber pressure can be made by the sum of two saw-tooth waveforms as shown in Figure 3.7.

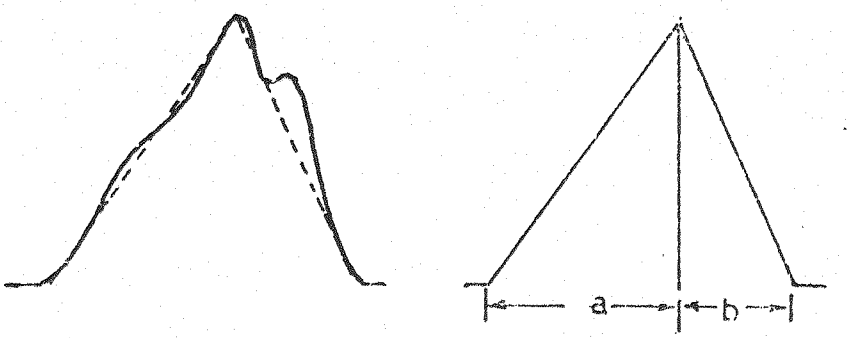

FIG. 3·7 TWO SAWTOOTH WAVE FORMS.

Starting from zero the pressure reaches a maximum at a certain rate of pressure rise in linear manner determined by (a). After reaching a maximum the pressure falls to zero, determined by (b).

$$P = P_o \left\{ \frac{t}{a}\, U(t) - (t-a)\left(\frac{1}{a}+\frac{1}{b}\right) U(t-a) + \frac{(t-(a+b))}{b}\, U(t-(a+b)) \right\} \quad \text{---- (1)}$$

For equation (1) occurring periodically, with period 2ℓ, we have

$$P = F(t) = \frac{A_o}{2} + \sum_{n=1}^{\infty} A_n \cos\left[\frac{n.\pi.t}{\ell}\right] + b_n \sin\left[\frac{n.\pi.t}{\ell}\right] \quad \text{---- (2)}$$

where $A_o = \frac{1}{\ell}\int_o^{2\ell} F.(t).dt$

$$A_n = \frac{1}{\ell}\int_o^{2\ell} F(t) \cos\left[\frac{N.\pi.t}{\ell}\right] dt.$$

$$B_n = \frac{1}{\ell}\int_o^{2\ell} F(t) \sin\left[\frac{n.\pi.t}{\ell}\right] dt$$

and $2\ell > (a + b)$

For A_n the results can be simplified

$$A_n = \frac{P_o}{\ell}\left\{\frac{1}{a}\int_0^{2\ell} t.\cos.\left[\frac{n\pi t}{\ell}\right].dt. - \left(\frac{1}{a}+\frac{1}{b}\right)\int_a^{2\ell}(t-a)\cos\left[\frac{n\pi t}{\ell}\right]dt + \frac{1}{b}\int_{a+b}^{2\ell}(t-[a+b])\cos\left[\frac{n\pi t}{\ell}\right]dt.\right.$$

$$\therefore\ A_n = \frac{P_o\ell}{n^2\pi}\left\{\frac{1}{b}\left(1-\cos\left[(a+b)\frac{n\pi}{\ell}\right]\right)-\left(\frac{1}{a}+\frac{1}{b}\right)\left(1-\cos\left[\frac{a.n\pi}{\ell}\right]\right)\right\}.$$

Similarly:

$$B_n = \frac{P_o}{\ell}\left\{\frac{1}{a}\int_0^{2\ell} t.\sin\left[\frac{n.\pi.t}{\ell}\right]dt - \left(\frac{1}{a}+\frac{1}{b}\right)\int_a^{2\ell}(t-a)\sin\left[\frac{n.\pi.t}{\ell}\right]dt + \frac{1}{b}\int_{a+b}^{2\ell}(t-[a+b])\sin\left[\frac{n\pi t}{\ell}\right]dt\right.$$

$$\therefore\ B_n = \frac{-P_o\ell}{n^2\pi^2}\left\{\frac{1}{b}\left[\sin\ (a+b)\frac{n\pi}{\ell}\right]-\left(\frac{1}{a}+\frac{1}{b}\right)\sin\ \frac{a.n\pi}{\ell}\right.$$

Amplitude of n^{th} harmonic is given by : $\sqrt{A_n + b_n}$

The amplitude of harmonics A_n and b_n can be determined directly from the equation or a computer program which has been developed by Anderton (3.1) for harmonic analysis of cylinder pressure development described in Appendix A. Using this derived program was found to be a faster method and important aspects of exciting propensities of hydraulic pressure pulse could be defined.

Figure 3.8. shows the spectra of an assumed symmetrical pressure pulse a = b = 15^o with the peak pressure of 415 bar. As can be seen up to 8th harmonic the level is constant whereas above this order the level of harmonics generally decay at a constant rate of 40 dB/decade. It shows the typical troughs of zero value starting at 500 Hz and its multiples.

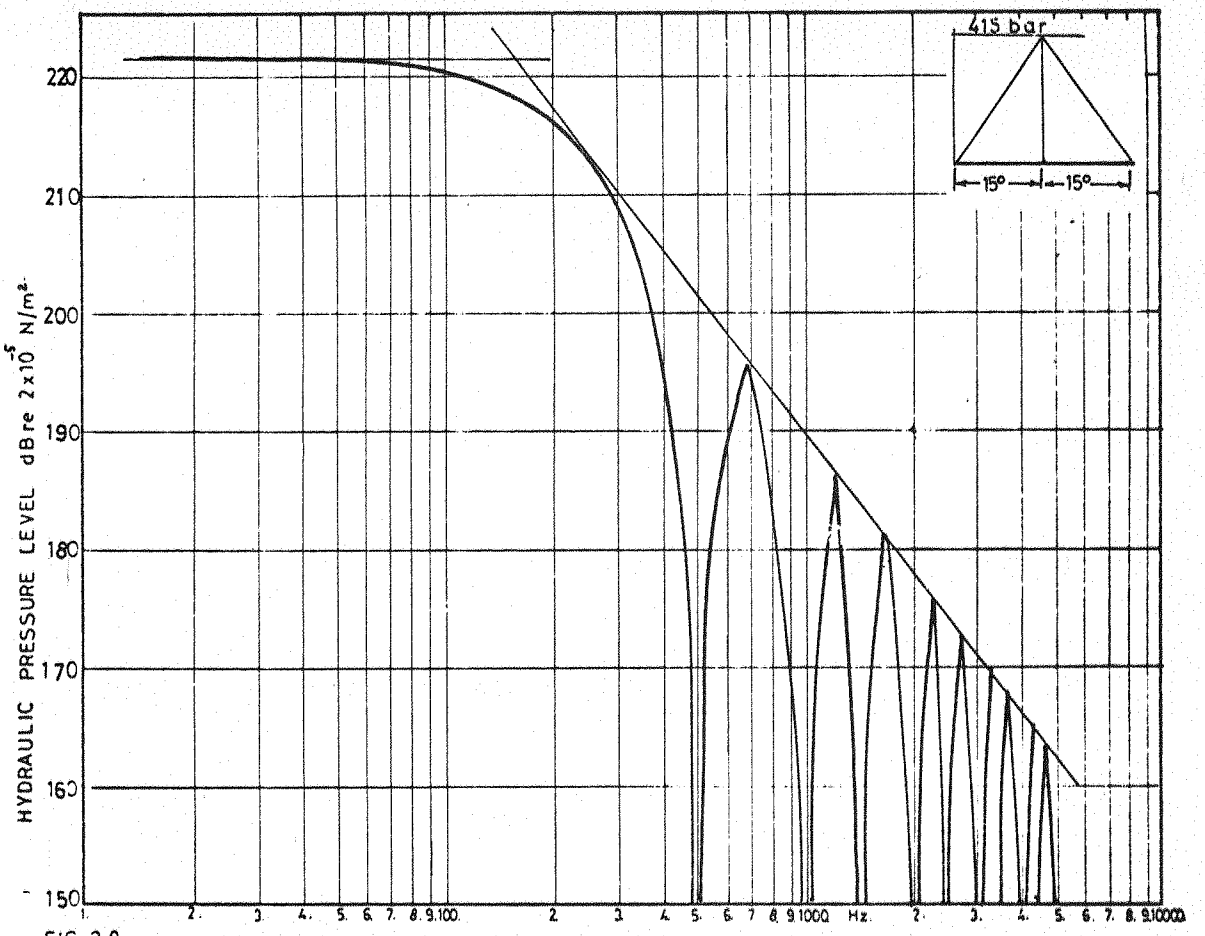

FIG. 3.8 SPECTRUM OF SYMETRICAL PRESSURE PULSE

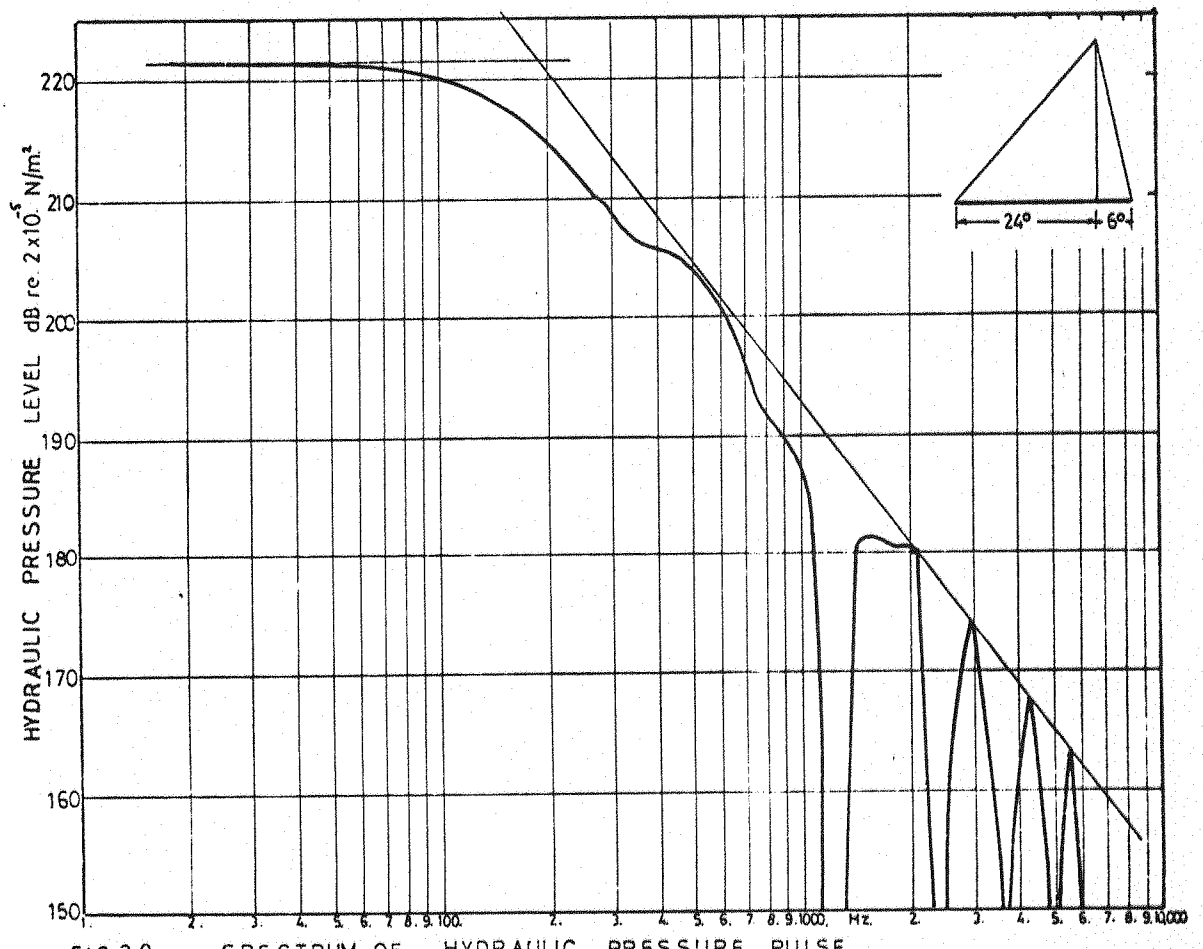

FIG. 3·9 SPECTRUM OF HYDRAULIC PRESSURE PULSE.

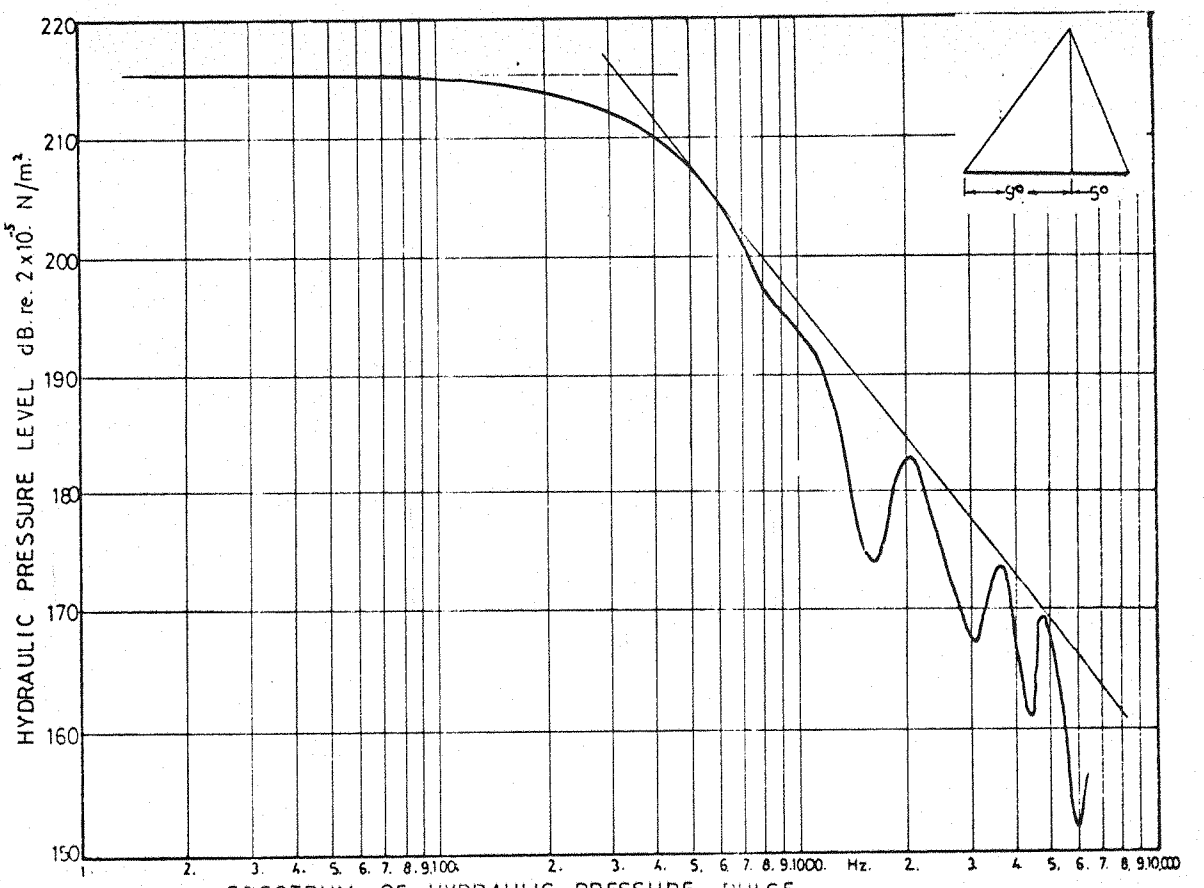

FIG. 3.10 SPECTRUM OF HYDRAULIC PRESSURE PULSE.

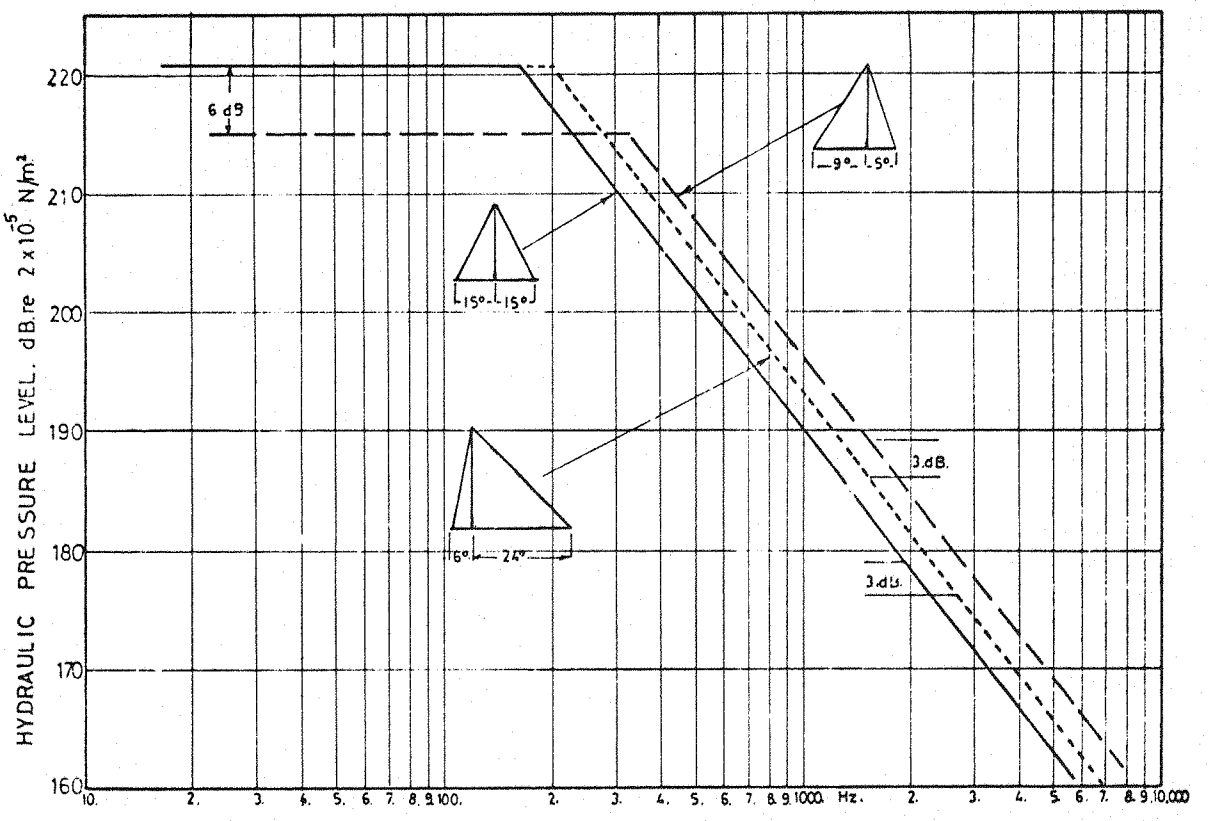

FIG. 3.11 CAMPARISON OF GENARAL OUTLINE OF PRESSURE PULSE SPECTRA

Figure 3.9 shows a hydraulic pulse of the same total duration of 30^{o} but with the rise time a = 24^{o} and fall time b = 6^{o}. The results are similar but there are significant changes in the spectrum. The level of low frequency harmonics are exactly the same as for the symmetrical pulse and harmonic decay at the same rate 40 dB/decade. The typical troughs are clearly defined but are more widely separated. The separation of troughs has increased from 600 to 1300 Hz.

Figure 3.10 shows the spectrum of a shorter pulse of total duration of 14^{o} with rise time of a = 9^{o} and fall time of b = 5^{o}. The total duration of the pulse in this instance is not a divisor of π. As can be seen the shape of the spectrum is similar with the typical decay of harmonics by 40 dB/decade. The typical troughs, however, do not reach the low values as in the previous cases and the broad peaks tend to be unsymmetrical.

Figure 3.11 shows the comparison of general outline of the spectra pressure pulses considered in Figures 3.8, 3.9 and 3.10, and the effects of various characteristics of pressure pulses.

These can be listed as follows:

(a) For a given amplitude of pressure pulse the magnitude of low frequency harmonics decreases with decrease of the width of the pulse, whilst the high frequency components (range of 40 dB slope) increases in magnitude.

(b) Asymmetry for a given amplitude and width of the pulse does not affect the low frequency components, but increases the magnitude of high frequency harmonics.

(c) The marked effect of the troughs occurs only when the pulse width is integer divisor of π. Otherwise the troughs and peaks are less marked and become of unsymmetrical shape.

The expected spectrum shapes can be devised from a simplified waveform as shown in Figure 3.12. In this waveform the amplitudes of harmonics are of a considerably simpler form.

$$A_K = \frac{2N}{\pi\,(N^2 - K^2)} \cos Ka$$

where $N = \frac{\pi}{2a}$

K = Harmonic number

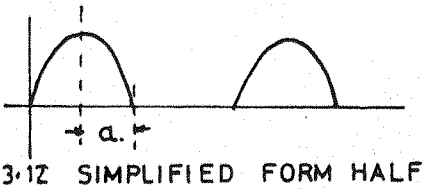

FIG 3·12 SIMPLIFIED FORM HALF SINE WAVE.

If the pulse half width is an integral divisor of $\pi/2$ then the cos Ka term becomes zero. If not then there will be no marked troughs in the spectrum, and the density of the harmonics causing excitation will be greater. Table I gives relevant details of the expected shape of the spectrum for various pulse widths (a. deg's) harmonic at which the spectrum begins to turn into a 40 dB/decade slope (K_t) and the corresponding frequency values for various pump speeds.

TABLE I

Pulse half width (a. deg)	A. in rad's	$N = \frac{\pi}{2a}$		K_t Harmonic at which spectrum turns ($N^2 = K^2$)	Frequencies at which spectrum turns for various engine speeds			
					1250	1000	750	500
1	0.01745	90.01	No zero	90	1872	1500	1125	750
2	0.0349	45.00		45	936	750	563	375
4	0.0698	22.50	No zero	22	458	367	275	183
6	0.1047	15.00		15	312	250	188	125
8	0.1396	11.252	No zero	11	229	183	138	92
10	0.1745	9.000		9	187	150	113	75
14	0.2443	6.429	No zero	6	125	100	75	50
15	0.2618	6.000		6	125	100	75	50
30	0.5236	3.000		3	63	50	38	25
60	2.0472	1.500	No zero	2	42	33	25	17
120	2.0944	0.750	No zero	1	21	17	13	8

From this analysis it is clear that the detailed form of the chamber pressure pulse has a considerable effect on the exact shape of the frequency analysis spectrum. The very narrow pulse width in comparison to a cylinder pressure development extends over the low frequency range in which high harmonic levels occur, and thus the frequency at which harmonic amplitudes start their rapid fall.

3.4. Experimental Assessment of Exciting Propensities of Pump Chamber and Pipe Line Pressure and their Relation with Emitted Noise

To assess the exciting propensities of the hydraulic forces acting on the plunger, it is necessary to measure pressure development

* The natural frequency of the Kistler 601A pressure transducer is very high, of the order of 130 KHz. First order calculations show that added plunger mass of 8 grammes reduces the natural frequency to about 22 KHz, which is adequate for measurements over the frequency range under consideration. Other techniques which employ passages in pressure measurement were not considered because the effect of lowering natural frequency is greater.

in the pump chamber. This presents considerable difficulties since pressure transducers of extremely small diameter (about 2 mm) were not commercially available.

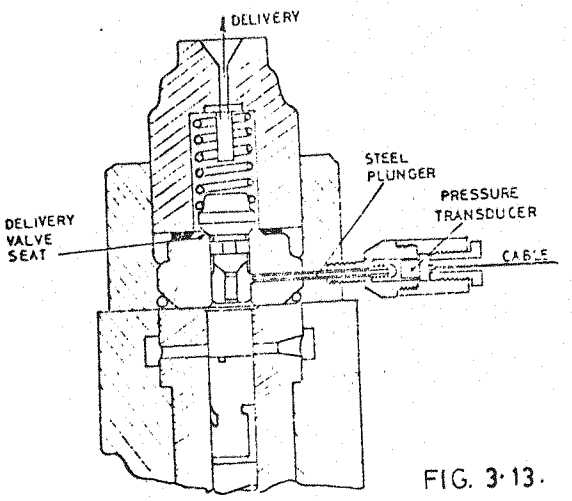

FIG. 3·13.

It was, however, decided to explore the shape of the pump chamber pressure diagram by using a Kistler 601A pressure transducer fitted to a special adaptor. By use of a plunger of 3 mm diameter, lapped in a drilled hole through the delivery valve holder, the hydraulic force acting on the end of the plunger can be transmitted to the diaphragm of the pressure transducer as shown in Figure 3.13.

This system of measuring has certain disadvantages since it is inevitable that some leakage of high pressure fuel will occur through the clearance between plunger spindle and lapped hole. This leakage was minimised to some degree by machining circular grooves in the plunger spindle. It was found, however, at low pump speeds, that leakage affected the peak pressures to some degree.*

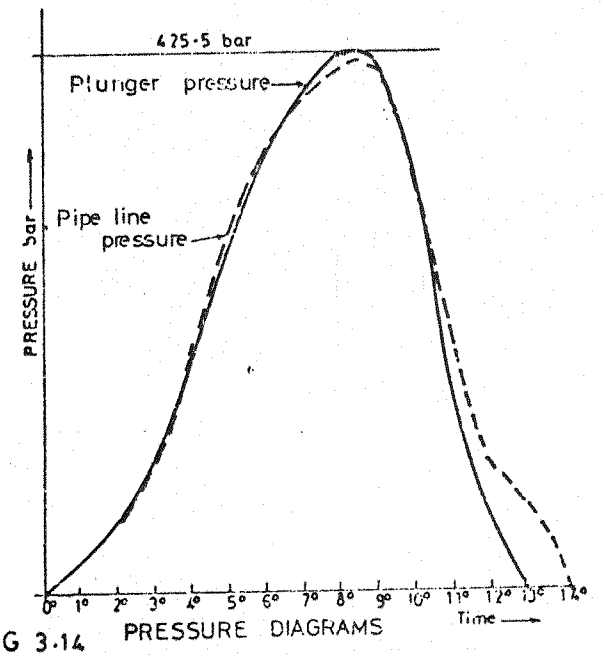

FIG 3·14 PRESSURE DIAGRAMS

At the rated speed condition the pressure changes in the pump were unaffected by the presence of the transducer system. Figure 3.14 shows the comparison of the pressure diagram in the pump chamber and in the high pressure pipe line a few inches above the delivery valve outlet. As can be seen there is only slight difference between the pipe line and plunger pressure diagrams.

Analysis of the waveform above and below the delivery valve

were checked and the differences in the spectrum obtained were insignificant, which is supported by the theoretical analysis described in Section 3. Because of this, and so as not to introduce any changes in the pump operation, the pressure diagram in the pipe lines during the period of injection was taken as the pump chamber pressure diagram.

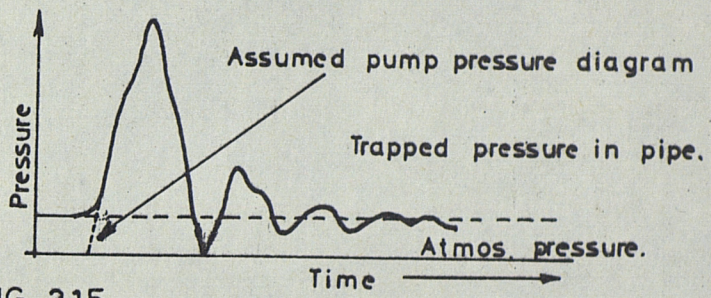

FIG. 3.15

The diagram (Figure 3.15) thus is corrected by removing the effect of residual pressure and the secondary pressure oscillations after the injection.

In this instance direct analysis by electronic wave analyser cannot be carried out on the waveform and all data therefore were obtained from harmonic analysis using a computer program developed by Anderton (3.1). Details of the program are given in Appendix A.

Three pumps were chosen to assess the exciting propensities of the pump chamber pressures :

(1) Six in-line (approximately 1 litre/cyl. engine capacity)

(2) Ten in-line (approximately 1.6 litre/cyl. engine capacity)

(3) Twin 5 in-line (approximately 1.4 litre/cyl. engine capacity)

Photographs of the pumps are shown in Figure 3.16.

3.4.1. In-line six injection pump force and noise.

Figure 3.17 shows the pump chamber pressure diagrams and their respective spectra for a 6 in-line pump at full load condition over the speed range from 500 to 1400 rev/min (engine speed 1000-2800 rev/min).

TWIN. 5. IN-LINE.

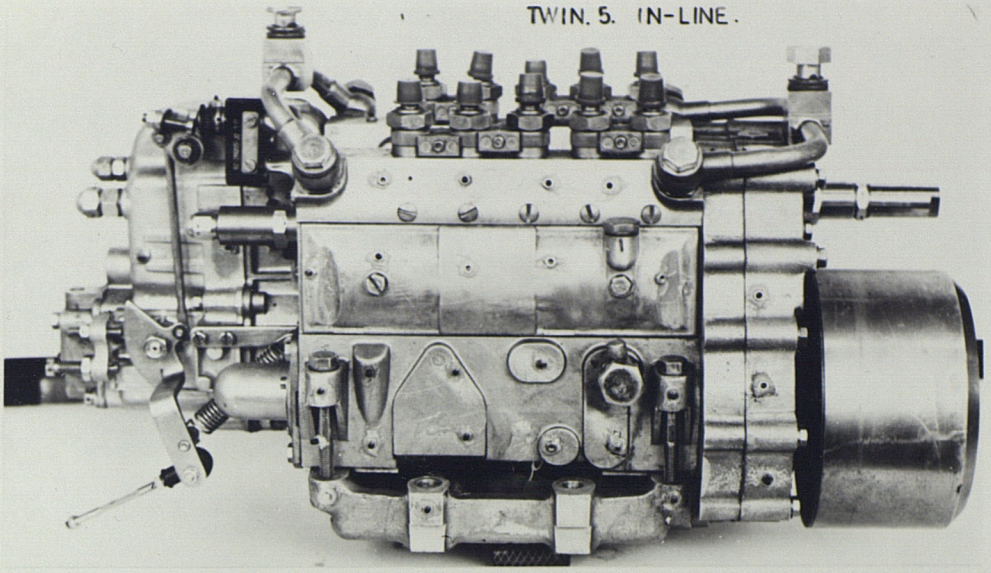

6. IN-LINE.

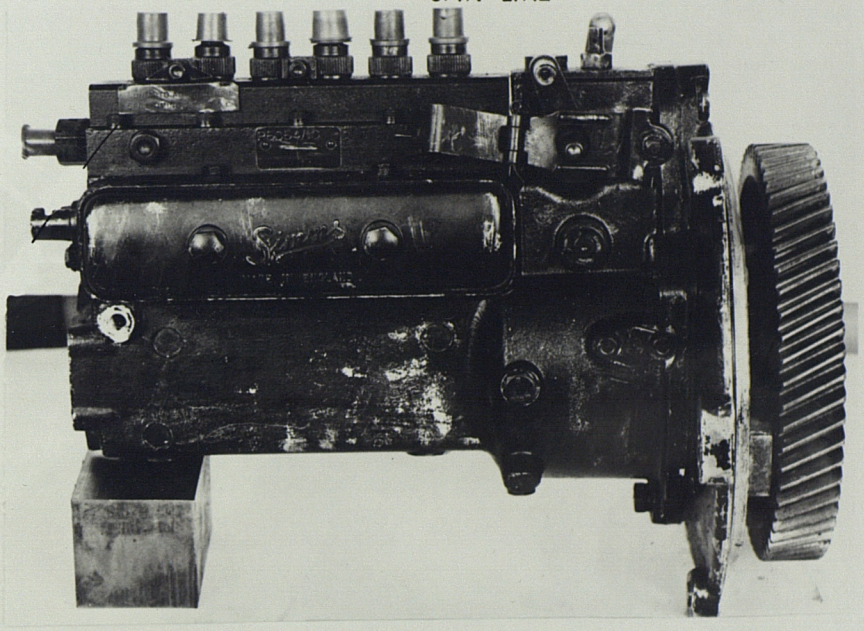

10. IN-LINE.

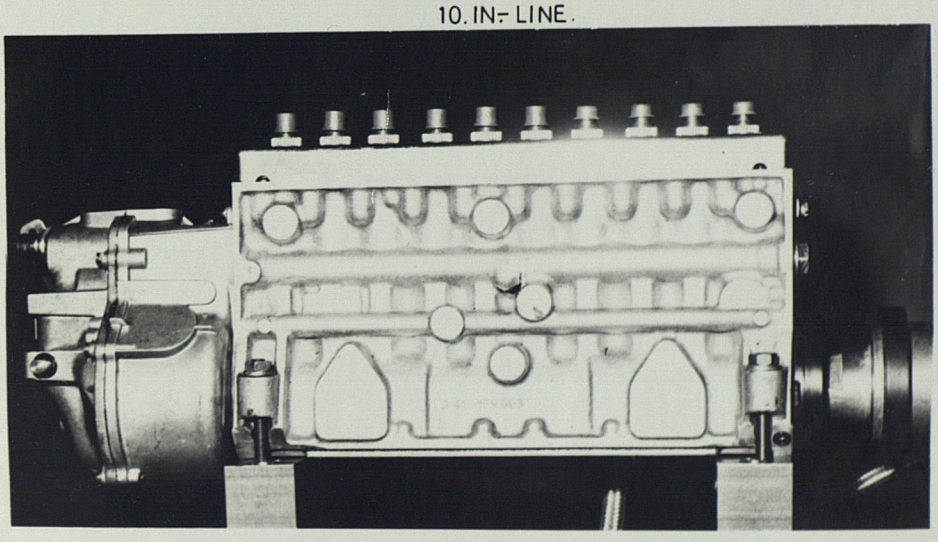

FIG. 3·16. FUEL INJECTION PUMPS.

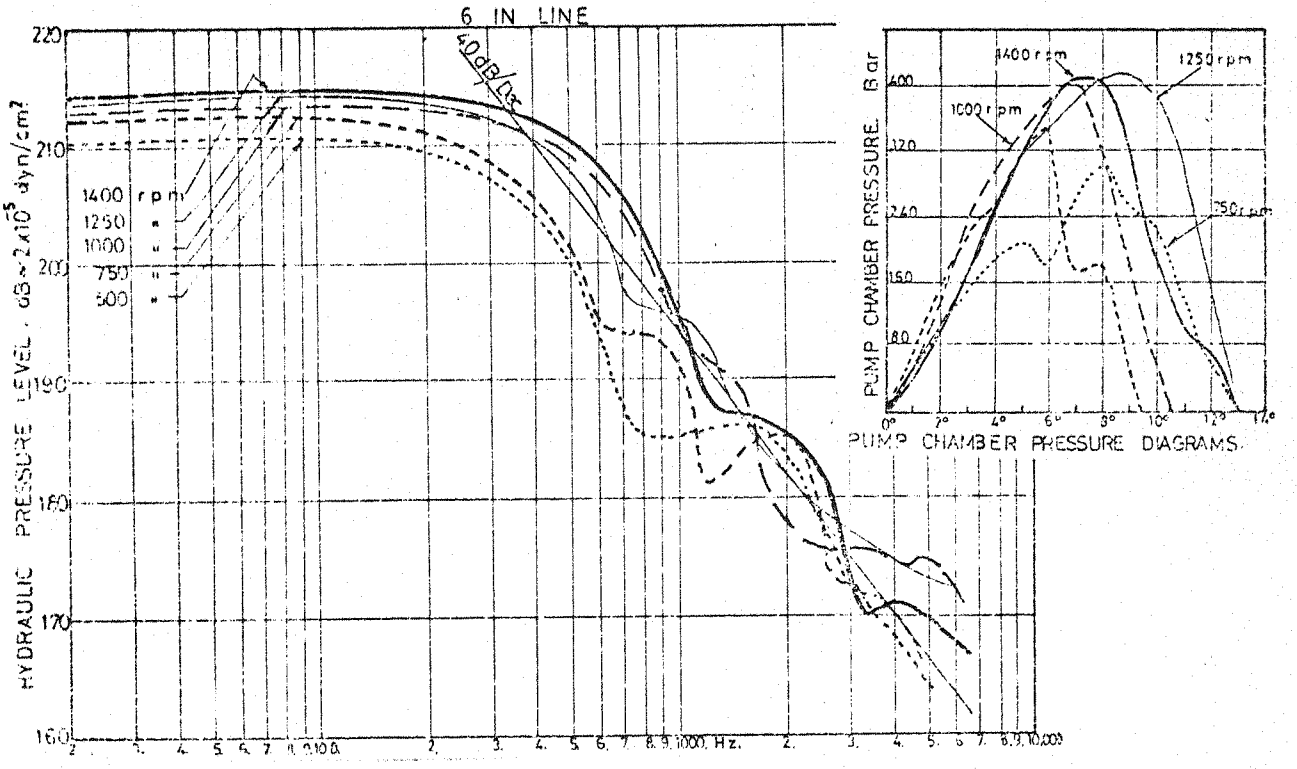

FIG 3·17 EFFECT OF SPEED ON PUMP CHAMBER PRESSURE.

It can be seen that there is a rapid increase of peak pressure from 500 rev/min (310 bar) up to 1000 rev/min (400 bar). Above 1000 rev/min up to 1400 rev/min there is only a slight increase of peak pressure reaching the valve of 420 bar.

The variation of injection duration, however, changes in an irregular manner. At 500 rev/min the duration of injection is 13°, this reduces to a duration of 9.5° at 750 rev/min. Above this speed the duration of injection gradually increases again from 10.5° at 1000 rev/min to 13° at 1250 rev/min and above. It is possible that these discrepancies are due to effects of pressure waves from the high pressure pipe line system influencing the pump chamber pressure.

As can be seen these irregular changes in pressure diagram characteristics with speed are clearly reflected in the corresponding chamber pressure spectra. There are, however, significant trends which can be clearly observed in the low frequency range (flat part of spectrum). It can be seen that there is a general increase in the level of the harmonics by about 5 dB over the speed range which can be accounted to increase of peak pressure and also to some extent to the injection duration.

The high frequency part of the spectra, i.e. the 40 dB slope range clearly shows the broad troughs and peaks as discussed in Section 3.1.

If the pump chamber pressure spectra (Figure 3.17) are compared now with the emitted noise of the pump (Figure 3.18) over the speed range from 500 rev/min to 1400 rev/min it would be seen that the maximum increase of noise (15 dB) of the pump occurs in the frequency range between 500 Hz and 800 Hz. Over the lower frequency range below 500 Hz the increase in noise is only some 6 dB which, as can be seen, corresponds with the relevant increases in pump chamber pressure spectra.

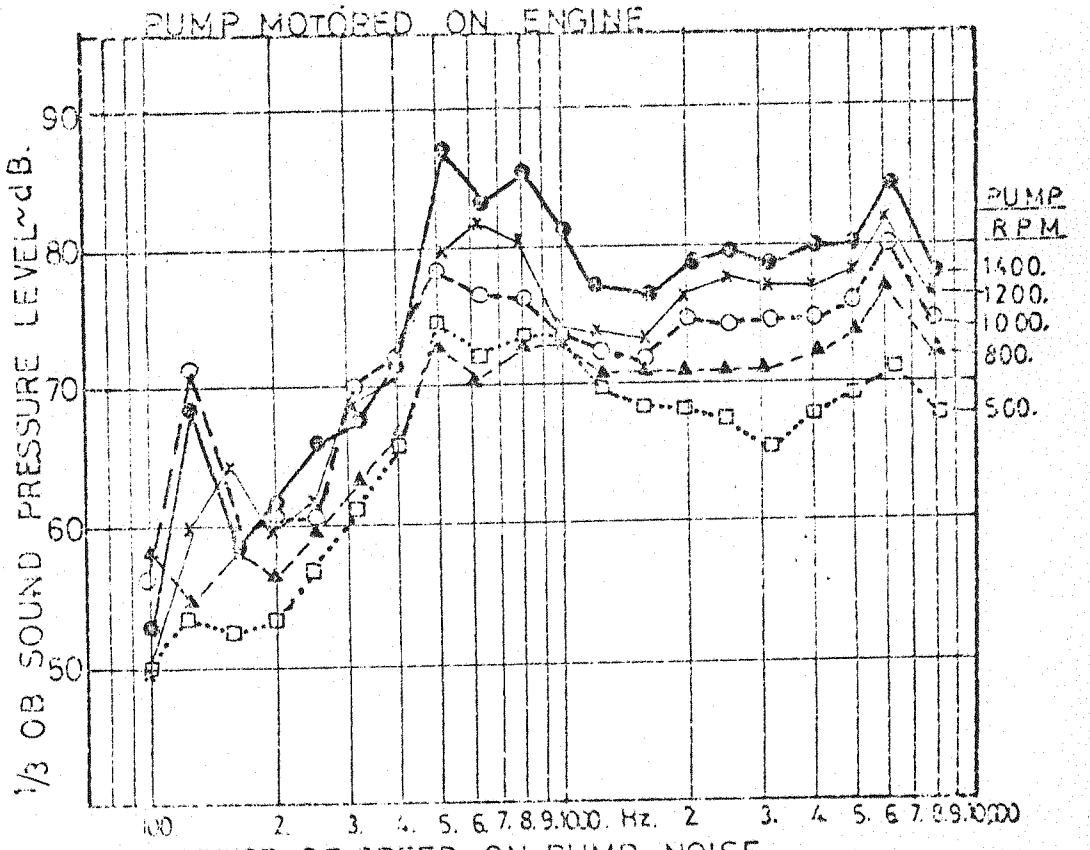

FIG. 3·18 EFFECT OF SPEED ON PUMP NOISE.
ENGINE LEAD COVERED. PUMP EXPOSED.

From 1000 Hz to 2000 Hz the increase is smaller which is also reflected in the pressure spectra. Above 2000 Hz the relationship between noise and pump chamber pressure spectra does not correlate.

Figure 3.19 shows plots for various one-third octave band frequencies between pump chamber pressure level and noise level for 400 Hz, 500 Hz, 630 Hz and 800 Hz, respectively. The relationship is reasonably close to the 45^{o} slope which confirms that in this frequency region the exciting force in the pump chamber controls the noise of the pump.

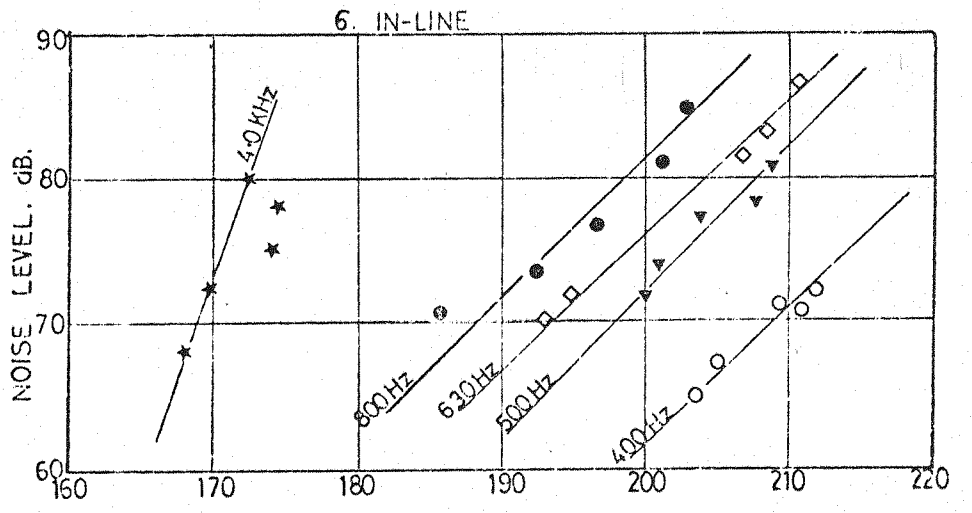

FIG. 3·19. PUMP CHAMBER PRESSURE LEVEL. dB.

As regards the high frequency region of the pump, namely from 1000 Hz to 2000 Hz, there is significant increase of pump noise with speed amounting to some 14 dB. There are no significant increases however, in level of pump chamber pressure as shown in Figure 3.17. A plot, shown in Figure 3.19 at the one-third octave band of 4000 Hz of chamber pressure versus noise level, clearly indicates a large increase of pump noise but with negligible increase in pump chamber pressure level. This suggests that other exciting forces should be responsible for the increase of high frequency noise and therefore it was decided to consider the possibility of pipe line pressure development being the cause of the high frequency noise.

Analyses of the pipe line pressure over the speed range 500, 750, 1000, 1250 and 1400 rev/min respectively, were carried out using a Muirhead Pametrada wave analyser and the spectra are shown in Figure 3.20. The pipe line pressure diagrams are shown in Figure 3.21. It can be seen that the pipe line pressure levels in the high frequency region also increase markedly with increase in pump speed.

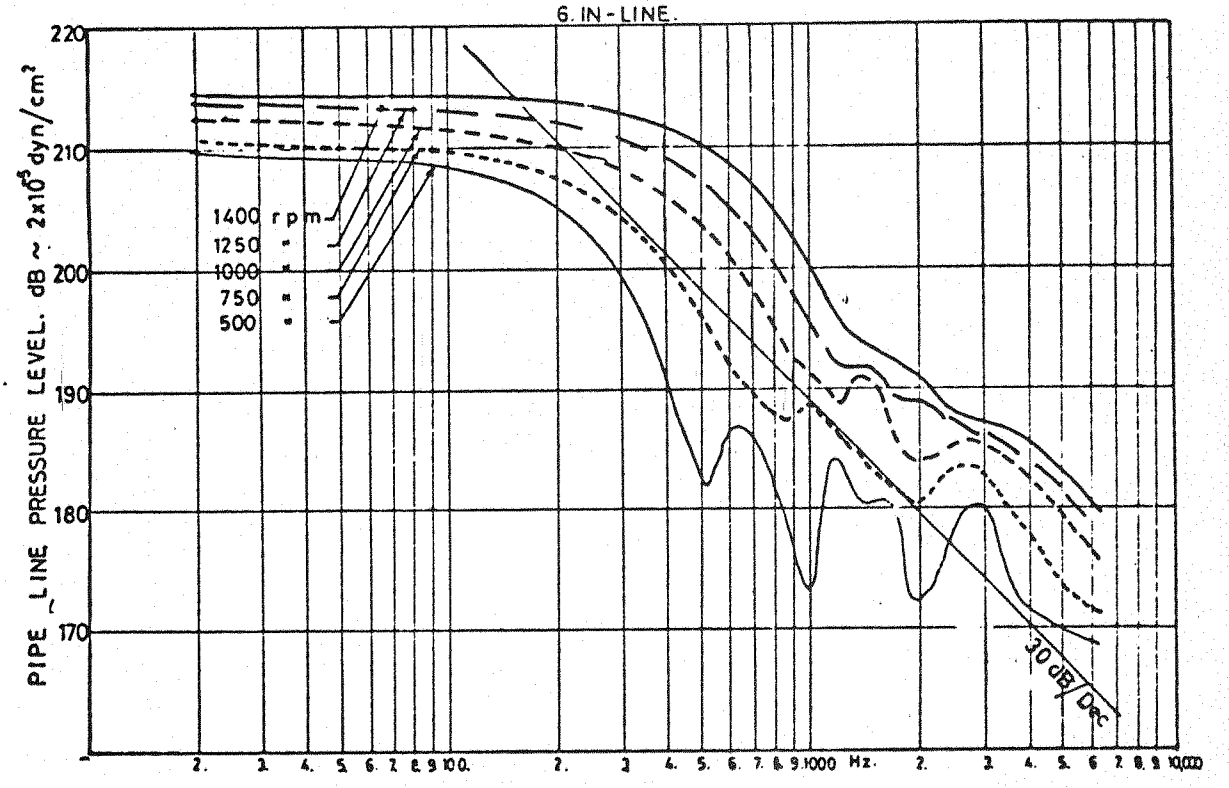

FIG. 3·20. EFFECT OF SPEED ON PIPE LINE PRESSURE SPECTRA.

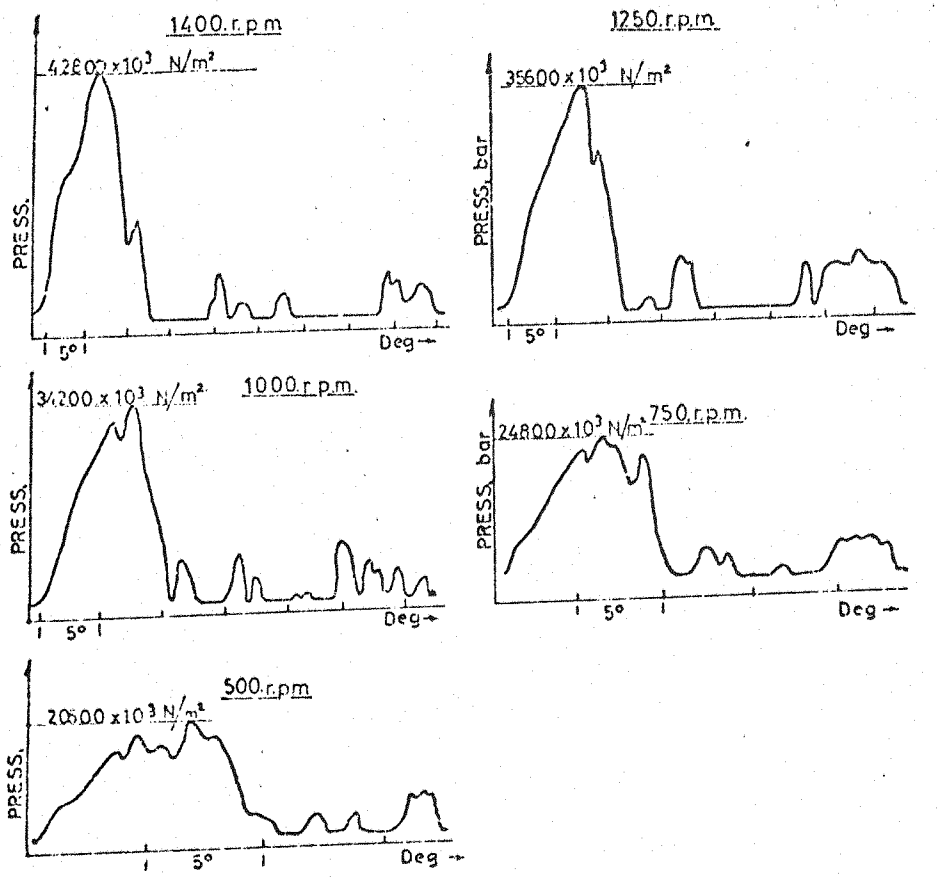

FIG. 3·21. PIPE LINE PRESSURE DIAGRAMS.

The pipe line pressure spectra are similar to those of the pump chamber pressure spectra in the low frequency range (flat part of spectra) but the levels in the high frequency range are considerably greater. Figure 3.22 compares the pipe line pressure spectrum with the pump chamber pressure spectrum at the maximum rated speed of 1400 rev/min. This clearly shows that above 1000 Hz the pipe line pressure levels are progressively greater than the pump chamber pressure levels by some 5 to 15 dB. It is also of interest to note that the slope of the higher frequency components in the pipe line pressure spectrum are about 30 dB/decade as compared to the 40 dB/decade slope for pump chamber pressure spectrum.

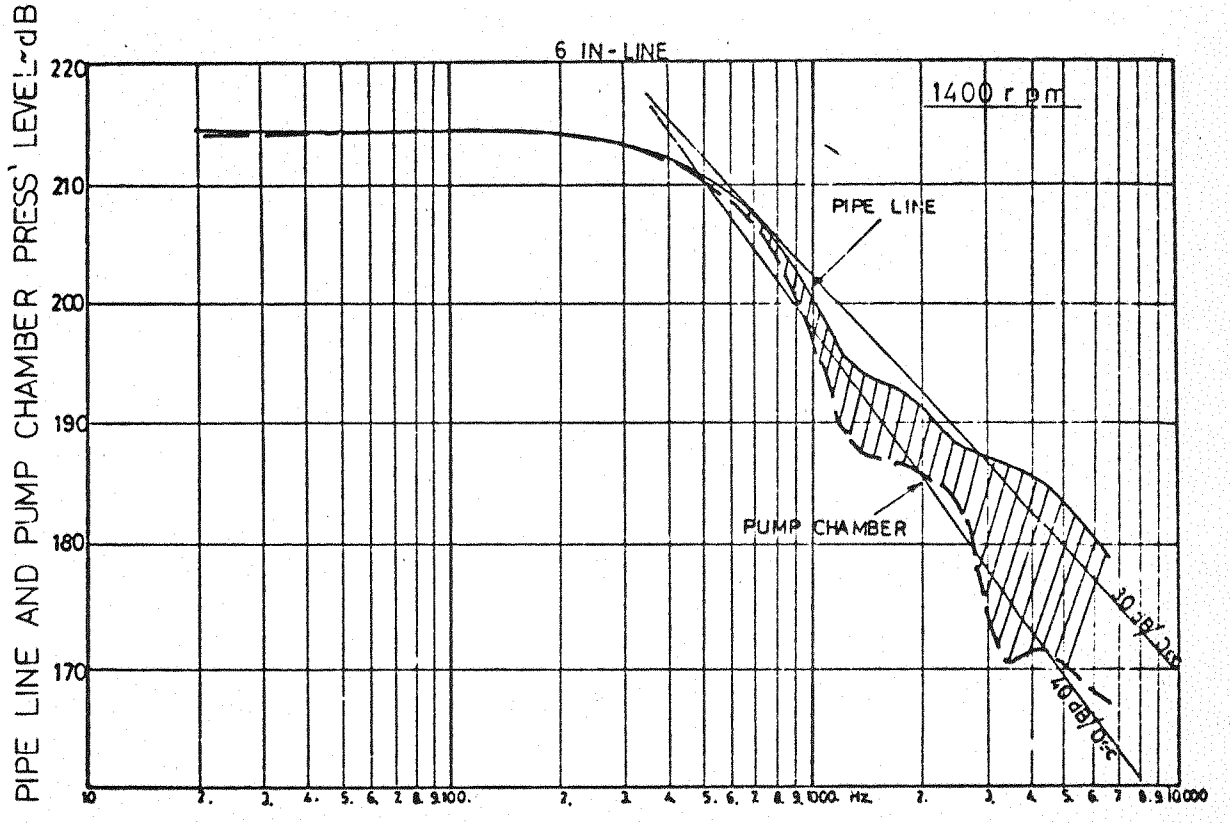

FIG. 3·22. COMPARISON PUMP CHAMBER AND PIPE LINE PRESSURE SPECTRA.

Figure 3.23 shows the relation between noise and pipe line pressure levels at various frequencies which illustrate that 45° slope corresponds with reasonable accuracy in the higher frequency region of the pump noise from 2000 Hz upwards.

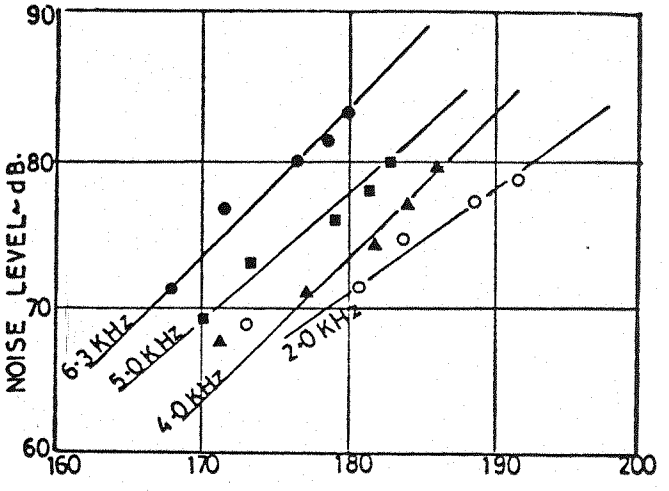

FIG 3·23 PIPE LINE PRESS LEVEL~ dB

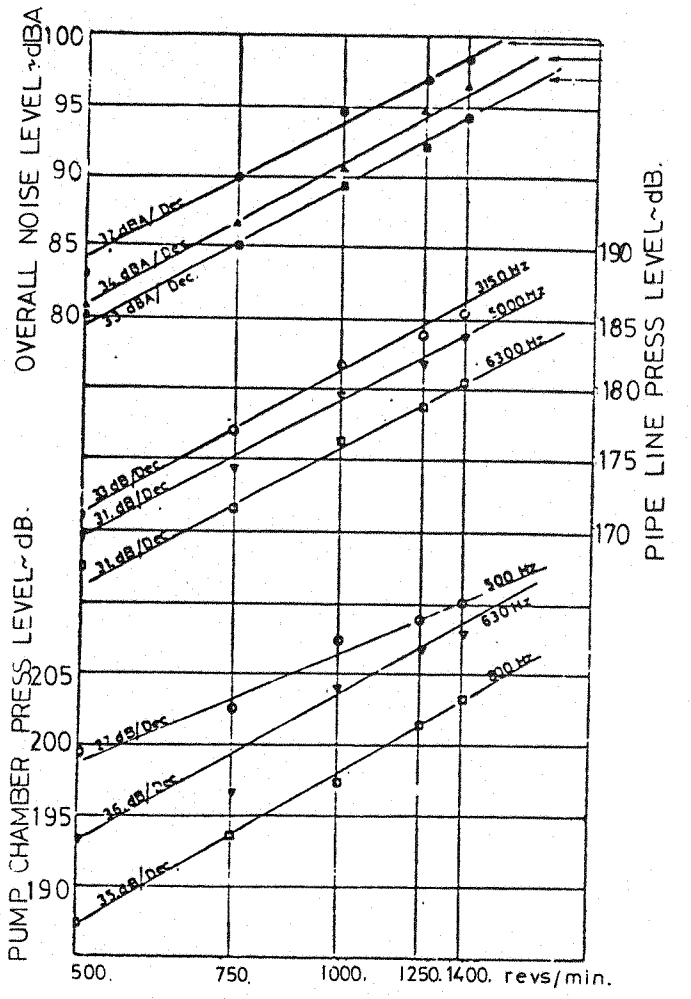

FIG 3·24 INCREASE OF NOISE WITH SPEED.

The noise in the remaining frequency range between 1000 Hz and 2000 Hz (i.e. dip in the noise spectra) is definitely not controlled by pipe line pressure. Despite the fact that correlation with pump chamber pressure is not very precise, it can be assumed that pump chamber pressure here is the major controlling factor.

The overall (dB(A)) increase of noise with speed and the increase of level of pump chamber and pipe line pressure in various frequency regions are shown in Figure 3.24.

As can be seen the slopes of pipe line pressure levels with speed vary between 31 and 33 dB/decade in the high frequency regions of 3150, 5000 and 6300 Hz. Similarly the slopes of the pump chamber pressure levels vary between 27 and 35 dB/ decade in the low frequency region of 500, 630 and 800 Hz. The increase of pump noise (overall dB(A)) at various test conditions, i.e. motored on the I.S.V.R. quiet rig, base mounted and flange mounted on the

engine, show the range between 32-34 dB(A)/decade.

This can be considered as reasonable correlation regarding the origin of the pump noise which is therefore mainly controlled by hydraulic pressure characteristics, i.e. both pump chamber and pipe line pressure.

3.4.2. In-line Ten fuel injection pump force and noise

The pump chamber pressure spectra and pressure diagrams (superimposed) for the 10 in-line fuel injection pump are shown in Figure 3.25 for pump speeds of 500, 750, 1000 and 1250 rev/min It can be seen that there are significant changes in peak pressures ranging from 300 bar at 500 rev/min to 500 bar at 1250 rev/min. Duration of fuel injection also changes with speed, i.e. 9^{o} at 500 rev/min, 12^{o} at 750 and 1000 rev/min, and 13^{o} at 1250 rev/min. The rates of pressure rise and fall are more or less the same.

Because of the general increase of peak pressure and injection duration with speed, the low frequency harmonics have been increased by a greater amount (8 dB) than in the previous example.

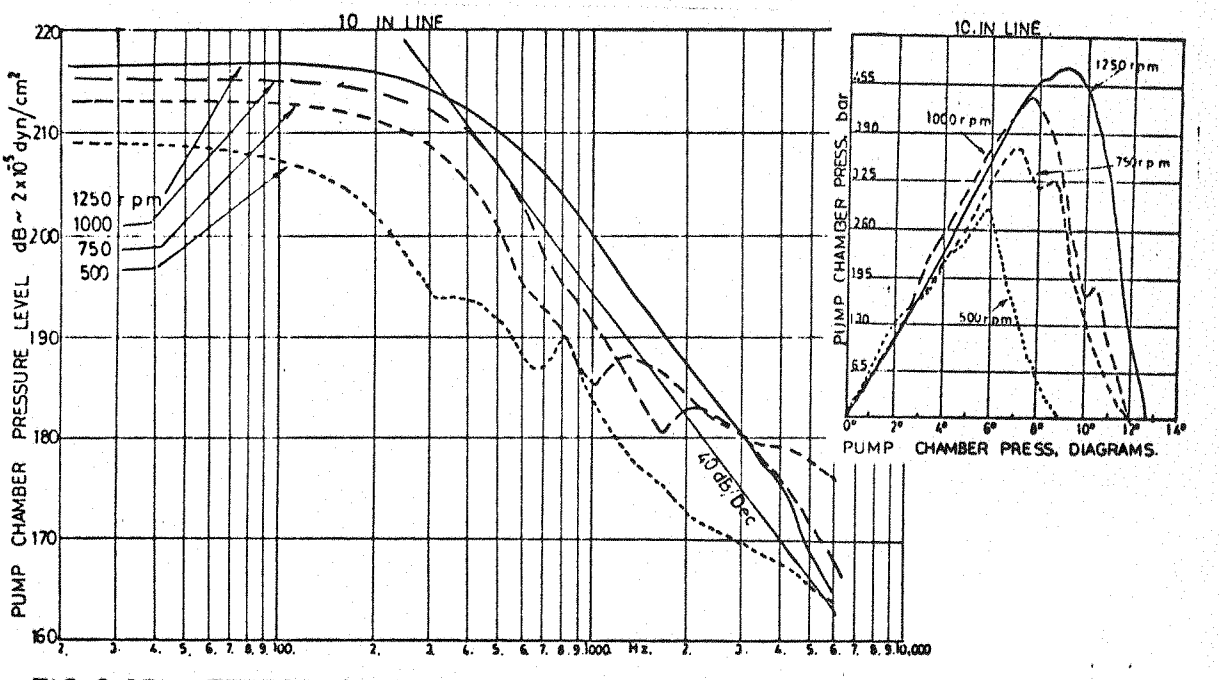

FIG. 3·25. EFFECT OF SPEED ON PUMP CHAMBER PRESSURE.

Over the middle frequency range from 400 Hz to 800 Hz, the pressure levels due to speed, tend to decrease with increase in frequency. This trend tends to be reflected in the pump noise spectra shown in Figure 3.26.

At high frequencies, i.e. 40 dB slope range, the pressure spectra appear to be influenced by the peaks and troughs shown in the pressure diagrams.

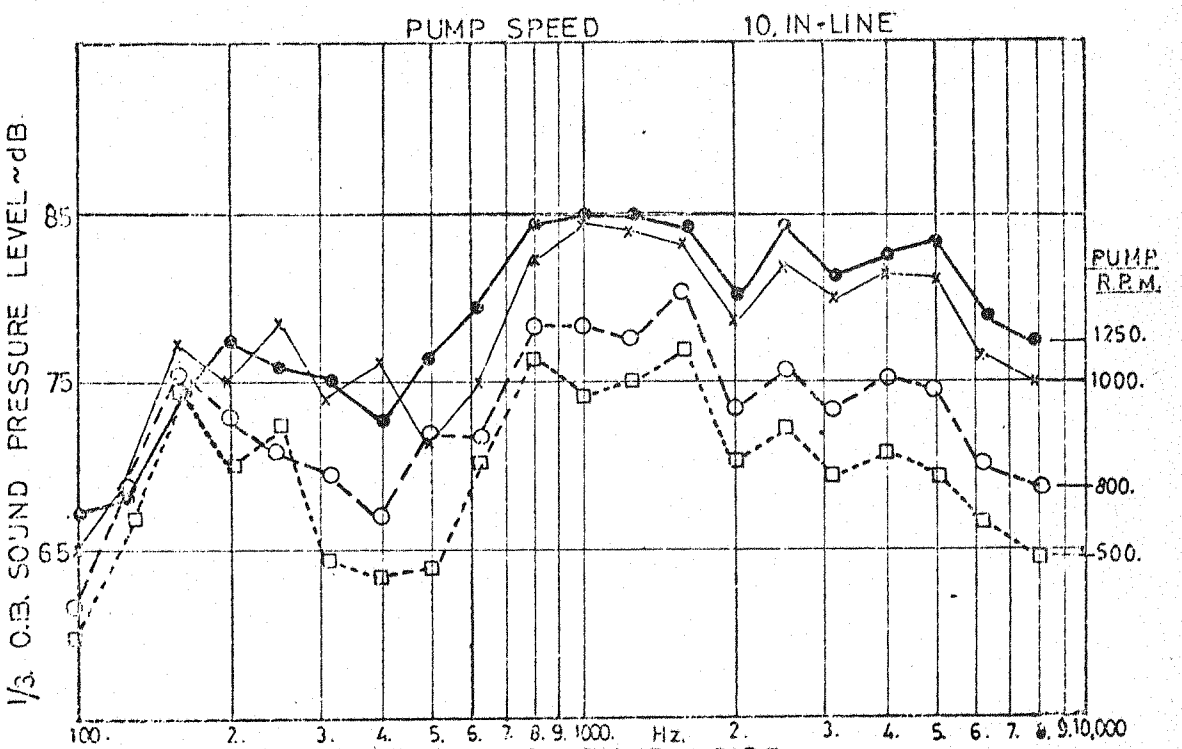

FIG. 3·26 EFFECT OF SPEED ON PUMP NOISE.

As with the 6 in-line pump, if the pump chamber pressures spectra are compared with the emitted noise of the pump over the speed range from 500 rev/min to 1250 rev/min, it would be seen that the maximum increase of noise (13 dB) of the pump occurs in the frequency range between 400 Hz and 800 Hz.

From 1000 Hz and above the relationship between noise and pump chamber pressure spectra are difficult to correlate. Figure 3.27 shows plots of various one-third octave band frequencies between pump chamber pressure level and noise level at 400, 500, 630 and 800 Hz respectively.

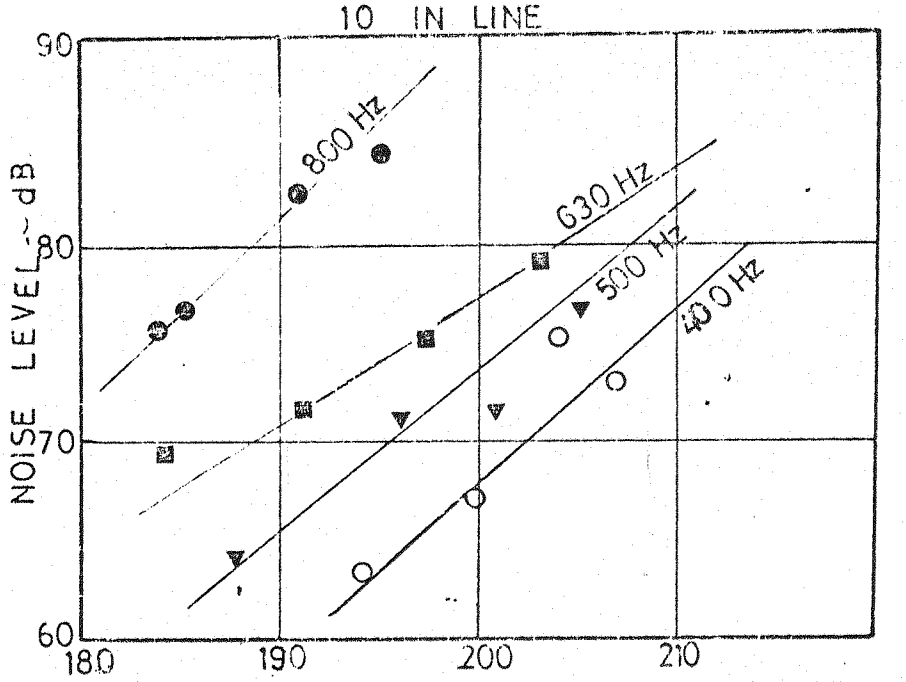

FIG. 3·27. PUMP CHAMBER PRESS LEVEL ~ dB.

This relationship is also reasonably close to the 45° slope which confirms that in this frequency region the exciting force generation in the pump chamber controls the noise of this pump.

3.4.3. In-line twin-five injection pump forces and noise

The pump chamber pressure diagrams of the twin 5 in-line fuel pump are less regular with far more pressure wave effects as shown in Figure 3.28. The peak pressures increase significantly with speed, i.e. 216 bar at 500 rev/min to 413 bar at 1250 rev/min and the durations over which peak pressures occur are very dissimilar. Fuel injection duration is from 12° at 500 rev/min to 14° at 1250 rev/min. With regard to rates of pressure rise and fall it appears that these are controlled to some extent by the severe peaks and troughs. Again it can be seen that these irregular changes in pump chamber pressure characteristics with speed are clearly reflected in the corresponding pump chamber pressure spectra (Figure 3.28) with particular reference over the high frequency range above 1000 Hz.

Over the lower frequency range, i.e. flat part of spectra there is a general increase of some 7 dB in level of harmonics, with increase of speed. Comparing the pump pressure spectra with the

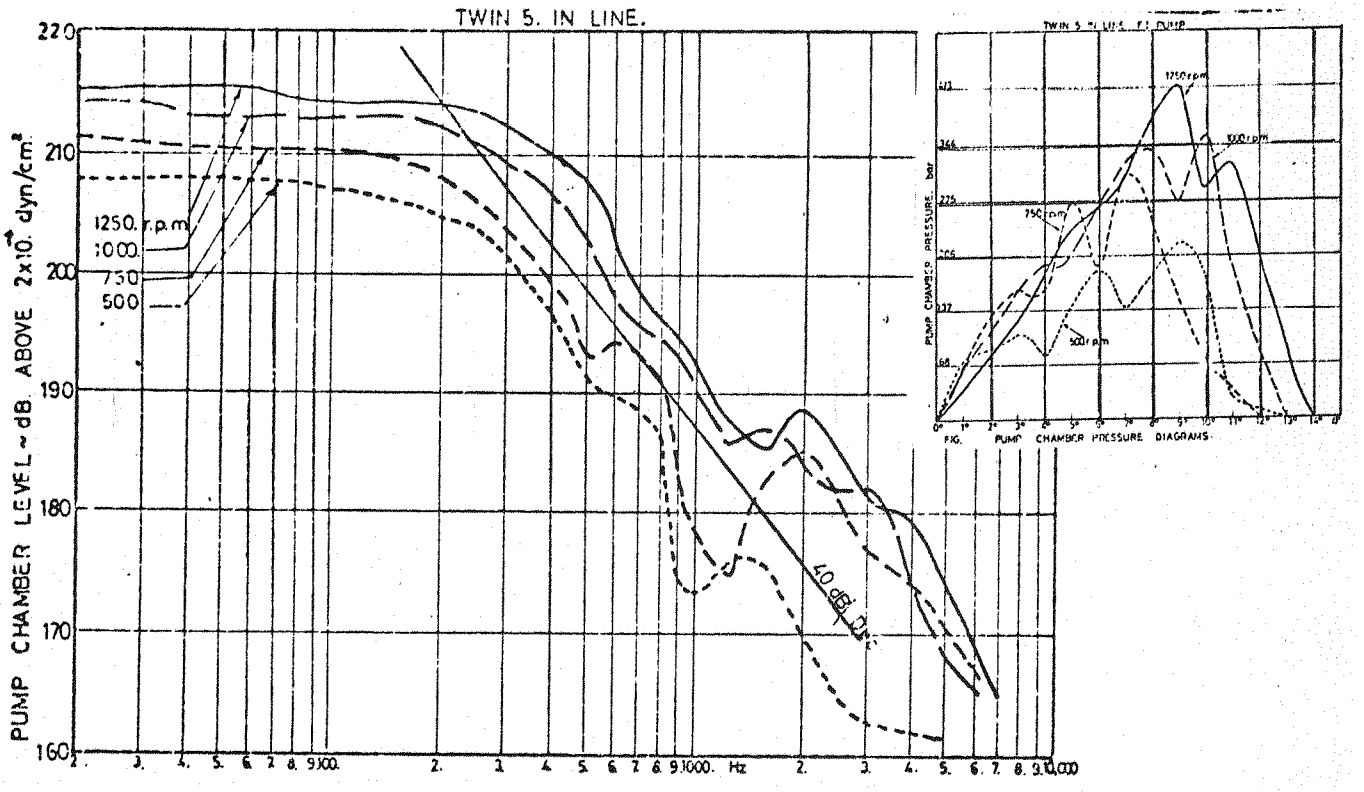

FIG 3·28. EFFECT ON PUMP CHAMBER PRESSURE SPECTRA WITH SPEED.

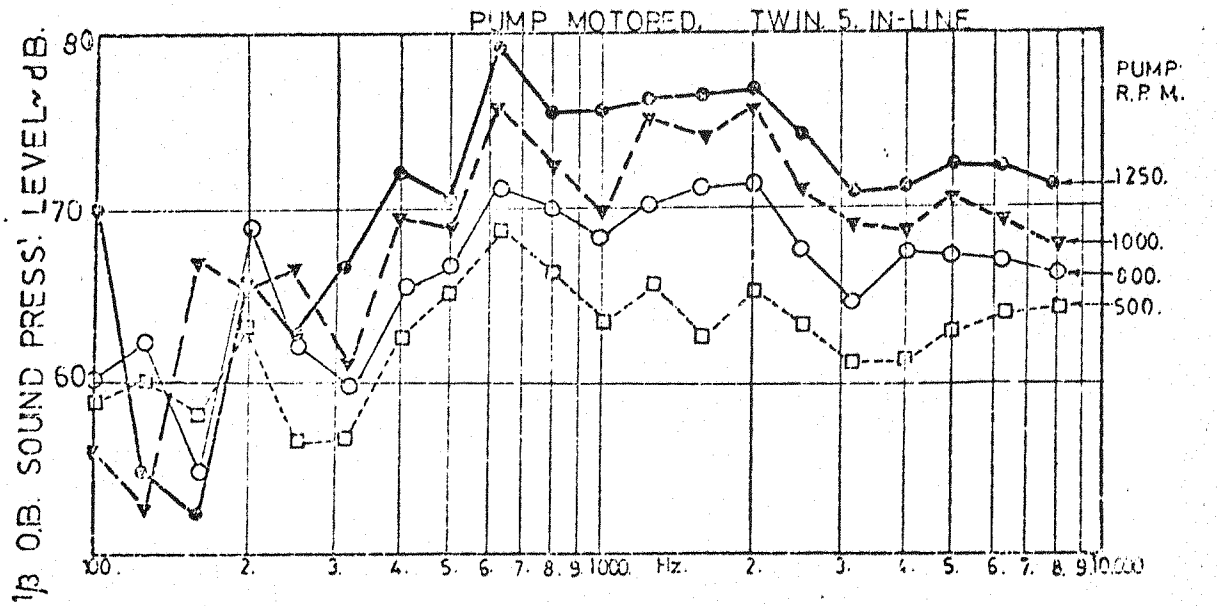

FIG 3·29. EFFECT OF SPEED ON PUMP NOISE.

emitted noise of the pump (Figure 3.29) it can be seen that the increase of noise from the pump with increase of speed is significant over the middle frequency range from 600 Hz to 2000 Hz, i.e. in the order of some 10 to 13 dB. This trend is also reflected in the pump chamber pressure spectra though the increase of levels with speed tend to be in the order of 13 dB to 18 dB.

3.5. Conclusions

The investigation of the three injection pumps show that hydraulic pressure exerted on the pump casing agrees with reasonable accuracy with theoretical waveforms.

The pressure spectra in the pump chamber show similarities, i.e. all the pumps tested show a typical decay by 40 dB/decade in the high frequency range. The pump noise in the low and mid-frequency range tends to be controlled by pump chamber pressure.

In the high frequency range the controlling factor, most probably, is the pipe line pressure when exciting only the top part of the pump structure. Pipe line pressure shows higher levels of excitation in the high frequency range by some 10 dB and the rate of increase of pump pressure excitation with speed corresponds more closely with increase of overall noise level with speed.

This finding does not exclude the effects of other exciting forces such as delivery valve, drive coupling and needle seating impacts. These effects will be discussed in later chapters.

4. VIBRATION CHARACTERISTICS OF FUEL INJECTION PUMP STRUCTURE

4.1. Description of Test Apparatus

In order to investigate the noise and vibration characteristics of the fuel injection pump without influence of noise and vibration transmitted from the engine, the pump was installed on a special "quiet" rig (Figure 4.1). The test rig was a converted Hartridge test machine, i.e. sound-proofed with a heavily damped bed plate.

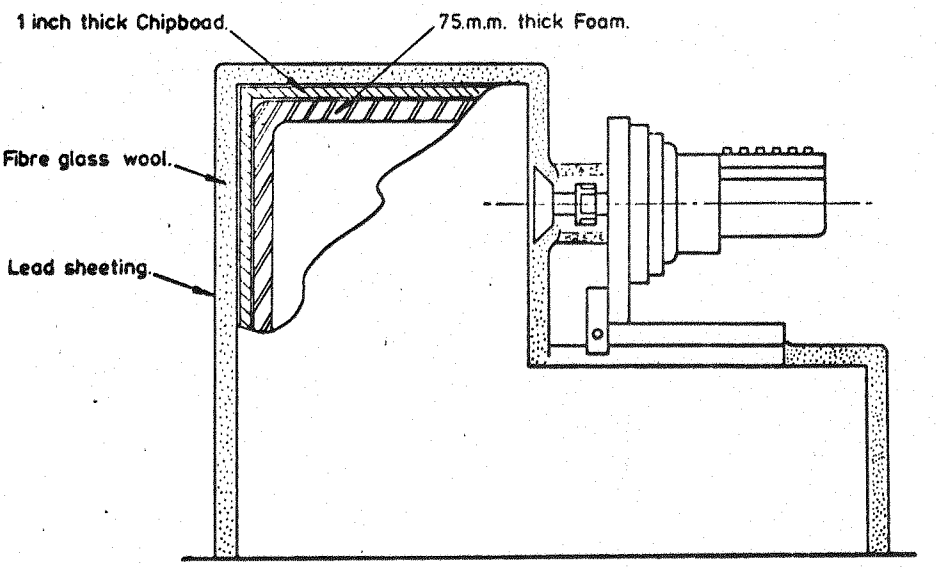

FIG 4·1 FUEL INJECTION PUMP TEST RIG. (I.S.V.R.)

The machine enclosure was made from 25 mm thick chipboard. In order to minimise the build-up of noise inside the enclosure, it was lined with sheet foam of 75 mm thickness. The outside of the enclosure was covered with lead sheeting lined with 25 mm thick fibreglass wool. The noise of the running machine was reduced by 30 dBA.

The drive-shaft and coupling were enclosed using lead sheeting lined with fibreglass wool formed as a tube. The fuel injection pipes were enclosed in thick rubber tubes and led outside the test cell to the injector distribution block.

Various techniques were employed to establish some understanding of what elements in the pump structure determine the characteristics of vibration and noise. These included the measurement of camshaft and pump body vibration.

4.2. Study of Camshaft Bending using Capacitance Transducer

Oscillographic studies of pump vibration were made on a six element in-line fuel injection pump to assess the nature of vibration from the application of hydraulic impulse loads. Since the camshaft is the first component of the pump which receives the application of the hydraulic load it was considered necessary to initially establish camshaft bending vibration.

In order to study the camshaft bending waveform, a capacitance transducer was designed. This consisted of an insulated brass shoe, with a turned radius at the toe equivalent to that of the camshaft and located in a housing attached to the base of the pump casing, as shown in Figure 4.2. Since the camshaft rotates it was essential to grind the centre part of the shaft to minimise any eccentricity.

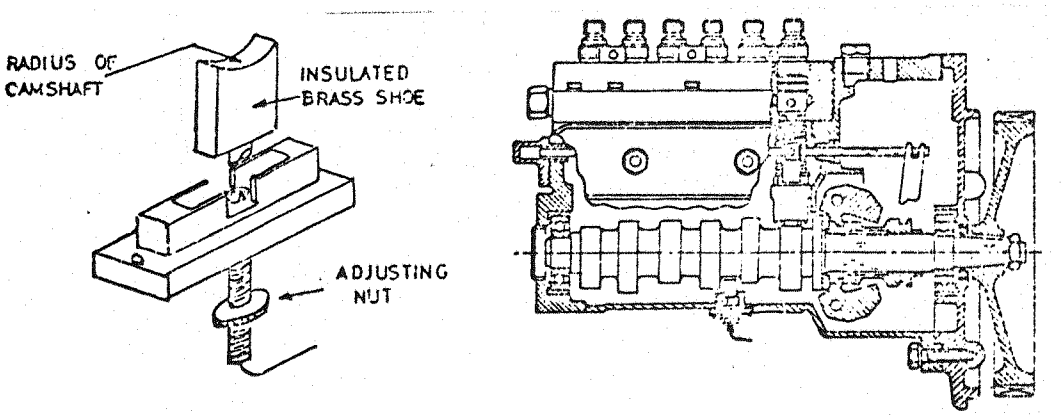

FIG.4.2 CAPACITANCE TRANSDUCER INSTALLATION IN PUMP.

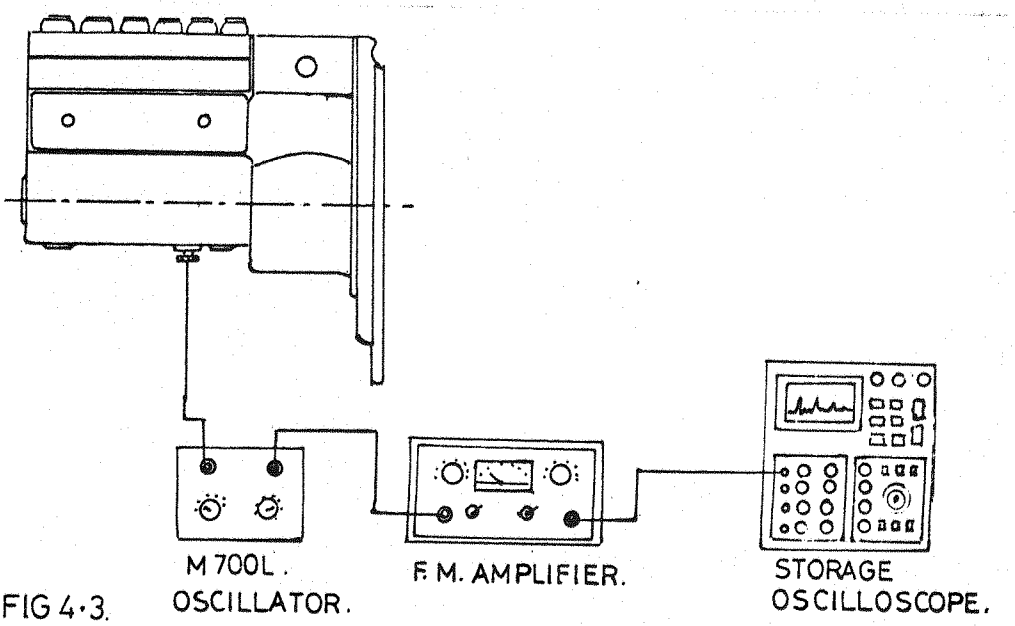

FIG 4.3.

A Southern Instrument F.M. System as shown in Figure 4.3 was used to obtain an electrical signal proportioned to the change of capacitance proportional to displacement. Since the capacitance gauge was fixed to the base of the pump casing, the resultant vibration oscillographs would truly represent only the relative vibration between the camshaft and the base of the pump casing. A typical oscillogram is shown in Figure 4.4 which also shows the pump chamber pressure in No.6 element. It will be seen that the measured relative deflection follows the form of the hydraulic force and the vibrations of any significance are seen to be induced by the drop in the pressure. Also they are heavily damped and thus reduced to a negligible value before the next impulse is applied.

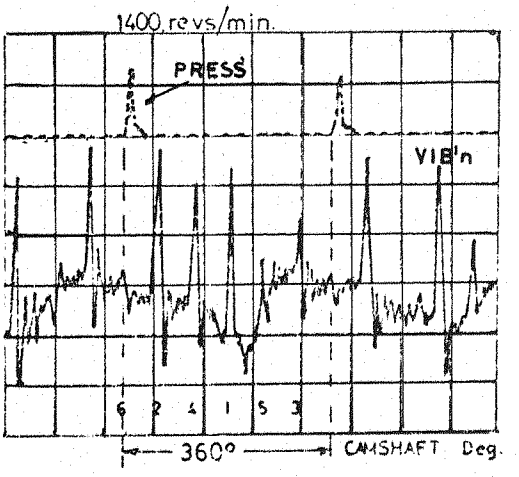

FIG4·4 CAMSHAFT VIBRATION

The frequency of vibration when determined from the oscillogram is around 700 Hz and thus corresponds to the broad band peak of the noise spectra (Figure 3.18, Section 3.4). The amplitude of the oscillatory part of the displacement diagram is about one-fifth of the total deflection which occurs during the time of hydraulic loading. This suggests that the forced components (particular integral) are considerably greater than the oscillatory components (complementary function).

The magnitude of deflection is dependent on the individual plunger operation. Near the cam shaft bearings, minimum deflections are produced by the working plungers while in the middle of the camshaft the working plunger produces considerably greater deflection amplitudes, this difference being in the order of some 2:1.

Figure 4.5 illustrates the distribution of deflection amplitudes as measured on the centre of the camshaft from the operation of the plungers.

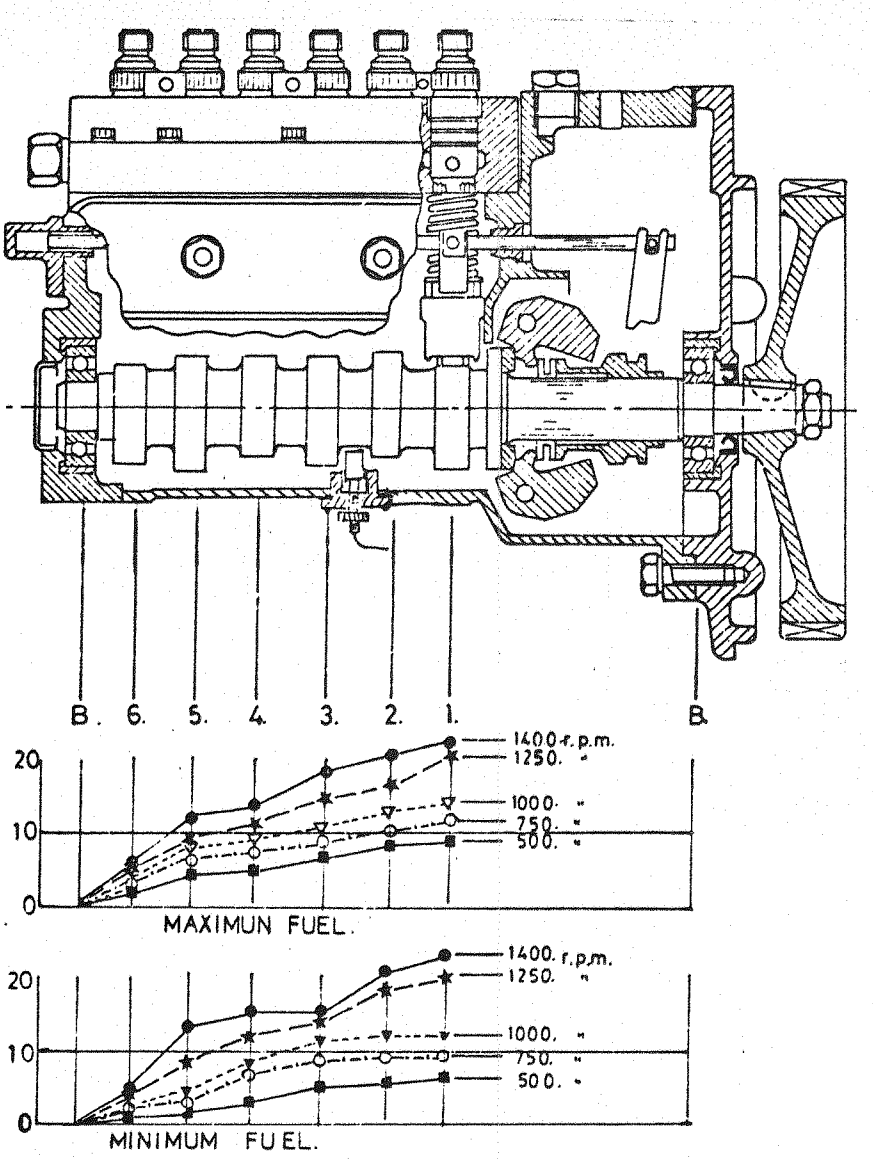

FIG.4·5. DISTRIBUTION OF DEFLECTION AMPLITUDES.

4.3. Study of Camshaft Bending Using Velocity Type Transducer

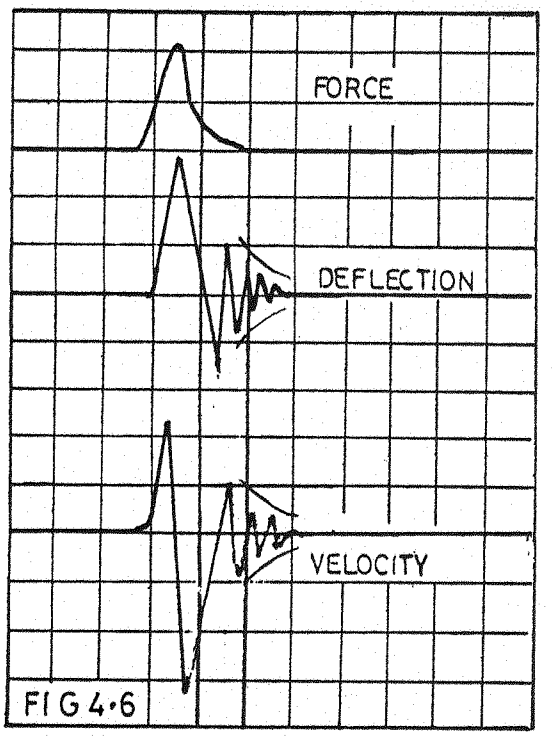

FIG 4·6

Similar results were obtained with a velocity type transducer. Figure 4.6 illustrates the deflection and velocity deflection in comparison with applied force diagram. The system also shows the presence of high damping, the Q factor was between 8.9 and 9.5.

The narrow band spectra of the velocity waveform and deflection waveform, obtained using a Muirhead Pametrada wave analyser are shown in Figures 4.7 and 4.8 respectively.

As can be seen the spectra contain predominantly the firing

harmonics, although the rotational harmonics can be detected but are of small amplitude. (The rotational harmonics are the result of known vibration amplitude resulting from different plungers operating).

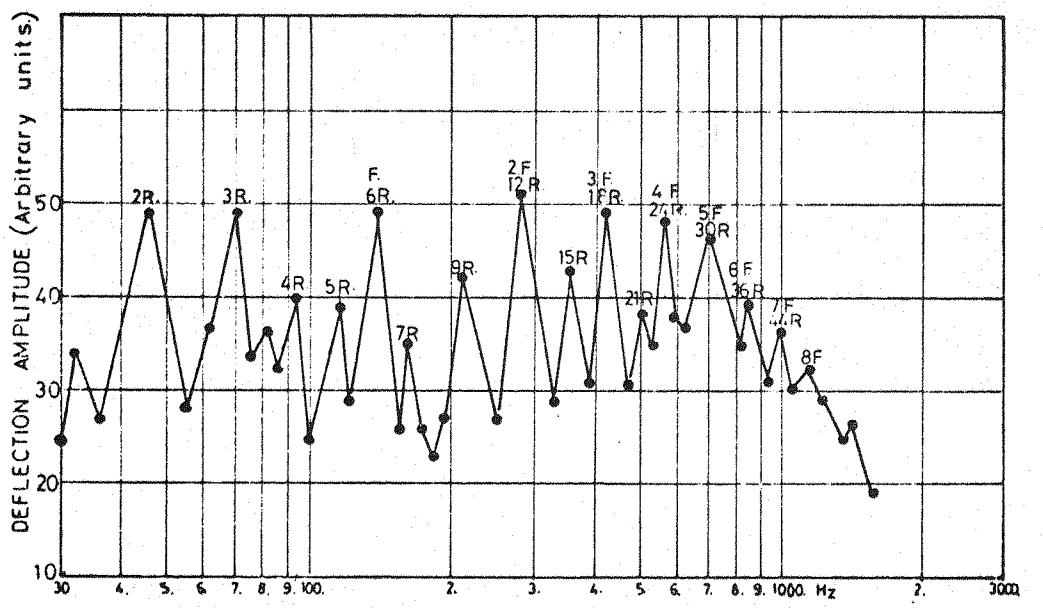

FIG. 4·7 SIX PLUNGERS OPERATING. (Capacitance probe)

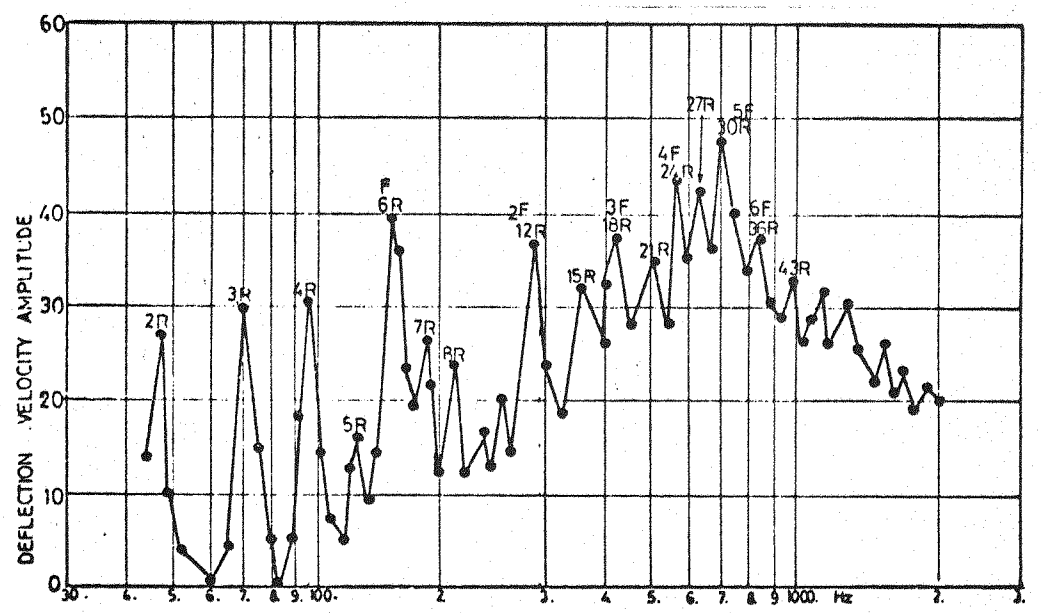

FIG. 4·8. SIX PLUNGERS OPERATING. (Electromagetic probe)

If the general outline (envelope of harmonics) is drawn and compared with force spectrum, as shown in Figure 4.9, they show very close similarity which suggests that pump vibration is stiffness controlled.

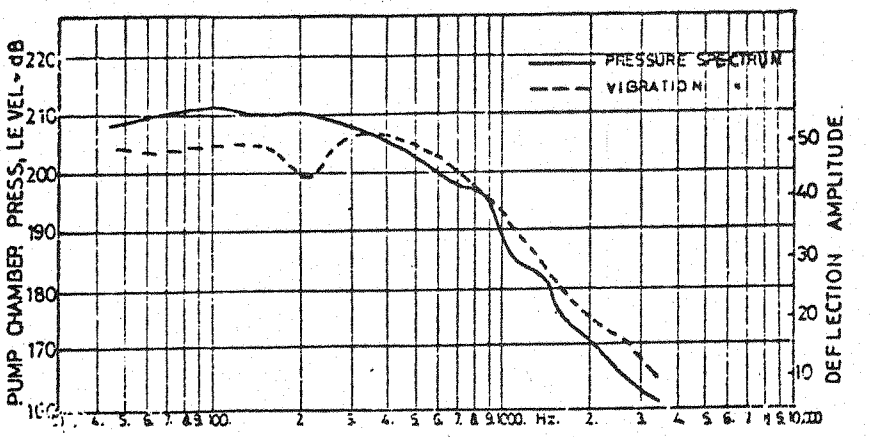

FIG4·9. SIX PLUNGERS OPERATING.

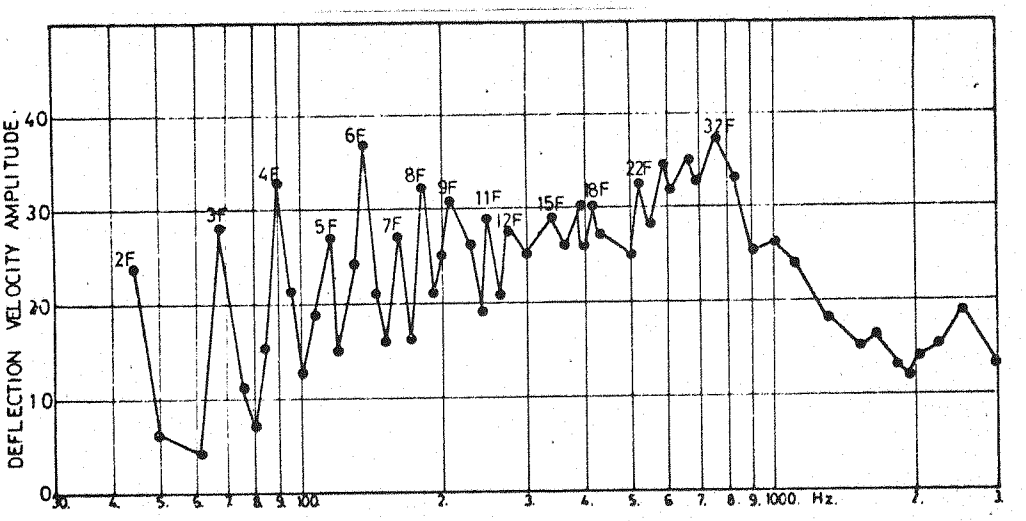

FIG 4·10 SINGLE PLUNGER OPERATING (Electromagnetic probe)

4.4. Study of Camshaft Bending - One Plunger only Operating

An experiment was carried out operating only one plunger. The spectrum is shown in Figure 4.10. It can be seen in this case that although the spectrum consists of harmonics of single plunger operation, the spectrum is similar. It was found also, that the noise was in no way different.

Comparison between force and vibration spectra is shown in Figure 4.11 which indicates the same mechanism of stiffness control. The damping in the pump is only marginally reduced, i.e. Q factor is reduced from 9.6 to 10.8.

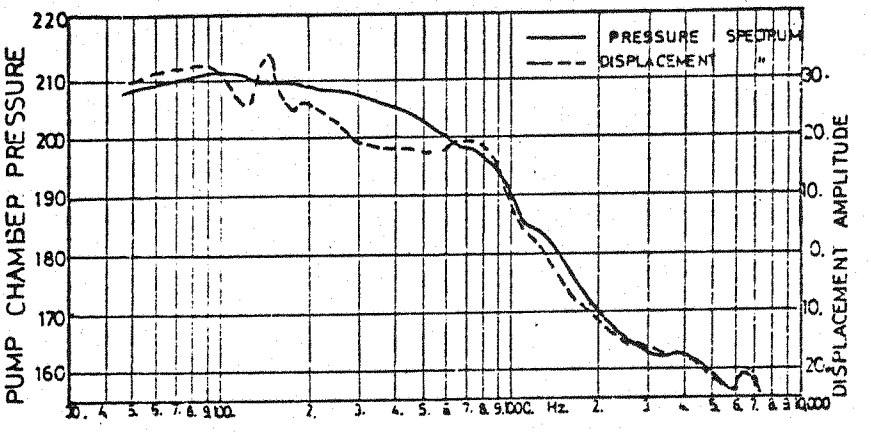

FIG.4·11. SINGLE PLUNGER OPERATING. 1400.r.p.m.

4.5. Study of Camshaft Bending Using Electro Magnetic Shaker

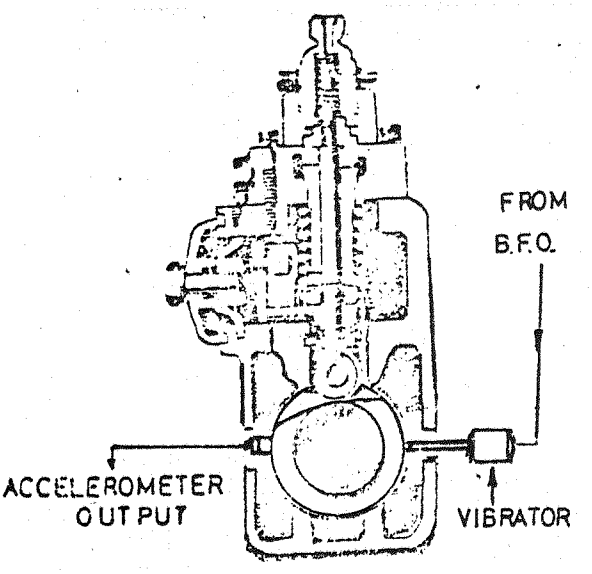

FIG 4·12

Camshaft vibration characteristics were investigated using a vibration generator attached to the centre of the camshaft via a drilled hole in the pump casing as shown in Figure 4.12. The vibratory response of the camshaft is shown in Figure 4.13 indicating predominant frequencies of 1250 Hz, 1400 Hz, 2500 Hz and 5000 Hz respectively. The response of the 700 Hz component is small, i.e. there is no evidence of resonance in this frequency region.

The pump casing response to camshaft vibratory force is shown in Figure 4.14. One-third octave band spectra were obtained in two horizontal planes (A and B) and one vertical plane (C). As can be

seen in both planes the 700 Hz component is very predominant. The horizontal components are some 5 to 11 dB higher than the vertical component.

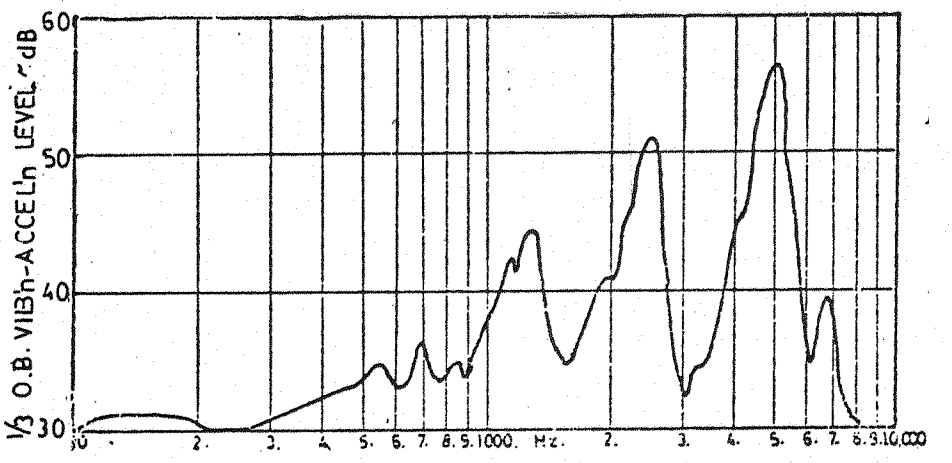

FIG 4·13 RESPONSE OF CAMSHAFT (Vibrated in pump casing.)

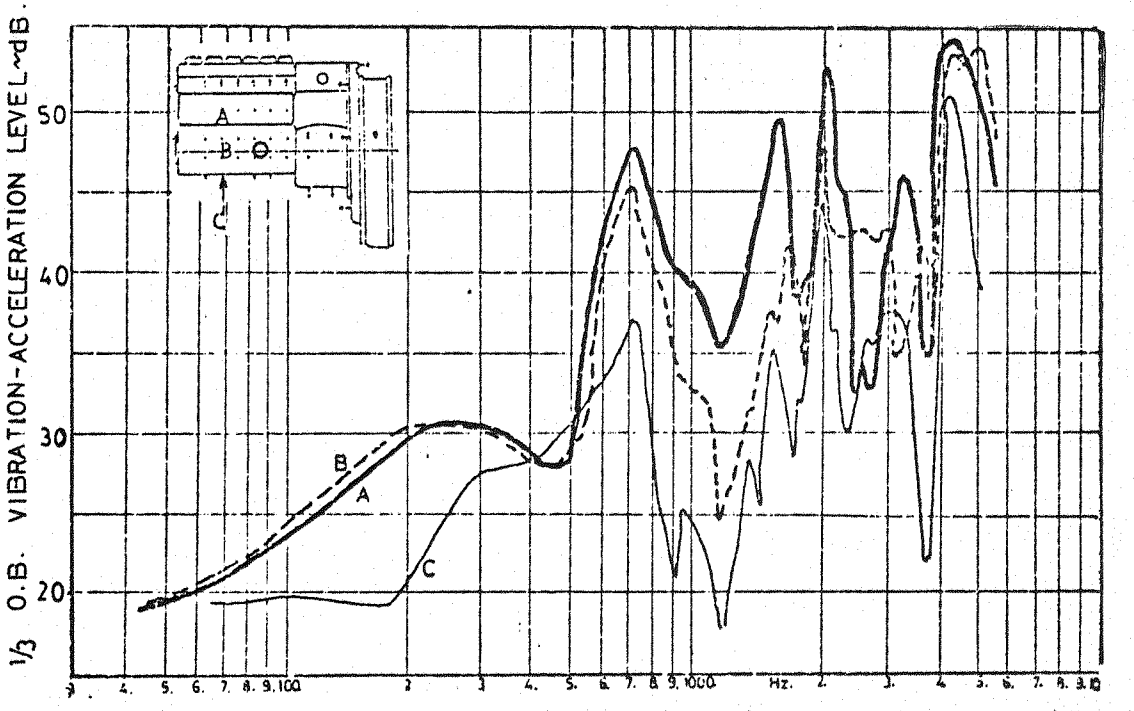

FIG 4·14 PUMP CASING RESPONCE. (Camshaft vibrated.)

From the vibration spectra taken on the pump casing along two horizontal rows and one vertical row, (i.e. A, B, C, 1-5,) the indication of a fundamental bending mode is observed at 700 Hz. At 2000 Hz there is indication of a second bending mode and a possible torsional mode. These results are shown in Figure 4.15.

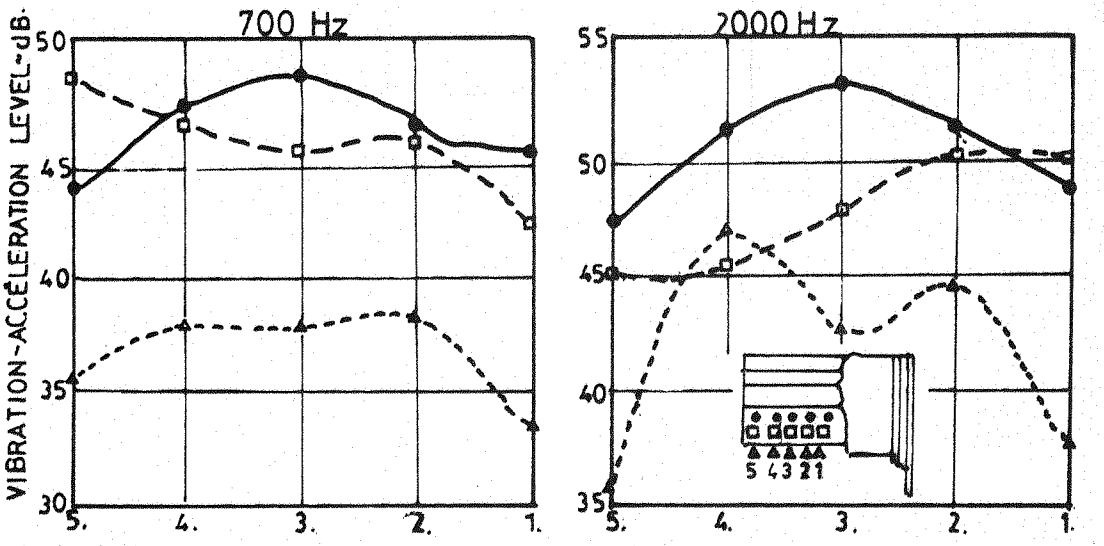

FIG.4.15. PUMP CASING VIBRATION SPECTRA.

4.6. Pump Structure Vibration Using "Proximity" Type Transducer

Pump housing vibration oscillograms were obtained at various positions on the pump casing using a "proximity" type velocity pick-up. As can be seen from Figure 4.16 the waveforms are very similar to those taken on the camshaft and clearly illustrate the effect of individual injectors and subsequent vibration.

Vibration spectra were obtained at twenty points on the pump casing. At each one-third octave band the vibration levels were summed and averaged, thereby producing one spectrum. This result is shown in Figure 4.17 which indicates a distinct broad band peak centred around 700-800 Hz. Above 1000 Hz the vibration levels are some 13 dB lower.

4.7. Conclusions

Vibration measurements between camshaft and base of the pump show that the measured relative deflection follows the form of the hydraulic force. Vibrations of any significance are seen to be induced only by the drop in pressure. The frequency of these vibrations is around 700 Hz.

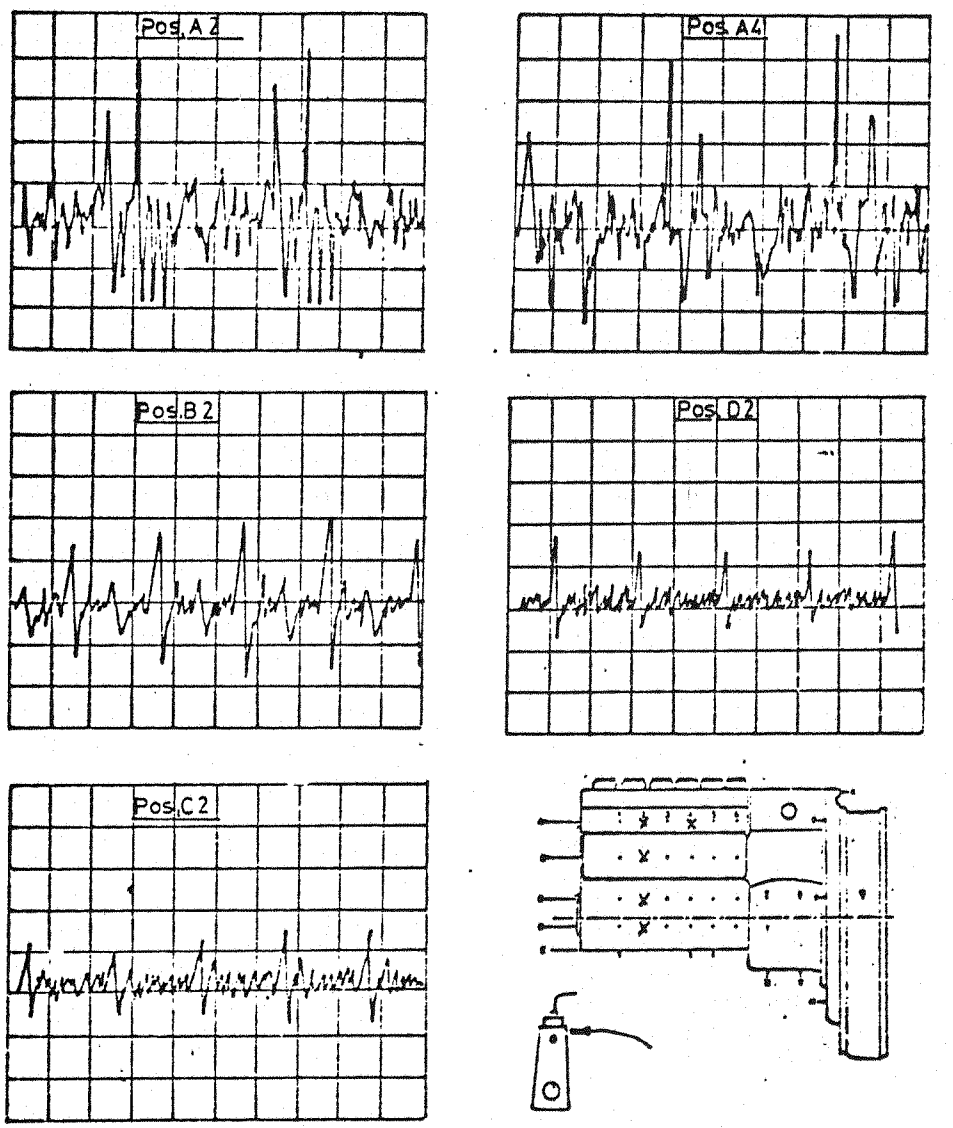

FIG.4-16. PUMP CASING VIBRATION OSCILLOGRAMS.
(Proximity type transducer.)

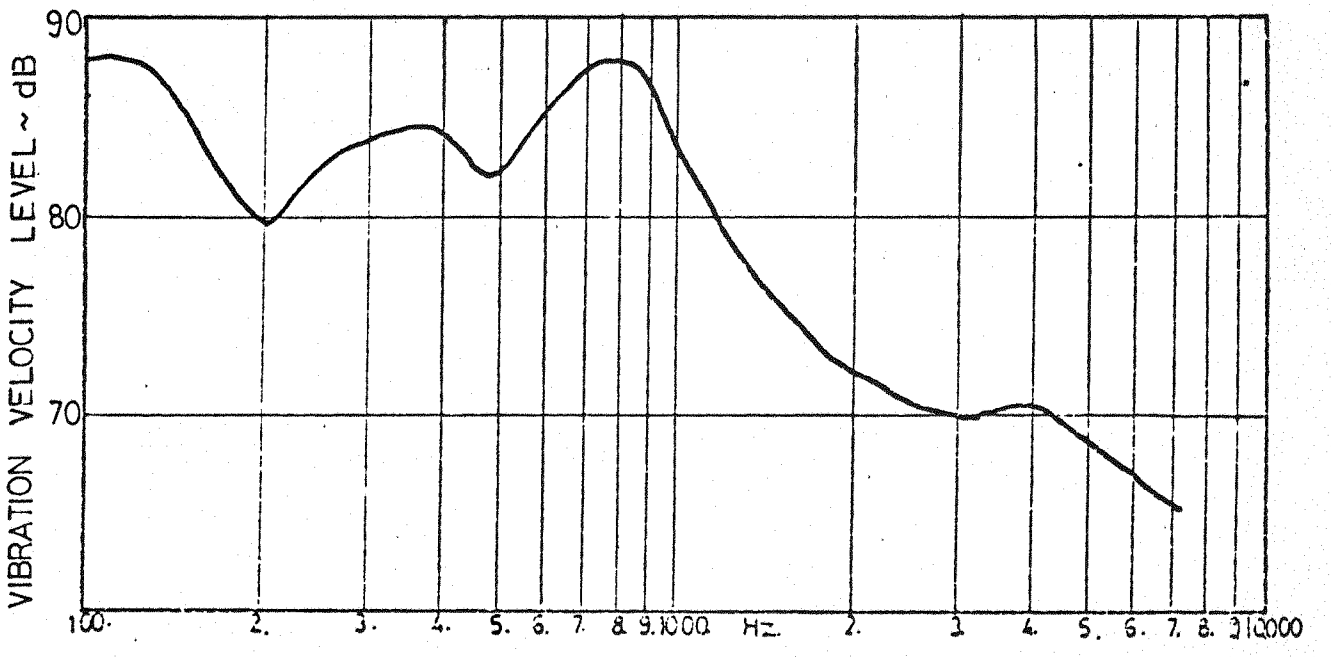

FIG.4-17. AVERAGED PUMP HOUSING VIBRATION SPECTRUM. 1400.revs/min.
(Proximity type transducer.)

Narrow band spectra of velocity and deflection waveforms contain predominantly the firing harmonics. Comparing the general outline of the harmonics with the pump chamber force spectrum results shows a very close similarity, indicating that pump vibration is stiffness controlled. Operating one plunger only, the narrow band spectrum shows harmonics of single plunger operation to be predominant above 300 Hz. Comparison between force and vibration spectra indicates the same mechanism of stiffness control. The damping in the pump is marginally reduced.

The vibratory response of the camshaft (using external vibrator) shows predominant frequencies of 1250 Hz, 1400 Hz, 2500 Hz and 5000 Hz respectively. The response at 700 Hz is small.

Response of the pump casing to camshaft vibration force, however, show that in both horizontal and vertical planes on the pump casing the 700 Hz component is clearly predominant. Vibration spectra taken on the pump housing indicate a fundamental bending mode around 700 Hz. At 2000 Hz there is indication of a second bending mode and possibly a torsional mode.

5. COMPARISON OF GENERAL VIBRATION CHARACTERISTICS OF THE PUMP AND ENGINE

There is a considerable similarity between the injection pump and engine structure design. Both structures are complex castings, and as shown by Lalor (5.1) the mode shapes are complex. In particular in the higher frequency range, the modal density (number of modes per unit bandwidth) can be very high. It has also been found experimentally by Lalor and Croker (5.2) employing a vibration generator to excite an undamped engine structure crankcase/block without running parts fitted, that even the slight damping present prevents the full identification of all the individual modes. The existence of all modes can only be determined by the finite element modal analysis of the engine structure.

Figure 5.1 illustrates the mode shape at one particular frequency in the high frequency range of a simplified engine block casting showing the amplitude, phase and modal lines.

Another way to compare and identify structure vibration is by measurement of the distribution of vibration level over the structure at a large number of points in one-third octave bands. This provides a time average vibration level of the engine or the pump. These data do not give any more detailed modal information but provide general information as to which parts of the structure are responsible for radiation of noise in a particular frequency range. The variation in vibration level over the structure is considerable largely up to 10 to 15 dB.

A technique for measurement of vibration distribution has been defined at I.S.V.R. On the engine block the practice is to divide the surface into grids of approximately 50 mm square and thus on average some 65 measuring points are used. On the pump structure (smaller physical size) the measuring grid is considerably finer, i.e. the structure is divided into a grid of about 25 mm square and thus on average some 25 measuring points are used. The photograph (Figure 5.2) illustrates the positioning of measuring grids on the pump and the engine.

Investigations by Anderton and Chan (5.3) have shown that radiated noise in a particular one-third octave band is directly related to the mean vibration level averaged over the whole surface of the engine. They have also shown that radiated noise in the same

2201 Hz

LHS

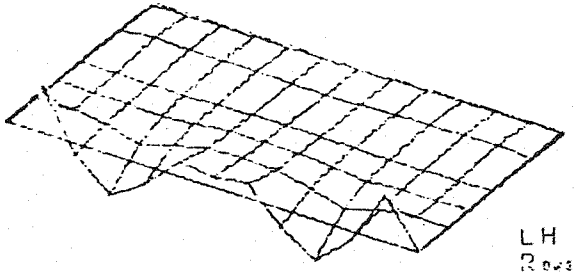

LH
Rows = 6
Columns= 13
Horizontal angle 30.00
Vertical angle 30.00
Y Scale 0.00000
Y Max 0.04194
Y Min -0.03713

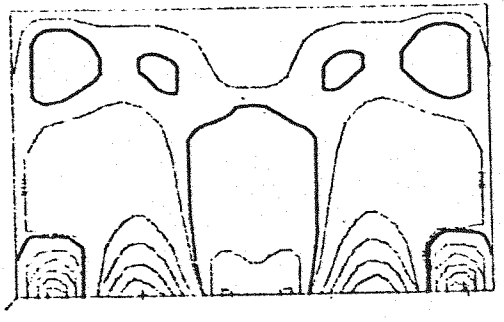

Contours of file LHC
No of Levels = 10
Maximum = 0.04212
Minimum = -0.03704

Levels
-0.02984
-0.02265
-0.01545
-0.00825
-0.00105
0.00614
0.01333
0.02053
0.02773
0.03493

RHS

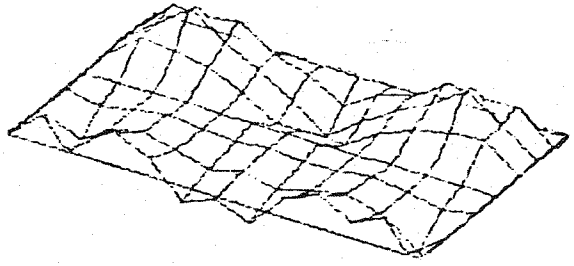

RH
Rows = 8
Columns= 13
Horizontal angle 30.00
Vertical angle 30.00
Y Scale 0.00000
Y Max 0.05346
Y Min -0.05700

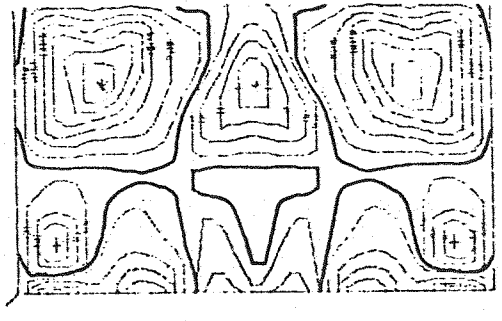

Contours of file RHC
No of Levels = 10
Maximum = 0.05341
Minimum = -0.05695

Levels
-0.02819
-0.02083
-0.01347
-0.00611
0.00125
0.00861
0.01597
0.02333
0.03069
0.03805

FIG 5·1 ILLUSTRATION OF MODE SHAPE.

way can be calculated from individual surfaces of structure, for example valve cover, block, exhaust and inlet manifolds, crankcase and sump, thus assessing quantitatively the noise making potential of each of these engine components.

In the present investigation therefore the basis of mean vibration levels distributed over the frequency range will be used for comparison of the characteristics of engine and pump vibration.

TABLE 2
ENGINE DATA AND PUMP DATA

ENGINE A	Bore Stroke Capacity HP	107.18 mm 120.7 mm 6.54 litres 125 HP @ 2400 rev/min	6 in-line	N.A.
ENGINE B	Bore Stroke Capacity HP	125 mm 130 mm 15.95 litres 330 HP @ 2500 rev/min	V 10	N.A.
ENGINE C	Bore Stroke Capacity HP	130 mm 150 mm 11.98 litres 350 HP	6 in-line	T.C.
ENGINE D	Bore Stroke Capacity HP	120 mm 130 mm 8.822 litres 182 HP @ 2400 rev/min	6 in-line	N.A.
ENGINE E	Bore Stroke Capacity HP	104.7 mm 114.7 mm 5.89 litres 113 HP @ 2800 rev/min	in-line	N.A.
ENGINE F	Bore Stroke Capacity HP	115 mm 120 mm 12.6 litres 286 HP @ 2800 rev/min	V 10	N.A.

Six engines of power range from 110 to 350 HP as employed in medium to heavy trucks, were chosen for the investigation. All these engines are fitted with in-line injection pumps. Four of the engines are in-line 6 cylinder engines, two are V 10 engines. One of the six in-line 350 HP engines is turbocharged. The chosen engines also represent relevant differences in pump drive and pump mounting arrangements.

The data of engines and pumps are given in Table 2.

5.1. General Vibration Characteristics of Injection Pump

Most of the detailed study was carried out on the Engine (E) fitted with a flange mounted injection pump as shown in the photograph (Figure 5.2). The vibration spectra plotted along the horizontal rows A, B, C and D, are shown in Figure 5.3. As can be seen in some frequency bands the variations in vibration level along the lines are quite large, i.e. about 10 dB, while in others they are as small as 2 dB. The spectra, however, exhibit certain similarities; they all have broad peaks in the frequency range from 800 Hz to 1000 Hz and in the high frequency range from 3000 Hz upwards.

The distribution of vibration, from the spectra shown in Figure 5.3, can be defined by plotting the variations of the vibration levels along the horizontal lines A, B, C, D, in each of the one-third octave bands as shown in Figures 5.4a,b,c,d. From these it is possible to identify the shape of the vibration in a horizontal direction. In the same way plots can be made in vertical planes as shown in Figures 5.5a,b, indicating the distribution of vibration in the vertical direction.

A clearer illustration can be provided by the construction of asymmetric diagrams of vibration distribution over the whole pump surface (three dimensional plots) in various one-third octave bands as shown in Figures 5.6a,b,c,d,e,f,g. These graphs illustrate that, based on Lalor's classification of engine modes in two groups (namely plate type modes and panel modes,) the pump appears to exhibit only plate type modes over the whole frequency range from 100 to 8000 Hz. These, as can be seen, are a combination of bending and torsional type modes.

At the broad peak around 800 Hz at the free end of the pump there is high vibration at the top and bottom surfaces while in the middle it is low, suggesting a torsional mode of the whole pump body. In the high frequency range from 2000 Hz upwards there is a general increase of vibration from the top part of the pump towards the lower part, thus resembling a 'conical mode' where from the applied forces the lower part of the pump structure distorts considerably more. The top part of the pump is extremely rigid and

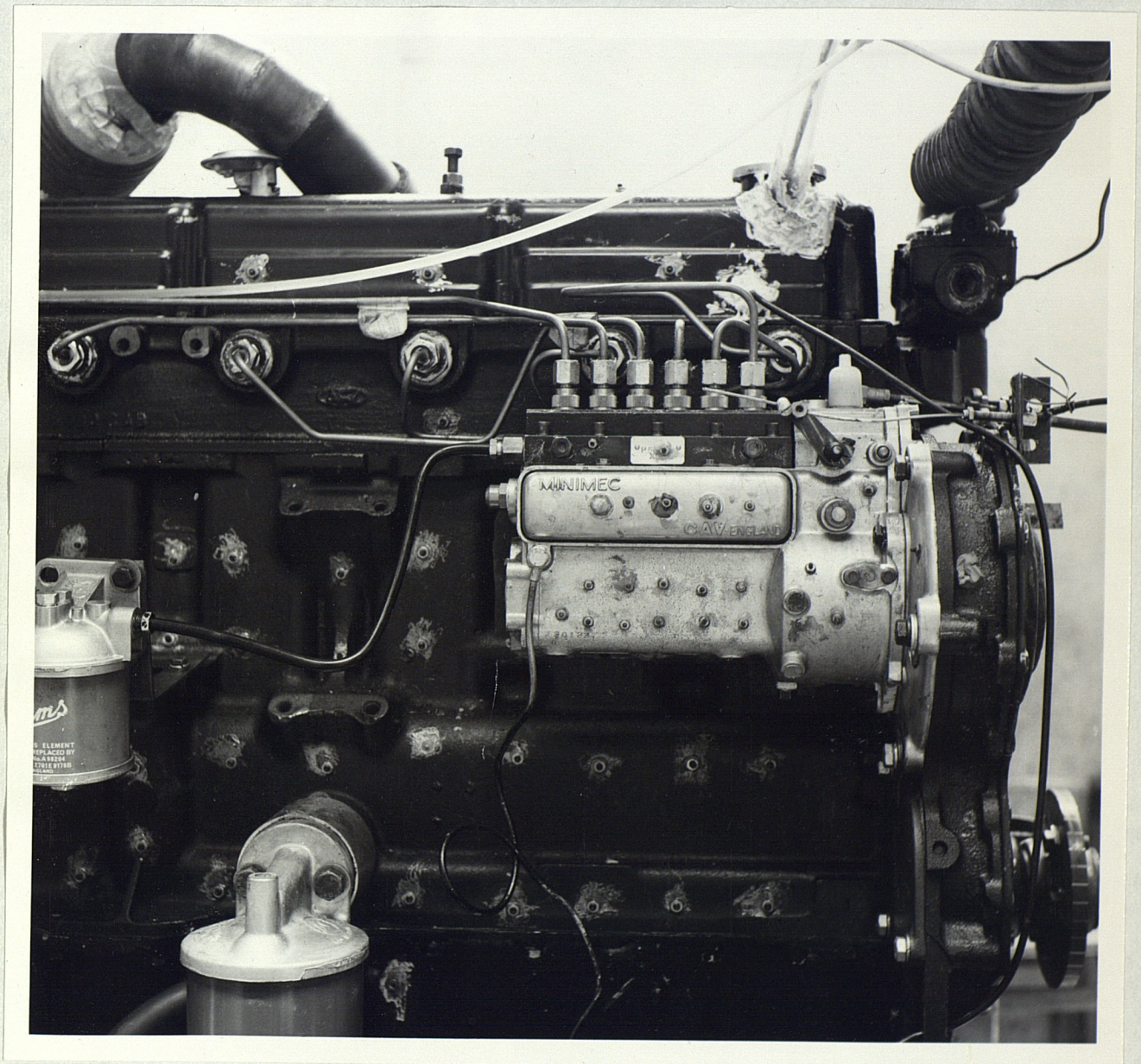

FIG. 5·2. ACCELEROMETER FIXING POSITIONS.

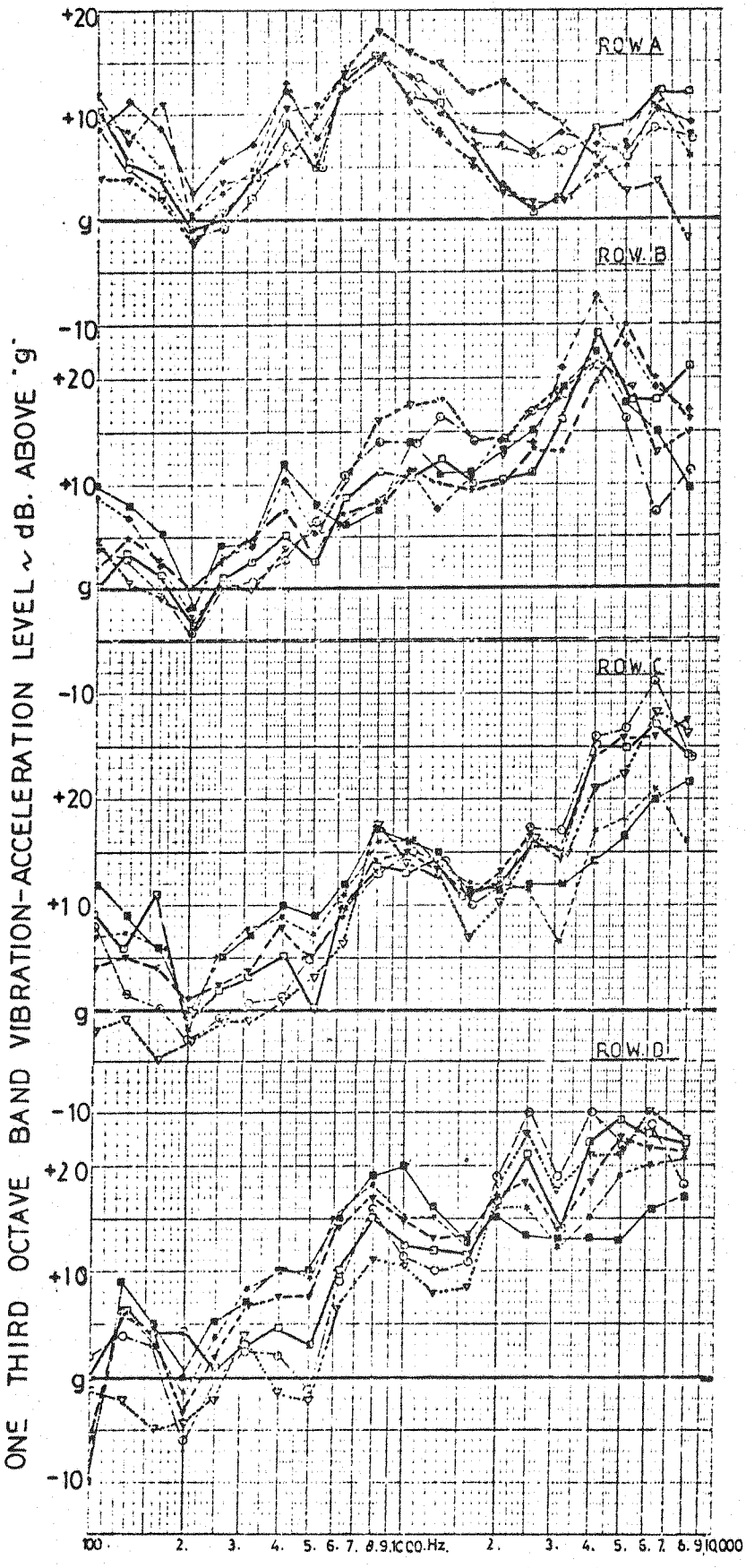

FIG. 5.3. VIBRATION SPECTRA. HORIZONTAL PLANE ON PUMP CASING.

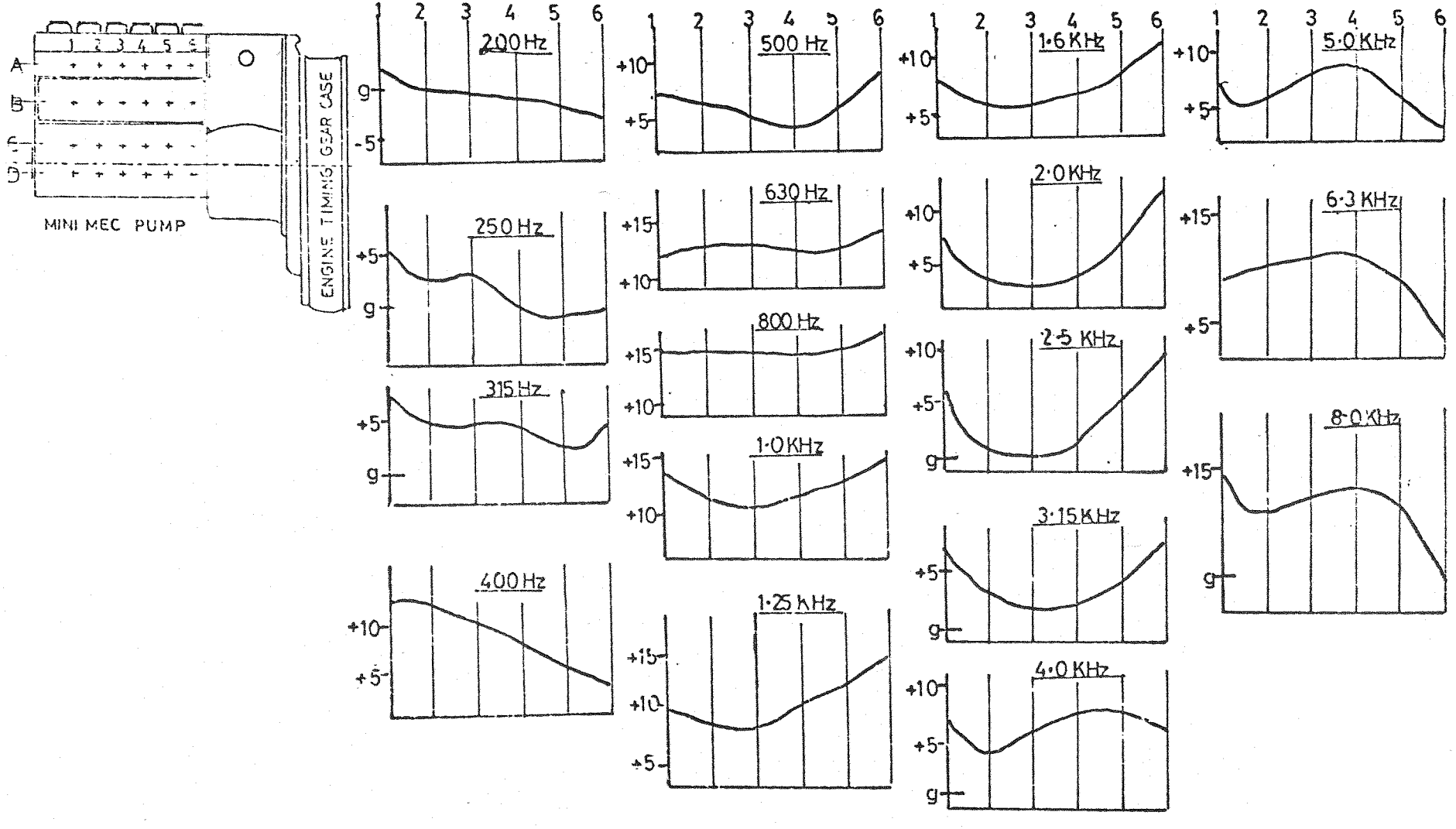

FIG. 5·4a. VIBRATION PATTERN HORIZONTAL PLANE. ROW.A.

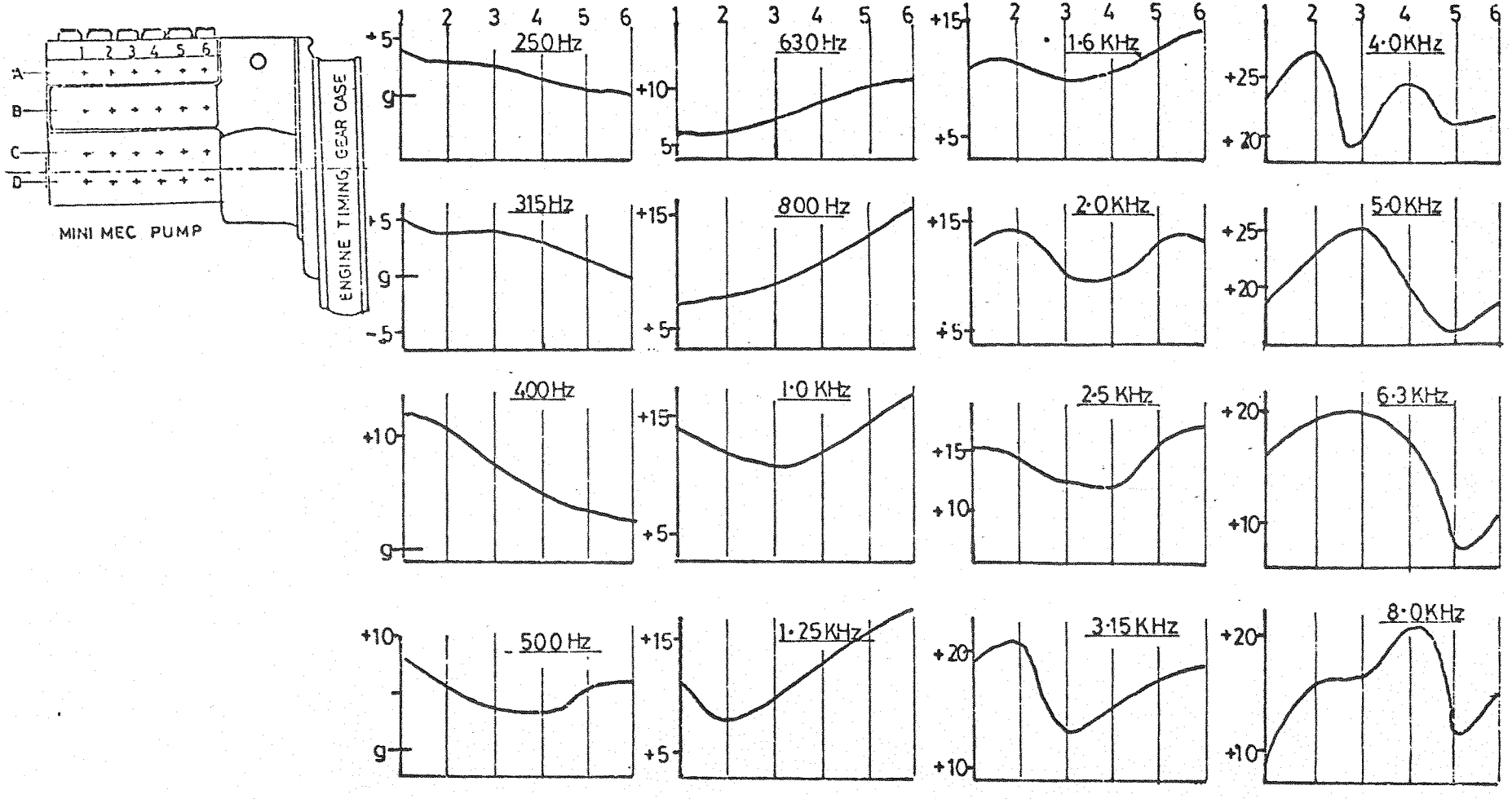

FIG. 5·4 b. VIBRATION PATTERN HORIZONTAL PLANE. ROW. B.

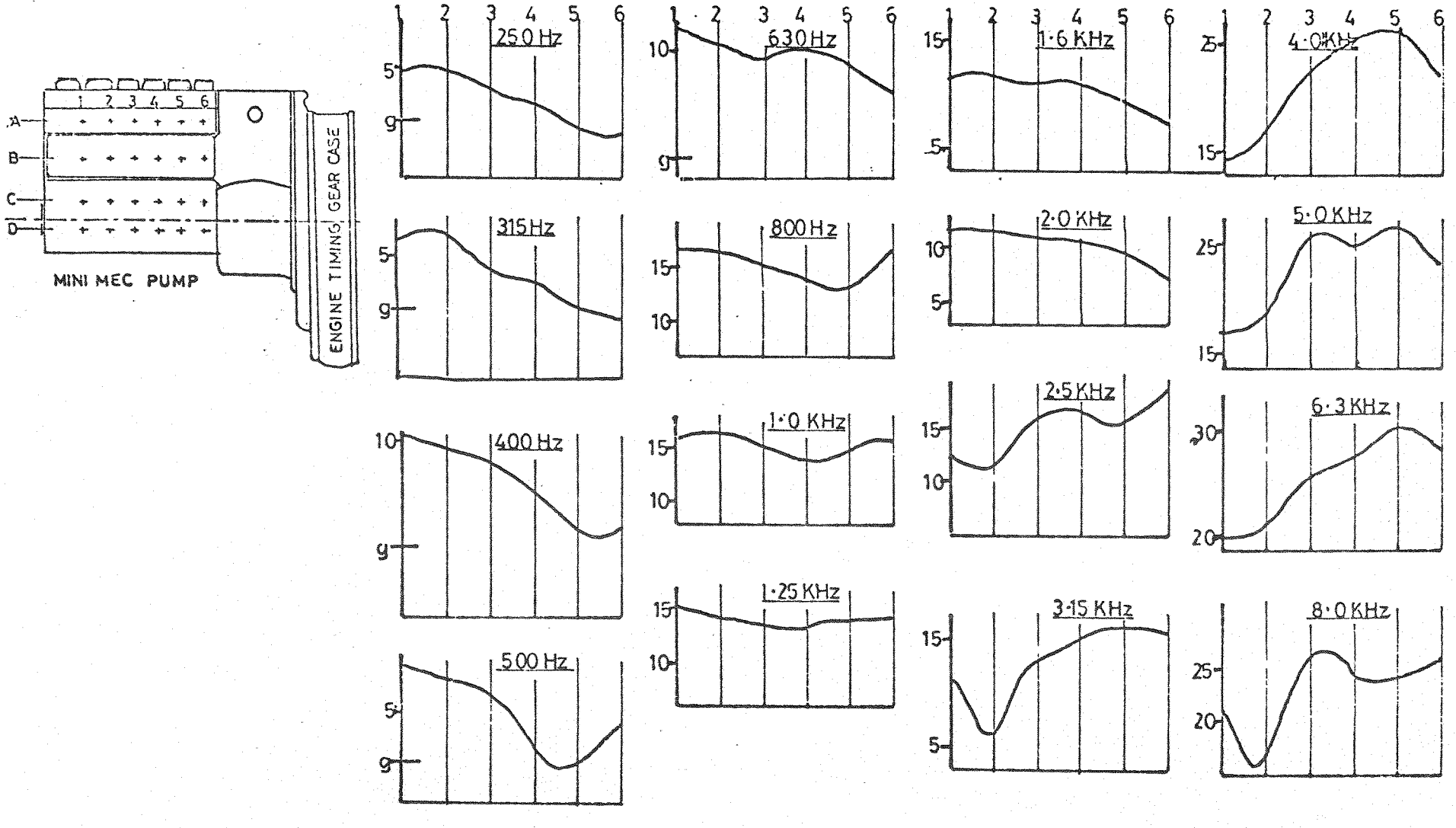

FIG. 5·4 c VIBRATION PATTERN HORIZONTAL PLANE. ROW. C.

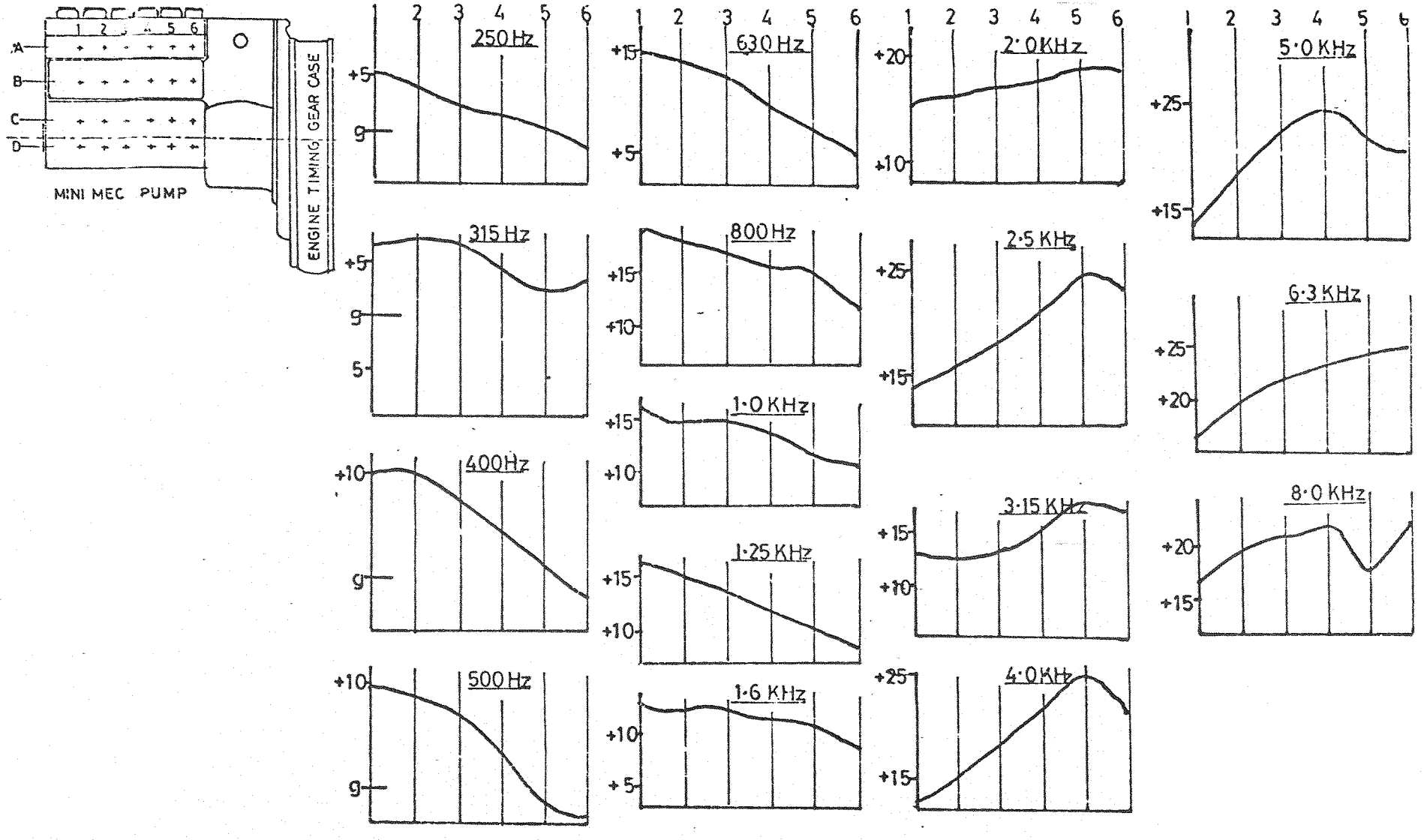

FIG. 5·4d. VIBRATION PATTERN HORIZONTAL PLANE. ROW. D.

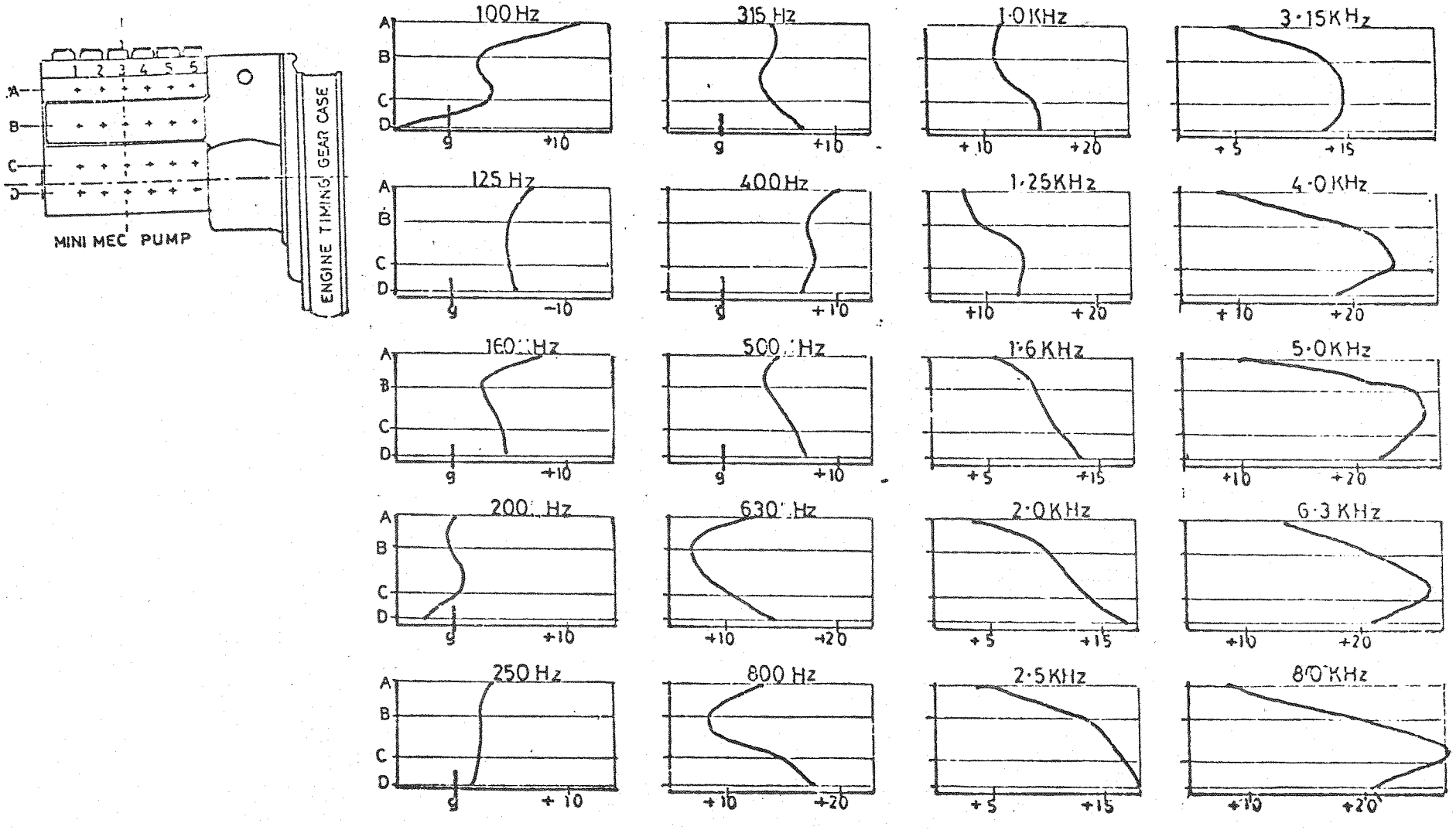

FIG. 5·5a. VIBRATION PATTERN. VERTICAL PLANE. ROW. 3.

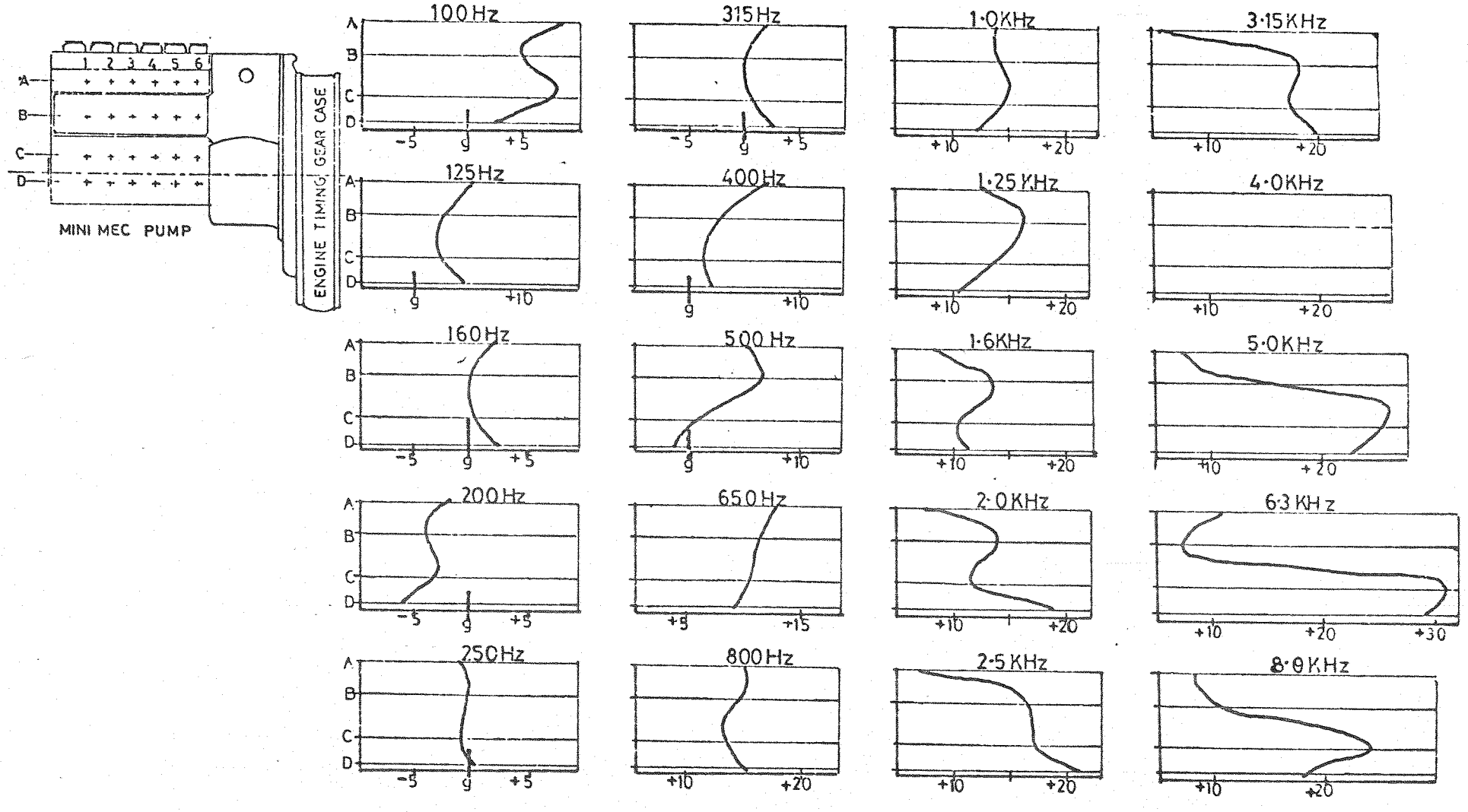

FIG.5·5b. VIBRATION PATTERN. VERTICAL PLANE. ROW.5.

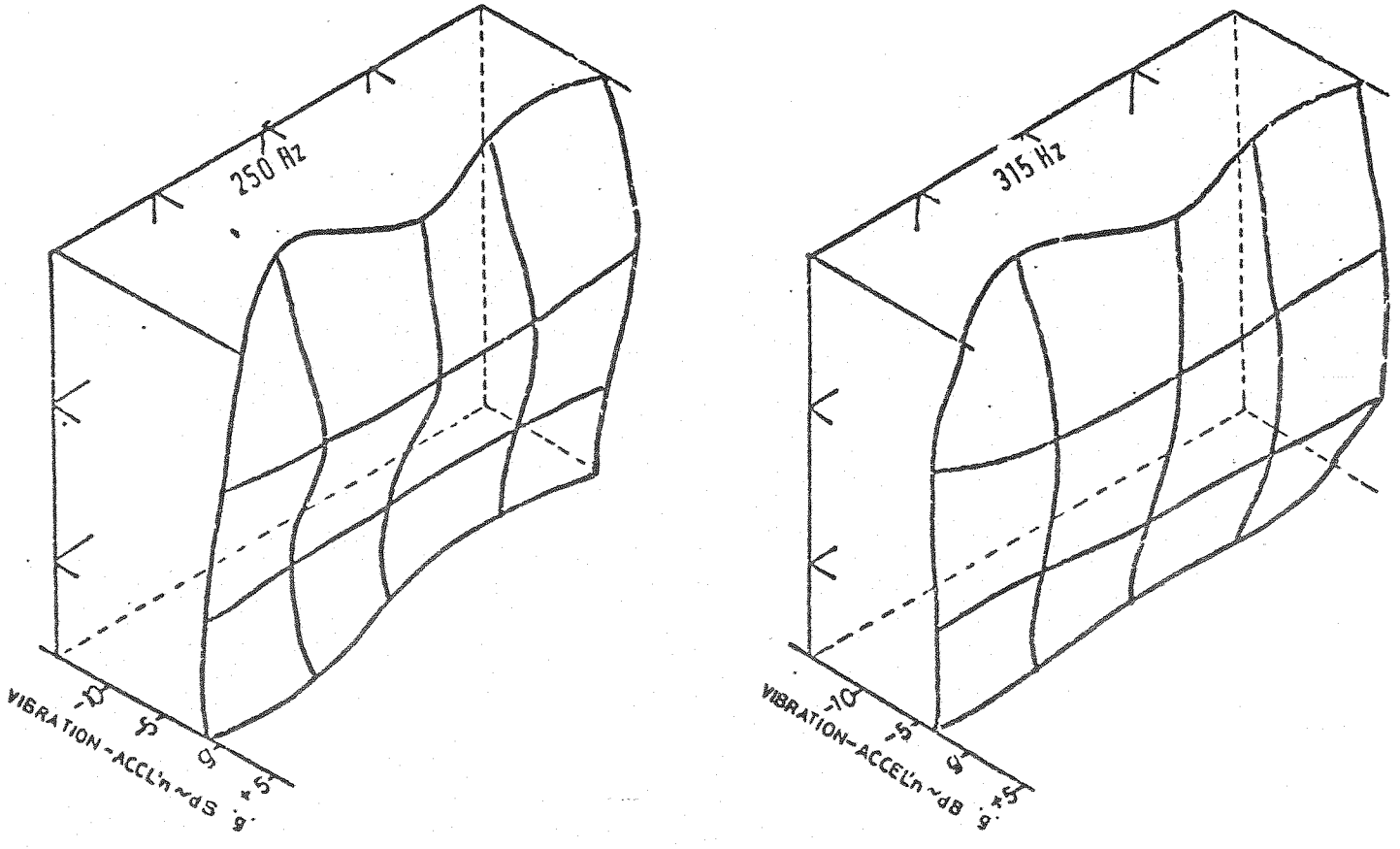

FIG 5.6a THREE DIMENSIONAL PLOTS OF PUMP BODY VIBRATION.

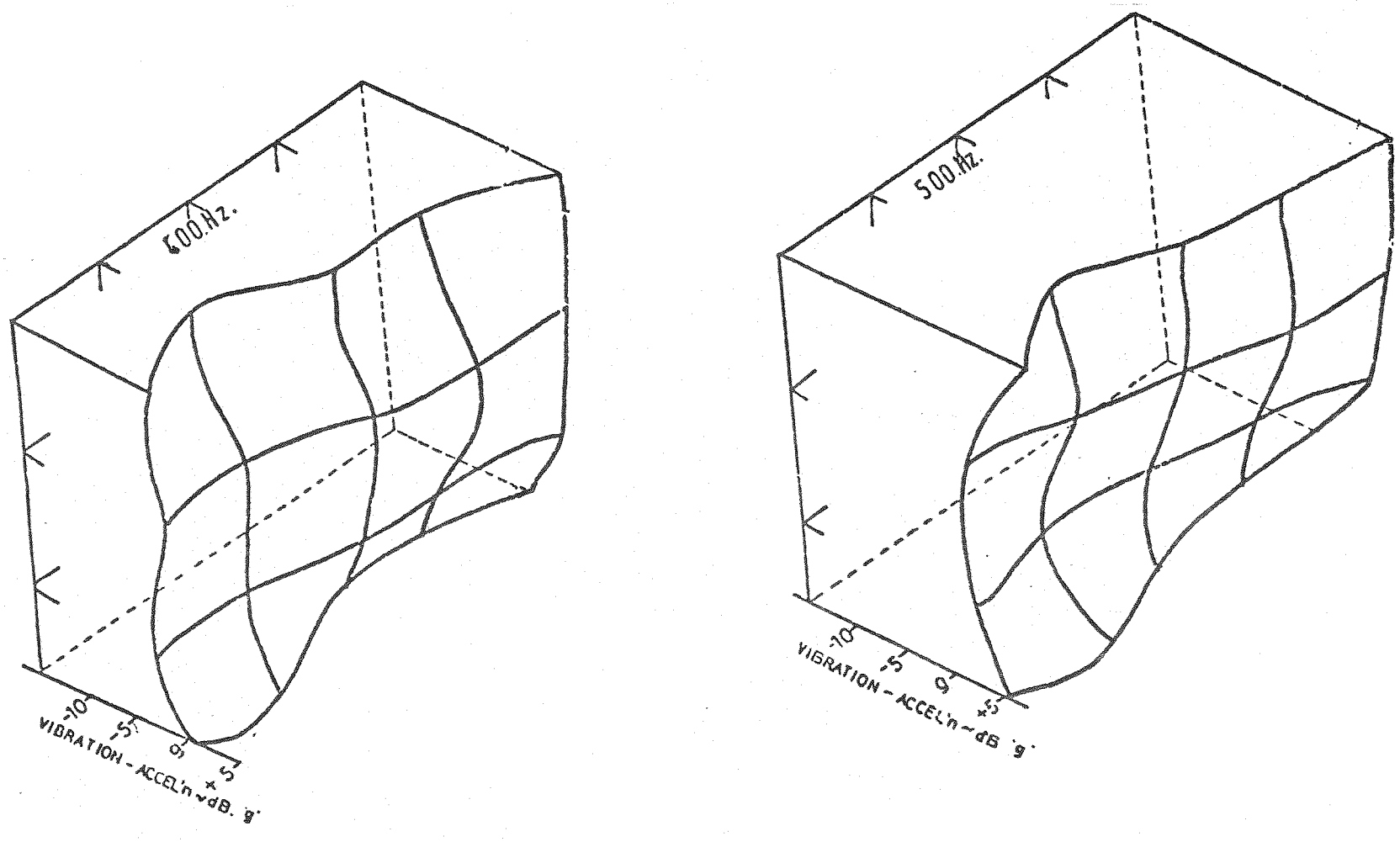

FIG. 5·6.b. THREE DIMENSIONAL PLOTS OF PUMP BODY VIBRATION.

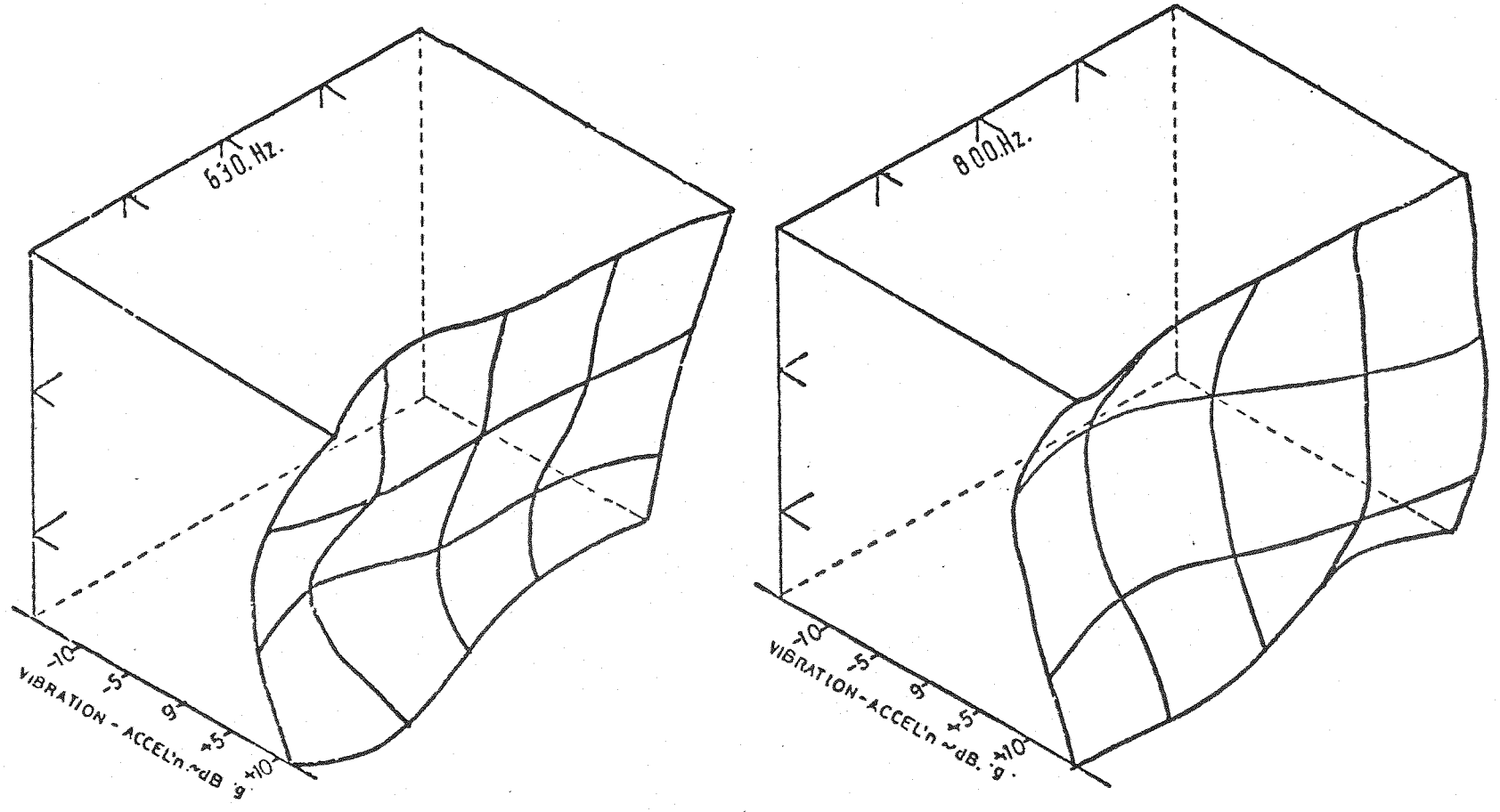

FIG. 5·6.c. THREE DIMENTIONAL PLOTS OF PUMP BODY VIBRATION.

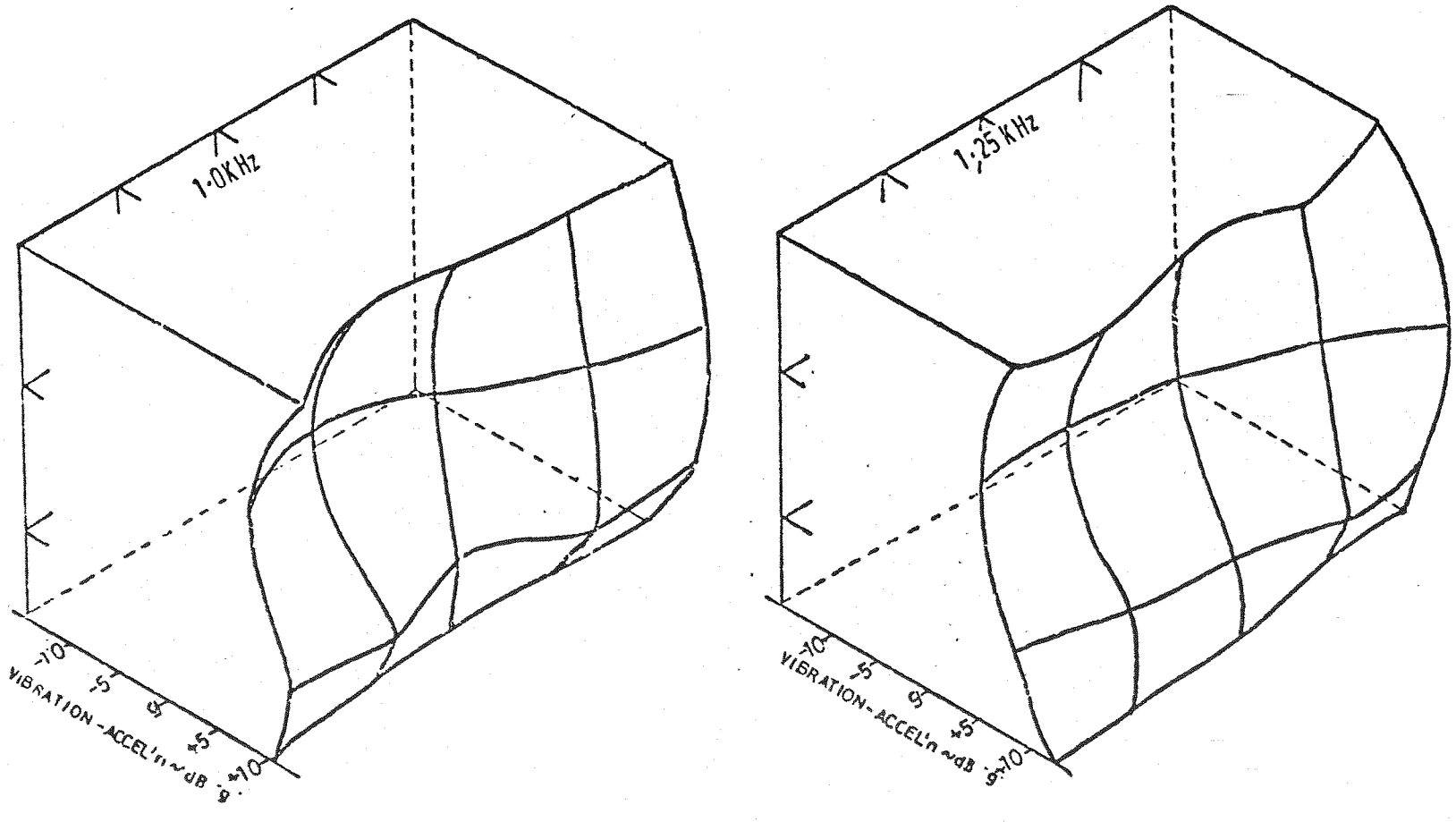

FIG. 5·6·d. THREE DIMENTIONAL PLOTS OF PUMP BODY VIBRATION.

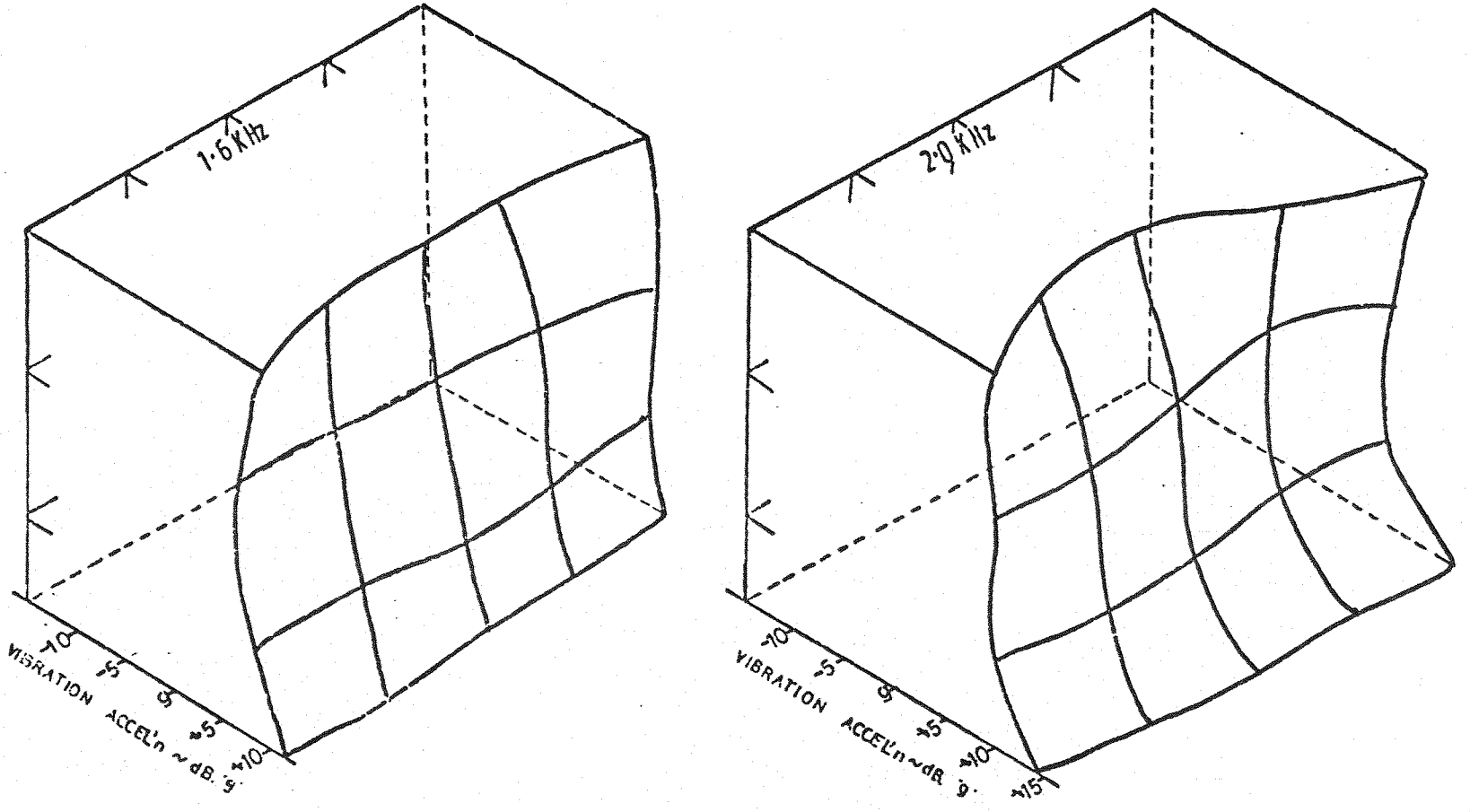

FIG. 5·6 e. THREE DIMENTIONAL PLOTS OF PUMP BODY VIBRATION.

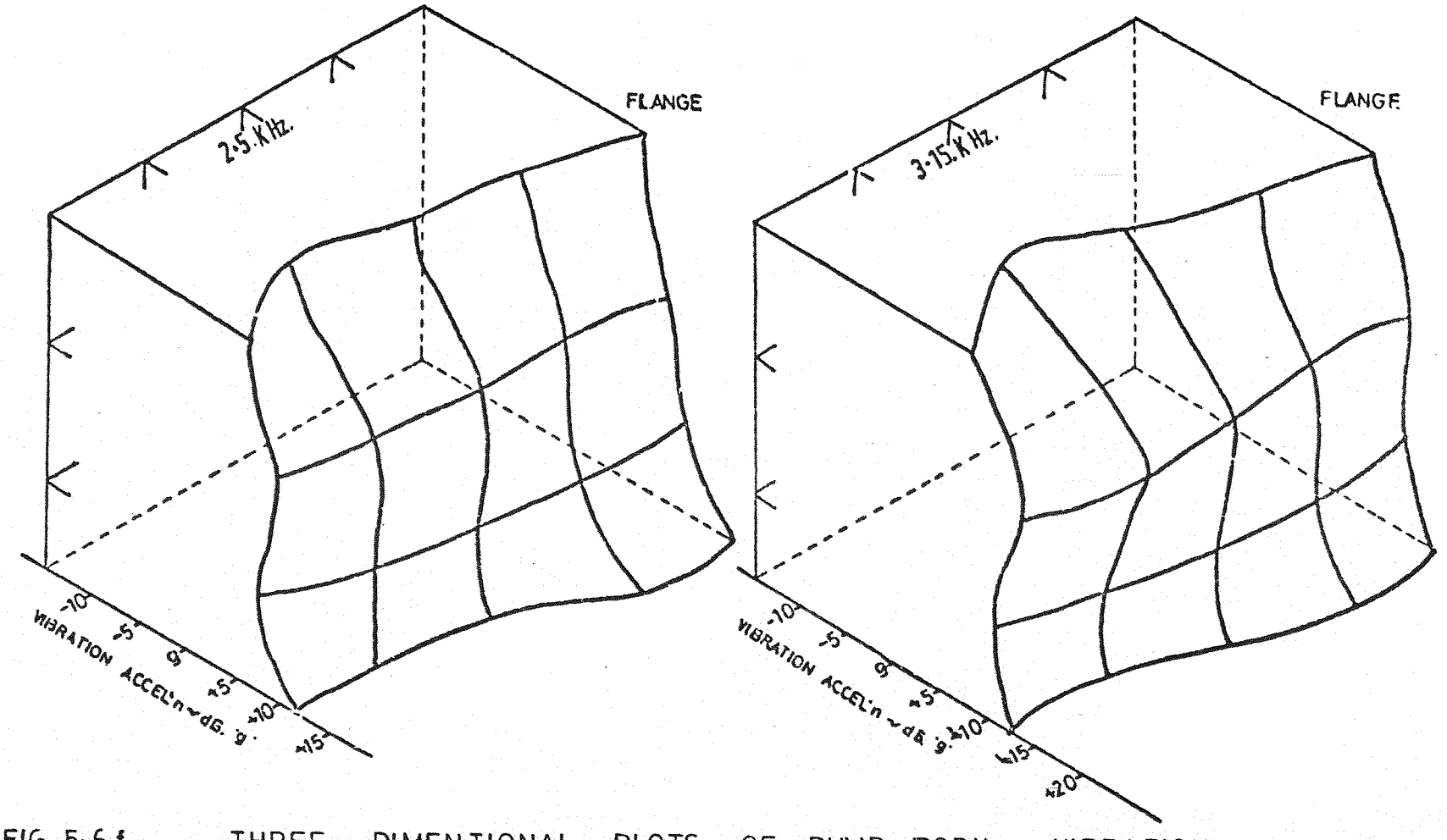

FIG. 5·6.f. THREE DIMENTIONAL PLOTS OF PUMP BODY VIBRATION.

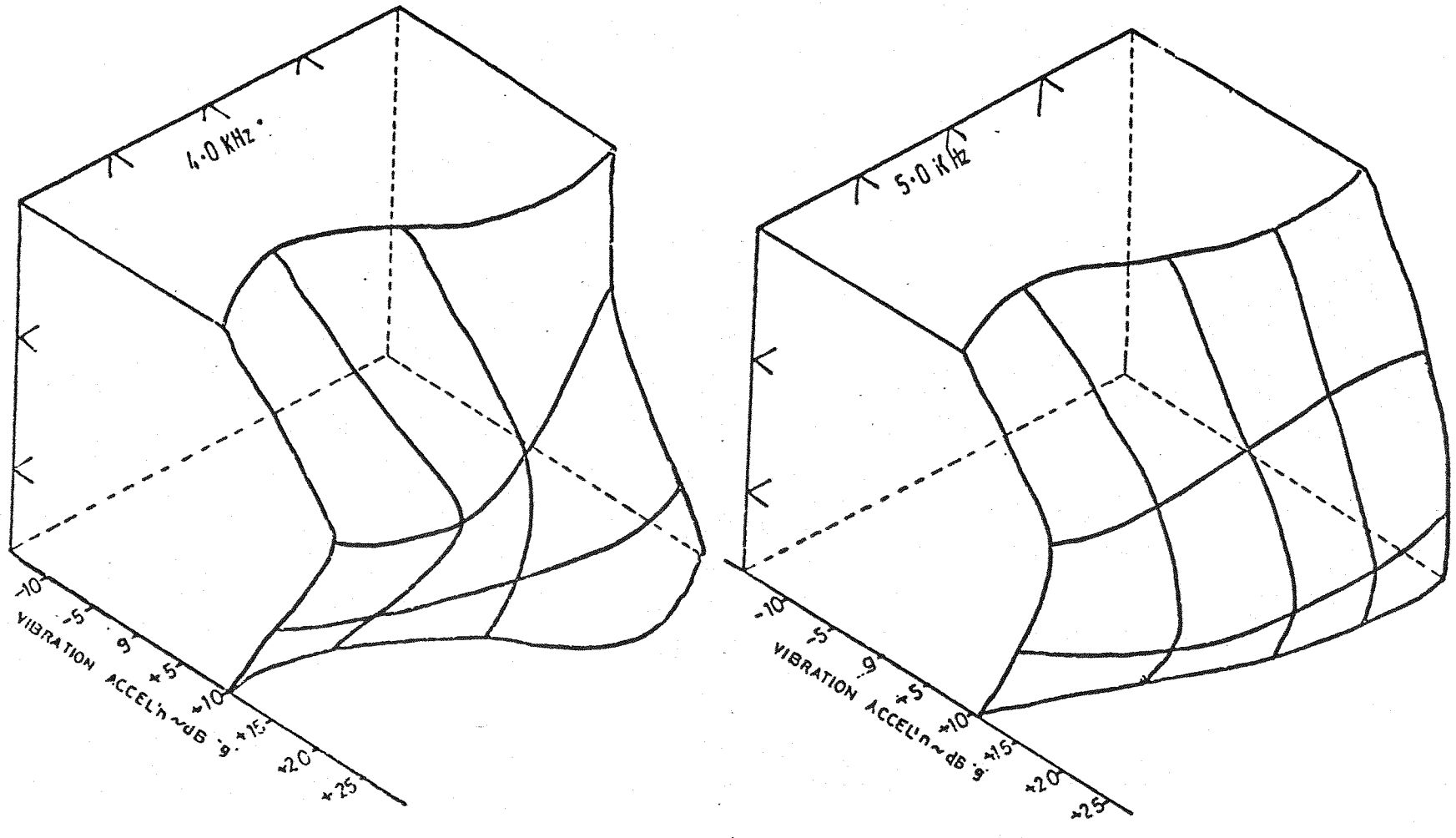

FIG. 5.6. g. THREE DIMENTIONAL PLOTS OF PUMP BODY VIBRATION.

thus vibrations are low. Due to the complexity of pump vibration a clearer indication of characteristics of vibration can be obtained by averaging vibration.

Figure 5.7 shows the vibration spectra averaged along the lines A, B, C, D. This illustrates how the four horizontal elements of the pump, i.e. top structure, inspection cover plate and the two sections of the cambox, vibrate. There is little variation of vibration in the vertical direction while in the high frequency range it is very clear that at the top of the pump the average vibration is about 10 dB lower than the lower part, i.e. clearly indicating the conical mode shape as it was observed from asymmetrical plots.

In the same way average spectra can be obtained along the vertical lines which enable the assessment of average distribution along the horizontal axis. Using the averaged lines, (i.e. horizontal elements of pump structure) average vertical plane vibration patterns can be obtained as shown in Figure 5.8. These, to some extent, provide somewhat clearer conclusions which enable one to classify vibration patterns as follows -

(1)	At 400 Hz	more or less uniform vibration in the vertical plane.
(2)	At 500, 650, 800 and 1000 Hz	minimum along the line B (inspection cover - where the pump structure is weak) and high levels at the top and the bottom.
(3)	1250 and 1600 Hz	high levels along the line (C) middle of the cambox decreasing towards top and bottom.
(4)	2000 and 2500 Hz	low levels at top and linear increase towards bottom of the pump.
(5)	3500, 6000 and 5000 Hz	low levels at top, uniform vibration of the rest of the pump.
(6)	6000 and 8000 Hz	low level at the top increases gradually towards bottom of the pump by some 15 dB.

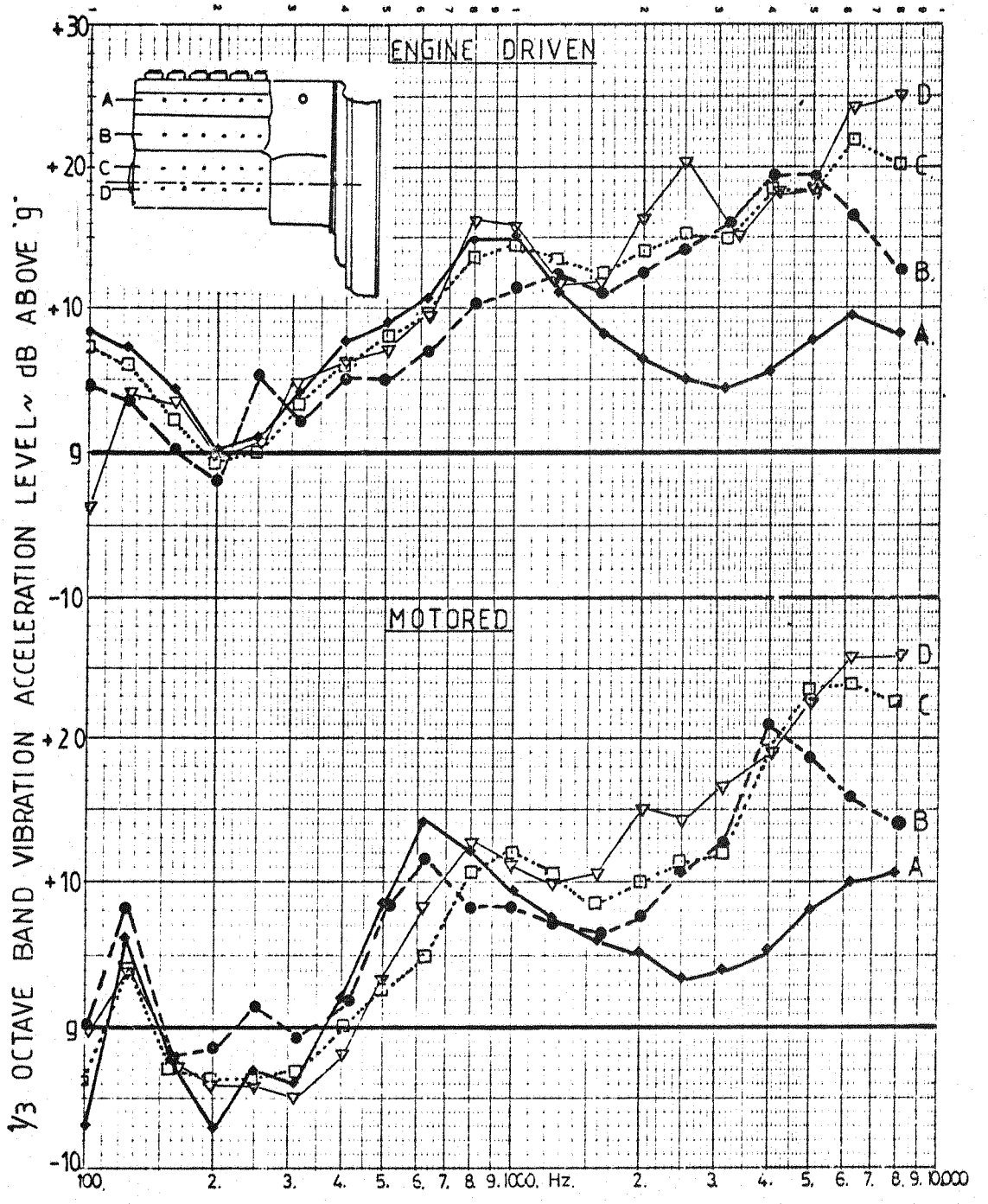

FIG.5·7. AVERAGED VIBRATION SPECTRA. DORSET PUMP. 1400.rpm.

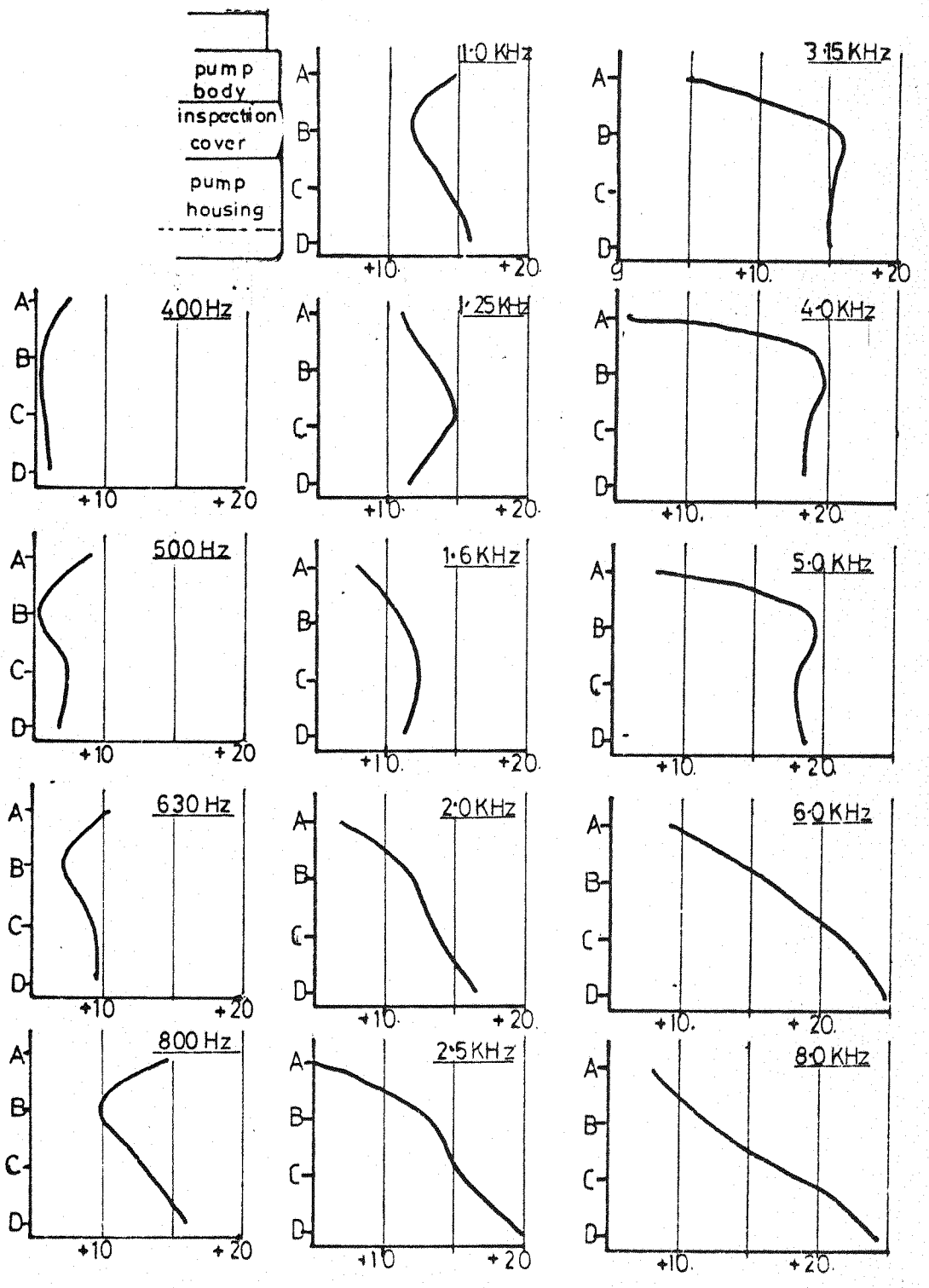

FIG.5·8 AVERAGED VIBRATION LEVELS IN VERTICAL PLANE ON PUMP CASING.

Finally, it is possible to arrive at and represent the pump vibration by average vibration spectrum as shown in Figure 5.9. Vertical lines on the spectrum indicate the maximum and minimum variation of vibration in a particular frequency range. The minimum, is about 8 dB (amplitude variation 13:1) while the maximum is about 30 dB (amplitude variation about 22:1).

5.1.1. Conclusions

From the three-dimensional plots of vibration distribution over the pump surface, the pump structure appears to exhibit plate type bending modes over the frequency range 1000 Hz to 8000 Hz. These are a combination of plate bending and torsional modes.

At around 800 Hz at the free end of the pump, high vibration levels at the top and bottom of the structure with low levels of vibration in the middle, suggest a torsional mode of the whole pump body.

Increase in vibration levels from the top part of the pump towards the bottom of the pump, over the frequency range above 2000 Hz suggest a conical mode, i.e. where the applied forces tend to be more effective at the lower part of the pump

The variation in vibration plotted in a vertical plane down the pump structure shows that over the high frequency range the average vibration levels, at the top of the pump, (stiff section) are some 10 dB lower than the lower part of pump indicating a conical mode as observed previously.

5.2. Vibration Characteristics of Engine Block

The engine vibration characteristics (in this instance only the block and crankcase) have been investigated in a similar manner to the pump. Figure 5.10 shows the vibration spectra plotted along the lines A,B,C and D, each group representing 11 spectra from individual measuring points along the particular line.

The spectra show strong broad peaks around 315 Hz and also significant levels of vibration in the high frequency range from 1000 Hz upwards. Figures 5.11a,b,c,d,e,f,g, show three dimensional plots of engine block and crankcase vibration.

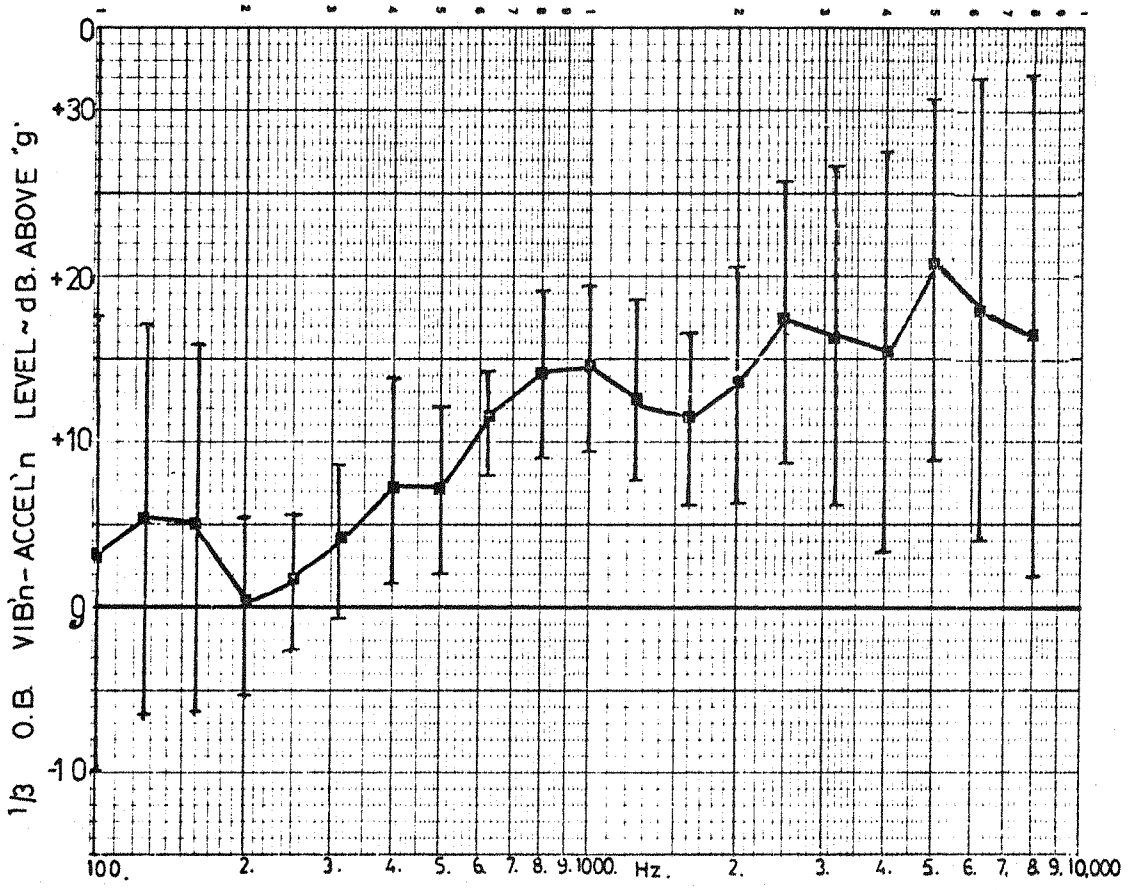

FIG.5·9. AVERAGE VIBRATION SPECTRUM.

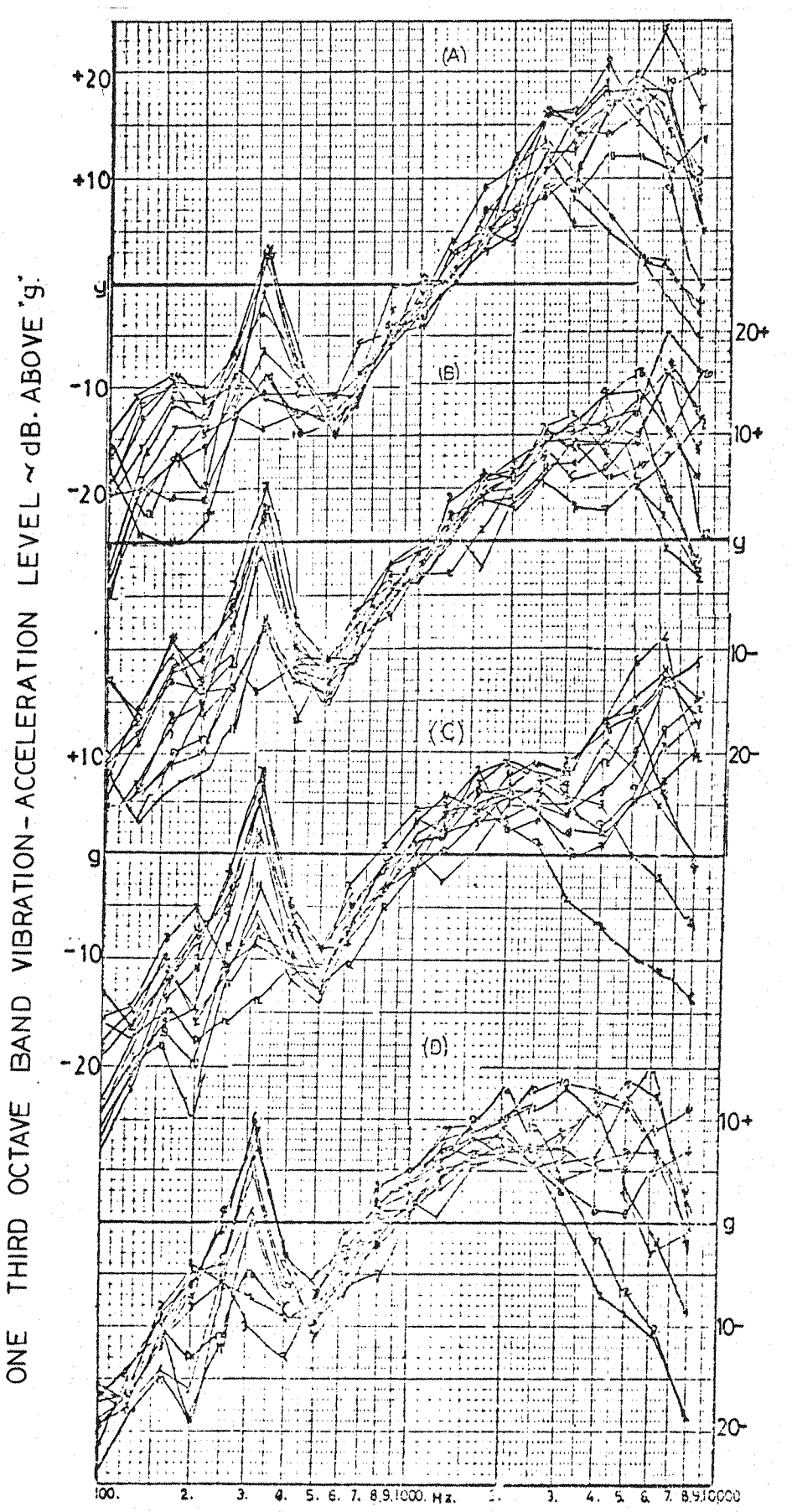

FIG 5·10 VIBRATION SPECTRA. HORIZONTAL PLANE. ENGINE BLOCK AND CRANKCASE.

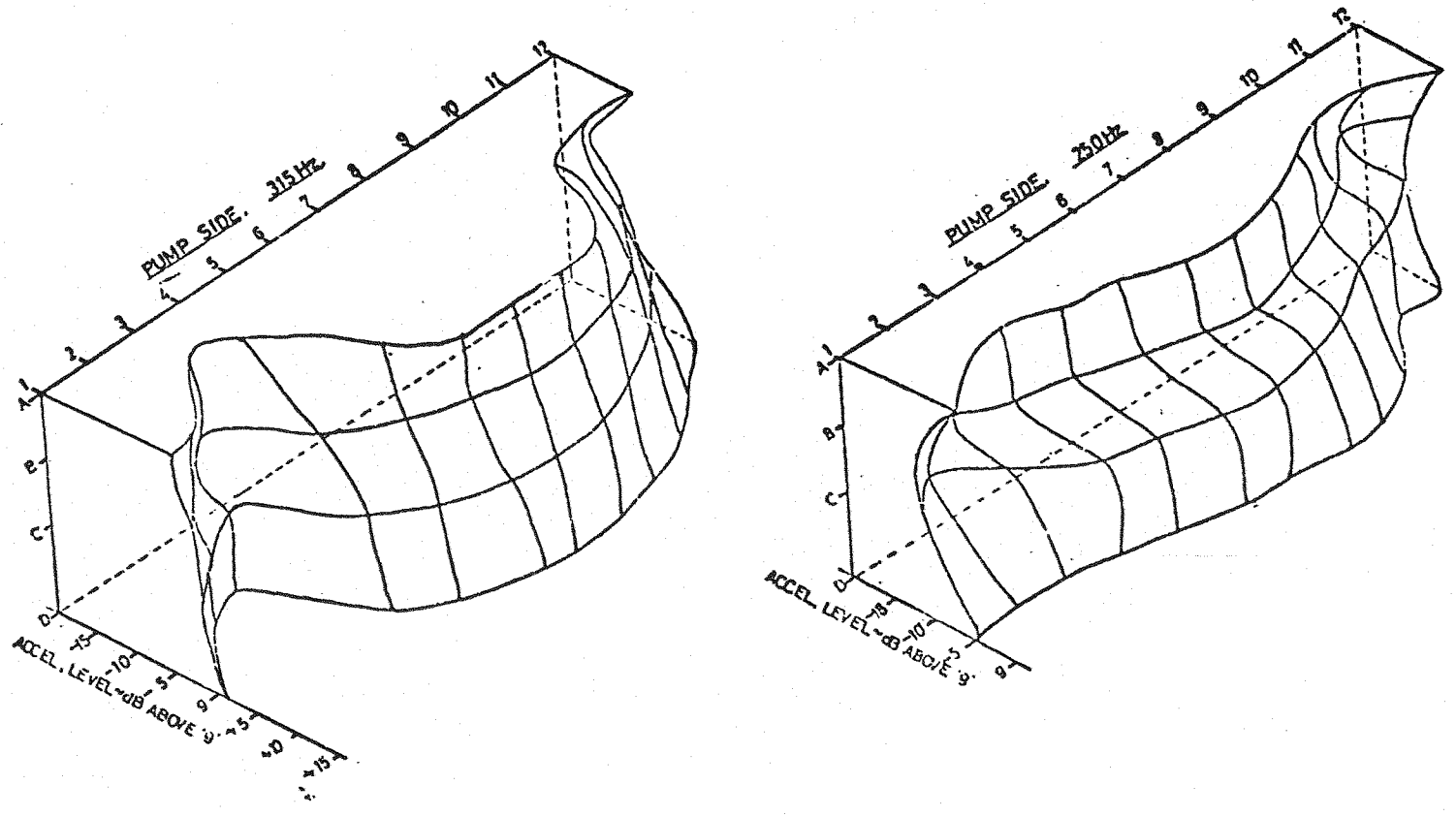

FIG. 5·11. a. THREE DIMENSIONAL PLOTS OF ENGINE BLOCK AND CRANKCASE VIBRATION.

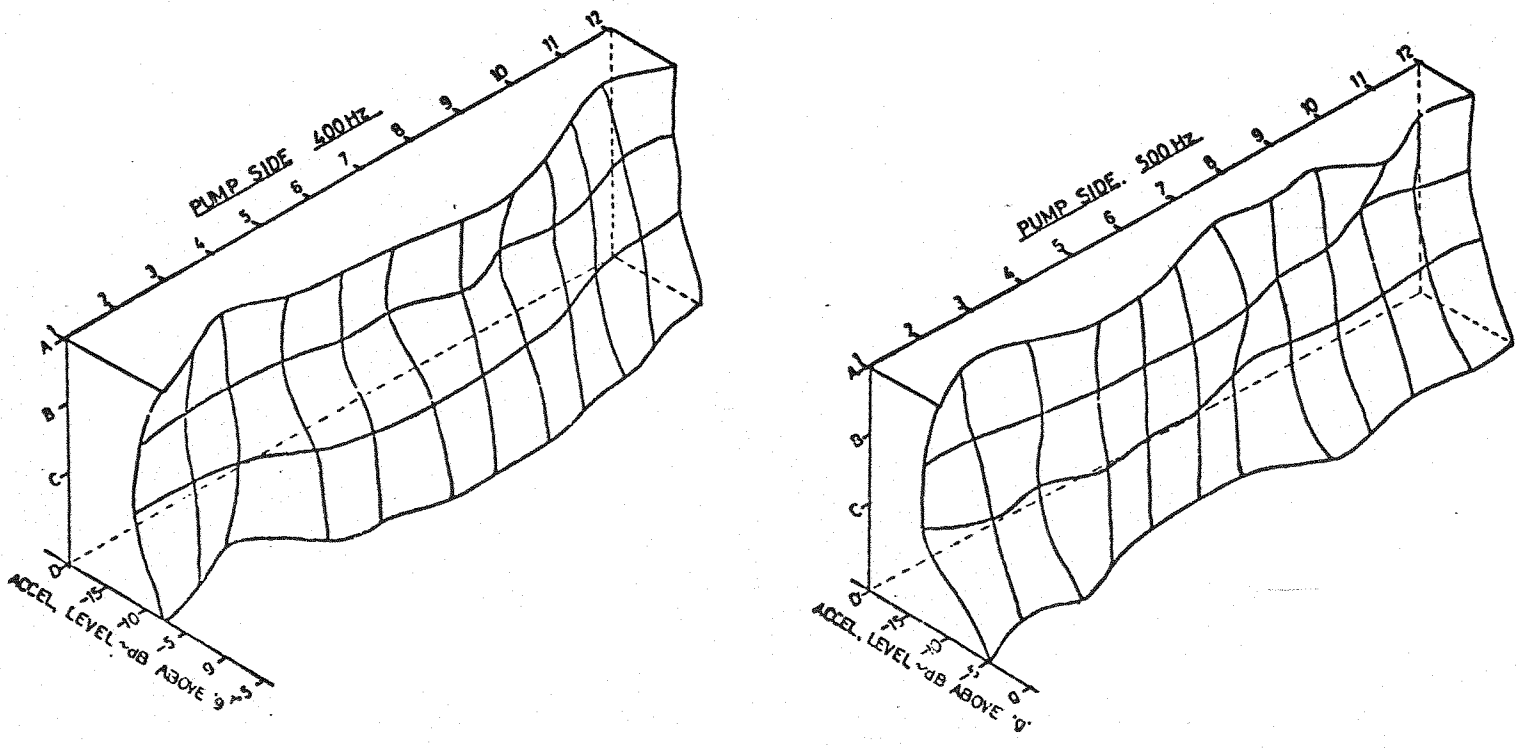

FIG. 5·11.b THREE DIMENSIONAL PLOTS OF ENGINE BLOCK AND CRANKCASE VIBRATION.

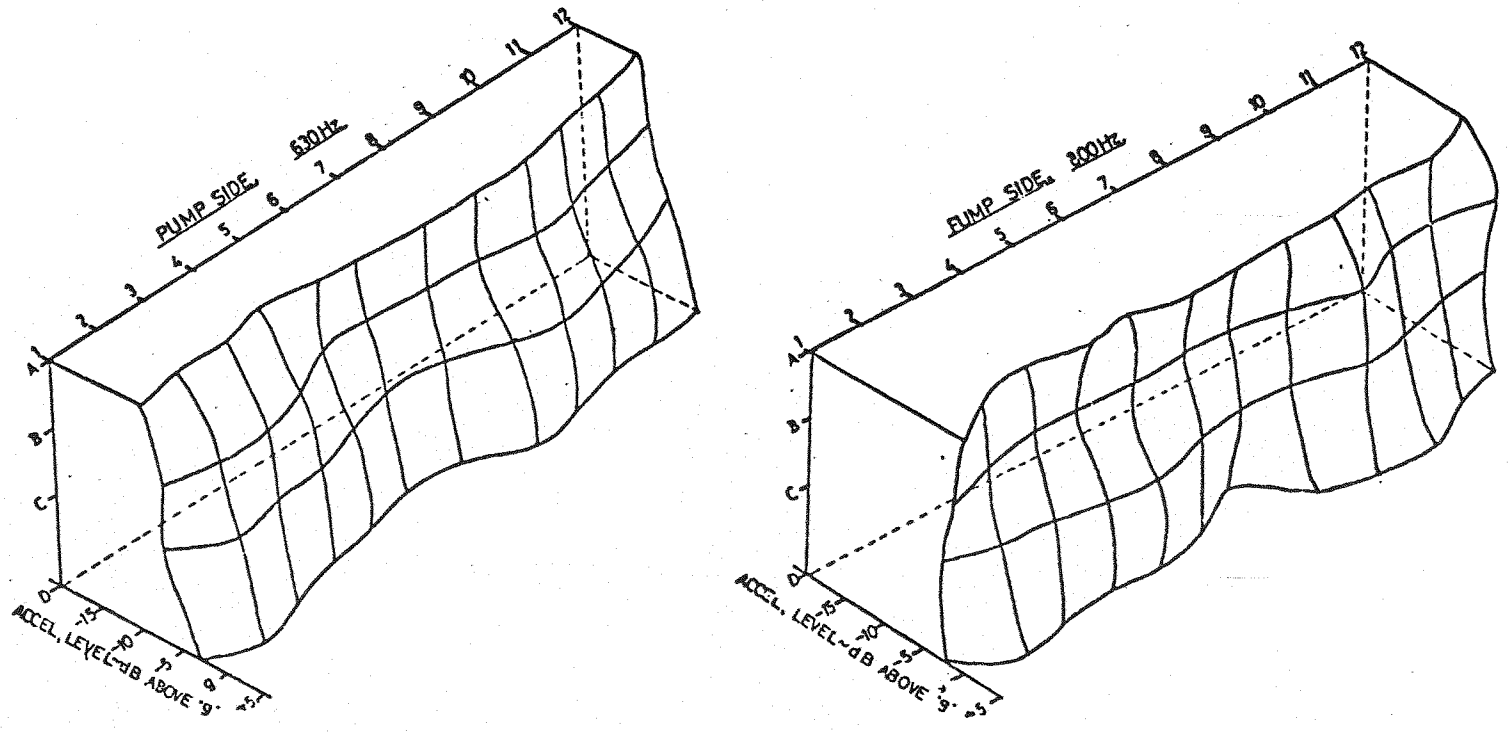

FIG. 5-11.c THREE DIMENSIONAL PLOTS OF ENGINE BLOCK AND CRANKCASE VIBRATION.

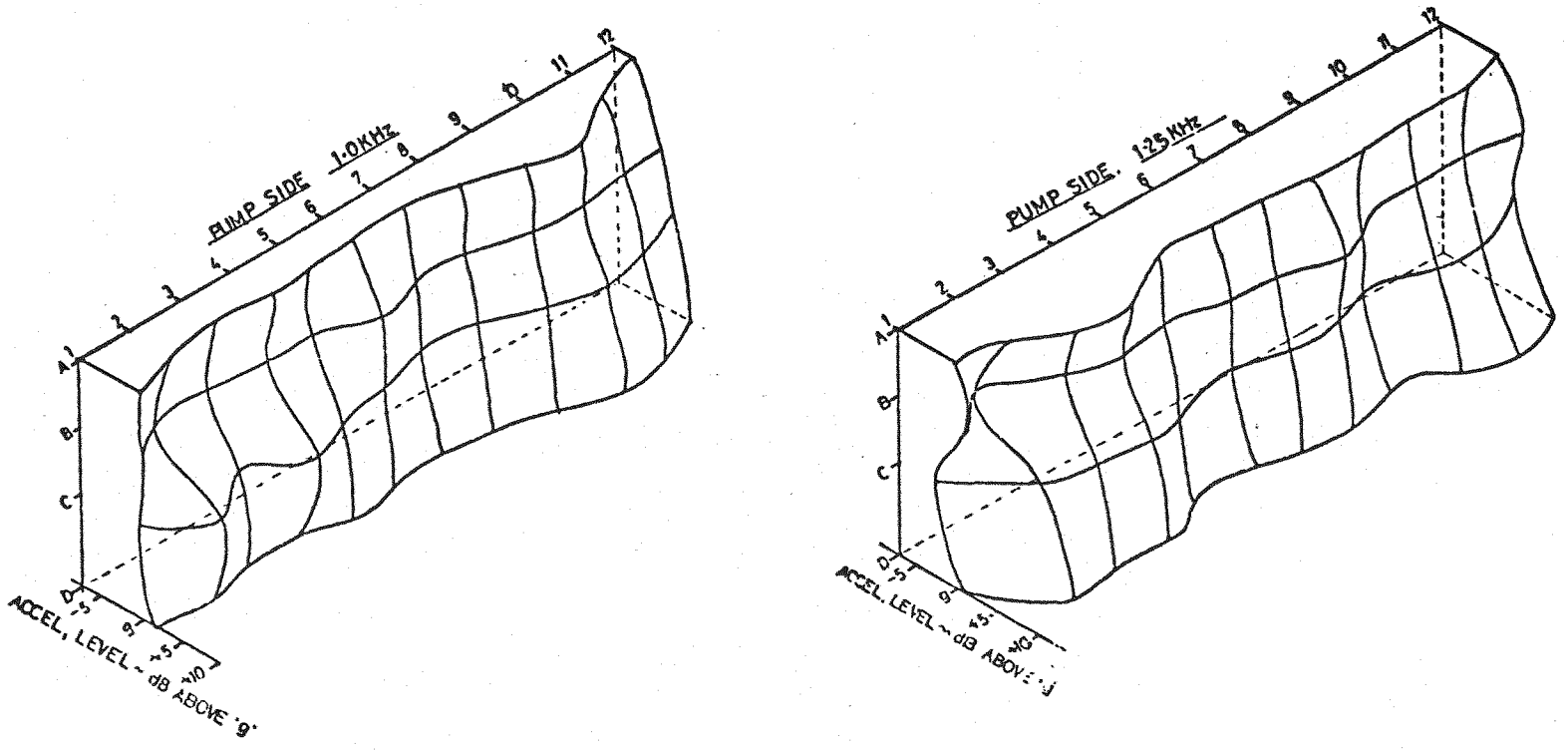

FIG. 5·11.d. THREE DIMENSIONAL PLOTS OF ENGINE BLOCK AND CRANKCASE VIBRATION.

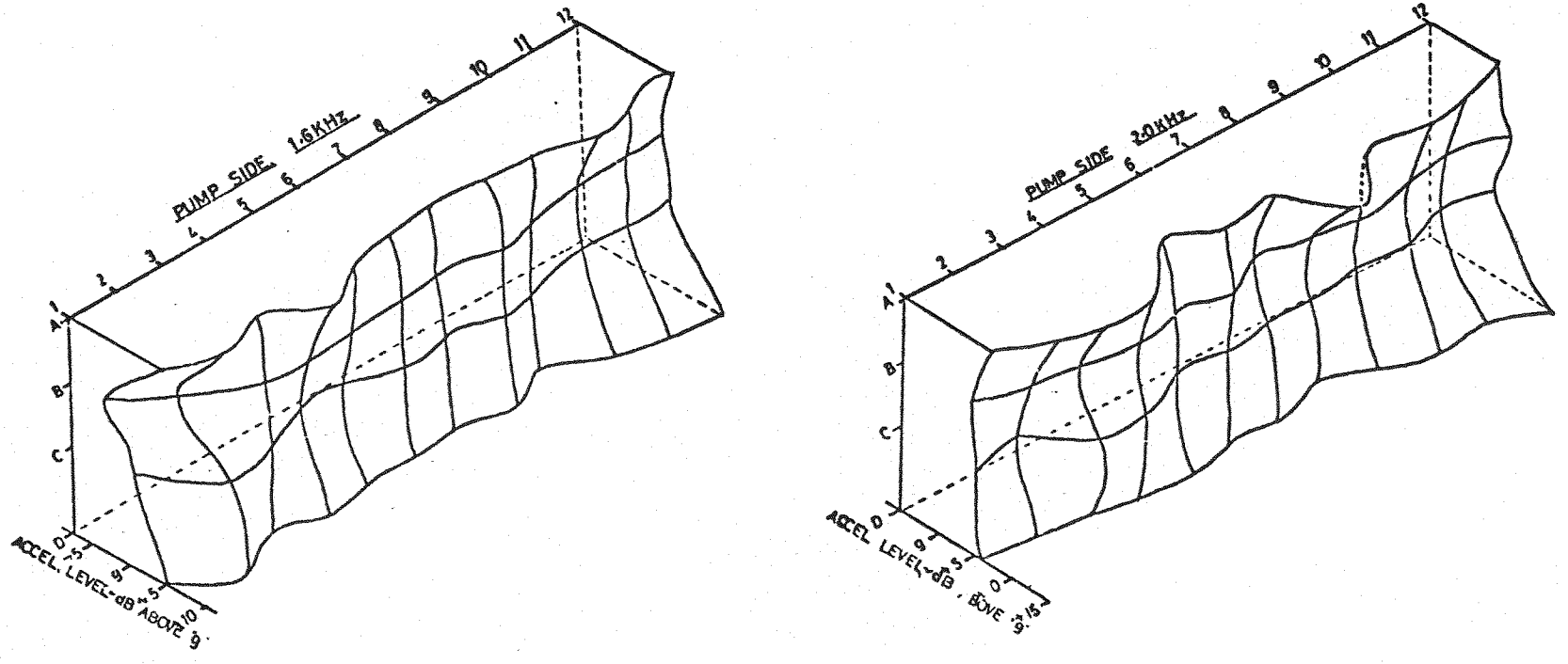

FIG 5·11.e THREE DIMENSIONAL PLOTS OF BLOCK AND CRANKCRASE VIBRATION

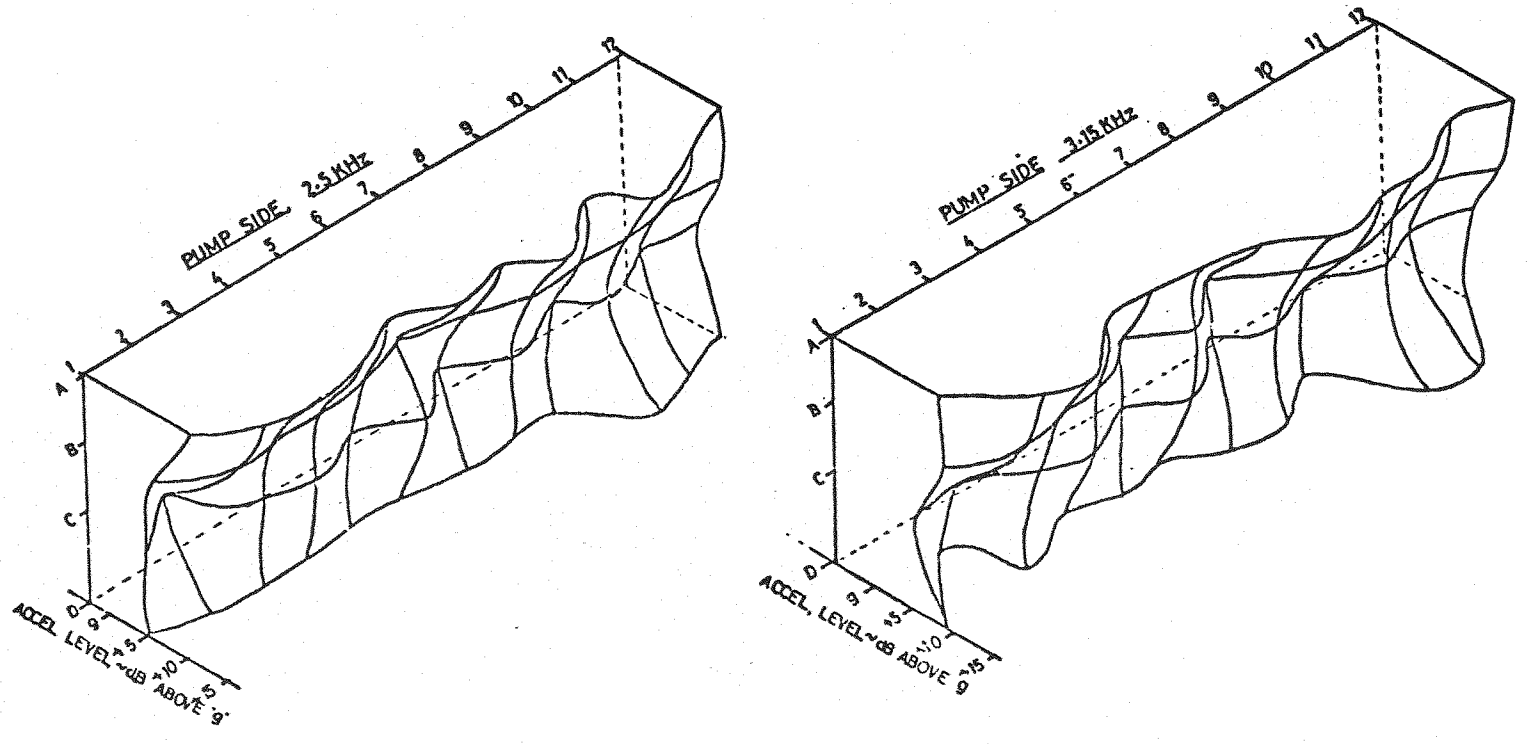

FIG.5.11.f. THREE DIMENSIONAL PLOTS OF BLOCK AND CRANKCASE VIBRATION.

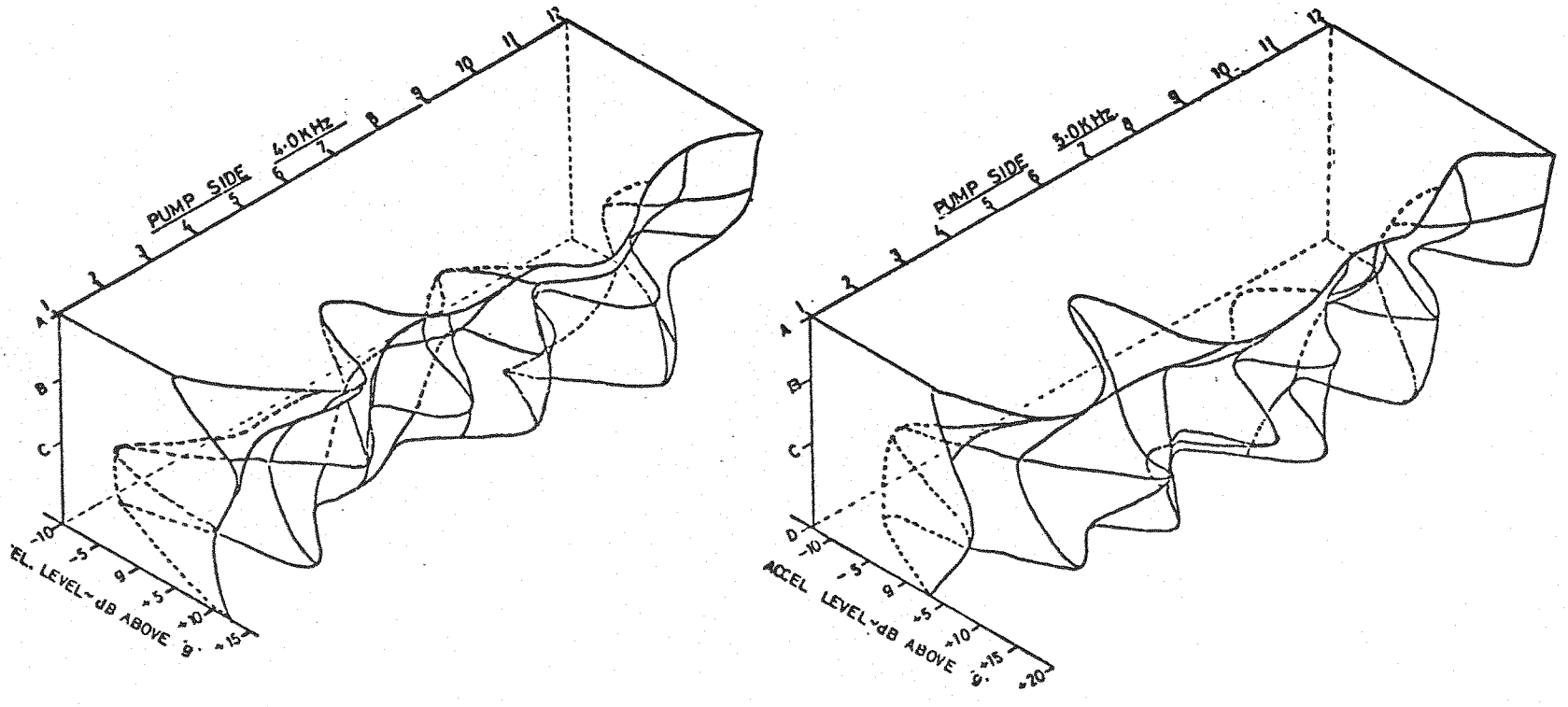

FIG.5·11.g. THREE DIMENSIONAL PLOTS OF ENGINE BLOCK AND CRANKCASE VIBRATION.

It is not intended to define in detail the engine vibration characteristics but it can be clearly seen that plate type modes of vibration occupy the low frequency range up to 1250 Hz. A very clear free-free beam type mode can be seen in Figure 5.11a at 315 Hz. Above 1250 Hz the structure breaks up in typical panel modes with the modal lines situated along the heavy sections of the casting, i.e. bulkheads, top and the bottom decks of the engine structure.

Comparing these asymmetric plots with those of the injection pump it is obvious that the injection pump has no panel modes present.

Figure 5.12 shows the vibration spectra averaged along lines A,B,C and D, respectively, of the engine structure and Figure 5.13 represents the engine vibration by average vibration spectrum. The vertical lines indicate maximum and minimum variations of vibration in each particular frequency range. The minimum, as can be seen, is about 10 dB variation in vibration level while the maximum is about 37 dB variation in vibration level.

5.3. Conclusions

Vibration spectra plotted along the block and crankcase show a very strong broad peak around 315 Hz. The vibration levels over the high frequency range from 630 Hz to 5000 Hz increase significantly with increase in frequency.

The three-dimensional plots of the block and crankcase vibration show a well defined free-free beam type mode. Over the high frequency range above 1250 Hz the structure breaks up into typical panel modes with modal lines situated along the heavy sections, i.e. bulkheads, top and bottom decks of engine casting.

Comparing these three-dimensional plots with those of the injection pump it appears that the injection pump has no panel modes present.

5.4. Comparison of Average Engine and Pump Vibrations

Figure 5.14 shows the average vibration spectra of the pump and engine block and crankcase. The pump vibration is significantly higher than that of the engine except for two regions (a) one at

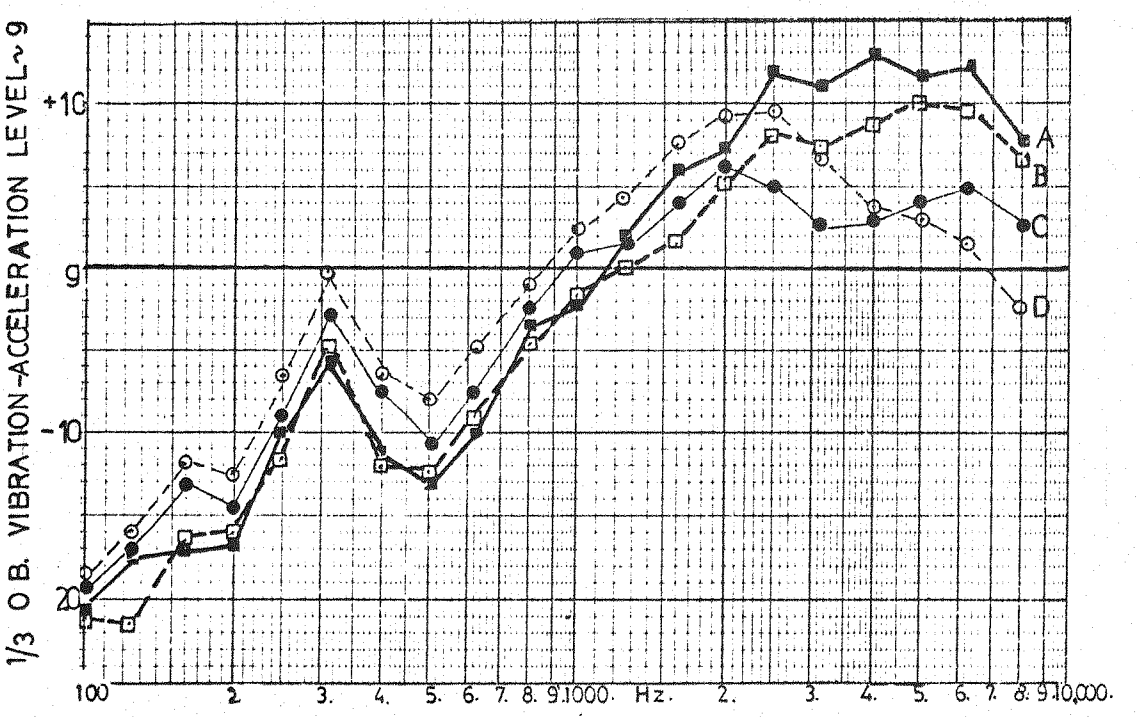

FIG.5·12. AVERAGE VIBRATION LEVELS ON ENGINE STRUCTURE

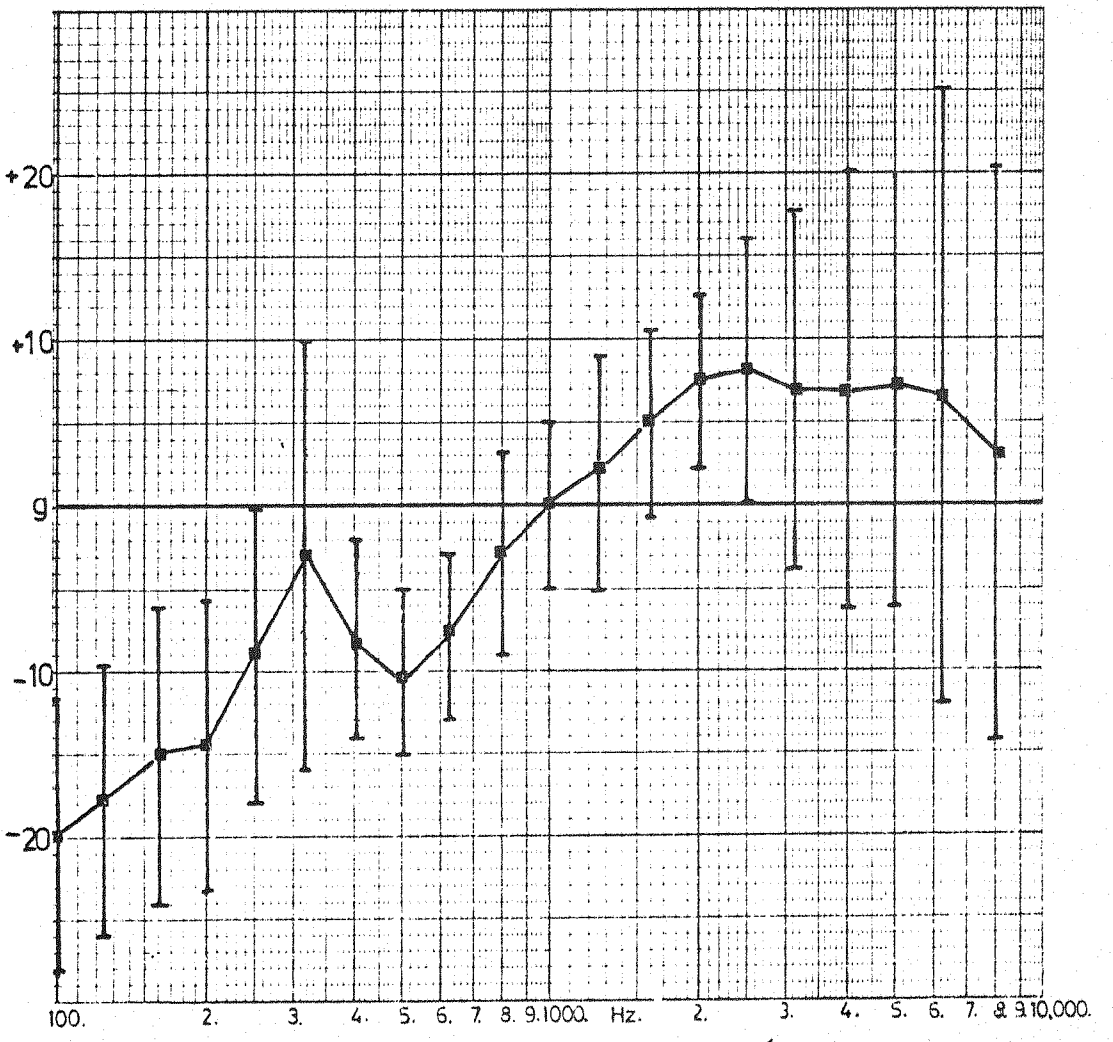

FIG.5·13. AVERAGE VIBRATION SPECTRUM. (LINES.A.B.C.D.)

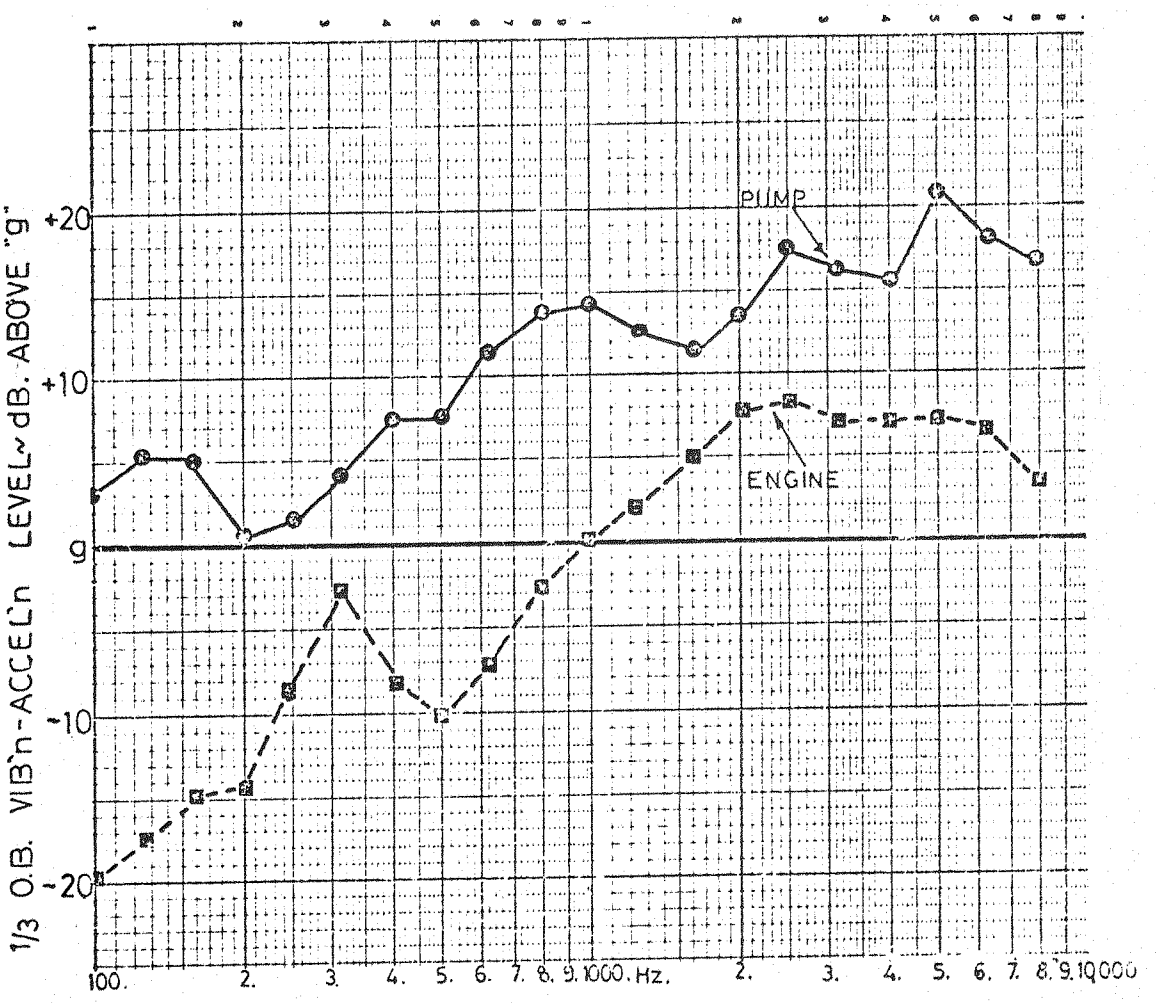

FIG.5.14 AVERAGED VIBRATION LEVELS ON ENGINE AND PUMP

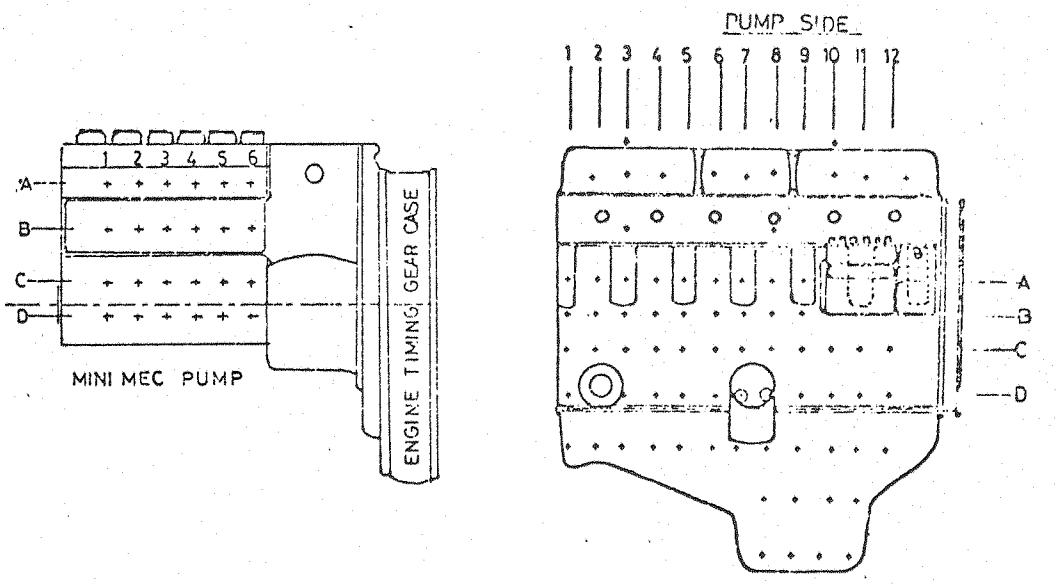

315 Hz where engine vibration is high due to its fundamental bending mode and (b) other at high frequencies from 2000 Hz to 4000 Hz where pump vibration is only marginally higher, 5-8 dB, than the engine vibration.

The same analysis was carried out for all other engines and pumps tested and the results in terms of average spectra are summarised in Figure 5.15. Pump vibrations in this instance were measured on the running engines.

In general, in all the normally aspirated engines the mean vibration levels of the pump are higher than those of the engine block. On the turbocharged engine (C) the pump vibration levels are higher than the block vibration levels over the low frequency range up to 400 Hz, but above 400 Hz the pump and engine block vibration levels are of the same magnitude.

The main reason why pump vibration levels are somewhat lower is that engine (C) was fitted with a low noise Maximec pump developed by C.A.V. Ltd., (5.3).

On the normally aspirated engine the pump vibration levels are on average about 10 dB to 15 dB higher than the engine block vibrations over most of the frequency range up to 3000 Hz. Above 3000 Hz the difference between the engine block and the pump in general becomes smaller and is about 3 to 6 dB. Only on one of the engines, i.e. engine (A), does the engine block vibration exceed the pump vibration in the higher frequency range over 2000 Hz by some 3 to 7 dB. On this particular engine the mounting arrangement of the pump appears to be responsible. Since the general trend is for the pump to have higher vibration levels than the engine, an attempt was made to find a basic explanation and relate the injection pump and engine structure vibration to the characteristics of the relevant exciting forces.

Engine (E) was chosen for the detailed analysis to explain the basic reasons why the pump surface vibrations are generally significantly higher than the engine surface vibrations. The analysis is based on comparing the characteristics of the engine exciting forces with those in the pump and relating them with relevant structural characteristics.

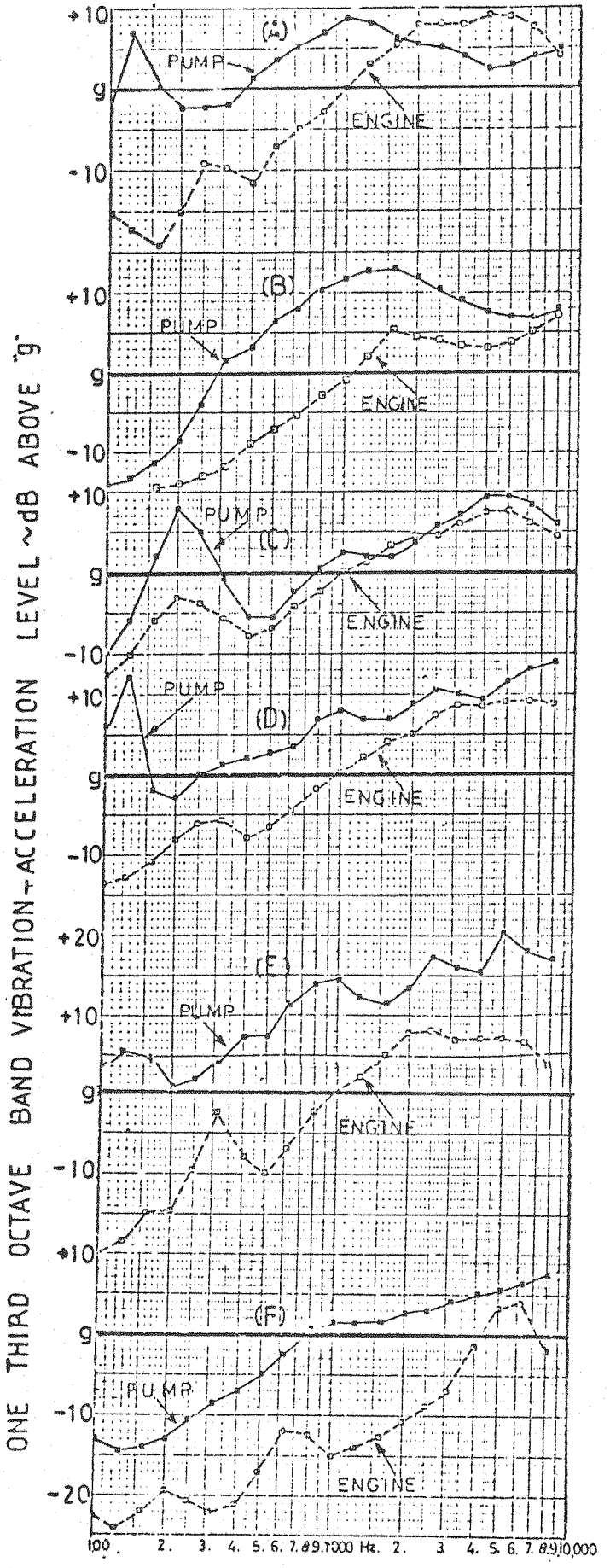

FIG 5·15. COMPARISON VIBRATION SPECTRA. (AVERAGED.)

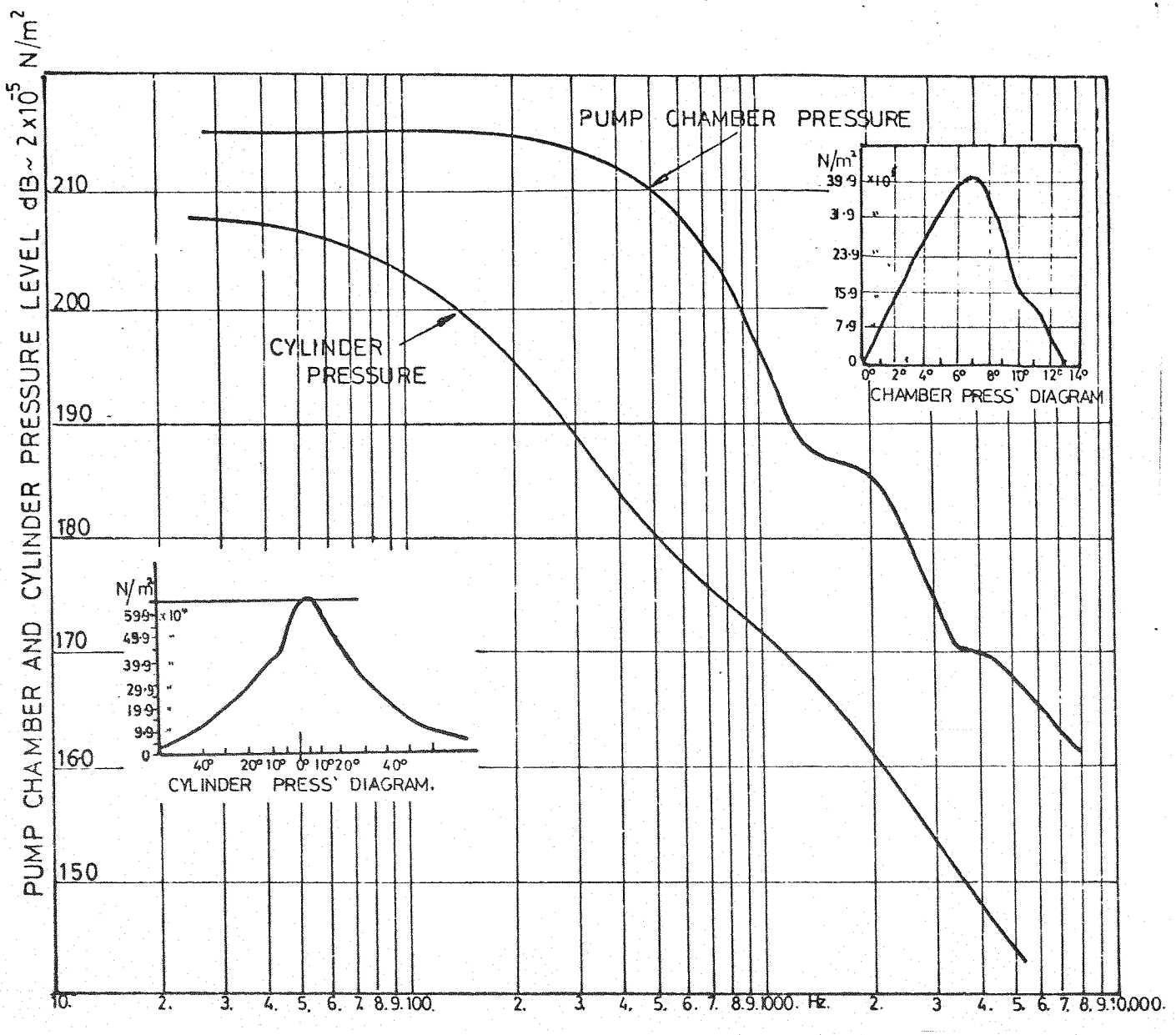

FIG. 5·16 PUMP CHAMBER AND CYLINDER PRESSURE SPECTRA.

Figure 5.16 shows the cylinder pressure spectrum of engine E and the hydraulic chamber pressure spectrum of its in-line pump. The spectra indicate that excitation per unit area of the pump is higher by 10 dB over the low frequency range up to 150 Hz, and 20-30 dB higher over the frequency range from 200 Hz to 1000 Hz, and some 20 dB higher over the high frequency range above 1000 Hz. Since the respective areas of the pump plunger and engine piston are different (area ratio 40 dB) it is more meaningful to consider the spectra of the forces acting on the pump structure and engine structure. The pressure spectrum shown in Figure 5.16 thus requires correction by 40 dB in order for comparisons in terms of relative force to be made.

i.e. ΔdB = L plunger - L cyl. pressure

Δ dB = 30 dB

Thus $20 \log_{10} \frac{P_{plunger}}{P_{piston}} = 30$ dB

the pressure ratio is therefore

$$\frac{P_{plunger}}{P_{piston}} = AL \frac{30}{20} = 31.5$$

The ratio of respective areas of piston and plunger are

$$\frac{\text{Area of piston}}{\text{Area of plunger}} = \frac{100}{1}$$

The ratio of force

$$= \frac{F_{piston}}{F_{plunger}} = \frac{P_{piston}}{P_{plunger}} \times \frac{A_{piston}}{A_{plunger}} = \frac{100}{31.5}$$

and the ratio of forces in terms of force levels in dB

$$20 \log_{10} \frac{F_{piston}}{F_{plunger}} = 20 \log_{10} \frac{100}{31.5} = 20(2-1.5) = 10 \text{ dB}$$

The plotted modified force spectrum is shown in Figure 5.17 which indicates that the level of combustion exciting force is higher than the pump exciting force over the whole frequency range. In the low

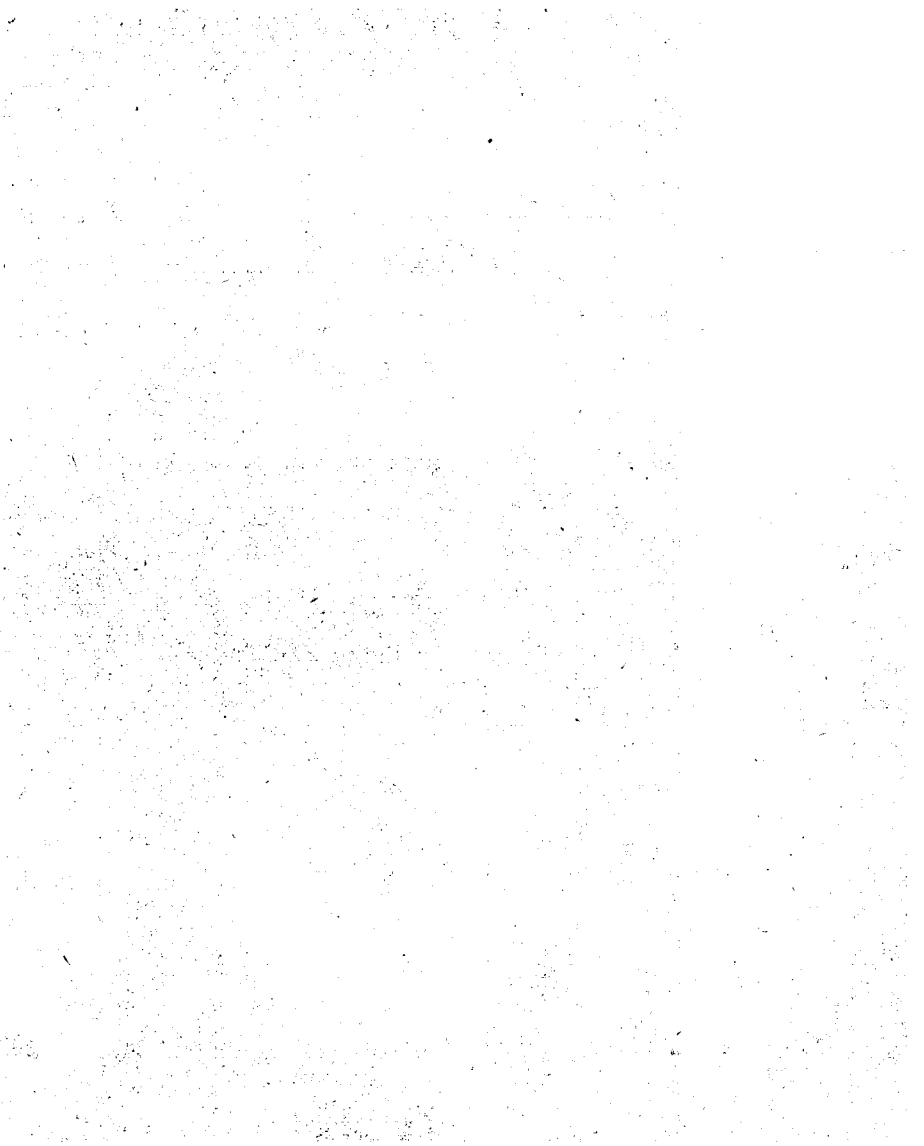

* For this simplified analysis, only vertical forces are considered for both systems. For the engine horizontal forces acting on piston and main bearings do exist but these are an order of magnitude lower than the vertical ones. On the fuel injection pump any horizontal force can only be transmitted via the roller/cam interface and this must always be considerably smaller than vertical force.

frequency range it is higher by some 32 to 28 dB up to 100 Hz, about 10 dB around 500 Hz to 800 Hz and some 15 to 20 dB over the high frequency range above 1000 Hz.

The basic reasons for the observed higher vibration levels on the pump, despite the considerably lower levels of exciting forces, can be shown by the following simple analysis.

The strength of the structure is proportional to the typical dimension L.*

$$\text{Deflection} = \frac{\text{Force}}{\text{Stiffness}} \qquad \frac{\text{Force}}{L}$$

The bore of the engine is about 10 times the pump plunger bore (B). The actual forces which are calculated on the engine and pump are therefore :

Force F on piston = 174.2 N
" F " plunger = 50.2 N
} calculated from Figure 5.16 at 400 Hz

If the principal dimension L is taken as diameter of the bore then ratio deflection

$$= \frac{\text{pump}}{\text{engine}} = \frac{50.2/B}{174.2/10B} = 2.88$$

Expressing this ratio in decibel units the difference in vibration levels between engine and pump can be derived thus:

$$20 \log_{10} \frac{\text{Vibration level pump casing}}{\text{Vibration level engine structure}}$$

$$= 20 \log_{10} 2.88 = 9.2 \text{ dB}$$

This analysis indicates, for example, that at a frequency of 400 Hz, the average vibration level of the engine should be some 9.2 dB below that of the pump. The difference, as can be seen, is somewhat greater which may be due to the fact that comparison is made between an aluminium structure (pump) and a cast iron structure (engine). The trend indicated by this simple calculation, however, shows clearly the basic fundamental principle involved.

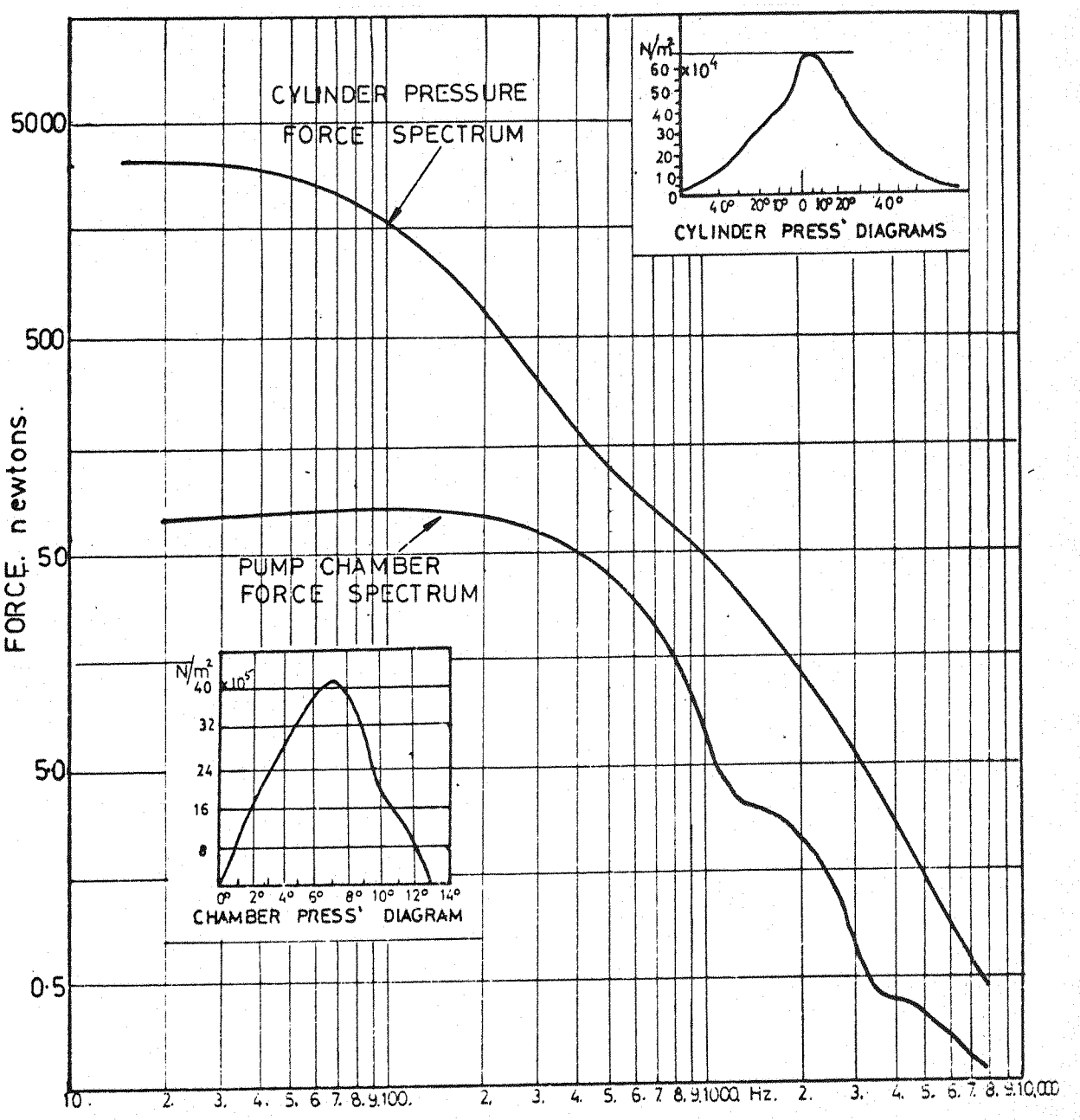

FIG. 5·17. PUMP CHAMBER AND CYLINDER PRESSURE FORCE SPECTRA.

5.5. Injection Equipment Excited Engine Structure Vibration

Numerous tests were made on stationary engines with only the injection pumps motored by means of a hydraulic motor. Figure 5.18 illustrates typical results. Spectrum (A) represents the mean pump vibration when it is driven by the running engine while the spectrum (B) shows pump vibration when driven from an external source. There are some discrepancies, but the general shape of the spectra are very similar and the differences between the two spectra from 500 Hz upwards do not exceed 2 to 3 dB. The running engine condition, however, does indicate that the pump vibration is by a small amount greater which may suggest that the engine input torque, which is transmitted through a series of timing gears, may be more impulsive and thus contributes to the slightly higher excitation. Similar findings were obtained on engine (F) (base mounted) as shown in Figure 5.20.

Spectrum D shown in Figure 5.18 shows the mean vibration of the engine block resulting from excitation from the injection system alone. As can be seen the block vibration is on average about 25 dB lower than in an actual running condition. This corresponds with the lower magnitude of exciting force generation in pumps (comparison of force level spectra, Figure 5.16, Section 5.4). It is of interest to note in this instance some similarity between the mean pump vibration spectra and the mean engine vibration spectra (spectrum B and D). The engine, tends to exhibit the broad humped peak around 800 Hz. On the running engine (spectrum C) this is not obvious due to generally higher levels.

The response of other engine components due to injection system excitation are also illustrated, namely sump (spectrum E) and valve cover (spectrum F). It is generally found on a running engine that both these components show considerably greater response, and as can be seen the response is also greater due to injection system excitation. These spectra show typical resonant peaks which correspond with the natural frequencies of lightweight covers of the engine. The response of the inlet and exhaust manifold tends to be some 10 dB lower.

Engine structure response can be expressed in terms of structure attenuation. This method was proposed by Austen and Priede (5.4),

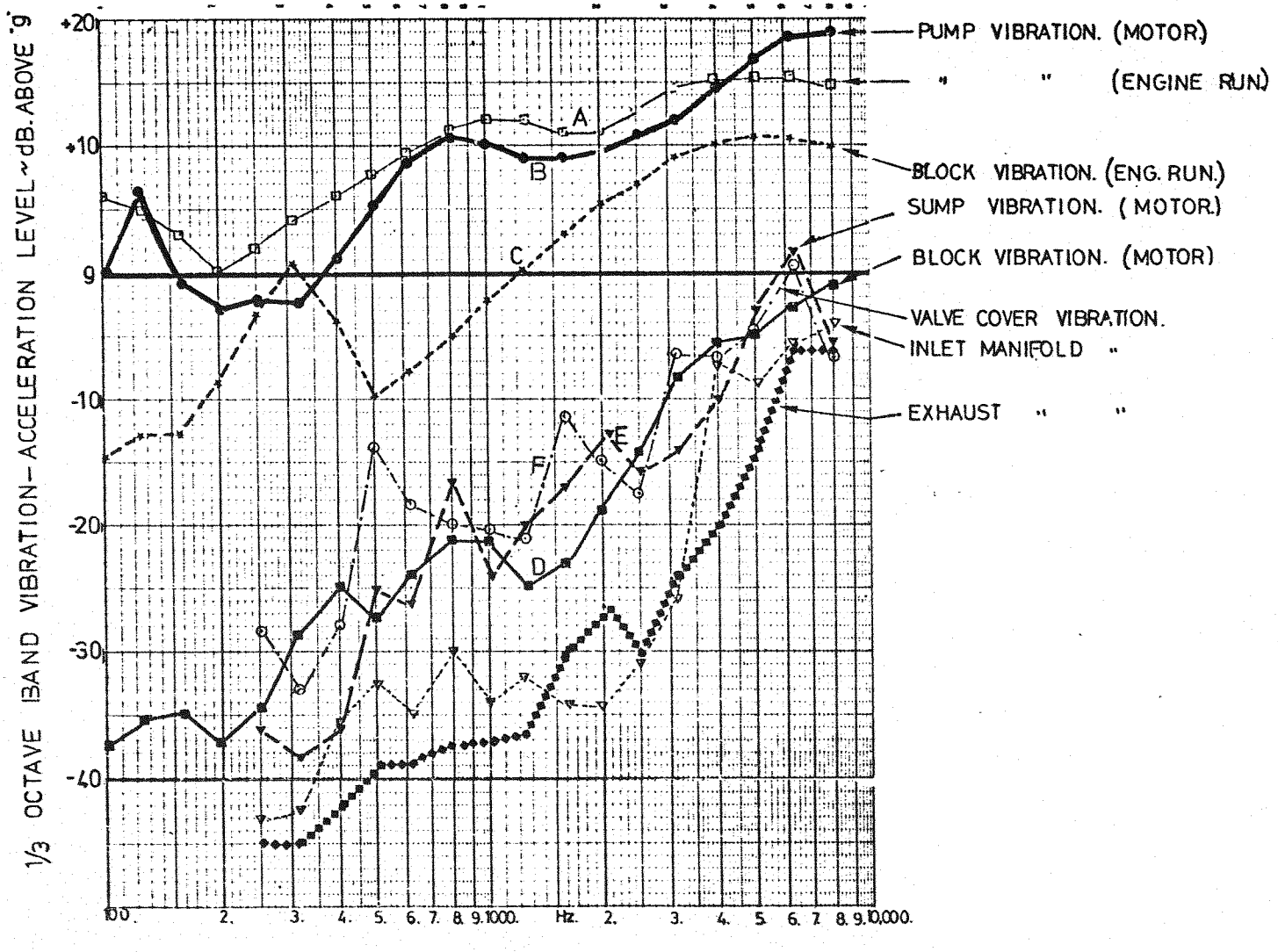

FIG.5.18. AVERAGED VIBRATION SPECTRA.

i.e. structure acoustical attenuation which was defined as differences between the exciting force level and emitted noise. Since the introduction of the principal of mean vibration levels of structure, in this study, it is possible to define attenuation itself from combustion exciting force and the injection pump exciting force. Thus two graphs of structure attenuation have been calculated:

(A) Structure attenuation EC = combustion force level - its mean block vibration level

(B) Structure attenuation EP = pump force level - its mean engine block vibration level

Figure 5.19 shows a line diagram of engine and pump illustrating the gas and hydraulic forces. As shown in Figure 5.20 both attenuation curves are of almost the same magnitude and shape. This indicates in effect that the engine block vibration is primarily determined by the force level irrespective of its origin, i.e. either gas force or hydraulic pump force. For comparison, structure attenuation curves of the injection pump are shown in spectrum C. This shows that the pump attenuation is considerably lower than that of the engine block as already discussed in the previous section (5.4) (Figure 5.16).

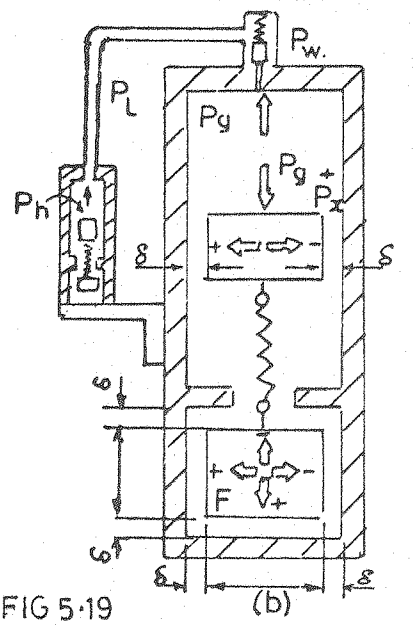

FIG 5·19

There is, however, indication that pump excitation and engine attenuation curves of the block are not exactly of the same magnitude. There are frequency regions where the differences may be as great as 10 dB but generally the orders of magnitude are the same. There is one aspect which still requires consideration and that is excitation from the injector. Injector operation in these comparisons is the same whether the engine is running under its own power or the injection pump is motored.

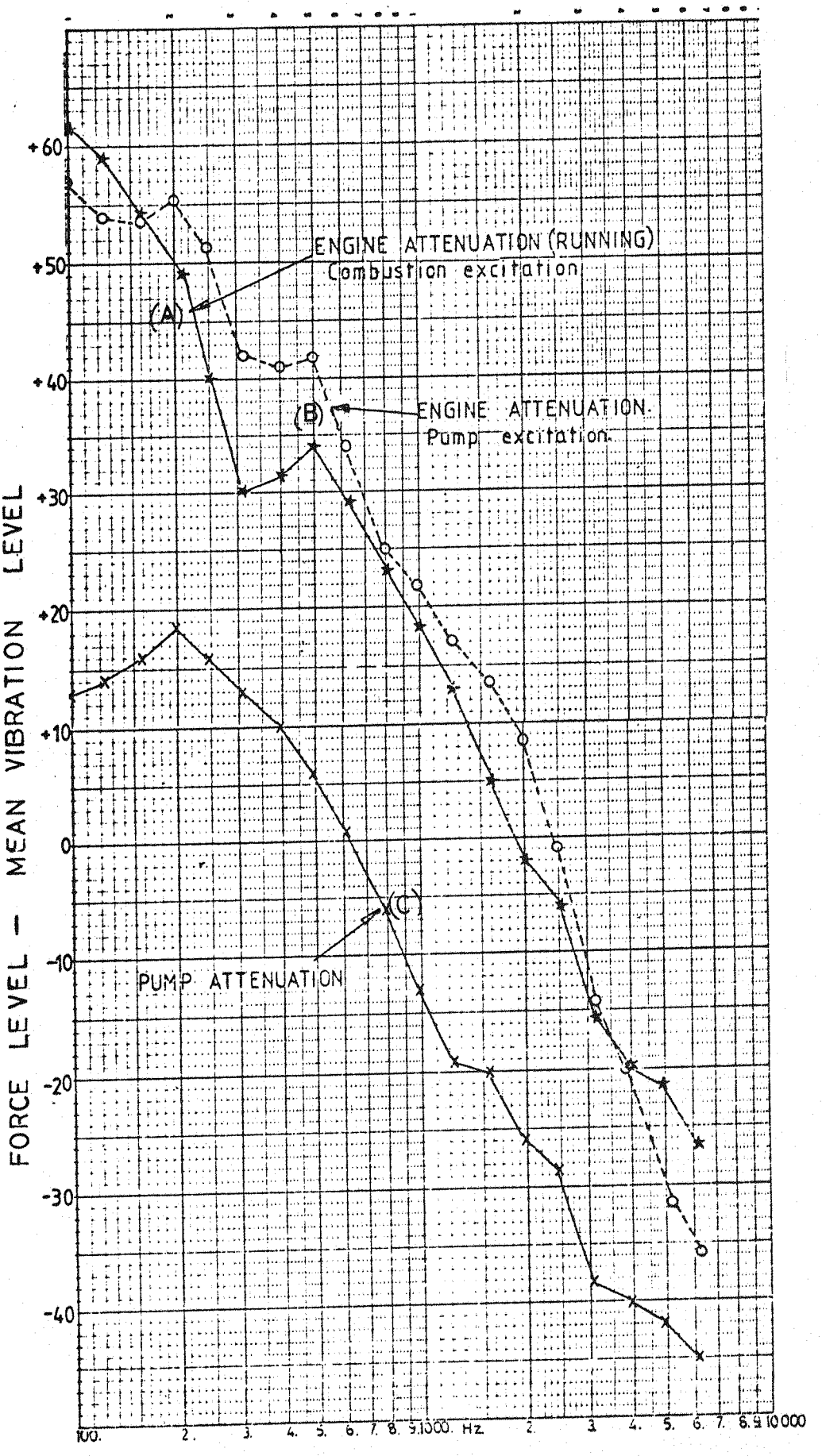

FIG. 5·20. STRUCTURE ATTENUATION CURVES.

6. INVESTIGATION OF VIBRATORY FORCE PATH BETWEEN INJECTION PUMP AND ENGINE

From studies made on two types of in-line fuel injection pump mounting systems namely "flange" and "base" fixing, it is apparent that instrumentation with force transducers on the flange mounted pump would present some problems since it is difficult to define the directions of the force inputs and thus triaxial force transducers would have to be employed. This would present unsurmountable problems related to necessary modifications to the timing gear drive system for driving the pump.

The base mounted pump, however, offered possibilities where only minor modifications to the mounting bracket were needed and a Kistler washer type force transducer was installed on engine A as shown in Figure 6.1.

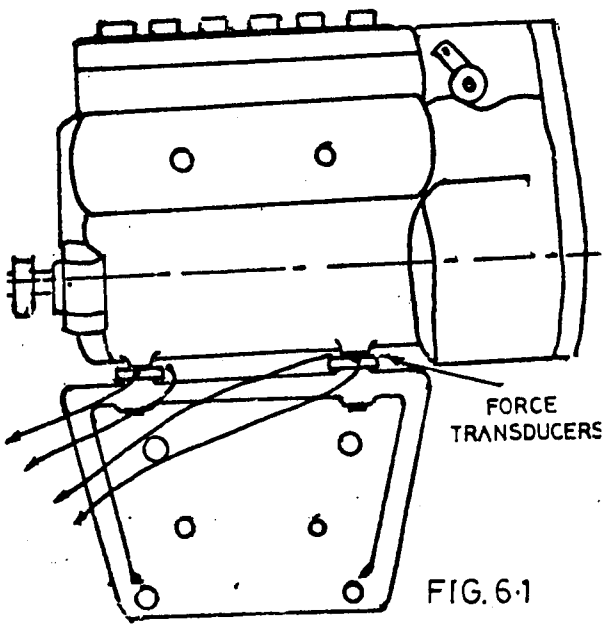

FIG. 6·1

The transducers were calibrated dynamically using a "Dawes" shaker. This consisted of a small vibrator operated at the mains supply frequency where the electro-magnetic circuit of the vibrator could be tuned to resonance by an external control.

Calibration was achieved by attaching the force transducer to a mass loaded system, including an accelerometer, as shown in Figure 6.2.

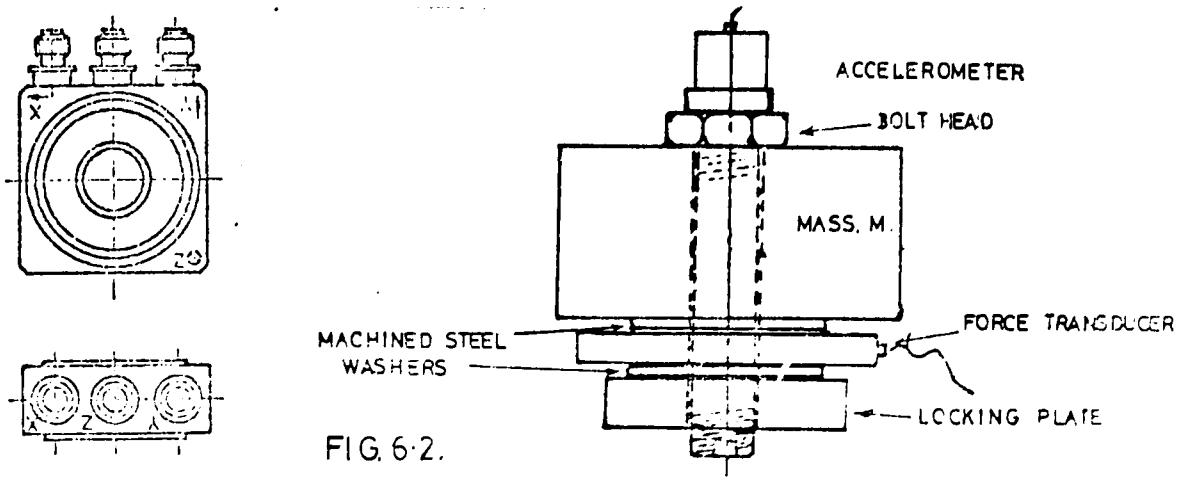

FIG. 6·2.

The same bolts as used for the calibration system were also used for pumps mounting on the bracket. The torque on the bolts was kept constant at 21 N.m in both applications. A line diagram of the calibration system is shown in Figure 6.3

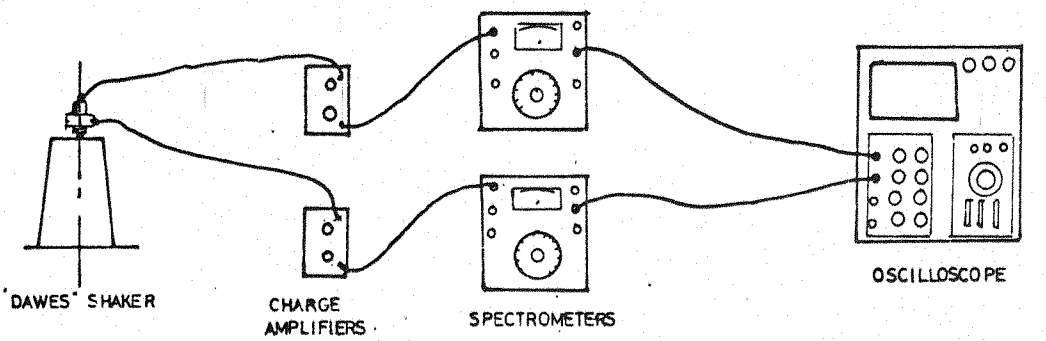

FIG.6·3 LINE 'DIAGRAM 'FORCE' TRANSDUCER CALIBRATION.

With the system operative, four sets of readings were obtained for each respective transducer, i.e. for each change in vibration level, the corresponding output from the transducer was recorded. The charge amplifier sensitivity setting was kept constant throughout the tests. The calibration curves obtained for the four transducers are shown in Figure 6.4

Measurements were carried out on the fuel injection pump with engine running, (i.e. normal pump operation) and also with the pump driven via an hydraulic motor as shown in Figure 6.5

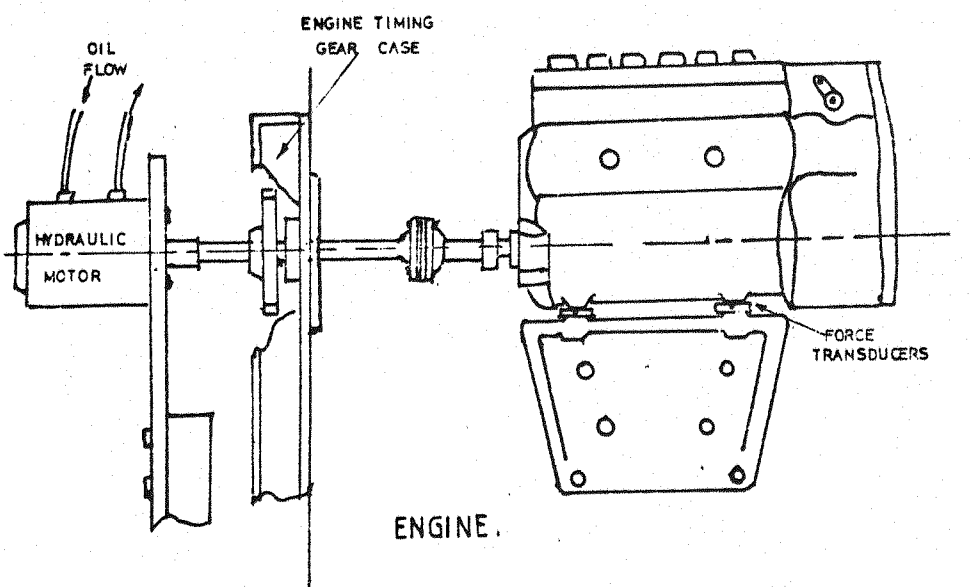

FIG.6-5. LINE DIAGRAM PUMP MOTORING SYSTEM.

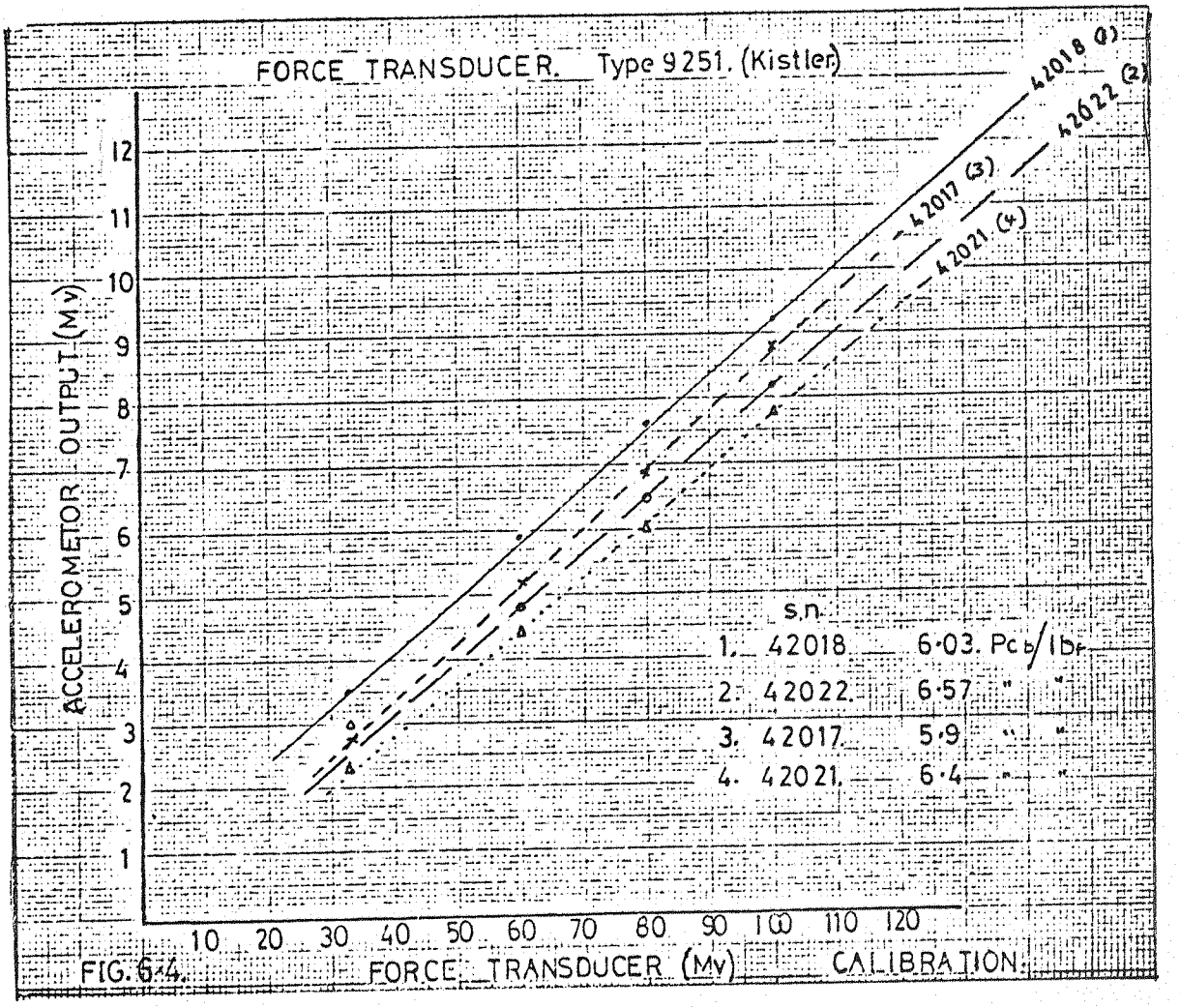

FIG. 6·4.

FIG 6·4. CALIBRATION CURVES FOR THE FOUR FORCE TRANSDUCERS.

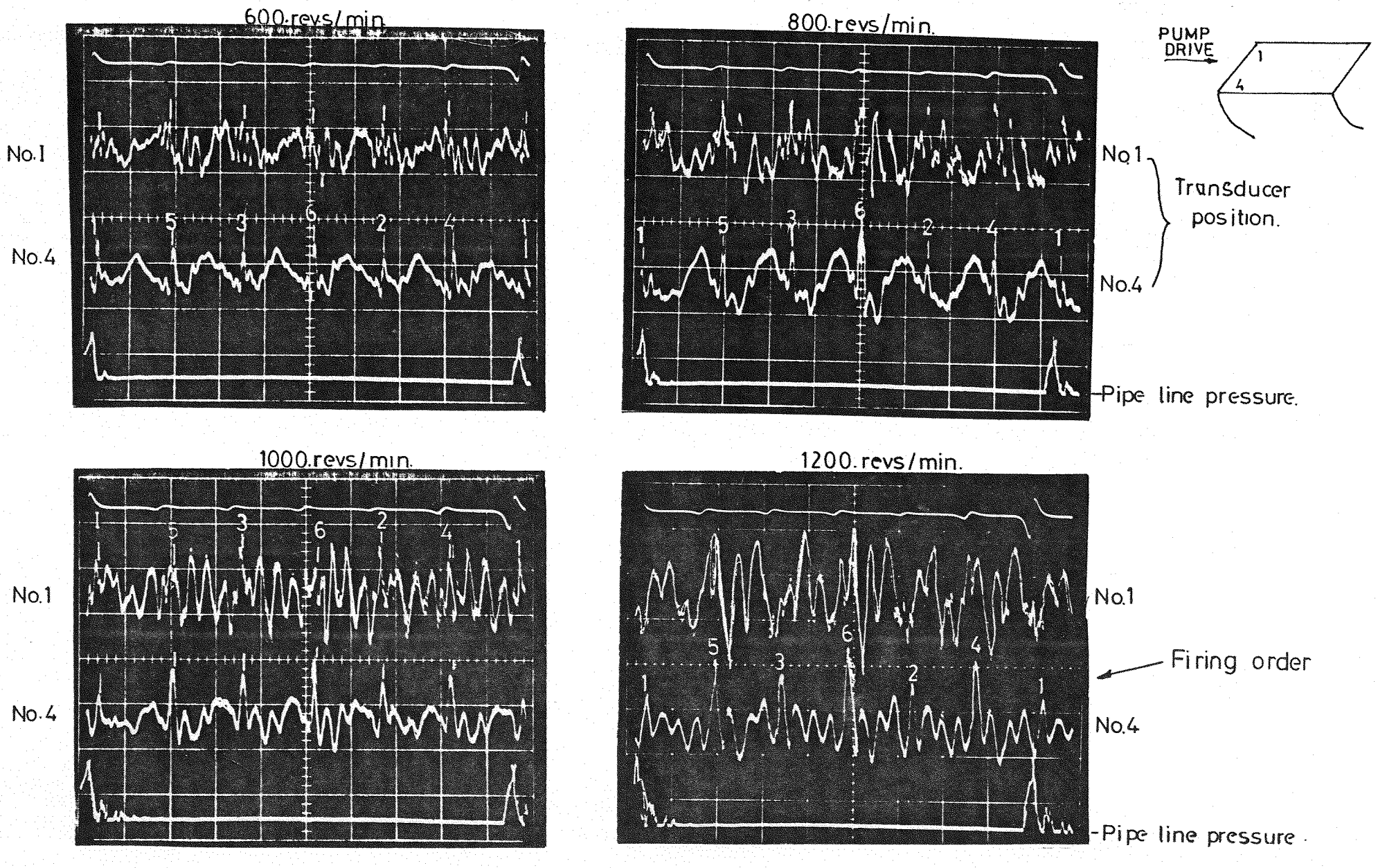

FIG.6·6. OSCILLOGRAMS OF WAVEFORM FROM FORCE TRANSDUCERS.

Figure 6.6 shows the force oscillograms at No.1 and No.4 positions on the bracket together with pipe line pressure diagrams and timing marks at pump speeds of 1200, 1000, 800 and 600 rev/min. The oscillograms clearly show the triangular peaks corresponding to the shape of the injection pressure diagrams. The impulsive peaks, as can be seen, induce transient force oscillations which are transmitted through the bracket.

The firing sequences of the pump are marked on the oscillograms indicating which of the elements is pumping at any particular instance. It will be noted that the amplitude of the force impulses from pumping are different for each plunger element, i.e. No.1 plunger which is nearest to camshaft bearing has the lowest impulse, whereas No.6 plunger, nearest to the centre of the camshaft, has a maximum force impulse.

The frequency of the waveform oscillations between each impulse are calculated as follows:-

1200 rev/min 480 Hz; 500 rev/min 492 Hz;
1000 rev/min 510 Hz; 600 rev/min 506 Hz.

These results indicate a strong resonant frequency of the pump bracket system, centred around 500 Hz which is reflected in the structure attenuation curves (Figure 5.20) and force spectra (Figure 6.8). The distribution of the individual force impulses is shown in Figure 6.7 at various speeds, which, as can be seen, follows the same pattern observed in the study of camshaft bending.

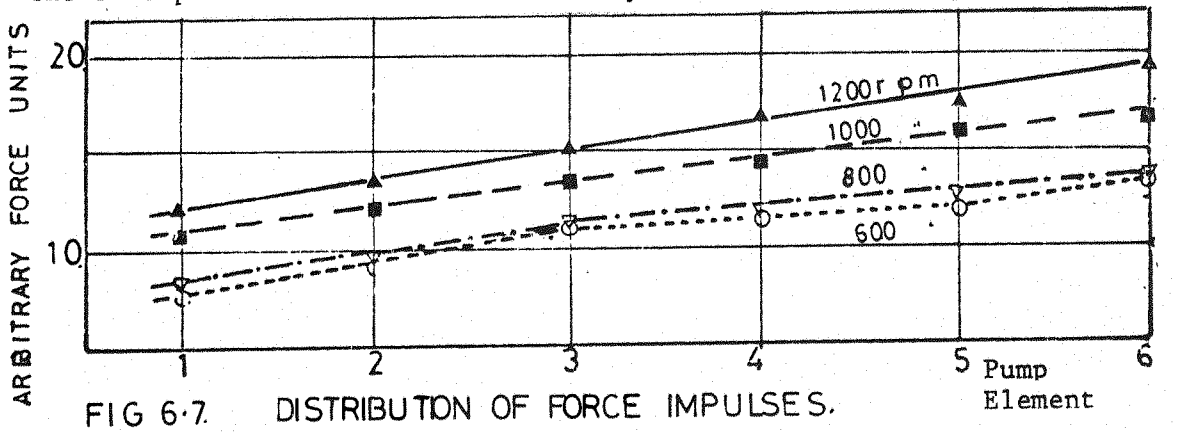

FIG 6·7. DISTRIBUTION OF FORCE IMPULSES.

Figure 6.8 shows the spectra of the force at position 1, at pump speeds of 1200, 1000, 800 and 600 rev/min. Force in Newtons is plotted on a logarithmic scale (a scale defining force

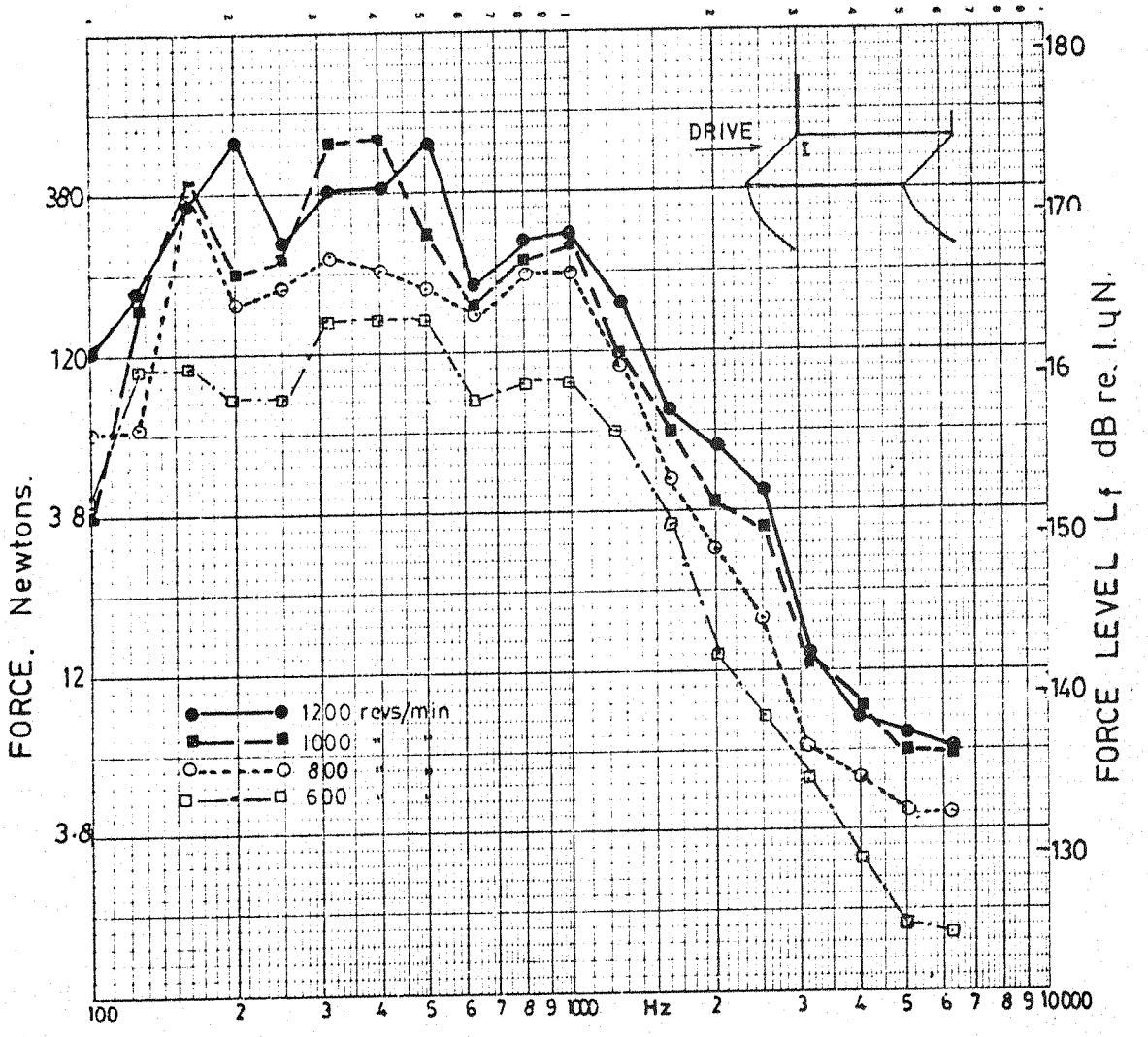

FIG. 6-8. EFFECT OF SPEED ON FORCE SPECTRA. Pos. I.

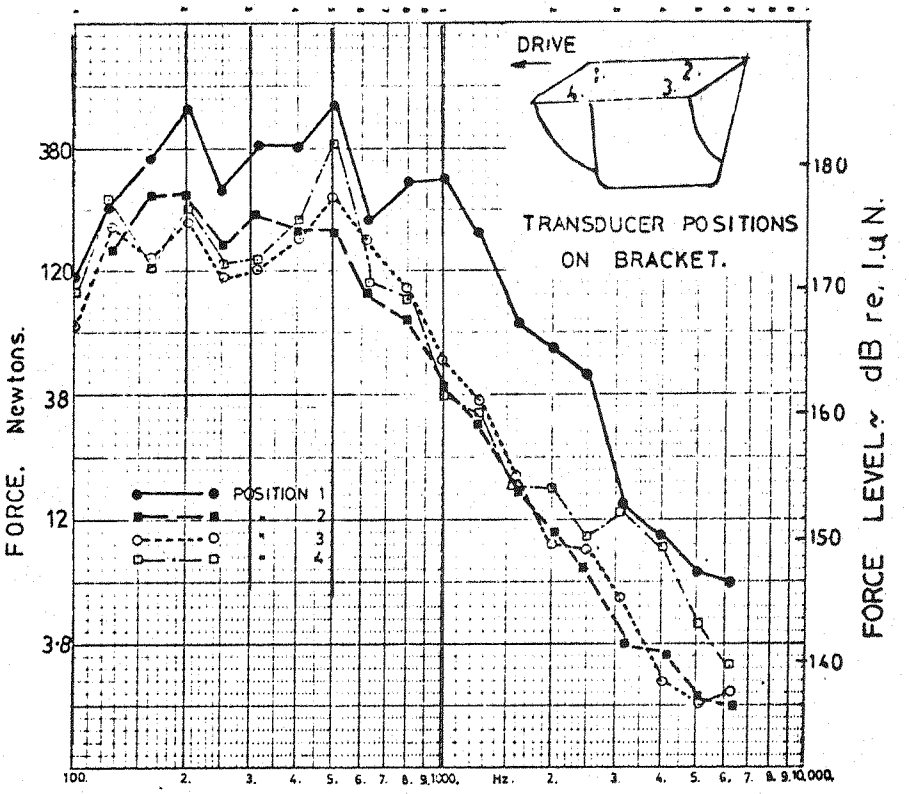

FIG. 6·9 FORCE SPECTRA. 1200.revs/min.

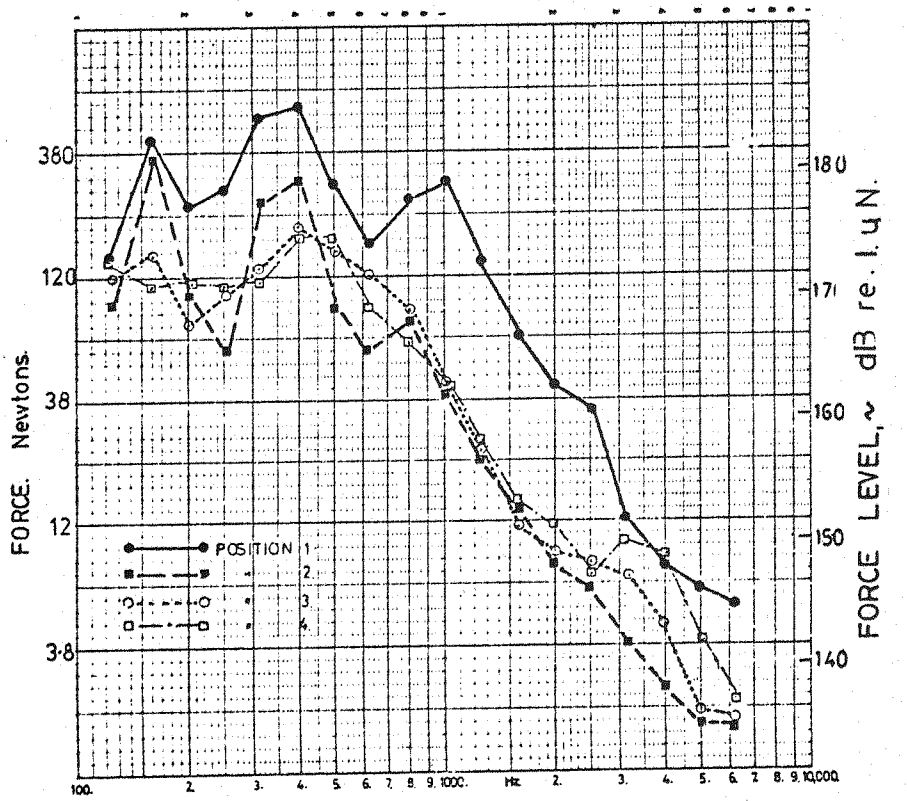

FIG. 6·10 FORCE SPECTRA. 1000.revs/min.

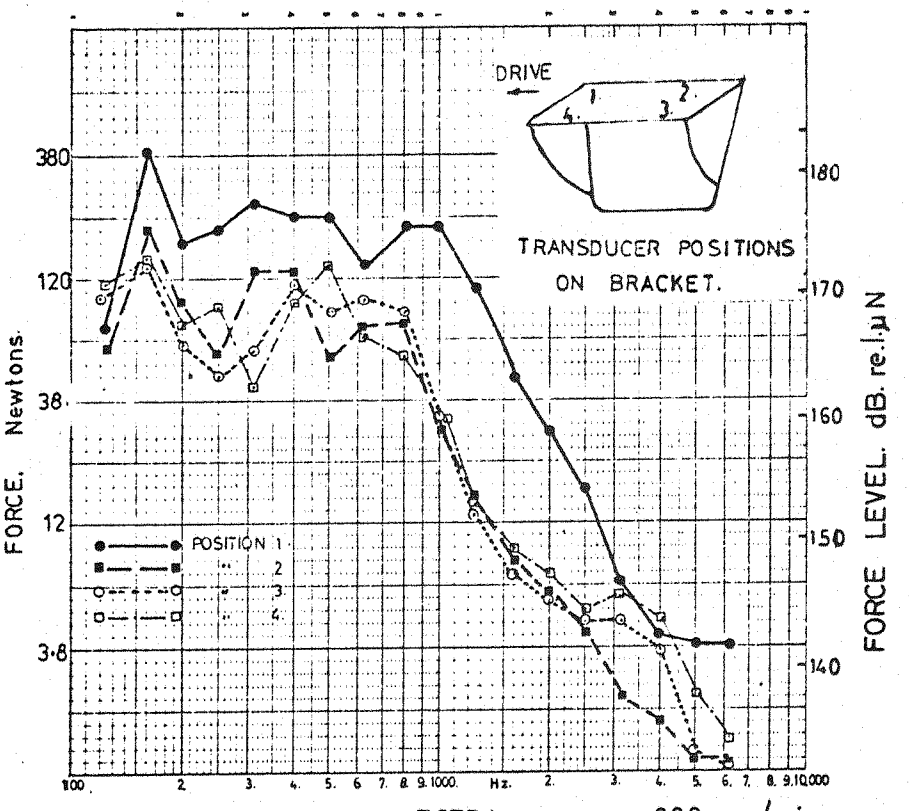

FIG. 6·11 FORCE SPECTRA. 800.revs/min.

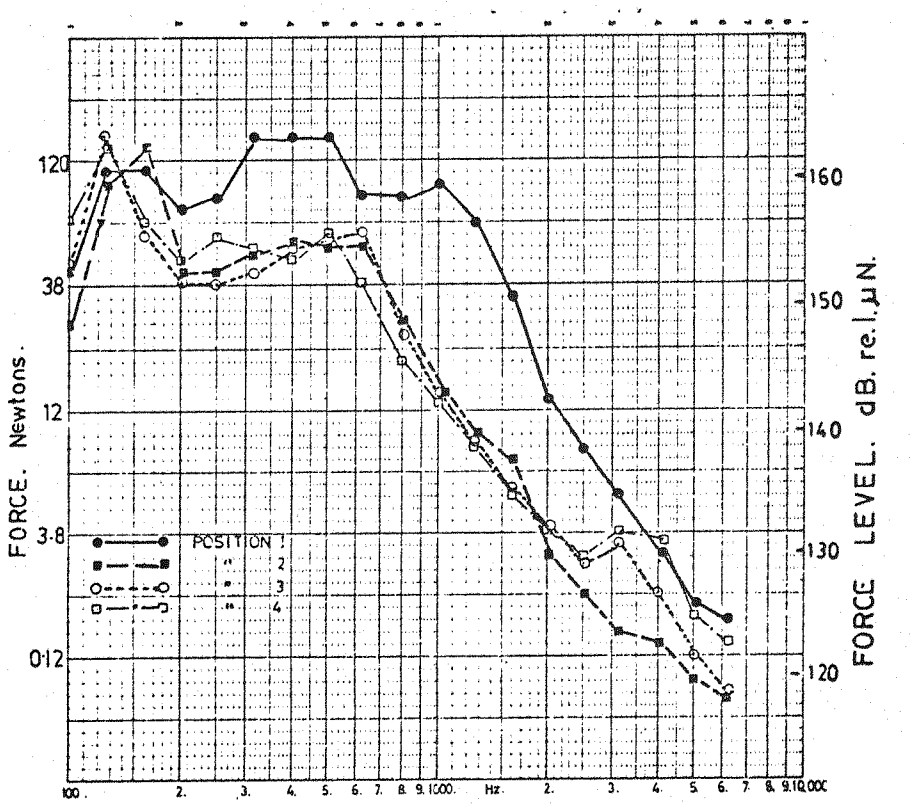

FIG. 6·12 FORCE SPECTRA. 600.revs/min.

level in dB re 1 μN is also included). The maximum force transmitted occurs in the frequency range from 100 Hz to 1000 Hz. Above 1000 Hz the transmitted force level decreases rapidly at about 40 dB/decade.

In this frequency region from 100 Hz to 1000 Hz there are definite broad peaks in the spectra which are closely related to the characteristics of the pump vibration. The frequency regions of the broad peaks are between (a) 100 to 160 Hz; (b) 300 to 400 Hz and (c) 800 to 1000 Hz, and are identical to the pump body vibrations.

As shown in Figure 5.3, Chapter 5, since the harmonic density of the exciting force in the low frequency range is low, the peaks (a) and (b) show irregular changes with speed. The higher frequency peak (c) from 800 Hz to 1000 Hz shows a constant steady increase with speed.

The increase of force transmitted at the mounting point also shows the same trends as observed in pump vibration with speed.

Figures 6.9 to 6.12 compare the force and level at each of the respective fixing points at pump speeds of 1200, 1000, 800 and 600 rev/min respectively. The shape of the spectra at each of the points is similar. The force level at the points 2,3, and 4, are more or less identical, but force transmitted from the fixing point, 1, is of the order of some 10 to 15 dB higher over the whole frequency range. This indicates that the force "flow" is largely occurring through one fixing point, i.e. No.1, on the drive end of the pump near the engine structure. At frequencies above 3000 Hz, the force flow shows a maximum at position No.1, followed by position No.4, then 3, with lowest force flow at position No.2.

This phenomenon was observed during the tests and in order to eliminate experimental error, No.1 transducer was fitted in turn to the other three positions. The results verified the original findings.

It is to be expected that the front two mounting points at Nos. 1 and 4 positions (i.e. nearest the input drive) could take the greatest torque reaction load because the flexibility of the pump body in torsion prevents this load being shared equally. Since mounting point No.1 is nearest the engine side the bracket support will be stiffer than at No.4 position. Therefore by similar reasoning No.1 support will take the greatest load.

Since correlation between hydraulic force spectrum (pump chamber force spectrum) and the vibration amplitude spectrum of the pump showed similarity (Chapter 4, Figure 4.9) it was of interest to correlate the mounting point force spectrum with the hydraulic force spectrum.

This comparison is shown in Figure 6.13.

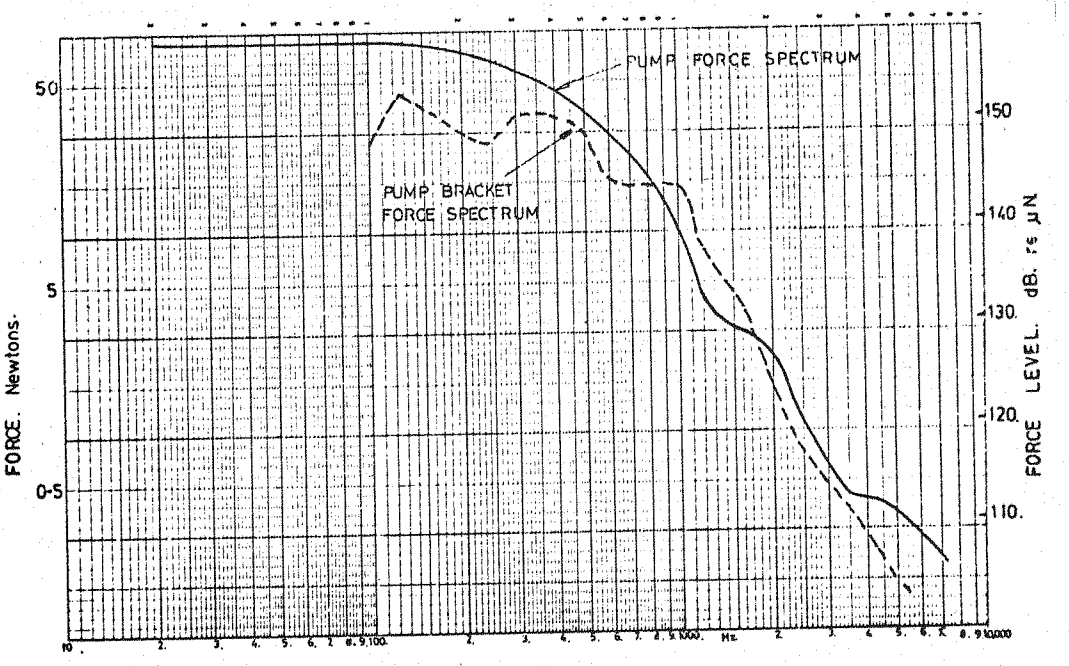

FIG. 6.13. PUMP AND BRACKET FORCE SPECTRA

The one-third octave band spectrum of the mounting point force has been corrected for 1 Hz bandwidth. The basic shapes of the two force characteristics are similar. This therefore indicates that the force generated in the pump chamber is fed into the engine structure without any appreciable modification, thus supporting the findings of the previous section, whence the spectrum of the pump vibration amplitude follows closely the force spectrum shape.

7. ASSESSMENT OF FUEL INJECTION PUMP NOISE FROM SURFACE VIBRATION MEASUREMENTS

Assessing noise of various engine components by lead covering techniques can, in some cases, be misleading, i.e. exposing the individual components often involves exposing other radiating sections of the engine. Also it has been found that the lead jacket enclosing the engine vibrates as a result of the forces transmitted through the lead jacket absorbent. Furthermore small leaks through overlapping sections of lead and joins allow more engine noise to reach the microphone than intended. Accumulation of these defects lead to inaccurate results with particular reference to pump radiated noise.

For the assessment of one particular 10 element in-line pump, noise tests were carried out using the facilities at C.A.V. Ltd, London. The pump was motored on a special 'quiet' rig in an anechoic chamber.

On the 'quiet' rig every effort was made to ensure that the pump noise could be measured without interference from other vibration sources. The rig was constructed so as to radiate little noise in response to pump vibration. The pump was mounted via solid blocks to a massive cast iron table which was supported on a stiff frame. The pump body was rigidly held. The drive torque was supplied from a motor outside the soundproof cell in which the rig was situated. The pump driveshaft, running in stiffly mounted bearings, was equipped with a large flywheel. It was connected to the camshaft of the pump via special couplings with high torsional stiffness. The coupling consisted of thin spring discs separated by a length of shaft which allowed misalignment between pump and camshaft to be taken up.

The investigation into the noise radiated by a 10 element fuel injection pump showed that pump radiated noise, when the pump was fitted to the engine, (all other engine surfaces lead shielded) was up to 10 dBA noisier than the same fuel pump motored on a quiet rig for the same fuelling and speed conditions. This is shown in Figure 7.1a.

The differences between noise apparently radiated by the pump on a running engine, and the noise when the pump is driven on the

quiet rig, can be seen more clearly from the spectra of the two noise measurements in Figure 7.1b.

7.1. Calculating Radiated Noise from Vibration Spectra "Russell's" Method

In order to assess the validity of these results, a further measurement of noise radiated from the pump surfaces was made. To obtain this estimate, one-third octave band vibration spectra were measured at 29 points on the side of the pump and governor, on the side facing the microphone. These measurements may be conveniently made with the pump mounted upon the engine or on the quiet rig.

The mean square values of vibration acceleration were estimated in each one-third octave band was estimated from the expression:

$$1/3 \text{ OB SPL} = 10 \log_{10} \left(\frac{\bar{u}^2 \rho \ \sigma \text{ rad}}{2\pi r^2} \right) + D$$

where $\bar{u}^2$ is the mean square vibration velocity, calculated from the measured acceleration values (α) $u = \alpha/2\pi f$

ρ is density of air

c is speed of sound in air

A is area of noise-radiating surface

σ rad is the radiation efficiency of the normal modes of surface area A

r is the radius, from the pump centre, to the measurement microphone position

D is the directivity factor expresses in decibels

The noise spectrum derived from spatial mean square vibration levels is compared with the noise radiated by the exposed pump on a lead jacketed engine in Figure 7.1b. As can be seen there is reasonable agreement over the frequency range 800 Hz to 2.5 K and at 8.0 kHz.

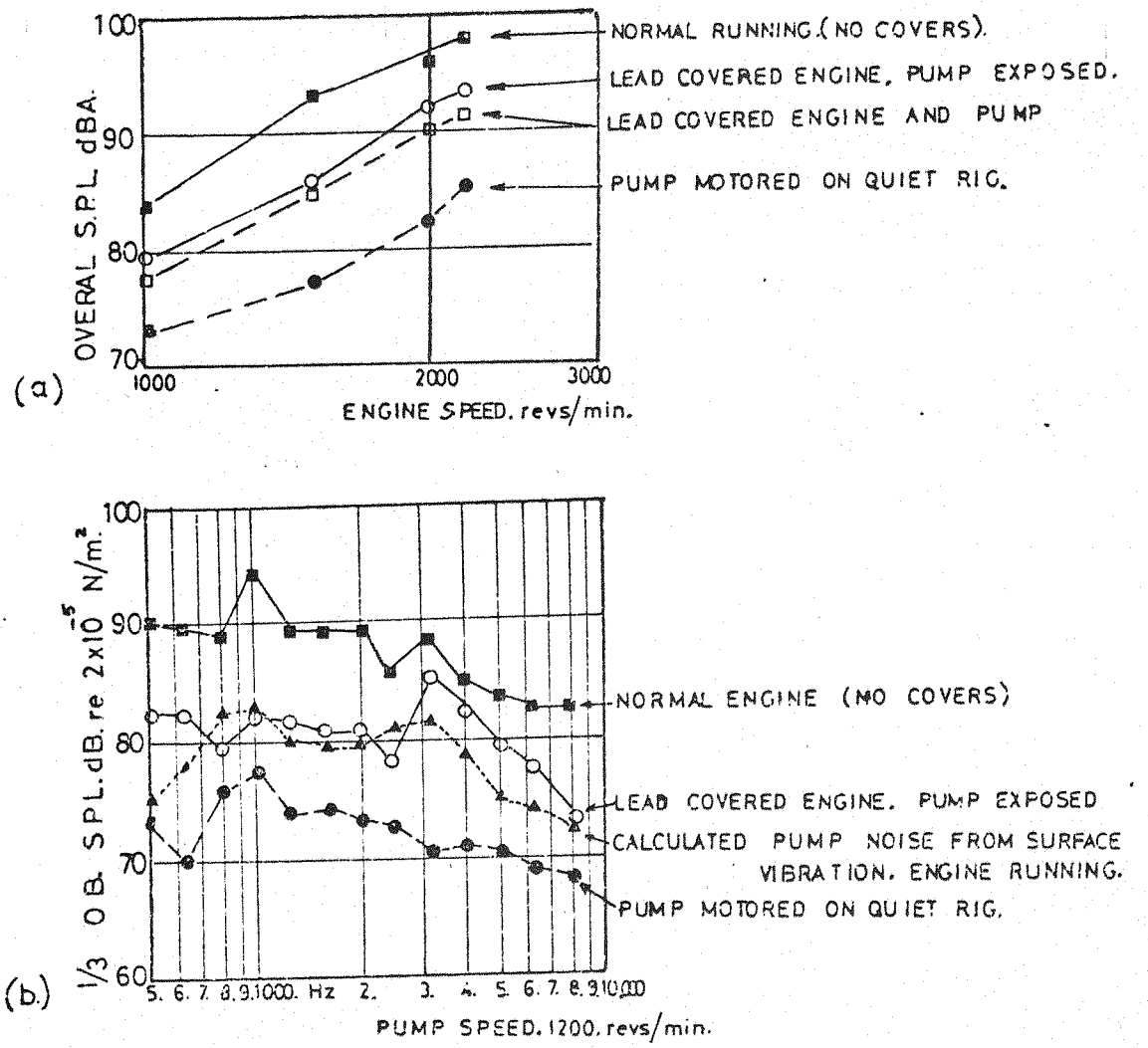

FIG. 7·1. NOISE RADIATED FROM PUMP AND ENGINE SURFACES. 10. ELEMENT IN-LINE PUMP.

There are significant differences in the low frequency range below 630 Hz and over the high frequency range above 3150 Hz. The results however, confirm the direct noise measurements indicating that the pump radiates more noise when mounted on a running engine than when motored on a "quiet" rig. The increase in noise is due to increased pump body vibration levels when mounted on the engine. This may be due to extra vibration excitation from sources within the engine or to some effect of pump mounting.

The method of calculating the radiated noise from structure vibrations was devised by M. Russell (5.5). A photo of the C.A.V. "quiet" rig on which some of these tests were carried out is shown in Figure 7.2.

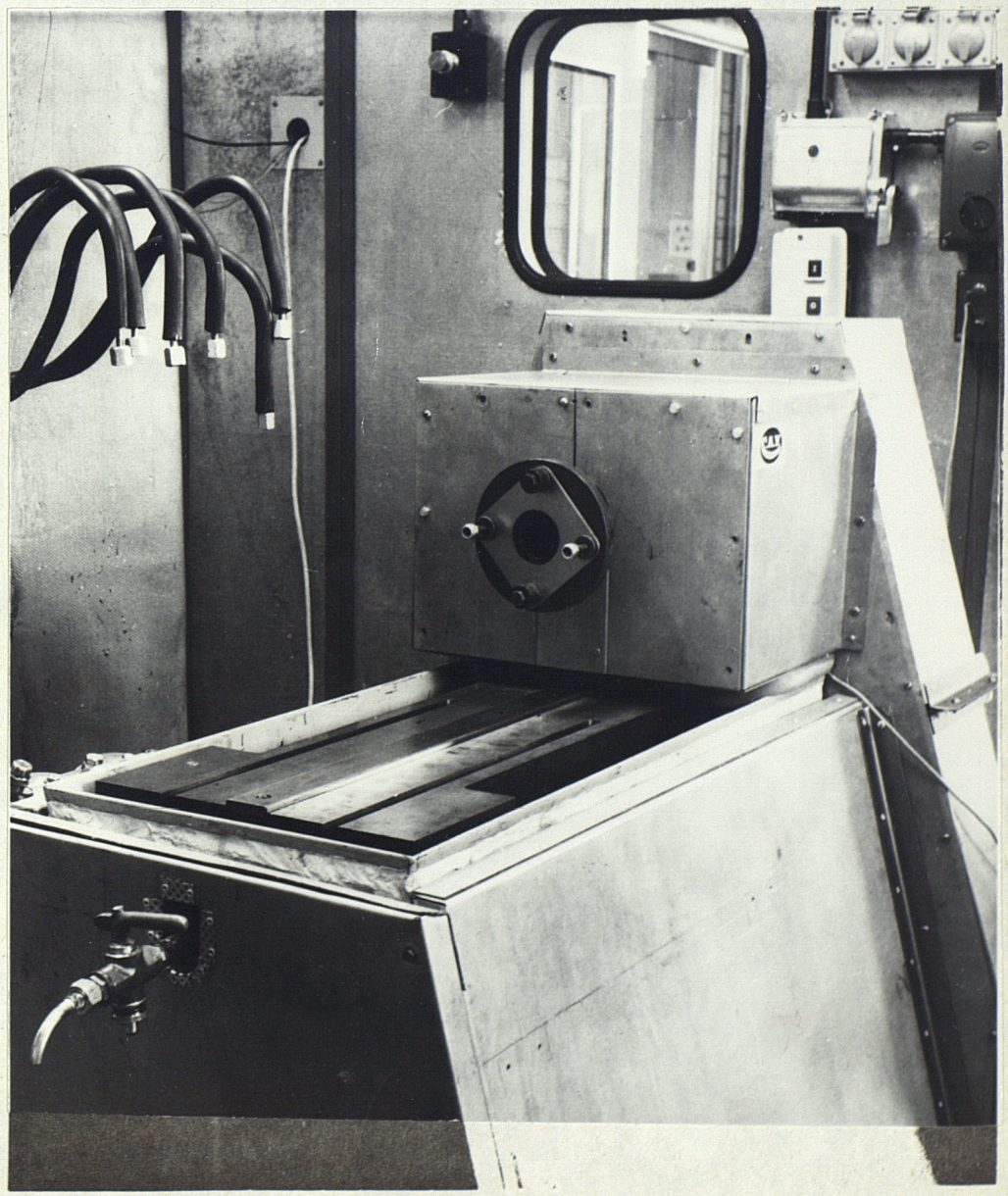

FIG. 7·2. C.A.V. "QUIET" TEST RIG FOR F.I. PUMP NOISE AND VIBRATION ASSESSMENT.

7.2. Calculating Radiated Noise from Vibration Spectra "Anderton's" Method

Another method of calculating the radiated noise from structure vibrations, though very similar in application, was devised by Dr. Anderton, I.S.V.R. (5.6).

His method of calculating radiated noise is as follows:-

Noise dB re. $2 \times 10^{-5} N/m^2$ is given by

$$dB(f) = L\bar{v}(f) - 10 \log_{10} \frac{S(trav)}{S(rad)} + K_1$$

S(rad) = radiating area of surface (i.e. top, sides, front, etc) for the pump used in test

$$S(rad) = 0.176 \ m^2$$

S(trav) = area of imaginary transverse of spherical microphone array 1m from surface

$$= \pi \left(\left(\frac{S(rad)}{\pi} \right)^{\frac{1}{2}} + 2 \right)^2 m^2$$

$$\therefore \quad S(trav) = 15.71 \ m^2$$

$L\bar{v}(f)$ = average mean square surface velocity for the specific radiating area. This was obtained from acceleration spectra dB re 1g.

For one-third octave bands $20 \log_{10} (\frac{f}{4})$ is as follows -

1/3 OB	500	630	800	1000	1250	1600	2000	2500	3150	4000	5000	6300	8000
$20 \log_{10}(\frac{f}{4})$	42	44	46	48	50	52	54	56	58	60	62	64	66 dB

For example, if acceleration is 1g at 1000 Hz then acceleration = 0 dB re 1g and velocity = -48 dB

For this to be so the reference velocity is 0.39 m/sec

For this reference velocity the value K_1 becomes

$$K_1 = 20 \log_{10} \left(\rho_c \frac{Uo}{Po}\right) \qquad \text{where } Uo = 0.39 \text{ m/sec}, \; Po = 2\times10^{-5} \text{ N/m}^2$$

$$= 20 \log_{10} \frac{1.21}{(\text{Kg/1m}^2)} \times \frac{343}{\text{m/sec}} \times \frac{0.39 \text{ m/sec}}{2.10^{-5}\text{N/m}^2} = 138.16 \text{ dB}$$

$$\text{SPL dB(f)} = L\bar{v}(f) - 10 \log_{10} \frac{S(trav)}{S(rad)} + 138.16 \text{ dB}$$

It should be noted that in this calculation the acoustic radiation ratio is assumed to be unity.

In order to assess Anderton's method for calculating pump radiated noise, tests were carried out on a six in-line fuel injection pump for conditions of (a) motored on the stationary engine, and (b) motored on the "quiet" rig at I.S.V.R.

Some 35 vibration measurements were taken from the pump casing and governor housing for each respective test. The pump was run at its maximum speed of 1400 rev/min, full rack condition. The results are shown in Figure 7.3.

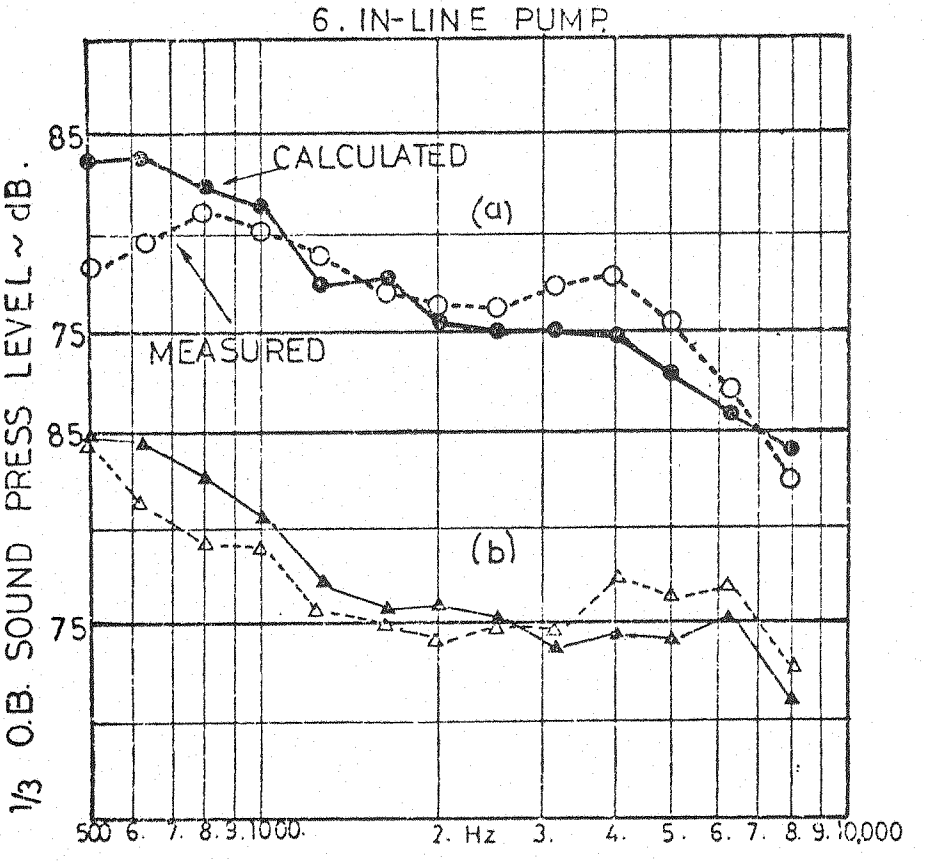

FIG 7.3 MEASURED AND CALCULATED NOISE SPECTRA.
(a). Motoring on engine.
(b). on. I.S.V.R. quiet rig.

It can be seen over the predominant noise frequency range 800 Hz to 3150 Hz, that the calculated noise levels are within 1 to 3 dB of the measured noise levels. Over the low frequency range below 800 Hz and over the high frequency range above 3150 Hz the calculated noise values differ by some 2 to 5 dB.

One further test was carried out on the 10 in-line fuel injection pump mounted on the engine as shown in Figure 7.4a. The engine was fully lead covered with the exception of the pump. The pump speed for this test was 1400 rev/min. Using Anderton's formula the results are shown in Figure 7.4b. The calculations are shown below :-

$$\text{SPL dB(f)} = L\bar{v}(f) - 10 \log_{10} \frac{S(trav)}{S(rad)} + 138.16$$

$L\bar{v}(f)$	500	630	800	1000	1250	1600	2000	2500	3150	4000	5000	6500	8000
	-42	-44	-46	-48	-50	-52	154	-56	-58	-60	-62	-64	-64
From vibration spectrum re g	0	5	9	11	12	15	14	15	13	13	14	14	16
	-42	-39	-37	-37	-38	-38	-40	-41	45	47	46	-50	-50

S(rad) total surface area of pump + governor = 0.3723 m^2

$$S(trav) = \pi \left(\left(\frac{S(rad)}{\pi} \right)^{\frac{1}{2}} + 2 \right)^2 = 17.24 m^2$$

For $\frac{1}{4}$ area as shown in Figure 7.4

$$S(trav) = \frac{17.24}{4} = 4.316 m^2$$

$$-10 \log_{10} \frac{(S(trav))}{S(rad)} = -10 \log_{10} \frac{4.316}{0.3723} = \underline{-10.5}$$

(f)				dB
500	- 42	-10.5	+ 138.16	85.6
630	- 39	-10.5	+ "	88.6
800	- 37	- "	+ "	90.6
1000	- 37	- "	+ "	90.6
1250	- 38	- "	+ "	89.6
1600	- 38	- "	+ "	89.6
2000	- 40	- "	+ "	87.6
2500	- 41	- "	+ "	87.6
3150	- 45	- "	+ "	83.6
4000	- 47	- "	+ "	81.6
5000	- 48	- "	+ "	79.6
6300	- 50	- "	+ "	77.6
8000	- 50	- "	+ "	77.6

From the mean vibration spectra shown in Figure 5.15 which have been derived for the six engines covered in this investigation it is possible to compare the level of radiation of noise from the pumps and from the engine blocks. As can be seen the pump radiated noise in general is of lower magnitude than the engine block radiated noise. In some engine designs, however, in certain limited frequency ranges the radiation of noise from the pump may exceed the radiation of noise from the block.

This comparison, however, does not take into account the overall noise of the engine structure and it does not include radiation of engine noise from covers (sump, valve cover, timing cover) bellhousing and front pulley. These sources are sometimes greater than the noise from the block.

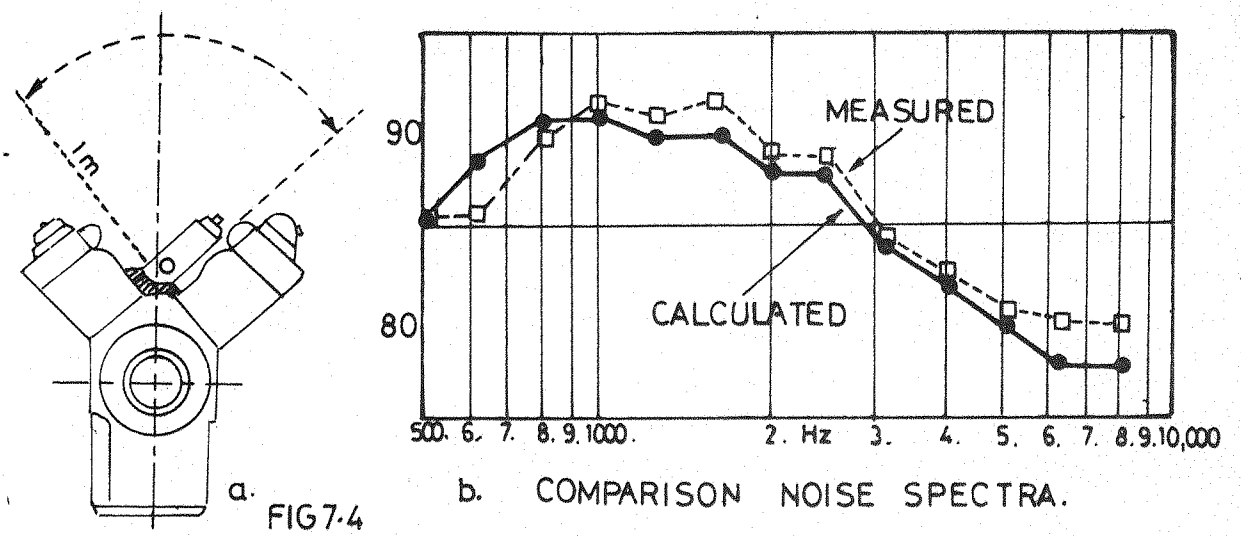

a. b. COMPARISON NOISE SPECTRA.

FIG 7.4

These results also show reasonable correlation between measured noise and calculated radiated noise. It is apparent that the limitations of this method of assessing noise from individual components are that, as in this particular case (a) all other noise radiating surfaces on the engine, must be completely enclosed such that the noise from the structure must be reduced to a minimum, and (b) consideration must be given in the calculation of S(trav), e.g. in this case due to the pump being mounted in the vee of the engine at angle in line with the plane of the cylinder bank. It was assumed that the noise was radiated into a quarter of a sphere.

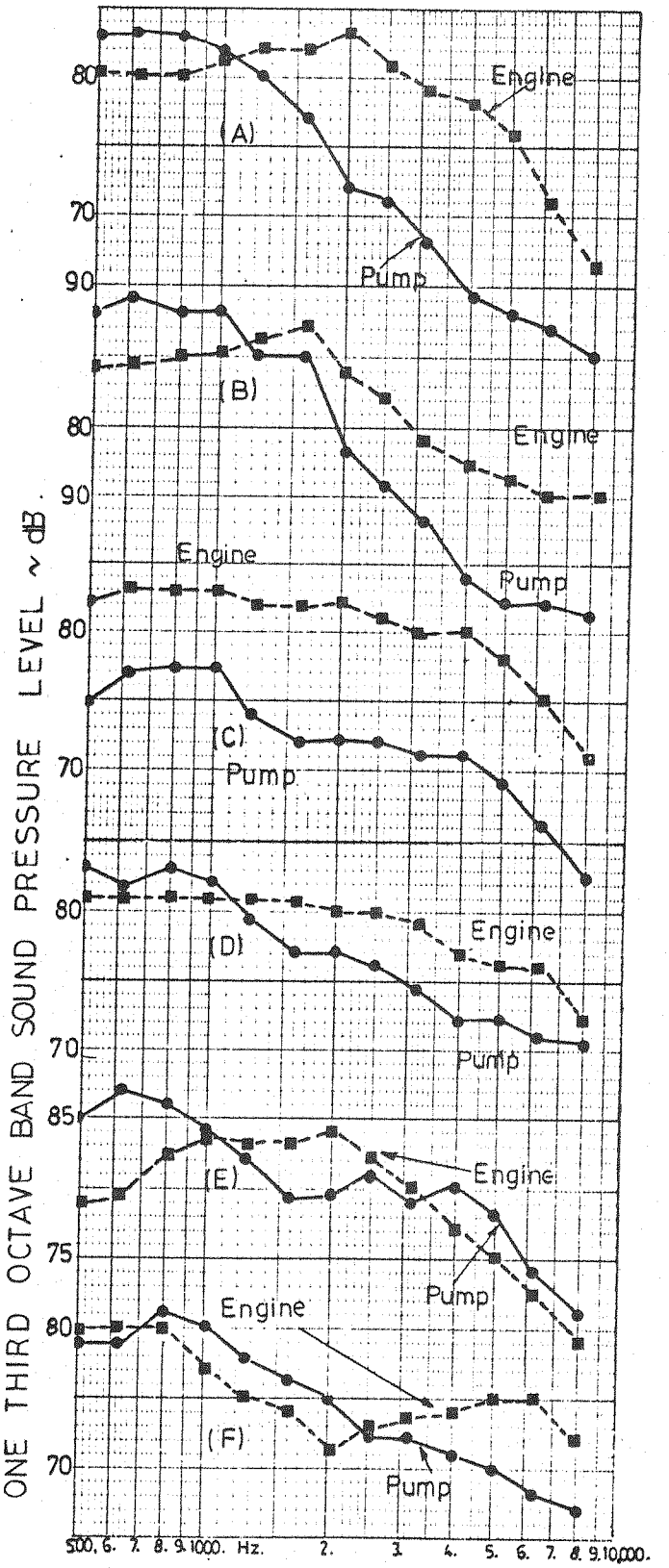

FIG. 7·5. CALCULATED NOISE LEVELS FROM VIBRATION SPECTRA. PUMP SPEED 1200. r. p. m.

CALCULATED USING TOTAL RADIATING SURFACES OF ENGINE AND PUMP.

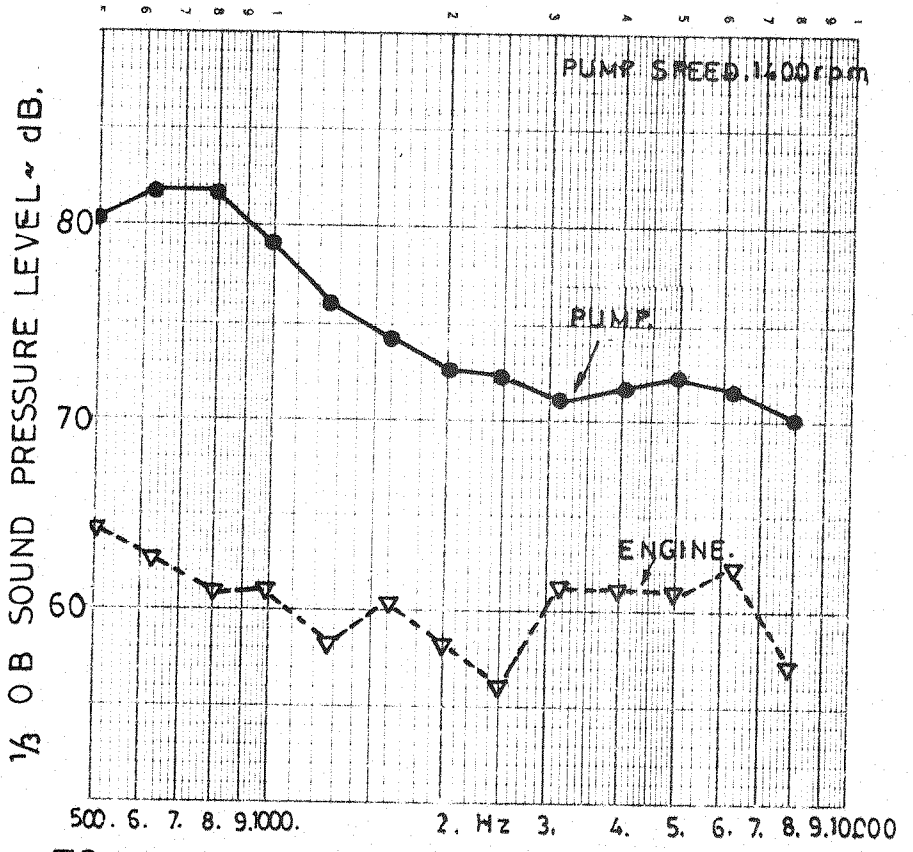

FIG. 7·6 CALCULATED NOISE LEVELS FROM VIBRATION SPECTRA. (PUMP MOTORED.)

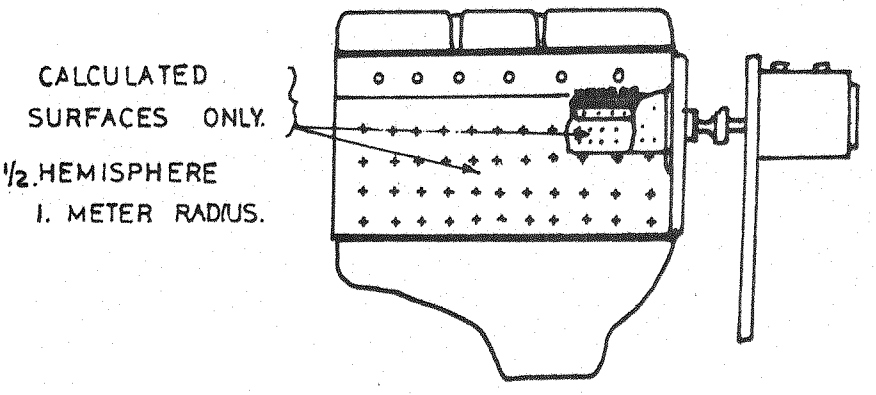

ACCELEROMETER STUDS ON ENGINE AND PUMP

7.3. Comparison of Engine and Pump Radiated Noise

From the mean vibration spectra shown in Figure 5.15, which have been derived for the six engines covered in this investigation, it is possible to compare the level of radiation of noise from the pumps and from the engine block. The pump radiated noise in general is of lower magnitude than the engine block radiated noise. In some engine designs, however, in certain limited frequency regions the radiation of noise from the pump exceeds the radiation of noise from the block.

This comparison, however, does not take into account the overall noise of the engine structure since it does not include radiation of engine noise from covers (sump, valve cover, timing cover) bellhousing and front pulley. These sources are sometimes greater than the noise from the block.

Figure 7.5 shows the comparison of mean vibration spectra of the pump and engine block on a non-running engine (Engine E) with motor driven pump. Using these data the radiated noise from both pump and block can be calculated and the results are shown in Figure 7.6 These results clearly indicate that contribution to the noise from the pump induced engine block vibration is negligible in comparison with the radiated noise resulting directly from pump surface vibrations.

8. INVESTIGATIONS OF PUMP MOUNTING, DRIVE COUPLING AND HIGH PRESSURE PIPES ON PUMP NOISE

As already described in Chapter 3 the pump structure as a whole, and in particular the thin sections of the pump surfaces, respond to vibration which originates from within the pump by deflecting under the applied forces (or when resonating in a multitude of normal modes when the forces are suddenly removed at spill). These normal modes may be excited also by vibration originating from within the associated engine via the pump mounting. Similarly vibration originating in the pump may be transmitted via the mounting to the engine.

This investigation has considered the exciting forces which develop by the operation of the injection system, with main emphasis on three vibratory transmission paths between the engine and the pump:

(a) the pump mounting,

(b) the pump drive coupling,

(c) the pipes connecting pump outlet to injector inlet.

This has been carried out to assess the effect of these vibratory forces on the noise emitted by the pump.

8.1. Comparison of Pump Radiated Noise with Alternative Mounting Brackets and Drive Couplings

Noise levels derived from pump surface vibration measurements were compared for two pumps with similar injection characteristics mounted to two engines of similar size and rating, but of different manufacture. The pump was mounted to one engine by the flange part of the governor chamber end-plate which was bolted to a cast aluminium timing cover. The camshaft of the pump carried a gear wheel, which acted as a flywheel, and which meshed with the timing gear idler as shown in Figure 8.1.

The base-mounted pump was secured to the engine crankcase via an inverted 'L' shaped aluminium alloy bracket which was stiffened by two webs. Six bolts secured the bracket to the engine crankcase panels and four bolts secured the base of the pump to the bracket.

This pump was driven via a short shaft from the timing gear case via a coupling. The drive and driven lugs of the coupling were connected by means of a plate fitted with hard rubber bushes to

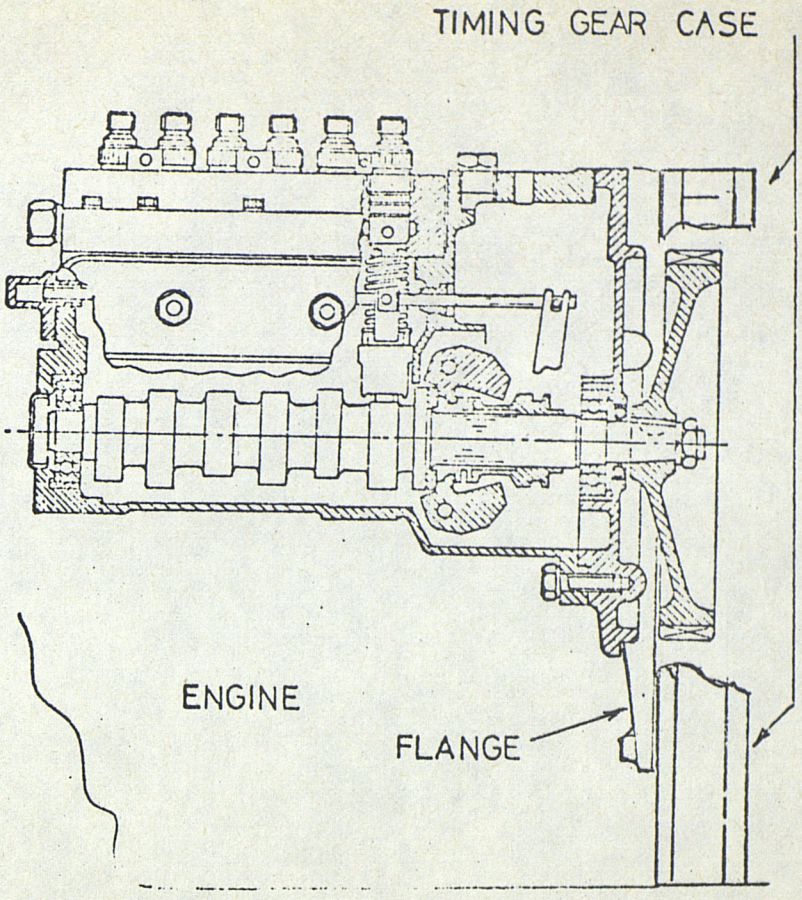

FIG. 8·1 DIAGRAM SHOWING PUMP DRIVE GEAR

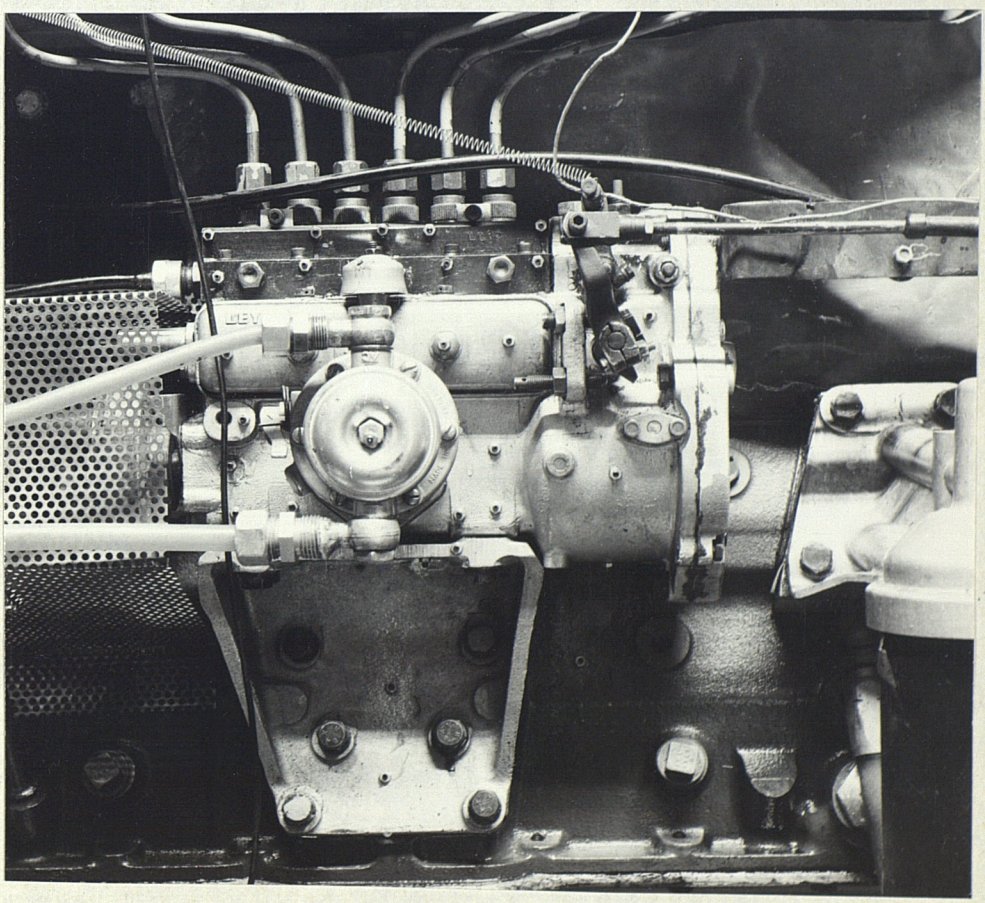

FIG 8·2 BASE MOUNTED PUMP.

accommodate any misalignment between gear and camshaft centre line. Details of the pump mounting on both engines are shown in Figure 8.2.

The spectra of noise radiated by the pumps, estimated from pump surface vibrations, for both pumps running at 1200 rev/min at full fuelling, are shown in Figure 8.3. The base mounted pump radiates less noise than the flange mounted pump when driven either from the running engine (Figure 8.3a) or driven via an hydraulic motor (Figure 8.3b) on a non-running engine; i.e. the noise levels are reduced by some 3 to 10 dB in the frequency range from 630 Hz to 8000 Hz. This indicates that the base-mounted pump is superior to the flange mounted pump.

It was considered, however, that the mounting may not be the only contributing factor, therefore it was necessary to obtain a comparison between flange and base-mounted pump arrangements on the same engine with the same pump using similar drive arrangements.

8.2. Comparison of Flange and Base Mounting Arrangements on Engine E

The mounting of the fuel injection pump on engine E was changed from the original flange mounting arrangement to a base mounted arrangement by fitting a special pad to the crankcase of Engine E, as shown in Figure 8.4a. This pad was made to take the pump bracket which was removed from engine A. The base of the pump from Engine E was drilled for bracket mounting. The base mounted pump and coupling drive assembly is shown in Figure 8.4b.

In order to minimise the effect of backlash in the pump drive coupling a Lucas CAV CR 100 coupling was used for these tests. The importance of coupling backlash on pump noise and vibration characteristics is detailed in the Section 8.4.

The noise radiated by the pump was calculated from surface vibration measurements for the following conditions:

(a) with the pump operating as for normal engine running, and

(b) driven by an hydraulic motor via the pump drive gear.

This provided a base/flange mounted comparison in which the drive, pump and engine were the same and the pump was not influenced from torsional vibration generated from the crankshaft and valve gear.

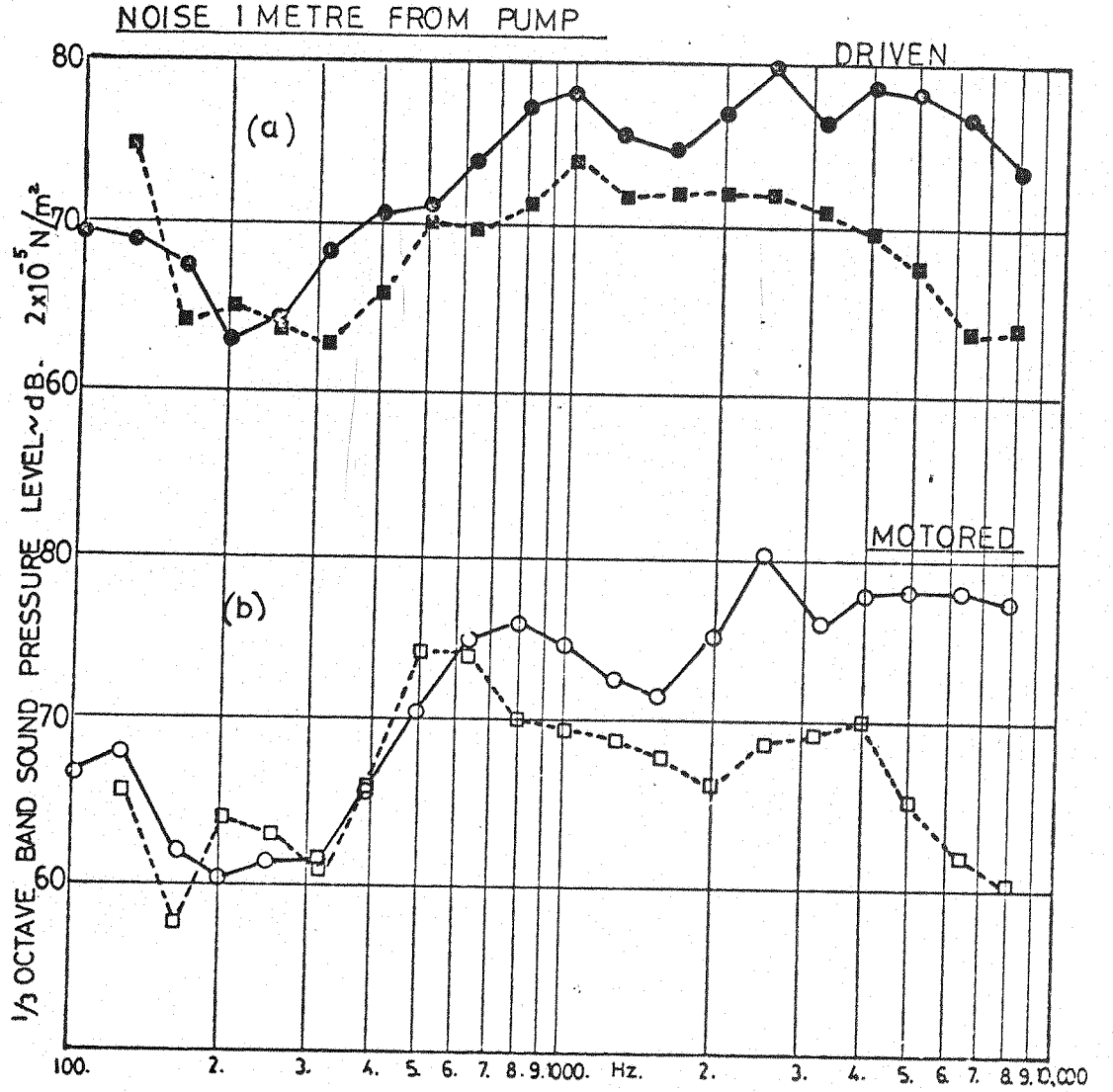

(a) TESTS WITH ENGINE RUNNING AT 2400revs/min. FULL LOAD.

FLANGE-MOUNTED IN-LINE PUMP

BASE - MOUNTED " " "

(b) TESTS WITH PUMP MOTORED AT 1200. revs/min.

FLANGE - MOUNTED IN LINE PUMP

BASE - MOUNTED " " "

FIG.8.3 COMPARISON NOISE RADIATED BY TWO 6 ELEMENT PUMPS MOUNTED ON TWO ENGINES WITH SIMILAR RATED POWER.

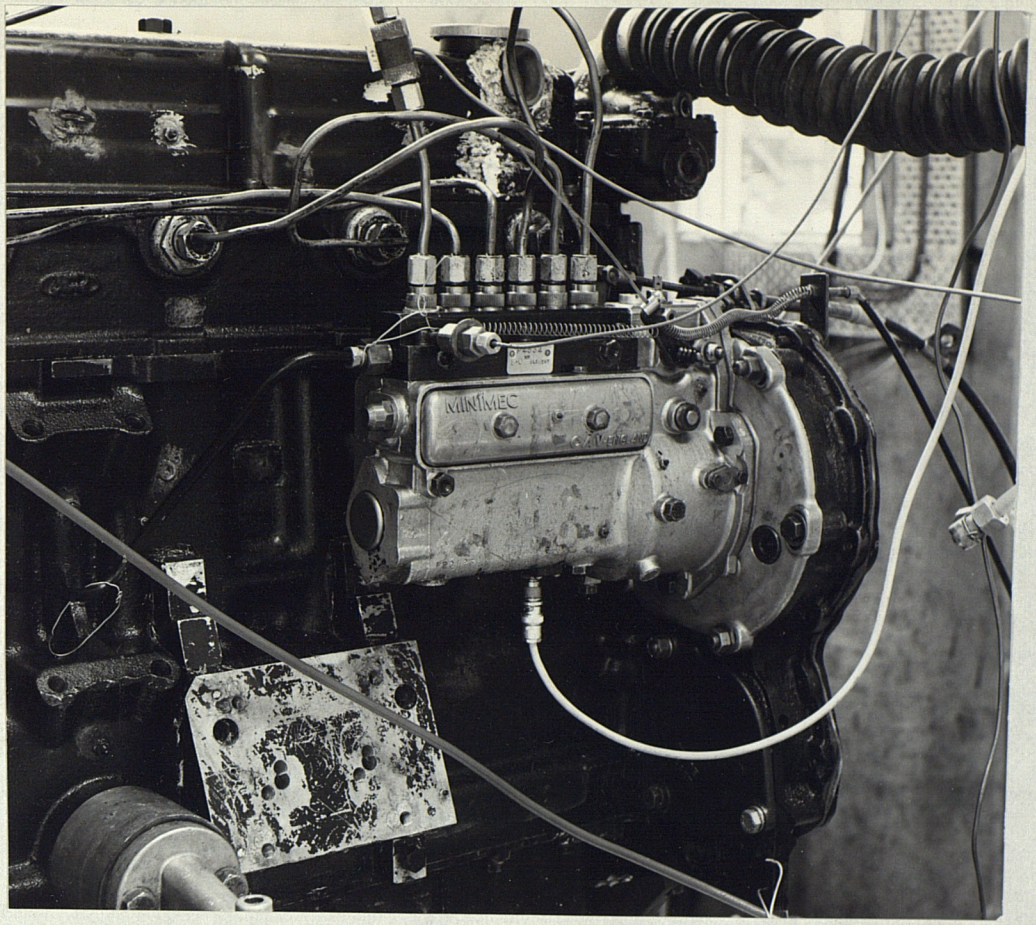

FIG. 8·4.a. PUMP MOUNTING PAD ARRANGEMENT.

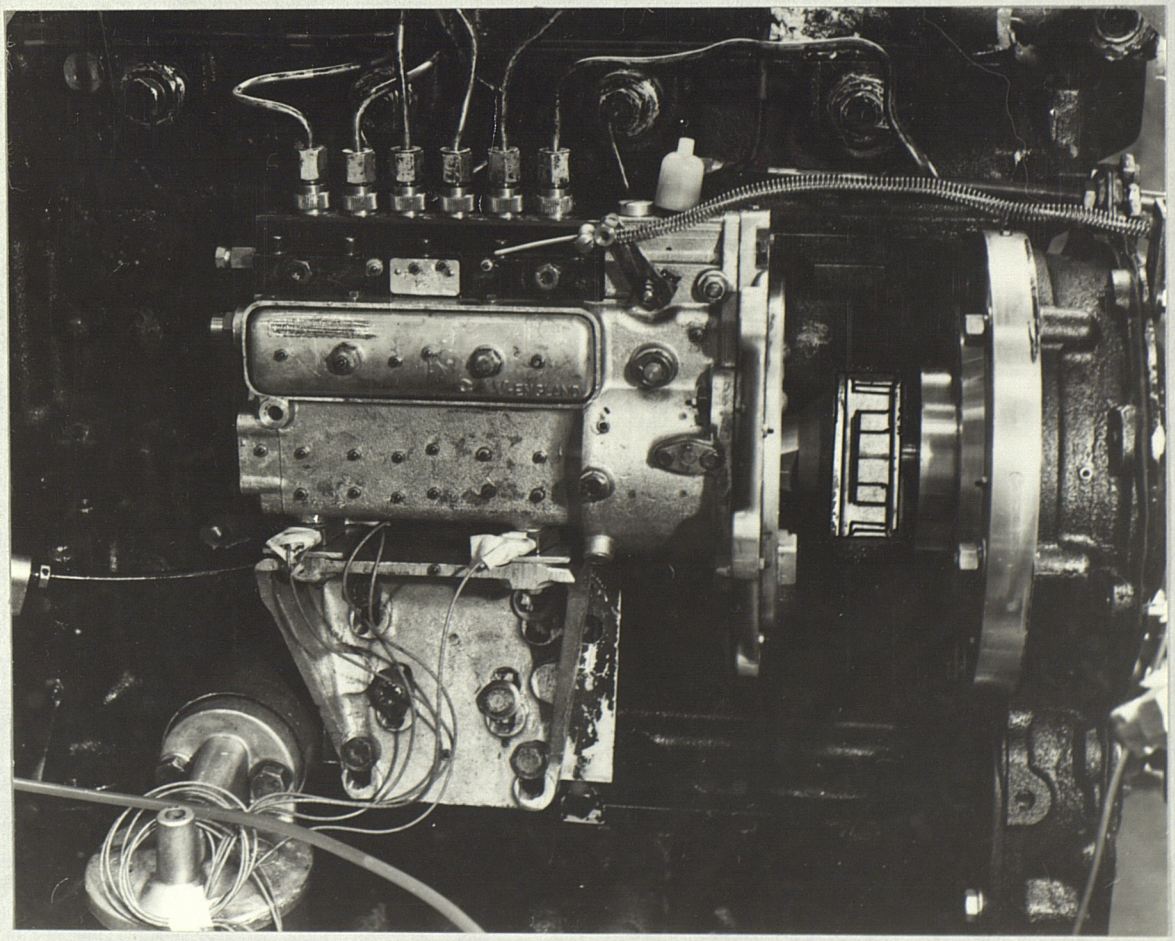

FIG. 8·4 b. BASE MOUNTED PUMP ASSEMBLY.

Figure 8.5b shows that when the base mounted pump was motored on the non-running engine the spectrum of the pump radiated noise is some 5 to 10 dB lower in the frequency range from 700 Hz to 8000 Hz than the noise radiated from the flange mounted pump. However, when the pump was driven by the engine under normal running conditions, the noise radiated by the base mounted pump was similar to that radiated by the flange mounted pump, as shown in Figure 8.5a.

8.3 Effect of Engine Structure Vibration on Pump Radiated Noise

Figure 8.5a compares the radiated noise from the base and flange mounted pumps on a running engine. The spectra show that the base mounted pump noise levels are increased by some 1 to 3 dB in the frequency range from 1250 Hz to 1600 Hz. This indicates that vibration originating from the engine structure had increased the pump surface vibration over the levels measured when the pump was motored on a non-running engine.

A comparison of the crankcase vibration spectra (Figure 8.6) measured on the bolts securing the base mounting bracket shows that the crankcase of Engine E has higher vibration levels than the crankcase of Engine A (normally fitted with a base mounted pump). The vibration levels measured have been converted into equivalent pump radiated noise. The differences between the vibration spectra of the engine crankcases of Engines A and E, is similar to the difference between the noise spectra of the base mounted pump driven on Engines A and E; i.e. within some 3 dB in the low frequency range from 3150 Hz (Figure 8.5a).

These test results showed that the base mounted pumps on Engines A and E radiated less noise than the flange mounted pumps when the excitation was from internally generated pump forces alone. As already stated the vibration levels measured on crankcase E were much higher than those measured on Engine A, therefore when the pump was base mounted to the crankcase of Engine E excitation of the engine structure increased the noise levels of the pump to match those of the flange mounted pump arrangement.

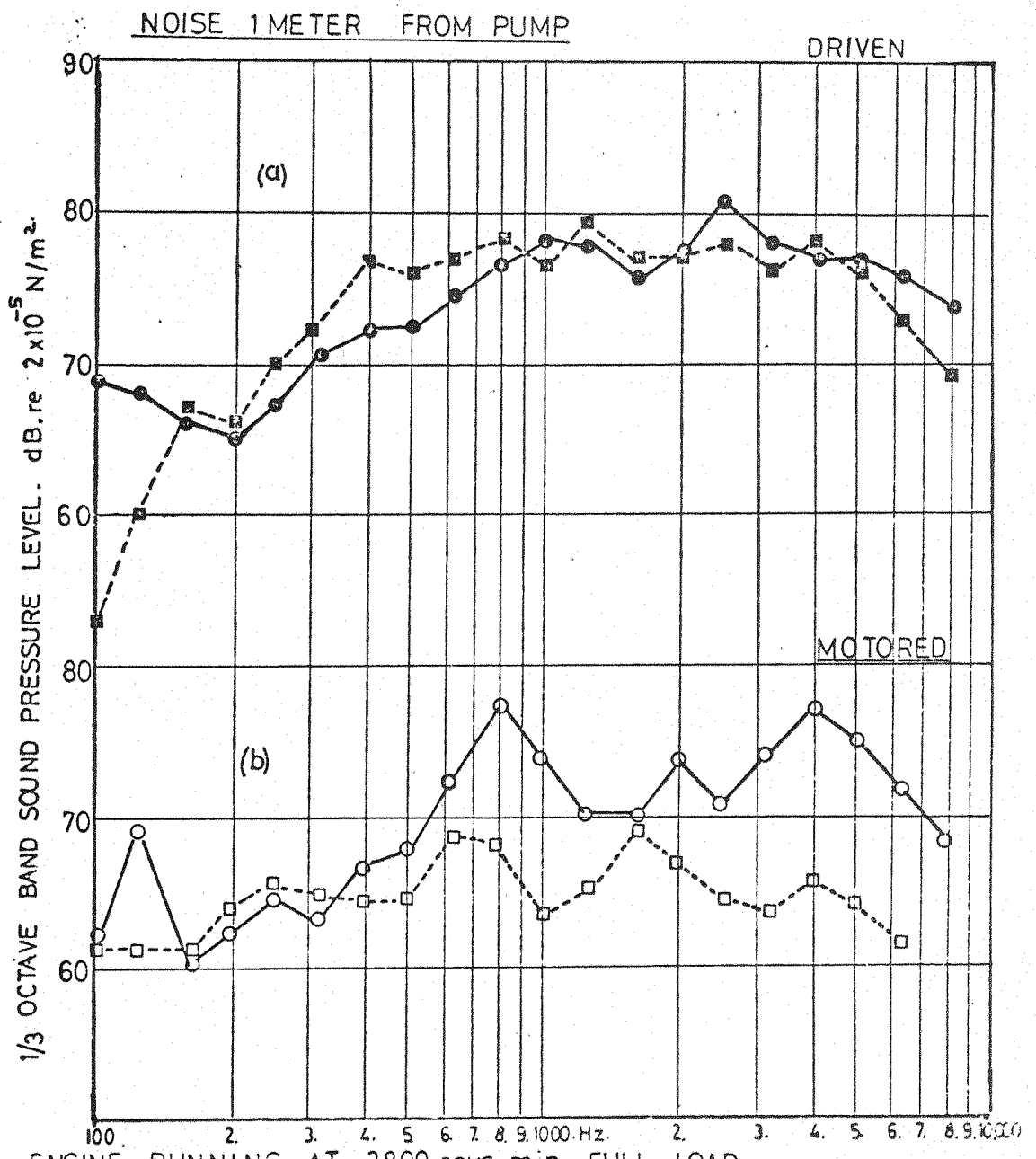

(a) ENGINE RUNNING AT 2800 revs min FULL LOAD

●——● FLANGE MOUNTED PUMP. DIRECT GEAR DRIVE.

■- - -■ BASE MOUNTED PUMP. C R.100. RUBBER COUPLING.

(b) PUMP MOTORED ON STATIONARY ENGINE. 1400revs/min. FULL FUEL

○——○ FLANGE MOUNTED PUMP. C R.100. RUBBER COUPLING.

□- - -□ BASE MOUNTED PUMP. " " " "

FIG. 8.5 COMPARISON BETWEEN FLANGE AND BASE MOUNTING OF SAME IN-LINE PUMP.

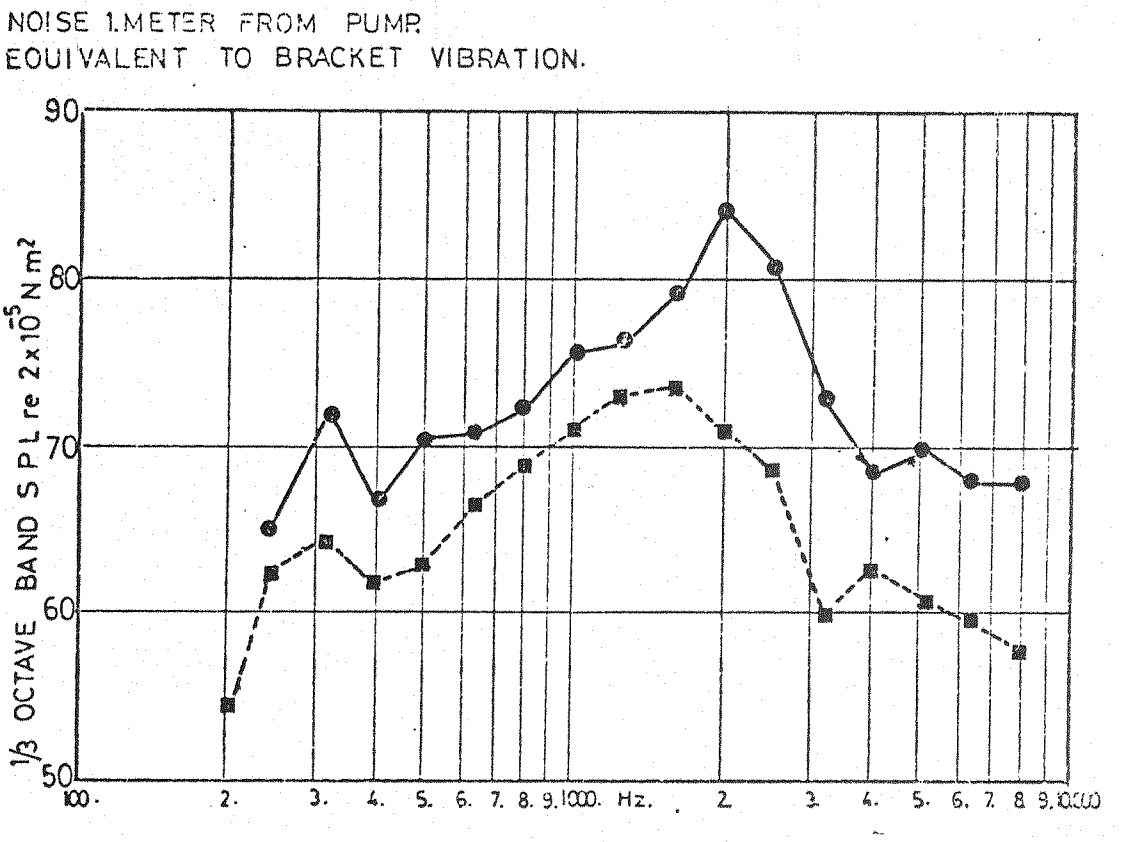

FIG.8·6. VIBRATION OF BRACKET WITH ENGINE RUNNING.

8.4 Effect on Pump Radiated Noise Due to Coupling

At all times during the investigation into noise from the pump the drive coupling was enclosed in order to minimise any noise from that source. With the aid of a stroboscope it could be seen that as pumping torque is applied, i.e. when the pump begins to force fuel to the injector, there is an impact due to backlash being taken up. The coupling itself does not radiate noise as stated by Russell and Pullen (5·7). This is a separate problem and has been a well known source of noise on pump test benches.

On Engine E an Oldham coupling, which had been in use for some time, was noted to have discernible backlash due to excessive clearances of the mating slots in the Tufnol disc. An Oldham coupling is shown in Figure 8.7.

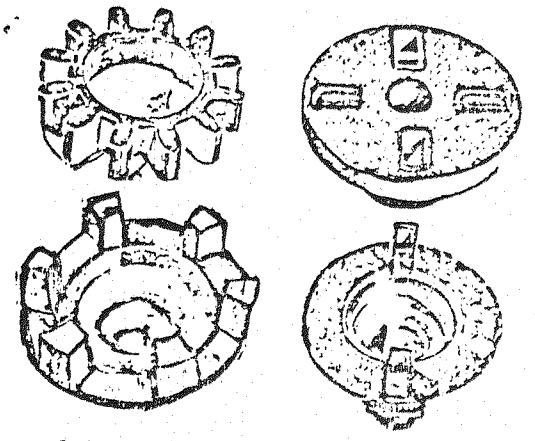

FIG.8·7 TYPES OF FUEL PUMP COUPLINGS.

When the Oldham coupling was modified with a new Tufnol disc with mating slots machined such that the dogs of the drive plate were a light push fit, the effect of backlash was then explored more thoroughly.

Results of the tests carried out on a base mounted pump driven via an hydraulic motor on a non-running engine compares the calculated noise radiated by the pump fitted with a sliding fit coupling and force fit coupling and are shown in Figure 8.8b. These results were calculated from vibration levels measured at some 29 points on the pump and governor casing. As can be seen the radiated noise from the pump has been significantly reduced by some 2 to 23 dB in the frequency range from 200 Hz to 8000 Hz.

Replacing the Oldham coupling with a CR 100 coupling, shown in Figure 8.7, the radiated noise spectrum shape was similar to that of the spectrum with the tight fit coupling. However there was a slight increase in noise levels of some 2 dB over the frequency range from

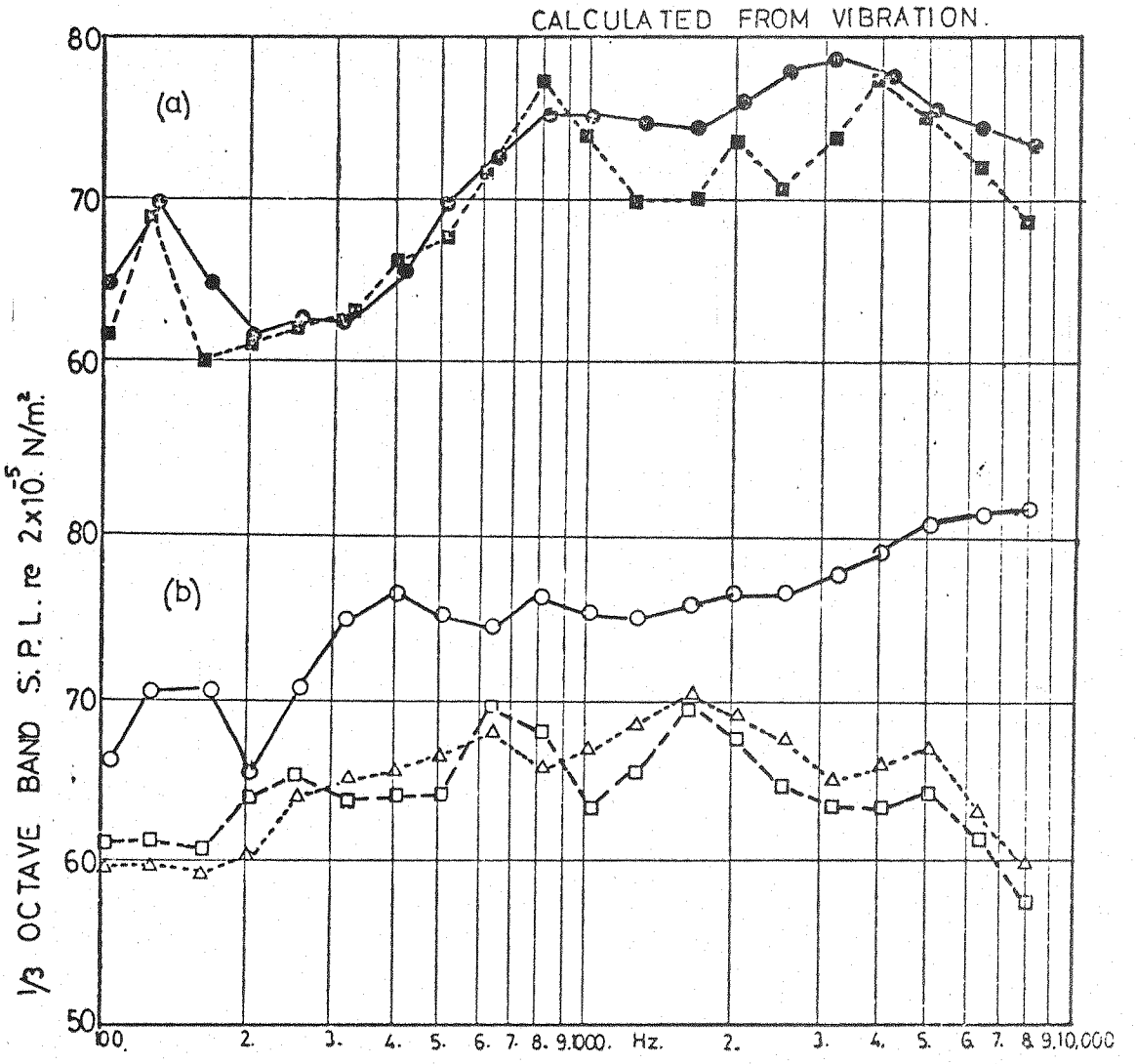

(a) FLANGE MOUNTED PUMP MOTORED ON STATIONARY ENGINE.

DRIVEN VIA OLDHAMS COUPLING. PRESS FIT.

DRIVEN VIA C R 100 RUBBER COUPLING.

(b) BASE MOUNTED PUMP MOTORED ON STATIONARY ENGINE

PUMP DRIVEN VIA OLDHAMS COUPLING SLIDING FIT.

" " " " " FORCE FIT.

PUMP DRIVEN VIA C R100 RUBBER COUPLING.

FIG 8·8 EFFECT OF BACKLASH IN DRIVE TO CAMSHAFT.

1000 Hz to 8000 Hz. This small difference could be the effect of changes in coupling stiffness rather than backlash.

Further tests were carried out on the flange mounted pump motored on Engine E with two types of coupling, (a) the tight fit Oldham coupling and (b) the CR 100 coupling. From the results shown in Figure 8.8a it can be seen that the CR 100 coupling reduces the radiated pump noise levels by some 1 to 4 dB in the frequency range from 1000 Hz to 4000 Hz.

8.5 Effect of High Pressure Pipes on Noise

Tests have shown that the radiated noise of the fuel injection pump can be influenced by the vibrating forces generated in the pipes due to the opening and closing of pump delivery valve and injector needle impacts.

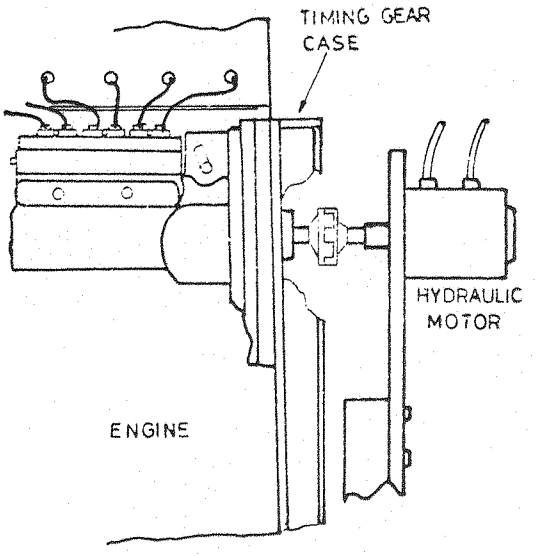

FIG. 8·9.

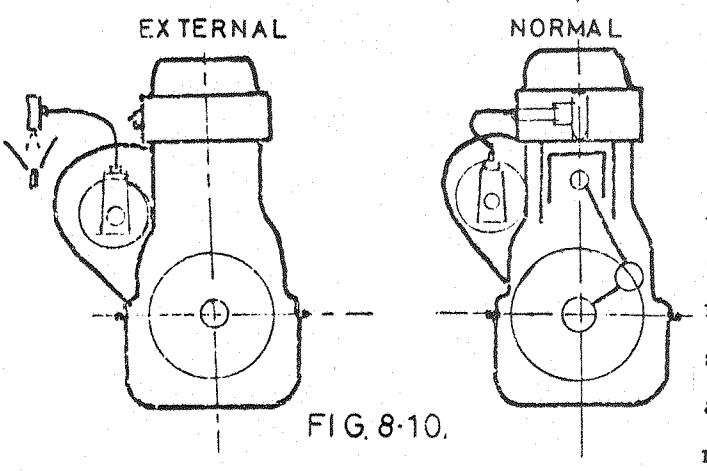

FIG. 8·10.

Considering the mass of the engine in comparison with that of the pump and, as in this particular case, the flange mounted pump is fixed as a cantilever (Figure 8.9), the 'free' end of the pump would be susceptible to forces due to the pressure pulses in the pipes. It is also possible that these forces that are set up in the pipes may be enhanced by the cylinder head vibration due to operation of injectors and combustion, i.e. the pipes would respond to the bodily movement of the cylinder head.

A paper published by Austen and Priede on the origins of injector noise states the noise is mainly produced by the sudden closing of the needle and two main components of the noise are due to spring surges

in the frequency range around 2.0 kHz and to needle impacts around 5.0 kHz.

To assess the effect of these transmitted forces, hence the noise of the pump structure, the pump was flange mounted on the engine as for normal operation but driven by an hydraulic motor as shown in Figure 8.9.

Noise was measured for the following conditions (a) injectors normal, as for running engine and (b) injection external from the cylinder head of the engine as shown in Figure 8.10.

For each test the engine and high pressure pipes were enclosed with lead sheeting lined with fibreglass wool, leaving the pump exposed.

The speed of the pump was measured using a Dawe stroboscope. Noise of the hydraulic motor was at least some 15 dB below the noise of the pump over the predominant frequency range. To minimise any coupling backlash and noise a CR 100 coupling was used. The drive shaft and coupling were also enclosed by lead sheeting.

Noise spectra taken at various speeds for injectors normal and external are shown in Figure 8.11.

It can be seen when the injectors are external to the engine structure, the noise levels at the maximum rated speed of the pump, i.e. 1400 rev/min, full rack condition, have been reduced by 2 dB to 5 dB over the frequency range from 630 Hz to 2000 Hz and by some 1 dB to 7 dB over the higher frequency range from 2500 Hz to 8000 Hz.

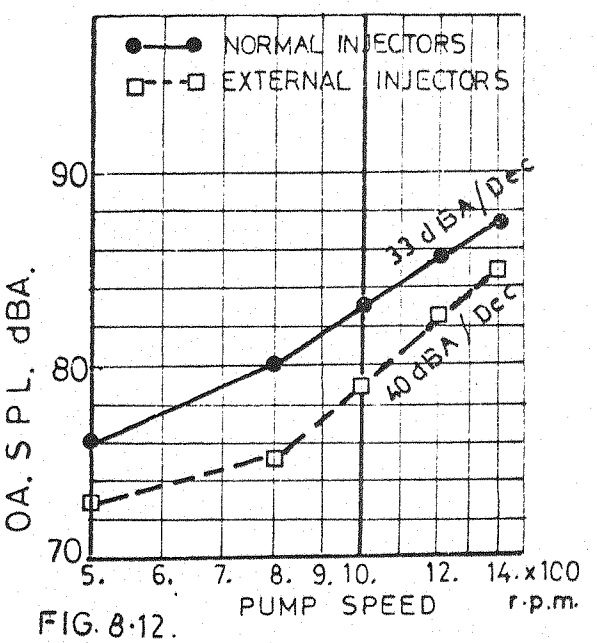

FIG. 8·12.

At pump speeds of 1200, 1000 and 750 rev/min, the noise levels have been reduced by some 2 dB to 10 dB over the frequency range from 160 Hz to 8000 Hz.

The significance of these results is more clearly seen by a plot of overall noise level versus speed as shown in Figure 8.12. The overall noise levels over the speed range have been reduced by 2 dBA to 5 dBA when the injectors were operated externally.

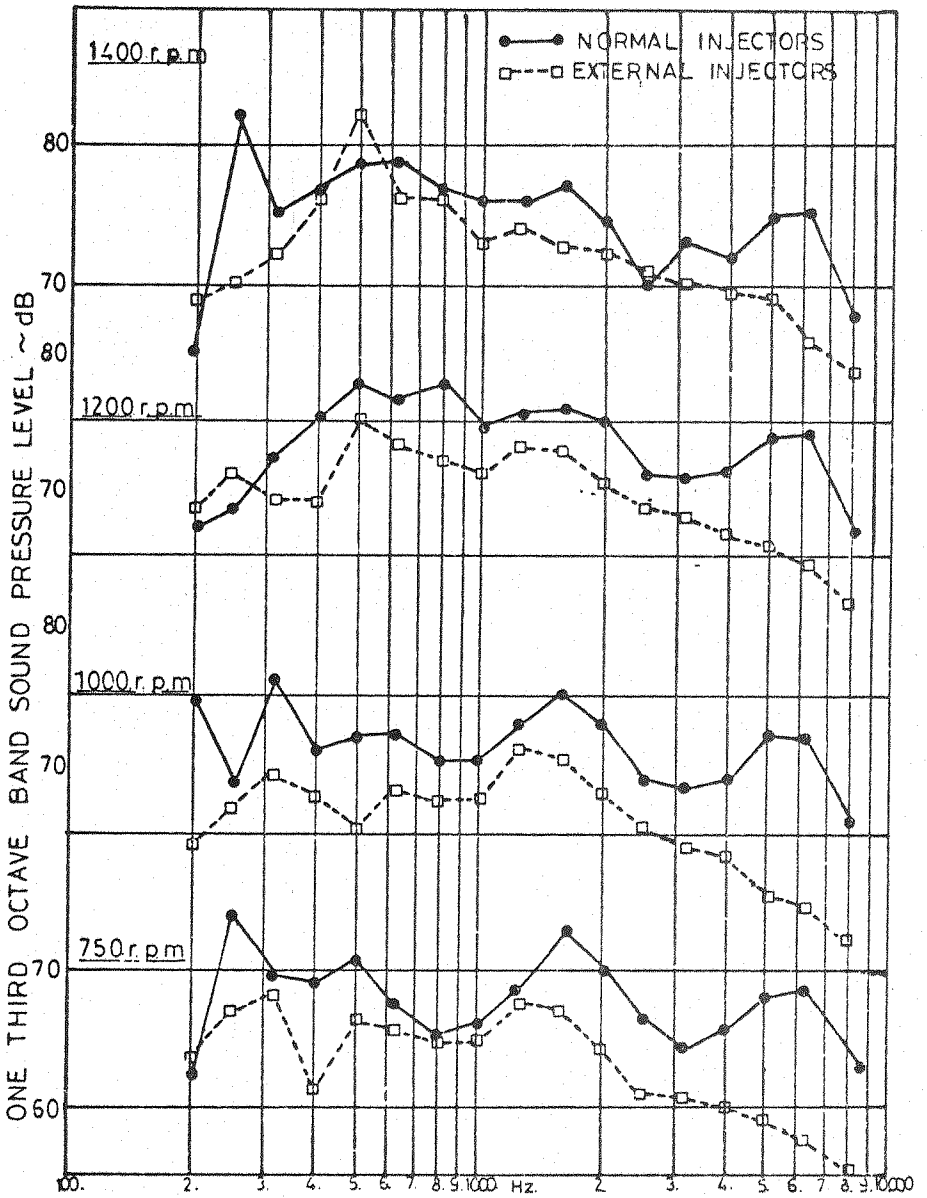

FIG 8·11. EFFECT OF HIGH PRESSURE PIPES ON NOISE RADIATING FROM PUMP

8.6. Vibration Assessment of Pump Structure - Injectors Normal and Externally Mounted

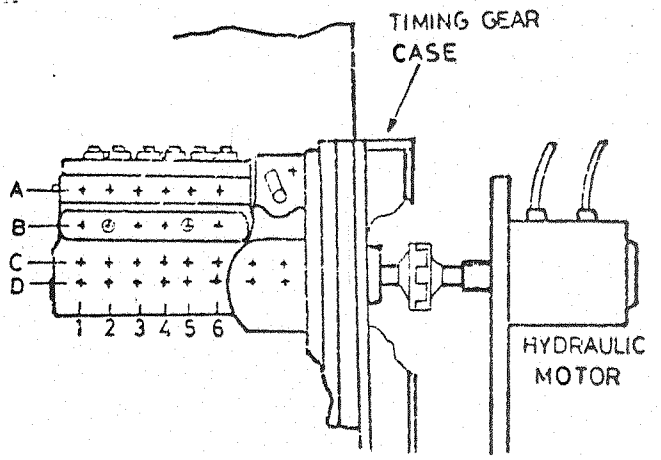

FIG. 8.13.

Vibration spectra were obtained for each of the 29 accelerometer pick-up points on the pump casing including governor housing as shown in Figure 8.13. The pump was motored at its maximum rated speed of 1400 rev/min full fuelling.

From the spectra taken at each respective point on the pump, the general variation in vibration levels for normal and externally mounted injectors are illustrated by (i) the three-dimensional plots for one-third octave band frequencies at 500 Hz, 800 Hz, 1250 Hz, 2000 Hz, 2500 Hz and 4000 Hz, (as shown in Figure 8.14), and (ii)by the plots of vibration patterns in a vertical plane on the pump casing (Figure 8.15).

In general these results show operating the injectors externally, the vibration levels of the pump casing have been reduced over a wide frequency range with the exception at 2500 Hz where levels of vibration have slightly increased.

From the spectra obtained from the pump casing (29 positions) the vibration levels for each respective one-third octave band were 'summed and averaged' producing a single spectrum for each operating condition, i.e. injectors normal and injectors externally operated. (Figure 8.16).

These results indicate the vibratory forces transmitted to the pump structure via the high pressure pipes are reduced by some 2 dB to 5 dB over the frequency range from 500 Hz to 8000 Hz with the exception of 2500 Hz where the levels have increased by 2 dB. With reference to Figure 8.11 it can be seen that the noise spectra at 1400 rev/min also show an increase at 2500 Hz.

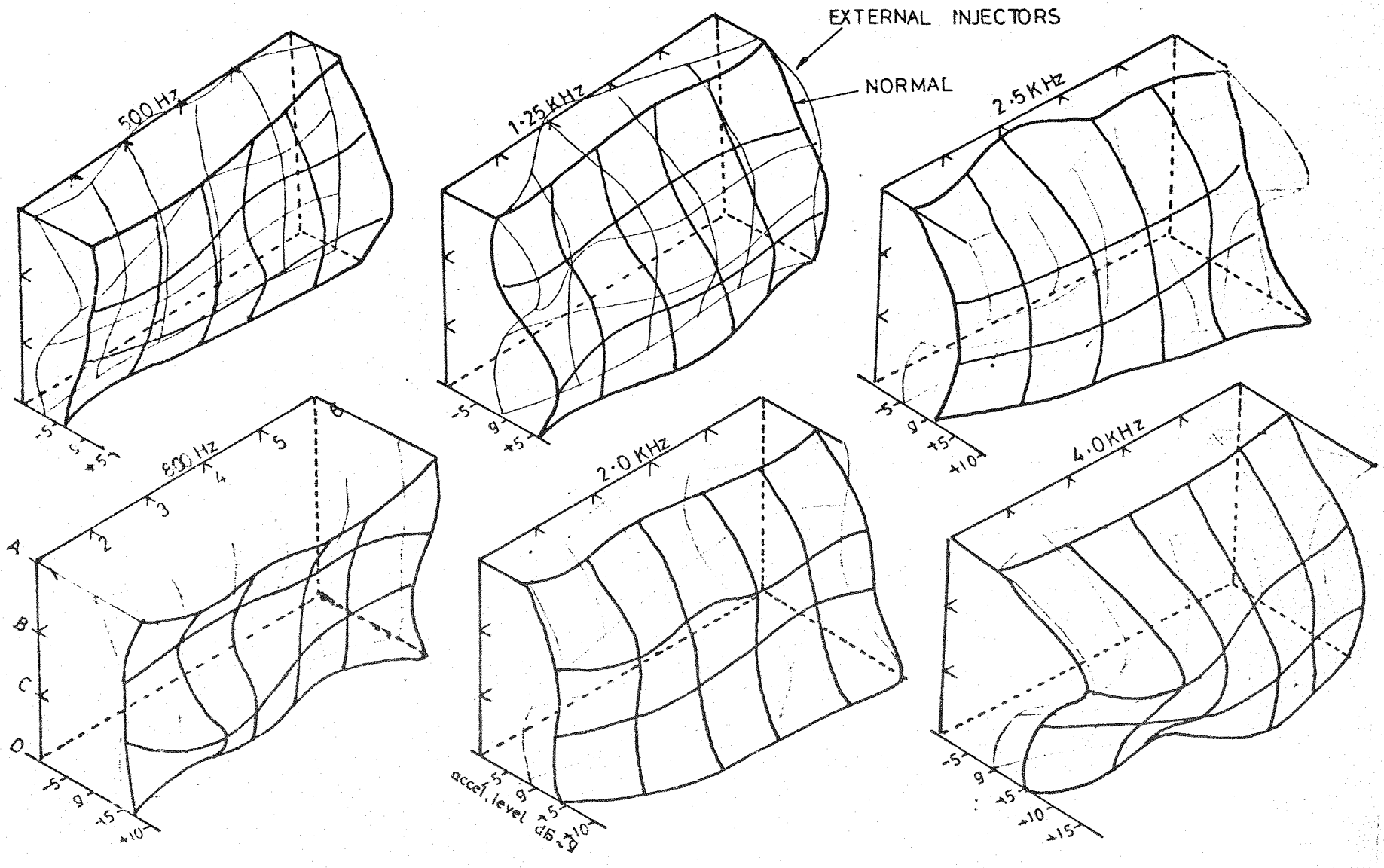

FIG. 8·14. THREE DIMENSIONAL PLOTS SHOWING VARIATION IN VIBRATION LEVELS.

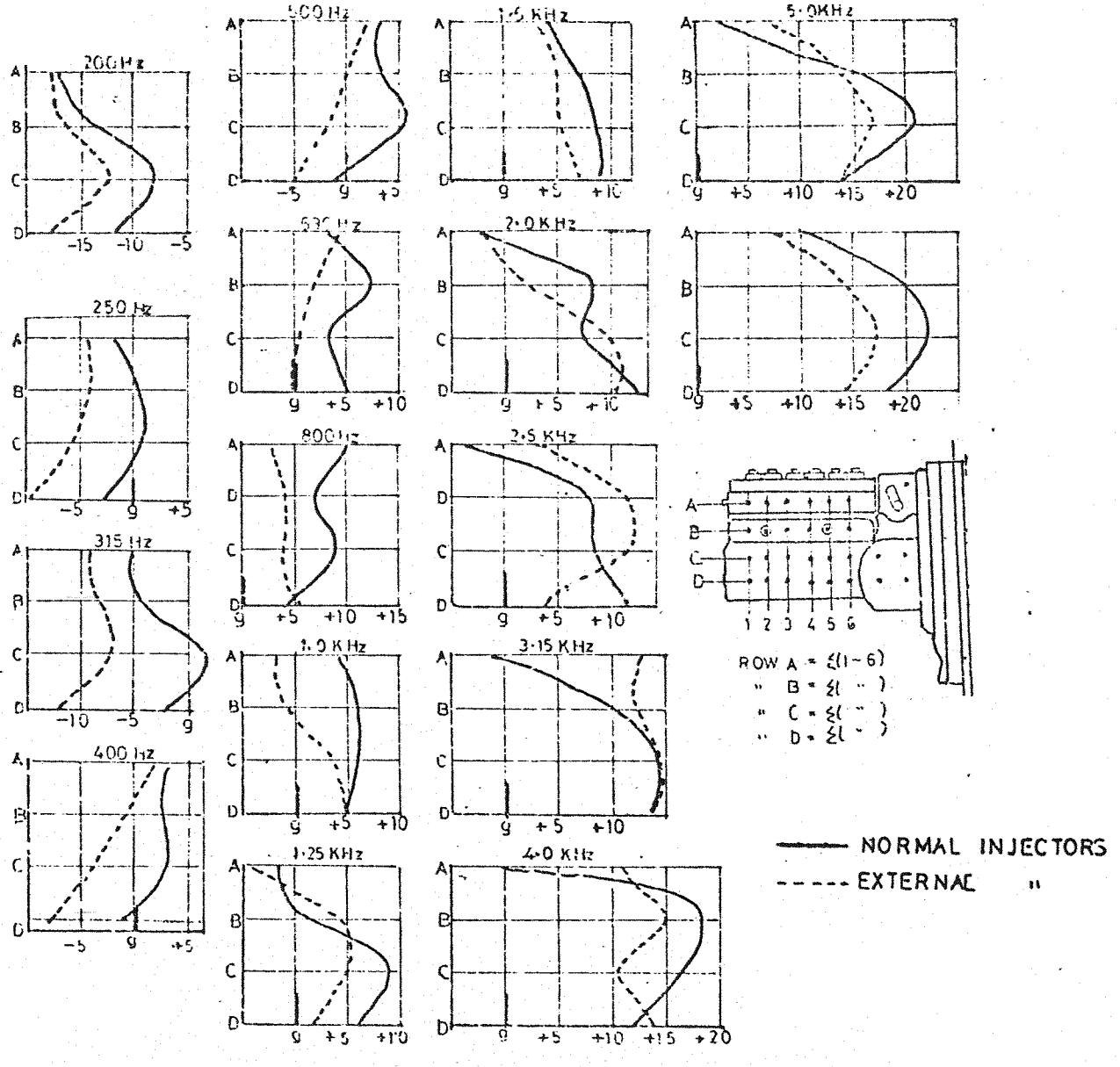

FIG. 8·15. VIBRATION PATTERN IN VERTICAL PLANE. (AVERAGED)

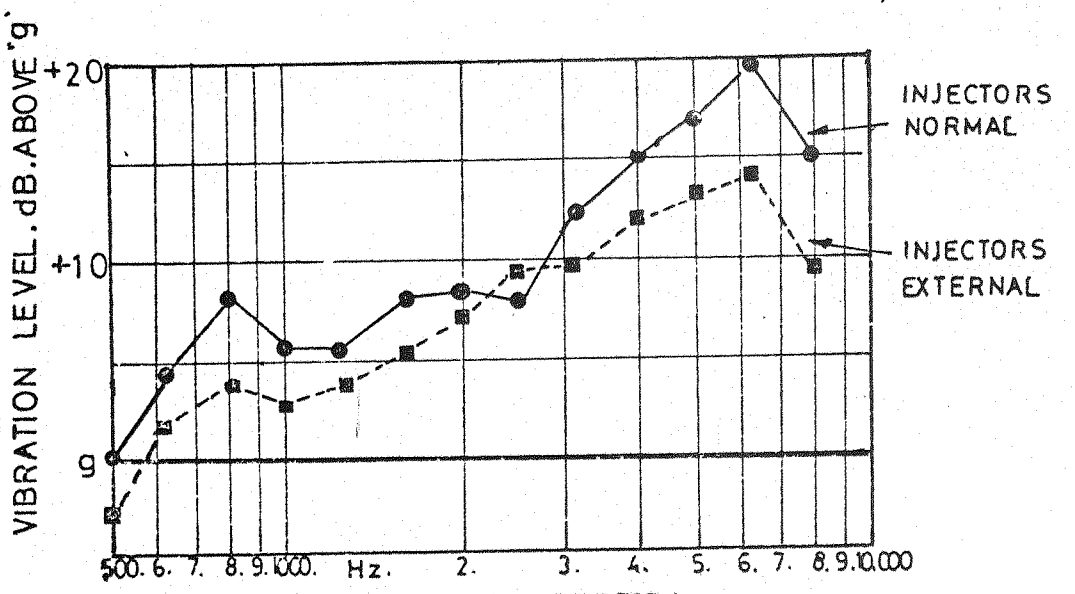

FIG.8·16 AVERAGED VIBRATION SPECTRA

In order to verify the measured noise results, noise levels were calculated from the pump surface vibration levels (detailed in Chapter 7). Figure 8.17 compares the measured noise spectra for normal and externally operated injectors for (a) the measured and calculated noise levels for injectors normal; (b) calculated and measured noise levels with injectors external; (c) and (d) compares the calculated noise levels of the injectors normal and externally operated.

These results show that the calculated noise levels conform to within a few dB of the measured noise levels.

8.7. Vibration Characteristics of Engine Structure Injectors Normal and Externally Operated

In order to assess the response of the engine structure due to the operation of the injectors, vibration acceleration levels were taken at 30 points on the engine block and crankcase as shown in Figure 8. 18 .

The pump was driven by an hydraulic motor on the stationary engine, at its maximum rated speed of 1400 rev/min full fuelling.

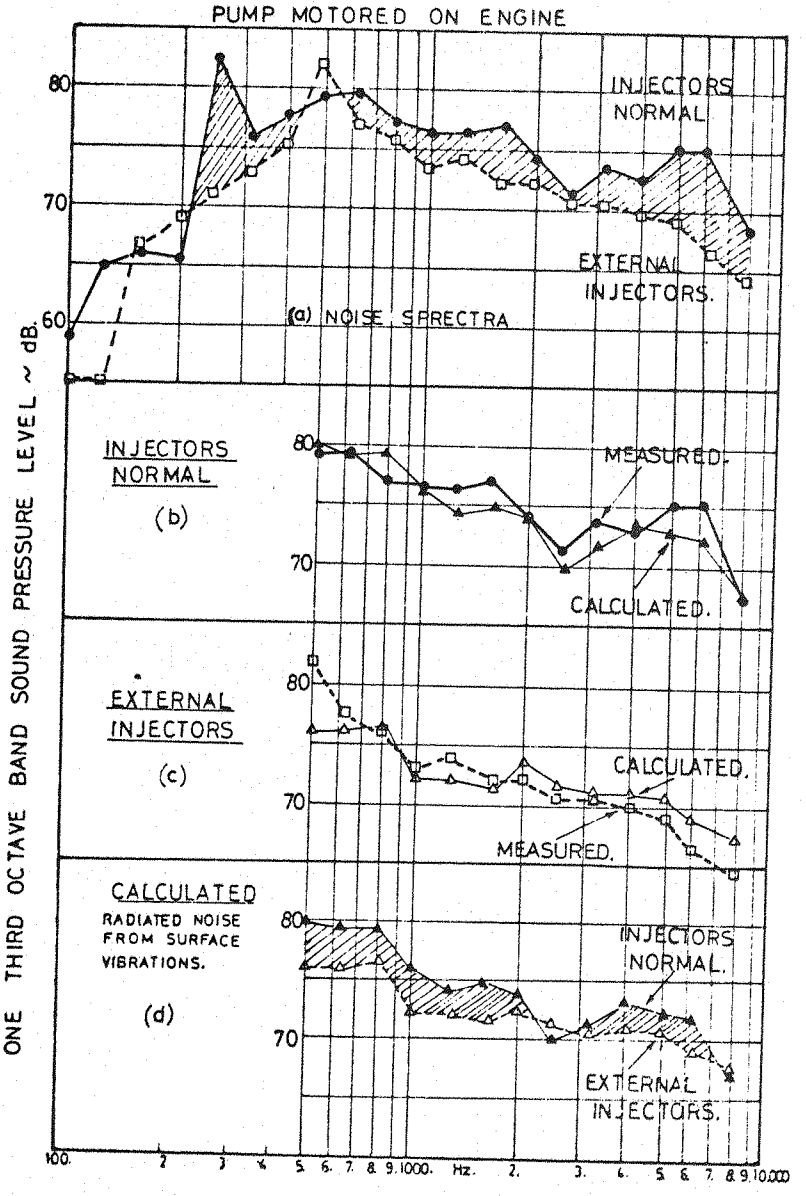

FIG. 8·17. EFFECT OF HP PIPES ON PUMP NOISE.

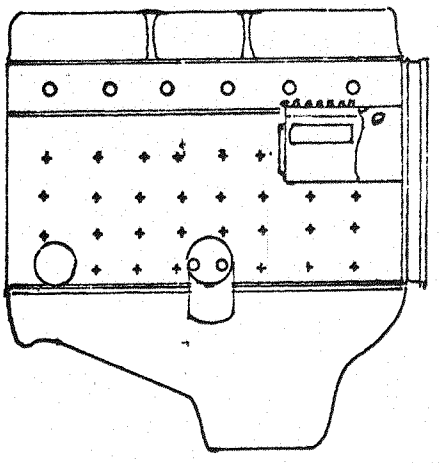

FIG. 8·18. ACCELEROMETER STUD POSITIONS.

As found by Austen and Priede (2·15) the injector structure, similar to that of the pump is being excited by two distinct transients. The noise produced by lifting the needle is negligible, but a large proportion of the noise results from the needle striking the seat. Due to the oscillatory nature of the injection in this instance, the needle strikes the nozzle twice, but the predominant noise impulse will coincide with the seating of the needle.

It can be shown that other parts of the engine structure, far removed from the cylinder head, responds effectively to injector vibrations.

From each respective point on the engine structure a vibration acceleration spectrum was obtained. The one-third octave band levels from each spectrum were 'summed' and 'averaged' hence producing a single spectrum indicating the general response of the structure when the injections were operated both normally and externally.

Figure 8.19 indicates that when the injectors were operated externally the vibration response of the engine structure shows little change in the low frequency range from 100 Hz to 1000 H z. In the high frequency range, however, the vibration levels reduce significantly by some 2 to 25 dB from 1000 Hz to 8000 Hz.

The 'averaged' vibration spectrum of the engine structure is also shown in Figure 8.19 for the engine running condition of 2800 rev/min, full load. The broad band peak in the low frequency range, centred at 315 Hz is due to the fundamental bending of the engine structure. In the high frequency range above 1000 Hz the rate of increase of vibration levels with increase in frequency is very similar to the response of the engine structure with the injection pump being operated by hydraulic motor. However the amplitudes of vibration levels

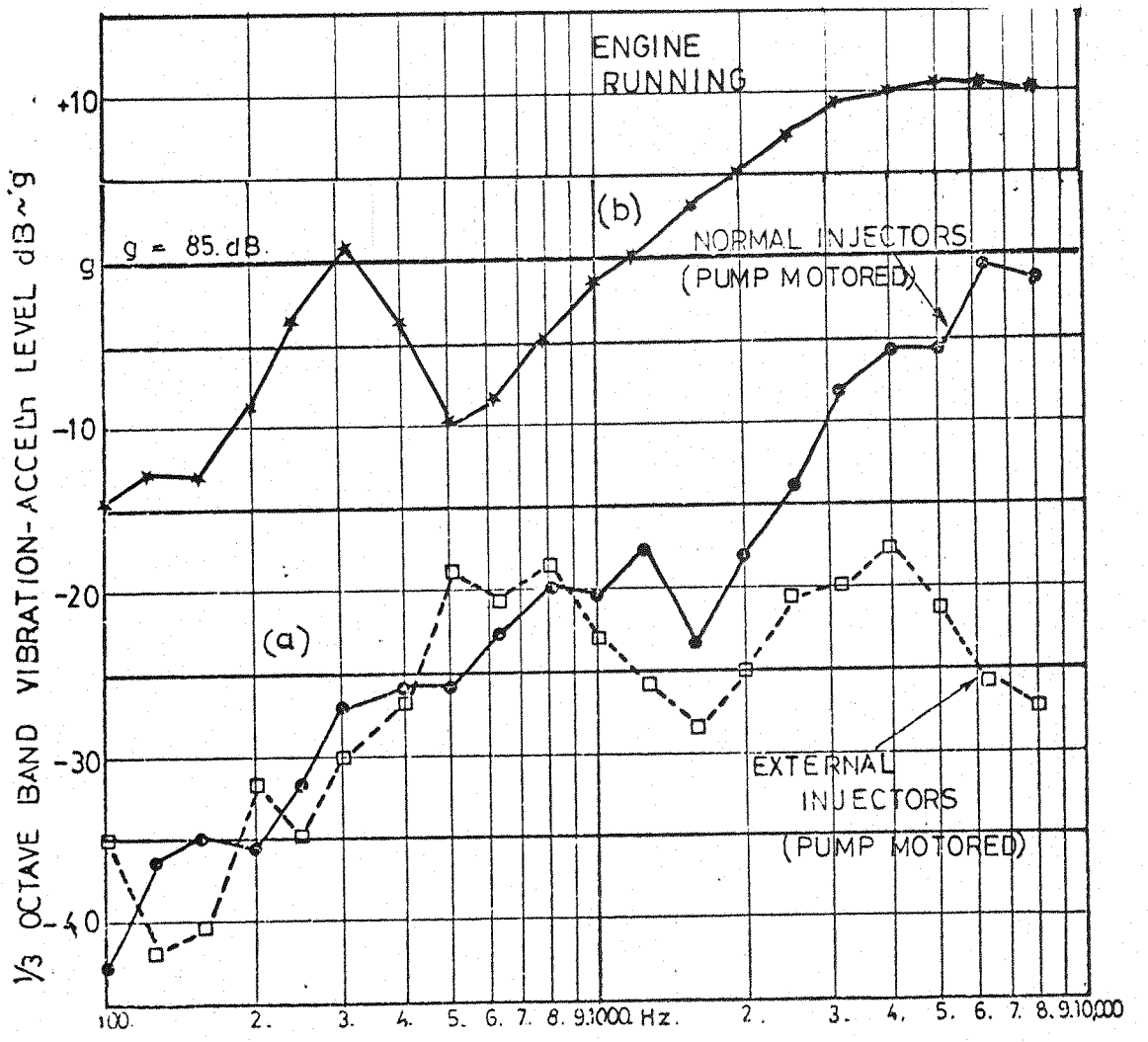

FIG 8·19 EFFECT OF INJECTORS ON ENGINE STRUCTURE VIBRATION.
("AVERAGED" VIBRATION LEVELS.)

are some 11 dB to 24 dB lower over the whole frequency range.

8.8. Conclusions

It has been found that one of the major factors influencing the noise radiated by the pump is backlash in the pump drive coupling. When the backlash is taken up the vibration levels of the pump surfaces can be significantly reduced by some 10 dB in the high frequency range from 1000 Hz to 8000 Hz.

With regard to crankcase vibrations affecting the pump radiated noise, when a particular engine crankcase was modified to enable the normally flange mounted pump to be base mounted, the crankcase vibrations were responsible for an increase of pump radiated noise of some 5 dBA when compared with another engine fitted with a base mounted pump. It is therefore essential that the pump bracket is secured to the engine structure where vibration levels are at minimum.

From tests made to compare the effect of base and flange mounting on the radiated noise from the pump, it is indicated that the pump radiated noise, due to vibration excitation originating from the pump, is greater when the pump is flange-mounted than when the pump is base mounted.

Tests carried out to assess the effect of the high pressure pipes on the pump radiated noise show that when the injectors are operating externally from the engine (i.e. removed from the cylinder head) the noise levels, at the maximum rated speed of 1400 rev/min are reduced by some 2 to 5 dB in the frequency range 630 Hz to 2000 Hz and by 1 to 7 dB in the high frequency range 2500 Hz to 8000 Hz. The overall levels over the speed range are reduced by 2 dBA to 5 dBA.

Tests carried out to assess the vibratory response of the engine structure due to the operation of the injectors, (pump being driven by an hydraulic motor) show that when the injectors are operating externally the 'averaged' vibration levels of the engine structure are reduced by some 2 to 25 dB in the higher frequency range from 1000 Hz to 8000 Hz, indicating injector needle impacts can in some cases significantly influence the vibration of the engine structure.

9. CONCLUSIONS

From the investigations presented in the thesis on various aspects of the origins of the noise of in-line injection pumps coupled to their appropriate engine structures, the following general conclusions can be drawn.

(1) The basic cause of injection pump vibration and emitted noise is the sudden application and removal of pump chamber hydraulic force of short duration which is applied via the injection pump camshaft to the pump body structure. The induced vibrations are of a transient nature similar to diesel engine block vibrations which are induced by rapid pressure rise resulting from diesel combustion.

The exciting propensities of the injection pump hydraulic force, which have been defined theoretically and experimentally, differ in characteristics from those of the gas force exciting propensities. The injection hydraulic force harmonics of constant amplitude extend to about the 20th harmonic above which there is a general decay of higher frequency force harmonics at about 40 dB/decade. At engine rated speeds, the range where harmonics are of constant amplitude thus may extend up to a frequency of 1000 Hz. For the gas force spectrum of a typical normally aspirated diesel engine the low frequency harmonics of constant magnitude are only few (4 or 5 harmonics followed by a steady decay by 30 dB/decade.

The increase of vibration and noise with speed is controlled by the force spectrum. In injection pumps it is due to two major parameters, the general increase of peak hydraulic pressure with speed, which causes a steady increase of the low frequency (below 1000 Hz) portion of the force spectra, and the increase in excitation levels due to a parallel shift of the force spectra along the frequency axis resulting from an increase of repetition rate (speed). In the engine the increase of excitation applied to the engine structure (peak cylinder pressure) remains constant with engine speed. Only the second effect is prominent and the slope of the gas force spectrum controls the rate of increase of noise with speed.

(2) The characteristics of the pipe line hydraulic force, which acts only on the top part of the pump structure, is more or less

identical to the pump chamber hydraulic force in the low frequency part of the spectrum. The high frequency part of the pipe-line hydraulic force spectrum is primarily controlled by the oscillatory pressure waves in the high pressure pipes. The general rate of decay is about 30 dB/decade. The experimental evidence shows that the high frequency range of the pump noise is controlled by these oscillations in pipe-line pressure.

(3) The pump structure vibration in the audio frequency range exhibits only solid body modes. The typical panel modes which control the engine block vibrations in the high frequency range from 1000 to 10,000 Hz are not important in pump structure vibration. These modes may be present but they are at very high frequencies and are thus of no specific interest.

(4) The evidence of various experimental tests and theoretical considerations indicate that pump vibration is primarily stiffness controlled. The pump structure is heavily damped (Q = 9), resulting in the vibration amplitude spectrum being of identical form to the force spectrum. Narrow band frequency analysis shows that pump vibration and noise contain mainly the firing frequency harmonics. Measurements made with various pump elements operating show that the elements further away from the camshaft bearings produce greater amplitudes of vibration in the pump structure.

A simple theoretical model based on general stiffness considerations of the pump structure and engine structure as excited by their relevant forces confirms the experimental results on six engines, that vibration levels of the pump are in general higher by about 10 dB than those of the engine block.

(5) Pump chamber hydraulic pressure not only excites the pump structure but also the whole engine structure. The measurements of the mean vibration levels of engine structure under running conditions and with injection pump motored on the engine show that the response of the engine structure expressed in terms of attenuation levels (force level dB/vibration level dB) is basically the same for both types of excitation. It is also found that the characteristics of the forces transmitted via the pump mountings are similar to those of the pump chamber hydraulic forces.

(6) Investigations on radiation of noise confirm that injection pump noise is emitted mainly by the pump surfaces and that the pump induced vibration of the engine structure is not a major contributing factor to overall engine noise.

(7) There are numerous other factors which control the noise emitted by injection systems and it was found that the back-lash in the drive coupling is very important. Methods of pump mounting produce considerable effects on emitted noise. The mass, stiffness and damping of the system to which the pump is mounted, whether on an engine or a test rig, influence significantly the pump body vibration. The very high frequency part of the spectrum tends to be controlled by injector needle impacts and in some cases the injection pipe configuration also affects the emitted noise.

REFERENCES

2. 1. A.F. Evans. 'History of the Oil Engine'. Publishers Sampson Low, Marston.

*2. 2. Priestman. Contemplation of Air-Less Injection.

*2. 3. A. Stuart. " " " " "

*2. 4. Capitaine. " " " " "

*2. 5. R. Diesel. " " " " "

*2. 6. McKechnie. Air-Less Injection for Large Diesel Engines.

*2. 7. Hornsby. Snail Cam Application.

*2. 8. Blackstone. Fuel Injection Accumulator System.

*2. 9. Robson. Conventional Suction and Delivery Valve.

*2.10. Harland and Wolf. Long Stroke Pump. Harmonic Motion.

* Extracts from Publication (reference 2.1).

2.11. F.H. Evans. 'A Review of In-Line Fuel Injection Pump Development'. Inst. Mech. Engrs. 1956.

2.12. R. Bosch. Design of In-Line Fuel Injection Pump.

2.13. Ruston. Differential Needle Valve.

2.14. Atlas Diesel Company. Unloading Delivery Valve.

Extracts from Publication (reference 2.11).

2.15. A.E. Austen and T. Priede. 'Noise of Diesel Engine Injection Equipment'. J.Sound Vib. 1967, p.443-459.

2.16. T. Priede. Considerations of Hydraulic Forces.

Extract from Publication (reference 2.15).

2.17. Zimmerman. 'The Noise Produced by the Injection Pump and its Relation to Total Engine Noise'. S.A.E. Paper 690449, 1969.

2.18. T.B. Barham. 'Comparison Between the Vibration Characteristics of Two Maxi-Mec Pumps on Their Respective Ford Devon and Leyland 5.10 Engines'. Lucas Industrial Noise Centre Note, No. 239.

3. 1. D. Anderton. 'Harmonic Analysis of Repetitive Waveform Using Digital Techniques'. ISVR Memorandum Nos.178 and 208.

5.1. N. Lalor. 'Computer Optimised Design of Engine Structure for Low Noise'. S.A.E. Paper 790364, 1979.

5.2. D.M. Croker, N. Lalor and M. Petyt. 'The Use of Finite Element Technique for the Prediction of Engine Noise'. Inst. Mech. Engrs. Conference Paper, 1979, C146/79.

5.3. C.M.P. Chan and D. Anderton. 'The Correlation of Machine Structure Surface Vibration and Radiated Noise'. Internoise Proceedings, Washington, 1972.

5.5. E. Madenic and R. Lyon. 'Static Method on Vibration Analyses'. A.I.A.A. Journal $\frac{2}{}$ pp. 1015-1024, 1964.

8.1. M.F. Russell and H.L. Pullen. 'The Influence of Mountings on Injection Pump Noise'. S.A.E. Paper, 790273, 1979.

Appendix - Harmonic Analysis Computer Programme.

HARMONIC ANALYSIS PROGRAM. (D. ANDERTON.)

APPENDIX. A

```
USER IS1003      JOB TEST1004O     FORTRAN F1.R.60 (01)      COMPILATION 1979/02/16  20:10:15   PAGE

LINE NUMBER   FORTRAN TEXT

    1              PROGRAM ANDER                                                                  1
    2               DIMENSION FR(23)                                                              2
    3               DIMENSION C(6050),D(400),E(400),A(1200),R(1200),DB(1200),AIAN(12              3
    4              *00),AK(1200),B(1200),X(6050),IXT(7),FREQ(1200),DC(310),EC(310)                4
    5               DIMENSION AIANT(1200),DBT(1200)                                               5
    6               INTEGER   IX1(2),IY1(7),IY2(8)                                                6
    7               INTEGER   IY3(6),IY3(3)                                                       7
    8               DATA IX1/7HDEGREES/                                                           8
    9               DATA IY1/28HCYLINDER PRESSURE INPUT DATA/                                     9
   10               DATA IY2/31HCYLINDER PRESSURE COMPUTED DATA/                                  10
   11               DATA IY3/23HCYLINDER PRESSURE LEVEL/                                          11
   12               DATA IX5/9HFREQUENCY/                                                         12
   13               DATAFR(1),FR(2),FR(3),FR(4),FR(5),FR(6),FR(7),FR(8),FR(9),FR(10),             13
   14              *  FR(11),FR(12),FR(13),FR(14),FR(15),FR(16),FR(17),FR(18),                   14
   15              *    FR(19),FR(20),FR(21),FR(22),FR(23),FR(24),FR(25),FR(26),                 15
   16              *    FR(27),FR(28)/20.0,25.0,31.5,40.0,50.0,63.0,80.0,100.0,                  16
   17              *    125.0,160.0,200.0,250.0,315.0,400.0,500.0,630.0,800.0,1000.0,            17
   18              *    1250.0,1600.0,2000.0,2500.0,3150.0,4000.0,5000.0,6300.0,                 18
   19              *    8000.0,10000.0/                                                          19
   20         11     CONTINUE                                                                     20
   21              READ(5,* )L,IX,IY,IB,IXX,ICASE                                                21
   22              READ(5,*  )AFAC,AFAG,AL,ENB,RPM                                               22
   23              READ(5,*  )(D(J),E(J),J=1,IXX)                                                23
   24         C    Y COORDINATE INPUT FORMAT CHANGED TO ACCOMODATE 6 FIGURE INPUT                 24
   25              IPA=1                                                                         25
   26              AH=1.0                                                                        26
   27          902 FORMAT(1X,25HX AND Y INPUT COORDINATES)                                       27
   28              WRITE(6,902)                                                                  28
   29              WRITE(6,901)(D(J),E(J),J=1,IXX)                                               29
   30              CAFA=/FAC/AFAG                                                                30
   31              DO 90 J=1,IXX                                                                 31
   32              E(J)=E(J)*CAFA                                                                32
   33           90 CONTINUE                                                                      33
   34              DO 93 J=1,IXX                                                                 34
   35              D(J)=D(J)*360.0*ENB/(D(IXX))                                                  35
   36           93 CONTINUE                                                                      36
   37              IK=2                                                                          37
   38              KID=0                                                                         38
   39              FL=D(IXX)-D(1)                                                                39
   40              ITCH=(IX-1)/5                                                                 40
   41              DIV=1.0/AL                                                                    41
   42              IXT=IX+1                                                                      42
   43              C(1)=E(1)                                                                     43
   44              X(1)=D(1)                                                                     44
   45              DO 89 IT=2,IX+1                                                               45
```

```
      AIT=FLOAT(IT)
      X(IT)=(AIT-1.0)*DIV*FL
      DO 88 J=2,IXX
      IF(D(J).LT.X(IT))GOTO 88
      IF(D(J).EQ.X(IT))C(IT)=E(J)
      IS=J-1
      IF(D(J).GT.X(IT))
     *  C(IT)=E(IS)+(E(J)-E(IS))*(X(IT)-D(IS))/(D(J)-D(IS))
      GOTO 750
   88 CONTINUE
  750 CONTINUE
      X(IT)=IT-1
      X(IT)=X(IT)*360.0*ENB/AL
   89 CONTINUE
      IX=IX+1
      DC(1)=D(1)
      EC(1)=E(1)
      IMAS=IX/20
      DO 3 J=2,IMAS
      I=J*20
      DC(J)=X(I)
      EC(J)=C(I)
    3 CONTINUE
      DO 92 LA=1,(IX-1)/2
      JOT=LA*2
      C(JOT)=C(JOT)*2.0
   92 CONTINUE
      C(1)=C(1)/2.0
      C(IX)=C(IX)/2.0
      IF(KT.GT.1) GOTO 4
    4 CONTINUE
      DO 15 K=IPA,IX,IY
      IF(K.GT.IB)GOTO 401
      AK(K)=FLOAT(K)
      IF(K.GT.((IX-1)/5))GOTO 401
      F1=0.0
      F2=0.0
      DARK=6.283185307*AK(K)/AL
C  VALUE OF PYE TO 11 SIG FIG INSTEAD OF 6 SIG FIGS
      COOK=COS(DARK)
      ACOC=2.0*COOK
      SOOD=SIN(DARK)
      DO 19 IZ=1,IX
      IM=IX1-IZ
      FC=C(IM)*F1*ACOC-F2
      F2=F1
      F1=FC
   19 CONTINUE
      A(K)=(FC-F2*COOK)*1.3333334/AL
      B(K)=(F2*SOOD*1.3333334)/AL
      R(K)=SQRT(A(K)*A(K)+B(K)*B(K))
      DB(K)=R(K)/(0.000000004416)
      IF(DB(K).LT.0.000001)GOTO 10
```

```
      DB(K)=20.0*ALOG10(DB(K))
      IF(DB(K).LT.0.0000001) GOTO 10
      GOTO 9
10    DB(K)=1.0
9     CONTINUE
      FREQ(K)=AK(K)*RPM/(60.0*ENB)
      AIAN(K)=ALOG10(FREQ(K))
15    CONTINUE
401   IX=IX
      IF(KTR.GT.5)GOTO 73
      WRITE(6,400)
400   FORMAT(5H PROGRA  V17E D.ANDERTON I.S.V.K.)
17    FORMAT(12H CASE NUMBER,I5)
      WRITE(6,17)ICASE
505   FORMAT(5X,4H IX ,7X,4H IY ,10X,4H IB ,7X,5H IXX )
      WRITE (6,505)
555   FORMAT(4X,I5,7X,I5,9X,I5,7X,I5)
      WRITE(6,555)IX,IY,IB,IXX
606   FORMAT(20X,3HAH ,23X,4H AL ,23X,4HAFAC,23X,4HAFAG)
      WRITE(6,606)
666   FORMAT(15X,4F20.5)
      WRITE(6,666)AH,AL,AFAC,AFAG
499   FORMAT(52X,24HHARMONIC AMPLITUDE IN DB)
      WRITE(6,499)
700   FORMAT(10X,4HA(K),20X,4HB(K),16X,4HR(K),13X,5HDB(K),18X,3H K )
      WRITE(6,700)
73    IF(IB.GT.ITCH) GOTO 78
      ITCH=IB
78    WRITE(6,800)(A(K),B(K),R(K),DB(K),AK(K),K=IPA,ITCH,IY)
800   FORMAT(1X,5F20.5)
901   FORMAT(2F12.1,2X)
      N=IB/IY
      IF(IY.EQ.1)GOTO 32
      J=0
      DO 30 I=1,IB,IY
      J=J+1
      AIANT(J)=AIAN(I)
      DBT(J)=DB(I)
30    CONTINUE
32    CONTINUE
      IF(IY.GT.1)GOTO 33
      DO 33 I=1,IB,IY
      AIANT(I)=AIAN(I)
      DBT(I)=DB(I)
33    CONTINUE
      IF(ITCH-IB)63,18,13
63    IX=((IX-1)*3)+1
18    CONTINUE
      IBK=1
      DO 14 I=1,28
      ICOUNT=0
      SUM=0.0
      HAT=FR(I)*0.115
      REM1=FR(I)-HAT
```

```
153             PER2=FR(I)+HAT
154             DO 6 J=INK,IP
155             IF(FREQ(J).LT.PER1)GOTO 6
156             IF(FREQ(J).GT.PER2)GOTO 8
157             SUM=SUM+R(J)*R(J)
158             ICOUNT=ICOUNT+1
159         6   CONTINUE
160             INK=IP
161             GOTO 29
162         8   INK=J
163         29  IF(ICOUNT.EQ.0)GOTO 28
164             DBC=SQRT(SUM/ICOUNT)
165             DBC=DBC/0.00000002?94
166             IF(DBC.LT.1.0)DBC=1.0
167             DB(I)=20.0*ALOG10(DBC)-3.0
168             GOTO 14
169         28  DB(I)=0.0
170         14  CONTINUE
171             WRITE(6,222)
172         222 FORMAT
173            *      (//10X,24H1/3 OCT BAND CENTRE FREQ,10X,10HBAND LEVEL/15X,
174            * 6HIN C/S,20X,21HDB RE 2*E-4 MICRO BAR//)
175             WRITE(6,20)(FR(I),DB(I),I=1,28)
176         20  FORMAT(15X,F12.6,12X,F12.6)
177             IF(L.GT.5)GOTO 11
178             STOP
179             END
```

DETAILS OF DATA CONTROL CARDS

L	=	Z program only accepts one data set
Ix	=	Number of calculated data points
	=	10 if it expects another data set
(Ix)	=	5 x number of harmonics calculated
IY	=	Harmonic spacing. One gives every harmonic
IB	=	Number of harmonics to be calculated
		2 gives every other harmonic
Ixx	=	Number of input data points
I case	=	Identification number
AFAC	=	Peak pressure in PSI
AFAG	=	Peak pressure in digits on input data
AL	=	Ix - 1 non integer number
EMB	=	2 for four-stroke, 1 for two-stroke
RPM	=	rev/min